WADC TECHNICAL REPORT 54-359
PART 2

EQUIPMENT COOLING SYSTEMS FOR AIRCRAFT

Part 2

Aircraft Penalty Methods and System Components Characteristics

R. H. ZIMMERMAN

THE OHIO STATE UNIVERSITY RESEARCH FOUNDATION

SEPTEMBER 1954

EQUIPMENT LABORATORY
CONTRACT No. AF 33(616)-147
TASK 61181

WRIGHT AIR DEVELOPMENT CENTER
AIR RESEARCH AND DEVELOPMENT COMMAND
UNITED STATES AIR FORCE
WRIGHT-PATTERSON AIR FORCE BASE, OHIO

Carpenter Litho & Prtg. Co., Springfield, O.
400 - May 1956

FOREWORD

This report was prepared in the Mechanical Engineering Department of the Ohio State University. The work was performed between June 1952 and August 1954 under Contract No. AF33(616)-147 with the Ohio State University Research Foundation. It was administered under the direction of the Mechanical Branch, Equipment Laboratory, Directorate of Laboratories, Wright Air Development Center, Wright-Patterson Air Force Base, Ohio. Mr. F. R. Ebersbach was the Equipment Laboratory project engineer in charge of the work which was accomplished under Task 61181, "Centralized versus Individualized Cooling of Aircraft Equipment", formerly RDO No. 664-803F-3.

The report is presented in three parts. Part 1 is concerned with an introduction to the scope of the study, the functional classification of cooling system components and types, and a summary and comparison of the characteristics of seven types of cooling systems. Part 2 contains methods of aircraft penalty evaluation, and the performance and physical characteristics of components used in the evaluation of cooling systems. Part 3 presents details of analysis and evaluation of seven types of cooling systems for design conditions up to 65,000 feet altitude and flight speeds up to Mach 1.8.

The authors acknowledge with thanks the contributions of the following research associates to the development of subject matter and the preparation of the three parts of this report. Part 1: K. G. Hornung. Part 2: S. E. Arnett, T. C. Taylor, W. Robinson, G. D. Hudelson and D. J. Masson. Part 3: C. F. Borteck and G. D. Hudelson.

ABSTRACT

Part 2 of the report contains data developed and compiled for use in the evaluation of cooling systems. Methods are given for the evaluation of aircraft penalty of cooling systems in terms of equivalent drag, increase in gross weight, reduced range, or reduced payload. The components of cooling systems are classified as equipment, distribution, intermediate and ultimate. Methods for the analytical simulation of equipment items by means of an equipment component are developed. The physical characteristics and performance of coolant distribution systems are analyzed for constant velocity, constant-pressure-gradient, and constant-diameter designs. Methods are developed for the analytical representation of cooling load distribution along the header of a distribution system. Various types of heat exchangers applicable as intermediate components in cooling systems are analyzed. Methods are developed for the evaluation of physical characteristics of air-to-air, liquid-to-air, and liquid-to-evaporant heat exchangers. Data on performance and physical characteristics are compiled for items serving as parts of the ultimate component of cooling systems. Included are: air intakes, air ducts, radial and axial blowers, compressors and turbines.

PUBLICATION REVIEW

The publication of this report does not constitute approval by the Air Force of the findings or conclusions contained therein. It is published for the exchange and stimulation of ideas.

FOR THE COMMANDER:

for S. T. SMITH Lt Col USAF
Colonel, USAF
Chief, Equipment Laboratory

TABLE OF CONTENTS

PART 2

CONTENTS OF PARTS 1, 2, AND 3 OF REPORT

PART 1

PART 2

PART 3

LIST OF ILLUSTRATIONS

LIST OF TABLES

SECTION III

AIRCRAFT PENALTY OF COOLING SYSTEMS

A problem fundamental to the study of aircraft equipment cooling systems is the evaluation of the flight performance penalty imposed on an aircraft by the addition of cooling systems. The overall evaluation and comparison of different types of cooling systems is affected to a great extent by their flight performance penalties. The purpose of this section is to present the methods of analysis and basic working equations employed to permit evaluation of flight performance or aircraft penalty for the various types of cooling systems studied and for various types of aircraft with which the cooling systems may be associated.

Flight performance penalty imposed on an aircraft by cooling systems results from system weight, external and momentum drags and change in powerplant performance. Indirectly, factors such as reliability, vulnerability, ease of maintenance, off-design performance of the cooling system, etc. affect the overall aircraft penalty. These factors are not considered within the scope of the presented working methods which aim for analytical evaluation and comparison of the more direct factors of cooling systems influencing the aircraft.

The penalty on an aircraft due to weight of cooling systems may be evaluated in terms of the effect on (1) aircraft gross weight at take-off for range and payload equivalent to that of the comparable aircraft without cooling systems, (2) on range for equivalent gross weight and payload, (3) on payload for equivalent gross weight and range. Also, in some cases other interpretations of the weight effect may be required, since with any aircraft having fixed mission characteristics, gross weight and payload, the introduction of a cooling system or systems might necessitate disposal or compromise of other equipment items and accessories of the aircraft. The general procedure employed in this study to define flight performance penalty is to determine the penalty relative to comparable aircraft without cooling systems. Thus, the weight of the cooling system is translated into effects on gross weight, range or payload.

External and momentum drags of cooling systems result whenever atmospheric air is used, either for direct or indirect cooling of equipment items. The external drag represents the parasitic drag added to the aircraft because of protuberances such as, for example, air intakes. The momentum drag represents the net drag on the aircraft for the process of taking air on board and subsequent ejection. It is possible for some cooling systems to have negative momentum drag, i.e., to produce thrust. Normally, however, systems impose a momentum drag penalty. The sum of external and momentum drags associated with cooling systems may be considered with good approximation to represent additional thrust required of the aircraft's powerplants to maintain comparable flight characteristics as without cooling systems.

Penalties imposed on powerplant performance by cooling systems can result from (1) shaft power extraction required in all indirect cooling systems for circulation of transfer fluids, circulation of air in direct cooling systems employing blowers, and input power to vapor cycle refrigeration machines, and (2) from air extracted intermediately or after the compressor of a powerplant for direct and indirect bleed-air cooling systems, and for remote power drives when air turbines are employed in preference to electric or hydraulic drives. Extraction of shaft power or air from the aircraft's powerplants requires increased fuel consumption of the powerplants in order to maintain comparable flight characteristics as without cooling systems.

Powerplant performance penalty must be integrated with drag and weight penalties to define the overall effect of the cooling systems on the aircraft. Of the many methods possible for defining flight performance penalty, two general methods are presented that have been used in the evaluation and comparison of the various cooling systems studied. The first method consists of evaluating the equivalent drag of the cooling system. The second method is based on evaluation of the effects of the cooling system on aircraft gross weight, payload and flight range.

Nomenclature

Symbol	Concept	Dimensions
C	constant	dimensionless
Dr	drag	pounds
Lf	lift of aircraft	pounds
p	static pressure	pounds per square foot, abs.
P	power	Btu per hour
Rg	range of aircraft	feet
SFC	thrust specific fuel consumption	pounds per hour-pound thrust
T	temperature	$^{\circ}R$
w	fluid flow rate	pounds per hour
W	weight	pounds
X	ratio of fuel weight at take-off to gross weight of aircraft	dimensionless
β	Mach number parameter, $1 + 0.2\ M_{\infty}^2$	dimensionless
Δ	difference or change of a quantity	

Subscript	Refers to
bd	bleed air
c	compressor
D	distribution component
e	exit
eq	equivalent
ex	external
g	gross weight
i	inlet

I	intermediate component
mom	momentum
para	parasitic drag
p-sy	power supply system
pl	payload
ref	reference value
sh	shaft power
sy	cooling system
U	ultimate component
τ	turbine
∞	free stream conditions

Superscript	Refers to
o	total or stagnation condition
'	power in units of horsepower

Equivalent Drag Method

Equivalent drag is defined as the sum of weight drag, external drag, momentum drag and any potential loss in thrust of a powerplant due to air bleed and/or shaft power extraction. External and momentum drags are defined directly by the system evaluation procedures as the parasitic drag introduced by air inlets and outlets, such as leading-edge or boundary-layer-air intakes, and the drag (possibly thrust) resulting from momentum change of atmospheric air taken aboard the aircraft and subsequently discharged. Weight drag is defined as the drag equivalent to the system's dead weight, converted to a drag basis by assumption of an operating lift-to-drag ratio for the aircraft.

Drag due to air bleed or shaft power extraction from a powerplant can be defined in one of several ways. The assumption may be made that the powerplant operating conditions remain fixed, and that the loss in propulsive thrust due to air bleed or power extraction suffices to define the powerplant performance penalty. Alternately, it may be assumed that best comparison of systems would be obtained by assuming constant flight characteristics, with or without air bleed or power extraction; so that constant thrust level, and, hence, flight speed, should be maintained. On this basis, an increased fuel rate is required and the drag penalty is defined by the potential gain in powerplant thrust corresponding to the increased fuel rate if the powerplant had no air bleed and power extraction. The latter procedure is believed preferable to that assuming a constant fuel rate, since evaluation of effects for an extensive range of flight Mach numbers is more satisfactory, the powerplant penalty effects can be more directly combined with other drags to define flight performance penalties, and, in general, the assumption of constant flight speed should provide a better datum plane for comparison of cooling systems.

The equivalent drag of a cooling system is defined, therefore, by

$$Dr_{eq} = Dr_{ex} + Dr_{mom} + W_{sy}/(Lf/Dr)_{ref} + \Delta w_{fuel}/SFC_{ref} \qquad (III-1)$$

where Dr_{ex} represents the external drag, Dr_{mom} the momentum drag caused by air taken on board, W_{sy} the dead weight of the cooling system, $(Lf/Dr)_{ref}$ and SFC_{ref} the operating lift-to-drag ratio and specific fuel consumption of the powerplants, respectively, and Δw_{fuel} the increase in fuel flow rate to the powerplants necessary to maintain constant thrust level with air bleed and/or power extraction. In defining the equivalent drag of a cooling system, the assumption is made that all changes in drag and engine performance are small in comparison to the corresponding values without a cooling system. Specifically, it is assumed that decremental thrust and incremental drags are small in comparison to the total drag of the aircraft, so that decremental values of thrust and incremental drags can be assumed equivalent aerodynamically and in their effects on flight performance, thus permitting summation of the individual effects to yield a total equivalent drag. Also, it is assumed that in defining the drag due to bleed air and/or power extraction, the specific fuel consumption SFC_{ref}, expressed in pounds of fuel per hour-pound net thrust, may be used as the specific fuel consumption of the powerplant without air bleed or power extraction. Evaluation of powerplant performance with air bleed rates needed for cooling systems in this study has shown this assumption to introduce a very negligible error in defining the equivalent drag.

Gross Weight, Payload and Range Methods

While the equivalent drag of a cooling system provides an index to the effect of the cooling system on the aircraft's flight performance, the use of this parameter has oftentimes the disadvantage that its magnitude cannot be readily translated into direct or concrete effects on aircraft flight performance, particularly when considering different types of aircraft, cooling systems and flight conditions. The alternate method of defining flight performance penalty is based on evaluation of cooling system effects on flight range, aircraft gross weight, fuel load and payload. For this purpose, the first assumption is that the Breguet range equation (Reference III-1) is accurate for relative comparisons of the effects of cooling systems. The range of any aircraft may, thereby, be defined in the form

$$Rg = \frac{C}{SFC\ Dr_{para}} \ln \frac{1}{1 - (W_{fuel}/W_g)} \qquad (III-2)$$

where the parameter C includes all flight conditions affecting the basic range of the aircraft, Rg, and Dr_{para} represents the total equivalent parasitic drag of the aircraft. The initial fuel load W_{fuel} is represented as a fraction of the aircraft's initial gross weight W_g. The second assumption is that the aircraft operates at a constant flight speed and altitude. Thus, the operating lift-to-drag ratio is assumed constant and the flight altitude will increase with flight time. The increase in altitude for operation above 35,000 feet depends upon the

value of W_{fuel}/W_g, and will normally be 5000 to 15,000 feet. The drag term is included in equation (III-2) to incorporate effects of drag increase (due to cooling systems) on the fuel consumption rate of the powerplants.

Since comparison of the effects of cooling systems is made on the basis of equivalent flight conditions with or without a cooling system, it is possible to define the reference range of the aircraft without cooling systems by

$$Rg_{ref}\ SFC_{ref}\ Dr_{para-ref} = C \ln \frac{1}{1 - X_{ref}}$$

where X_{ref} is the ratio of initial fuel load to gross weight of the aircraft without a cooling system. Hence, the range for an aircraft with a cooling system relative to the same aircraft having comparable flight conditions and powerplants but without a cooling system is defined by

$$\frac{Rg}{Rg_{ref}} = \frac{SFC_{ref}}{SFC} \frac{Dr_{para-ref}}{Dr_{para}} \left[\ln \frac{1}{1 - X} \Big/ \ln \frac{1}{1 - X_{ref}} \right] \qquad \text{(III-3)}$$

By this procedure, the flight plans of the aircraft are essentially equivalent, i.e., variations in altitude, flight speed, etc., which may occur will be similar in both cases since one might justifiably assume that cooling systems will not create pronounced effects on aircraft operational characteristics.

In order to introduce into equation (III-3) the effect of air bleed or power extraction, one may write

$$\frac{SFC}{SFC_{ref}} = 1 + \frac{\Delta W_{fuel}}{Dr_{ref}\ SFC_{ref}} \qquad \text{(III-4)}$$

To include the effects of external and momentum drags, it may be assumed that

$$\frac{Dr_{para}}{Dr_{para-ref}} = 1 + \frac{Dr_{ex} + Dr_{mom}}{Dr_{ref}} \qquad \text{(III-5)}$$

where Dr_{ref} is defined as the flight drag of the aircraft without a cooling system, being equal to the net thrust of the powerplants during unaccelerated level flight. It is reasonable to assume that in aircraft operating in the Mach number range from 0.5 to 1.8 the changes in fuel rate, external drag and momentum drag due to cooling systems are normally small in comparison to their reference values, i.e., the fuel rate and drag for the entire aircraft without cooling system. Thus, equations (III-4) and (III-5) may be introduced into equation (III-3) in the form

$$\frac{Rg}{Rg_{ref}} = \frac{\left[\ln \frac{1}{1-X} / \ln \frac{1}{1-X_{ref}}\right]}{1 + \left[Dr_{ex} + Dr_{mom} + \Delta W_{fuel}/SCF_{ref}\right]/Dr_{ref}} \qquad \text{(III-6)}$$

The relative range defined by equation (III-6) is assumed to be applicable to all types of aircraft, regardless of the flight speed or powerplant performance, since the range effect is related to a comparable aircraft having the same flight conditions, but no cooling system. Limitations on the accuracy of equation (III-6) depend on the correctness of the assumptions that drags are additive and that relative effects on range are described by the Breguet-type range equation.

1. Constant Range

Of considerable interest in the design and evaluation of cooling systems is the determination of effects on the aircraft when the flight range is equal to that for the same aircraft without a cooling system. For purposes of evaluation, let it be assumed that any change in a variable is small in comparison to the basic value of the variable. Thus, for the condition of constant range, equation (III-6) may be expressed as

$$\ln \frac{1}{1-X} = \ln \frac{1}{1-X_{ref}} \left[1 + \frac{Dr_{sy}}{Dr_{ref}}\right] \qquad \text{(III-7)}$$

or

$$d\left[\ln \frac{1}{1-X}\right] = \left[\ln \frac{1}{1-X_{ref}}\right] d \frac{Dr_{sy}}{Dr_{ref}}$$

where Dr_{sy} is hereafter referred to as the drag of the system, which is smaller than the equivalent drag of the system by the weight drag as defined in equation (III-1). Differentiation of this expression yields

$$\frac{dX}{1-X} = \left[\ln \frac{1}{1-X_{ref}}\right] d \frac{Dr_{sy}}{Dr_{ref}} \qquad \text{(III-8)}$$

Suppose now the condition is examined when it is permissible to increase the gross weight of the aircraft in order to maintain constant payload. Thus,

$$dX = X_{ref}(dW_{fuel}/W_{fuel}) - X_{ref}(dW_g/W_g) \qquad \text{(III-9)}$$

and

$$dW_g = dW_{fuel} + dW_{sy} \qquad \text{(III-10)}$$

so that equation (III-8) may be rearranged to the following form, assuming small finite changes in the variables,

$$\frac{\Delta W_{fuel}}{W_{fuel\text{-}ref}} = \left[\frac{1}{1-X_{ref}}\right] \frac{W_{sy}}{W_{g\text{-}ref}} + \left[\frac{1}{X_{ref}} \ln \frac{1}{1-X_{ref}}\right] \frac{Dr_{sy}}{Dr_{ref}} \qquad \text{(III-11)}$$

Equation (III-11) defines the fractional increase in fuel load required to maintain constant range under the condition that the maximum gross weight is permitted to increase. The fractional increase in gross weight, neglecting possible changes in the aircraft's fixed weight which might be required if the gross weight is increased during the aircraft design stage, is defined by

$$\Delta W_g = W_{sy} + \Delta W_{fuel}$$

or

$$\frac{\Delta W_g}{W_{g\text{-}ref}} = \left[\frac{1}{1-X_{ref}}\right] \frac{W_{sy}}{W_{g\text{-}ref}} + \left[\ln \frac{1}{1-X_{ref}}\right] \frac{Dr_{sy}}{Dr_{ref}} \qquad \text{(III-12)}$$

Numerical values of X_{ref}, the ratio of fuel load to gross weight, might be considered to vary for different types of aircraft designs and mission requirements from about 0.20 to roughly 0.75. Low ratios are characteristic of aircraft operating at relatively short range and high payload, while high ratios would normally be associated with high-speed aircraft having reasonably long range. The ratio would tend to increase somewhat with increased flight speed. Common values of this ratio for military aircraft are considered to be about 0.4 or 0.5.

Examination of equation (III-11) shows that under the conditions of constant range and assuming X_{ref} to be 0.5, a cooling system weight equal to 1% of the reference gross weight would increase the required fuel load by 2% of the reference fuel load; a 1%-increase in the aircraft's drag, due to air bleed and/or power extraction and external and momentum drag, would increase the required fuel load by 1.4% of the reference fuel load. The increase in gross weight required for constant range is, therefore, by equation (III-12), 2.7%. Suppose, for example, a cooling system is added to a bomber which has a basic gross weight and fuel load of 200,000 and 80,000 pounds, respectively. Let the cooling system weight and drag be 200 and 100 pounds, respectively. Assume, also, that the total net powerplant thrust for the flight condition is 15,000 pounds. Thus, by equation (III-11) the fuel load must increase by 1.02%, or 815 pounds. The required increase in gross weight would be 1015 pounds. For aircraft operating with low ratios of initial fuel load to gross weight, i.e., around 0.2, equation (III-11) reduces to, approximately,

$$\Delta W_{fuel}/W_{fuel\text{-}ref} = \left[1/(1 - X_{ref})\right] (Dr_{eq}/Dr_{ref})$$

which indicates that the fractional increase in fuel load is very nearly equal to the fractional increase in drag due to the equivalent drag of the cooling system. When the ratio of fuel load to gross weight is high, the effect of an increase in system weight is more critical. If X_{ref} is

0.75, 1 pound of cooling system weight requires 3 pounds extra fuel, and, thereby, a 4-pound increase in gross weight. For the same condition and a lift-to-drag ratio of six, 1 pound drag requires over 8 pounds extra fuel.

Useful alternate forms of equations (III-11) and (III-12) for comparison of aircraft cooling systems, based on constant range and payload, are

$$\Delta W_{fuel} = \frac{X_{ref}}{1-X_{ref}} (W_{sy}) + (Lf/Dr)(Dr_{sy}) \ln \frac{1}{1-X_{ref}} \qquad \text{(III-13)}$$

and, since

$$\Delta W_g = \Delta W_{fuel} + W_{sy}$$

then,

$$\Delta W_g = \frac{1}{1-X_{ref}} (W_{sy}) + \left[\ln \frac{1}{1-X_{ref}}\right] (Lf/Dr)(Dr_{sy}) \qquad \text{(III-14)}$$

This equation defining gross weight increase may be conveniently interpreted by noting that if the equation is rearranged to the form

$$(1-X_{ref})\Delta W_g = W_{sy} + \left[(1-X_{ref}) \ln \frac{1}{1-X_{ref}}\right] (Lf/Dr)(Dr_{sy}) \qquad \text{(III-14a)}$$

the coefficient on the drag term that is a function of X_{ref} varies only from 0.25 when X_{ref} is 0.3 to a maximum value of about 0.367 when X_{ref} is 0.633. Also, in the range of X_{ref} from 0.4 to 0.6, an average value of the coefficient of 1/3 is correct to within less than 10%. Thus, with good approximation, the gross weight parameter $(1-X_{ref})\Delta W_g$ is defined by the sum of the system weight and a term equal to the product of one-third of the lift-to-drag ratio and the drag of the system.

For fixed gross weight of an aircraft, constancy of range results in reduced payload when flight performance penalties are introduced. The reduction in payload is defined by letting the right-hand term of equation (III-9) be zero, so that equation (III-8) reduces to

$$\frac{\Delta W_{fuel}}{W_{fuel-ref}} = \left[\frac{1-X_{ref}}{X_{ref}} \ln \frac{1}{1-X_{ref}}\right] (Dr_{sy}/Dr_{ref}) \qquad \text{(III-15)}$$

In terms of the gross weight,

$$\Delta W_{pl}/W_g = (\Delta W_{fuel} + W_{sy})/W_g$$

so that

$$\Delta W_{pl}/W_g = W_{sy}/W_g + (1-X_{ref})\left[\ln \frac{1}{1-X_{ref}}\right](Dr_{sy}/Dr_{ref}) \qquad \text{(III-16)}$$

or

$$\frac{\Delta W_{pl}}{W_{pl-ref}} = \frac{-\left[(1-X_{ref}) \ln \frac{1}{1-X_{ref}}\right](Dr_{sy}/Dr_{ref}) - W_{sy}/W_g}{1 - X_{ref} - (W_{fixed}/W_g)} \qquad \text{(III-17)}$$

where W_{fixed} represents the operating empty weight of the aircraft. Using the previous example of a 200,000-pound airplane having a cooling system weight and drag of 200 and 100 pounds, respectively, the reduction in payload required for the same range of the aircraft without a cooling system is 609 pounds. For purposes of system evaluation, equation (III-16) may be rearranged to

$$\Delta W_{pl} = -W_{sy} - \left[(1-X_{ref}) \ln \frac{1}{1-X_{ref}}\right](Lf/Dr)(Dr_{sy}) \qquad \text{(III-18)}$$

Suppose, for example, that the fixed weight of the aircraft is 40% of the gross weight and the value of X_{ref} is 0.50. Thus, the reference payload is 10% of the gross weight. For these assumed conditions, equation (III-17) shows that a cooling system drag of 1% of the drag of the aircraft without a cooling system reduces the payload by about 3.5%. The weight of the cooling system, for constant range and gross weight, will always reduce the payload by an amount equal to the system weight. A comparison of equations (III-14a) and (III-18) shows that for any cooling system the ratio of the payload reduction required for constant gross weight to the gross weight increase required for constant payload is equal to

$$\Delta W_{pl}/\Delta W_g = 1 - X_{ref}$$

Thus, typically, the required reduction in payload is 40 to 50% of the required gross weight increase. Also, the ratio of the percentage of reduction in payload to the percentage of increase in gross weight is defined by unity plus the ratio of the fixed weight to the reference payload. Thus, on a percentage basis, the payload can decrease, typically, from 3 to 9 times the percentage of increase in gross weight. The basis of evaluation to be used, i.e., constant payload or gross weight, to determine cooling system penalty would depend upon the mission requirements and the design characteristics of the aircraft.

2. Reduced Range

When neither gross weight nor payload may be altered the cooling system penalties result in reduced range of the aircraft. The magnitude of range reduction for fixed gross weight and payload is defined by use of equation (III-6). The weight of the cooling system, W_{sy}, reduces the aircraft's fuel load. Thus,

$$dX = -dW_{fuel}/W_g = -W_{sy}/W_g$$

Then, the fractional reduction in range becomes, neglecting second-order correction factors,

$$\frac{\Delta Rg}{Rg_{ref}} = -\frac{W_{sy}/W_g}{(1-X_{ref})\ln\frac{1}{1-X_{ref}}} - \frac{Dr_{sy}}{Dr_{ref}} \qquad \text{(III-19)}$$

or,

$$\frac{\Delta Rg}{Rg_{ref}} = -\frac{\frac{W_{sy}}{W_g} + \left[(1-X_{ref})\ln\frac{1}{1-X_{ref}}\right]\left[\frac{Lf}{Dr}\right]\left[\frac{Dr_{sy}}{W_g}\right]}{(1-X_{ref})\ln\frac{1}{1-X_{ref}}} \qquad \text{(III-19a)}$$

The denominator of the system weight term in equation (III-19) is approximately 1/3, as previously noted, so that with good approximation

$$\Delta Rg/Rg_{ref} = -\left[3W_{sy} + (Lf/Dr)Dr_{sy}\right]/W_g \qquad \text{(III-20)}$$

If the fuel and payloads are fixed and the gross weight is permitted to increase to accommodate the weight of the cooling system, the fractional loss in range is defined by

$$\frac{\Delta Rg}{Rg_{ref}} = -\frac{(X_{ref})(W_{sy}/W_g)}{(1-X_{ref})\ln\frac{1}{1-X_{ref}}} - \frac{Dr_{sy}}{Dr_{ref}} \qquad \text{(III-21)}$$

3. Alternate Method

The basic equation for optimum range of jet aircraft is slightly different than equation (III-2). The range equation for jet aircraft appears in the literature in different forms based upon different conditions of analysis. Reference III-1 presents a range equation which when compared with the basic equation (III-2) differs, in effect, only in the term containing the ratio of the fuel load to the aircraft gross weight. The modified range equation for jet aircraft is placed in the form

$$Rg = \left[C/(SFC)(Dr_{para})\right]\left[1 - (1-X_{ref})^{0.5}\right] \qquad \text{(III-22)}$$

For constant range and payload, the required increase in aircraft gross weight, based on equation (III-22), is defined by

$$(1-X_{ref})\Delta W_g = W_{sy} + 2\left[(1-X_{ref})^{0.5} - (1-X_{ref})\right](Lf/Dr)(Dr_{sy}) \qquad \text{(III-23)}$$

This equation and the comparable equation based on the previous analysis, i.e., equation (III-14a), differ only in the term defining the effect of

the drag on the gross weight increase. The difference lies in the coefficient that is a function of the reference ratio of the fuel load to gross weight, X_{ref}. For typical values of X_{ref}, the coefficient on the right-hand term of equation (III-23) is 10 to 20% greater than that in equation (III-14a). Thus, for cooling systems imposing a small percentage of the total penalty because of dead weight, the difference between the two methods would be significant. However, since with most cooling systems the dead weight represents an important portion, or, in some cases, nearly all of the total penalty, the difference between the gross weight penalty predicted by the two methods would not be of great importance. For most cooling systems, the difference will be well within the limits of accuracy of the overall evaluation of drag, weight, etc.

A review of the literature indicates that a variety of basic range equations have been employed, depending upon the type of powerplant, desired simplicity of evaluation, etc. It is believed that the equations developed in the preceding sub-sections based upon the Breguet-type of range equation are on the average the most suitable for general evaluation of aircraft penalty resulting from the use of equipment cooling systems.

Powerplant Performance Penalty Resulting from Air Bleed and Shaft Power Extraction

The evaluation of powerplant performance penalty due to bleed air and/or shaft power extraction is based on the assumption that the powerplants are turbojet engines. The methods presented in the preceding sub-sections for evaluation of aircraft performance penalty can, however, be adapted to any type of powerplant. In general, the comparison of the relative penalties associated with different types of cooling systems will be similar for turbojet and turbine-propeller engines. Therefore, the results of the cooling system studies presented in this report are based only on aircraft having turbojet engines.

The penalty imposed on the powerplant due to bleeding air from its compressor is evaluated on the basis of the increased fuel flow required to operate the powerplant at constant net thrust. The resultant penalty imposed on the aircraft is evaluated by the methods outlined in the preceding sub-sections, either as a potential loss in thrust, when evaluating the equivalent drag of a cooling system, or, as the increased fuel flow affects the aircraft gross weight, payload or range. It is assumed that the air bleed occurs at discharge of the compressor. A number of methods for evaluating turbojet performance with air bleed have been examined. Most working methods and information available are based on performance of specific powerplants and, thereby, do not permit general use for the wide range of flight Mach numbers and aircraft considered in this study. Furthermore, available methods are based on correction of the generalized powerplant performance, so that evaluation of air bleed effects requires considerable computational effort, in addition to knowledge of the generalized powerplant performance. In order to avoid se-

lecting one or several specific turbojet engines, the following simplified equation is used in the cooling system studies of this report to define the increase in fuel rate necessary to maintain constant engine thrust.

$$\Delta w_{fuel} = 0.0335\ (T^{o}_{ti\text{-}ref}/2000)(w_{bd}) \qquad \text{(III-24)}$$

where w_{bd} represents the bleed air rate expressed in pounds per hour, $T^{o}_{ti\text{-}ref}$ the turbine inlet total temperature without air bleed and Δw_{fuel} the increase in fuel rate expressed in pounds per hour. Equation (III-24) was developed on the basis of general cycle studies of the effect of air bleed and the methods and data presented in References III-2, III-3 and III-5.

Similar studies based on cycle analysis and References III-4 and III-5 were conducted to define the penalty on turbojet engine performance due to shaft power extraction. The basis for determining the performance penalty is the increase in fuel rate necessary to maintain constant net thrust of the powerplant. The increase in fuel rate has been defined by

$$\Delta w_{fuel} = \frac{0.18(P'_{sh})(\beta_{\infty})^{0.87}\ (p^{o}_{ce}/p^{o}_{ci})^{0.25}}{\left[0.99(\beta_{\infty})^{0.87}\ (p^{o}_{ce}/p^{o}_{ci})^{0.25}\right] - 1} \qquad \text{(III-25)}$$

where the fuel rate is expressed in pounds per hour, the shaft power P'_{sh} in horsepower, p^{o}_{ce}/p^{o}_{ci} represents the total pressure ratio developed by the engine's compressor and β_{∞} a flight Mach number parameter equal to $1 + 0.2\ M^{2}_{\infty}$.

Equations (III-24) and (III-25) reveal the following order of magnitude of fuel flow penalties for air bleed and power extraction from turbojet engines operating at constant thrust. The fuel flow rate must increase about 30 pounds per hour for each 1000 pounds per hour of bleed air at typical cruise conditions. A survey of the bleed air cooling system indicates that should this type be employed for present-day or near-future aircraft, the minimum and maximum bleed air rates required would be from 500 to about 25,000 pounds per hour, respectively. Thus, the minimum and maximum fuel rate penalties to be expected for bleed air cooling systems would be from 15 to 750 pounds per hour. The equivalent in-flight load-carrying capacity corresponding to this range of fuel rate penalty could be from somewhat less than 100 to somewhat greater than 12,000 pounds, depending upon the flight lift-to-drag ratio of the aircraft. The increase in fuel rate required for shaft power extraction amounts to from 0.3 to 0.65 pound fuel per hour-horsepower, so that the fuel rate penalties for the present study due to shaft power requirements are likely to range from about 0.5 pound per hour to possibly 100 pounds per hour. This range of extra fuel rate required defines a range of equivalent in-flight load-carrying capacity of from about 3 to 1800 pounds. The above figures are intended to illustrate the range of penalty corresponding to the limits of maximum and minimum cooling capacity expected for present-day or near-future aircraft.

The effect of air bleed on the aircraft proper may be illustrated by examination of equation (III-14). Suppose an aircraft has a basic ratio of fuel load to gross weight of 0.50, an in-flight lift-to-drag ratio of 15 and an in-flight specific fuel consumption of 1.1 pounds per hour-pound net thrust. The drag due to 1000 pounds per hour air bleed is about 27 pounds, and by the right-hand term of equation (III-13) the fuel load at take-off for constant range must be increased by 280 pounds due to the 1000 pounds per hour air bleed only, i.e., exclusive of system weight and other drag introduced by the cooling system. If it is assumed, in the way of an example, that the weight of the bleed-air cooling system is comparable to the weight of an evaporative cooling system, i.e., one employing an expendable coolant, and that other drags of the bleed-air system are neglected, assumptions which favor the bleed-air system, then it is found that, typically for high subsonic Mach numbers, the breakeven point in terms of increased gross weight, using water for the expendable coolant, corresponds to about 4 hours flight time, i.e., for less than 4 hours flight the evaporative system would necessitate less increase in gross weight than would the bleed-air system.

The general effect of shaft power extraction on the aircraft may be evaluated in a similar manner. Consider, for example, a turbojet engine having an in-flight compressor pressure ratio of 5:1. For a flight Mach number of 0.9, the increased fuel rate, defined by equation (III-25), is 0.45 pound per shaft horsepower-hour. Assuming subsonic flight with a powerplant specific fuel consumption of 1.1, lift-to-drag ratio of 15 and a reference fuel load to gross weight ratio of 0.50, the required increase in take-off fuel load for constant range amounts to 4.3 pounds per shaft horsepower extracted. This increase in fuel load is the penalty due only to shaft power extraction, i.e., exclusive of system weight, external and momentum drag. In all probability, for cooling loads up to 100 kilowatts, the shaft power extraction for well-designed cooling systems, and other than vapor cycle machines, will not exceed 25 to 30 horsepower, so that the increase in fuel flow would not exceed 20 pounds per hour. The maximum increase in take-off fuel load for this power extraction would be around 400 pounds, although quite commonly it would be around 150 to 200 pounds for the 20 pounds per hour increase in fuel flow.

A vapor cycle refrigeration machine used as the intermediate component of a cooling system may require as much as 1 horsepower input power per kilowatt cooling. Thus, assuming a power transmission efficiency of 67%, the shaft power extraction from the powerplant amounts to about 1.5 horsepower per kilowatt, or an hourly increase in the fuel rate of roughly 0.75 pound per kilowatt cooling capacity. The increase in take-off fuel load due only to power extraction required for constant flight range would be, therefore, between 2 and 10 pounds per kilowatt cooling, depending upon the type of aircraft and mission. The increase in take-off fuel load for typical high subsonic flight due only to power extraction would be about 7 pounds per kilowatt, and about 2 to 4 pounds per kilowatt for typical flight at a Mach number of 1.5. For a conceivable cooling load of 100 kilowatts, the take-off fuel load of a large long-

range aircraft may require an increase of as much as 1000 pounds with a vapor cycle cooling system, excluding effects due to weight and drag of the cooling system.

Application of Methods for Evaluation of Aircraft Penalty of Various Types of Cooling Systems

In the previous sub-sections methods for evaluating aircraft penalty resulting from cooling systems are presented from the viewpoint of defining the equivalent drag, the required increase in aircraft gross weight for fixed payload and range, the required reduction in payload for fixed gross weight and range, the range reduction for fixed gross weight and payload, and the range reduction for fixed fuel load and payload. For study of the relative merits of aircraft cooling systems, it is believed that of these methods, the equivalent drag method and the method defining required increase in aircraft gross weight for fixed payload and range are the most suitable. The equivalent drag method has the advantage of defining a parameter which the aircraft designer can translate into the effects any cooling system has on the aircraft performance in any way he prefers. It has, however, the basic disadvantage of being difficult to interpret and does not present in a tangible way the effects cooling systems have on aircraft performance. The method evaluating gross weight increase required for fixed range and payload is believed to provide the most realistic basis for comparison of cooling systems. The increase in gross weight allows for the cooling system weight and the extra fuel load required. This basis of comparison most nearly reflects what changes in design of an aircraft, having fixed mission characteristics, are required when a cooling system is incorporated. The method does not account for change in fixed weight of an aircraft, which would normally result when the weight is increased during the design stage. No attempt has been made to include this effect on fixed weight. The method represents the case of an existing aircraft having its gross weight increased without undergoing structural modifications.

As an example of the use of the previously presented methods the following discussion is presented for the ram air cooling system. The application of the methods to other types of cooling systems would be similar.

Both direct and indirect ram air cooling systems require facilities for taking atmospheric air on board the aircraft, conveying the ram air to a heat exchanger, and then conveying it to the point of ejection from the aircraft. These facilities, comprising the ultimate component, introduce dead weight and drag; the latter resulting from external and momentum drags of the intakes, outlets and the ultimate cooling air flow. Since the equipment component is not considered as part of the cooling system, the weight of direct ram air systems is defined by

$$W_{sy} = (W_{intakes} + W_{ducts} + W_{outlets})_U = W_U \qquad \text{(III-26)}$$

The drag is defined by

$$Dr_{sy} = Dr_{mom-U} + Dr_{ex-intakes,outlets} = Dr_U \qquad \text{(III-27)}$$

since direct systems require no shaft power for distribution of transfer fluids. Thus, for direct ram air cooling systems, the increase in gross weight required for constant range and payload is defined on the basis of equation (III-14a) by

$$(1-X_{ref})\left[\Delta W_g\right]_{\substack{\text{ram air}\\ \text{direct}}} = W_U + \left[(1-X_{ref})\ln\frac{1}{1-X_{ref}}\right]\left[\frac{Lf}{Dr}\right](Dr_U) \qquad \text{(III-28)}$$

The equivalent drag, according to equation (III-1), would be evaluated by

$$\left[Dr_{eq}\right]_{\substack{\text{ram air}\\ \text{direct}}} = Dr_U + (Lf/Dr)(W_U) \qquad \text{(III-29)}$$

When ram air is employed for indirect cooling of equipment items, the effects of the intermediate and distribution components must be included in the previous relationships. The intermediate component increases the dead weight of the system and indirectly affects the drag of the system because of the increased flow resistance of the ultimate cooling air. The distribution component, in addition to increasing the system weight, requires power extraction from the aircraft's powerplants for circulation of the transfer fluid in the distribution component. Also, the power must be transmitted from the powerplants to the transfer fluid, and, thereby, requires a power supply system which might be a separate unit for the cooling system or be part of a general power supply system within the aircraft. The weight of the indirect ram air cooling system is represented by

$$W_{sy} = W_U + W_I + W_D + W_{p-sy} \qquad \text{(III-30)}$$

and the drag by

$$Dr_{sy} = Dr_U + (\Delta w_{fuel}/SFC_{ref}) \qquad \text{(III-31)}$$

where the right-hand term of equation (III-31) defines the drag equivalent of the increased fuel flow to the powerplants required to maintain constant propulsive thrust with shaft power extraction. The gross weight parameter and equivalent drag of indirect systems are defined by substitution of equations (III-30) and (III-31) into equations (III-14a) and (III-1). Should the power supply system be operated pneumatically by bleed air from the powerplants, the right-hand term of equation (III-31) would represent the increased fuel flow required because of the compressor air bleed.

Compromise in the design of direct and indirect ram air systems is obtained basically by distribution of the aircraft penalty between dead

weight and drag on the aircraft. One extreme of design is minimization of drag by sacrificing the weight of the cooling system. The drag of the ultimate component may be minimized by using non-protruding intakes handling low-energy boundary layer air. The weight flow rate of ultimate air may be minimized by employing heat exchangers of high effectiveness. Lowering the air flow rate reduces the external and momentum drags of the ultimate component. The reduction in drag, however, increases the system weight, since by utilizing low-energy boundary-layer air the pressure available for overcoming the resistance of the flow passages is low and, therefore, the size of the air ducts, etc., must be large. Increasing the effectiveness of the heat exchanger introduces greater flow resistance and, thereby, reduces the pressure loss available for the ducts. Oppositely, one may design for minimum dead weight by employing high-resistance flow systems.

A major problem in the design of ram air cooling systems is the determination of the optimum distribution between dead weight and drag so as to impose the least penalty on the aircraft. Similar compromise in design is required for the distribution component of all indirect systems. Small weight of the distribution component results in large pumping power and, thereby, appreciable power extraction from the aircraft's powerplants. It is apparent that for any system having specified operational conditions there exists an optimum weight or size of the distribution component that results in minimum overall penalty imposed on the aircraft.

REFERENCES

III-1 Perkins and Hage, Aircraft Performance, Stability, and Control, John Wiley and Sons, New York, 1949.

III-2 Hensley, R. V., Rom, F. E. and Koutz, S. L., Effect of Heat and Power Extraction on Turbojet-Engine Performance. I - Analytical Method of Performance Evaluation with Compressor-Outlet Air Bleed, Tech. Note 2053, NACA, 1950.

III-3 Rom, F. E. and Koutz, S. L., Effect of Heat and Power Extraction on Turbojet-Engine Performance. II - Effects of Compressor-Outlet Air Bleed for Specific Modes of Engine Operation, Tech. Note 2166, NACA, 1950.

III-4 Koutz, S. L., Hensley, R. V. and Rom, F. E., Effect of Heat and Power Extraction on Turbojet-Engine Performance. III - Analytical Determination of Effects of Shaft-Power Extraction, Tech. Note 2202, NACA, 1950.

III-5 Installation Handbook for Turbojet Engines, First Edition, Aviation Gas Turbine Division, General Electric Co.

SECTION IV

THE EQUIPMENT COMPONENT

For the evaluation of aircraft cooling systems it is necessary to know the heat transfer and flow resistance characteristics of the equipment items being cooled. With indirect cooling systems, these characteristics affect directly the pumping power, transfer fluid flow rate and permissible heat transfer temperature level in the intermediate component and, thereby, affect indirectly the required ultimate fluid flow rate and the overall performance penalty imposed on the aircraft. With direct cooling systems, the heat transfer and flow resistance characteristics of the equipment items being cooled affect directly the requirements of the ultimate component.

Since the types of equipment items which may require cooling in any aircraft vary widely in heat transfer and coolant flow design, it is considered impossible to establish a generalized relationship between heat transfer and flow resistance that would be applicable to any equipment item served by any cooling system. In order to take these characteristics into account in the evaluation of cooling systems, it would be necessary to specify the number of each of the various types of equipment items being cooled, the general type of cooling design employed for each item, and the relationship of heat transfer and flow resistance for each type of cooling design.

Since the present state of the art does not permit definition of these basic relationships without extensive experimental and analytical study, the heat transfer aspects of the equipment items are defined in this study by employing an equipment component of known characteristics which is considered to be an integral part of the equipment item. The equipment component is a heat exchange surface through which heat is transferred from the equipment item to the transfer fluid in an indirect system or directly to the ultimate fluid in a direct cooling system. The mechanism by which heat is transferred from the various parts of the equipment item to the equipment component remains unspecified in this study, so that, presumably, the equipment component may be serving any type of equipment item. The heat transfer surface representing the equipment component could be interpreted, for example, as the envelope surfaces of all parts contained in an equipment item having an open through-flow cooling arrangement, or as an external heat transfer surface for closed equipment items having an internal coolant which is circulated over the component surfaces within the equipment item and the internal surface of the equipment component.

Primarily, for the purposes of defining its physical make-up and interpretation of cooling system characteristics, the equipment component is simulated by a heat exchanger of tubular construction. The fluid transporting heat to the intermediate component with indirect cooling systems or the ultimate fluid with direct cooling systems is as-

sumed to flow through the tubes of the heat exchanger. The tube surface of this heat exchanger represents the heat transfer surface of the equipment component. The simulating heat exchanger serving as the equipment component represents the heat transfer link between the cooling system and the equipment items. It is necessary, therefore, that the desired temperature level and cooling rate of an equipment item be defined in terms of the equipment component. The required cooling rate for an equipment item defines the required cooling capacity of the equipment component. The desired or required temperature level of an equipment item must be indexed by selecting a temperature for the heat transfer surface of the equipment component. It is assumed in all instances that the temperature of the surface of the equipment component is constant and uniform for any selected steady-state operational condition of the equipment item and cooling system. Inasmuch as the heat transfer mechanism on the equipment side of the equipment component is not specified, it is not possible to specify the temperature level of the equipment component as a function of the desired temperature level of parts of equipment items. The temperature of the heat transfer surface of the equipment component must be considered as an independent variable of analysis, and the viewpoint must be taken that cooling system performance and physical characteristics shall be defined for a range of temperatures of the equipment component. On this basis, the major problem associated with the use of an equipment component to represent the equipment items becomes one of selecting the most appropriate range of temperatures to be used for evaluation of cooling systems.

The temperature of the heat transfer surface of the equipment component was specified for this study to range from 130°to 250°F. This infers roughly equipment items which have required mean temperature levels from slightly above 130°F (54.4°C) to 350-400°F (175-200°C) or higher. The summarization of the approximate limiting temperatures of a wide variety of equipment items presented in Reference IV-1 yields a distribution curve roughly as illustrated in Figure IV-1. Thus, typically, based on present and near-future temperature limits, about 75% of all equipment items have a limiting temperature between 130°and 250°F. As the state of the art improves the distribution curve will shift to the right in Figure IV-1, so that equipment component temperatures of 200° to 250°F will be required when the bulk of the equipment items have limiting temperatures in the range of 250° to 350° or 400°F. The specified range in surface temperature on the equipment component of from 130° to 250°F to be used for investigation of aircraft cooling system performance and physical characteristics appears to be most appropriate for existing and near-future equipment items in general.

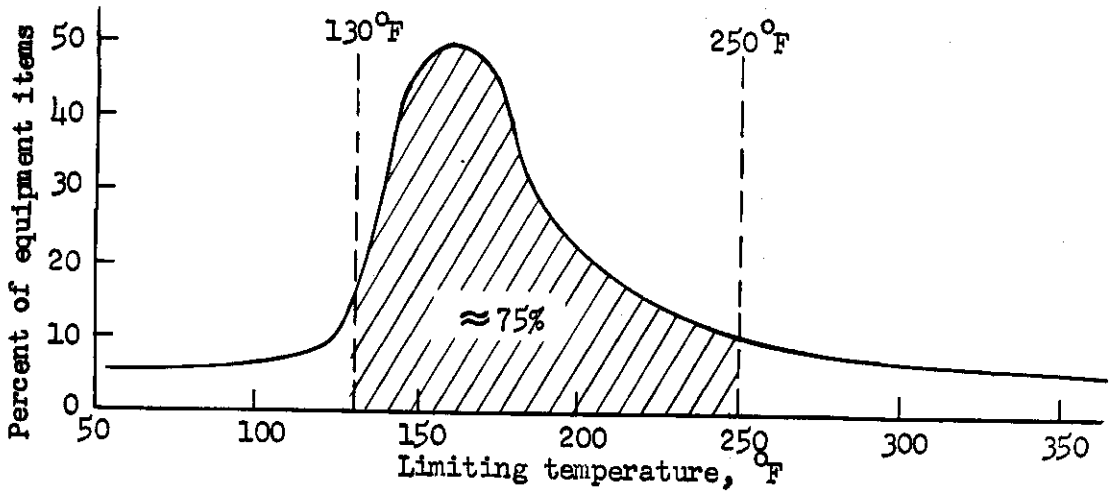

Figure IV-1. Approximate frequency distribution curve on temperature limits of various aircraft equipment items. Based on temperature limit data in Ref. IV-1.

Nomenclature

Symbol	Concept	Dimensions
c_p	specific heat at constant pressure	Btu per pound-°R
d	diameter	feet
e	heat exchanger effectiveness	dimensionless
f	Darcy friction factor	dimensionless
h	heat transfer coefficient	Btu per hour-square foot-°R
J	mechanical equivalent of heat	foot-pounds per Btu
k	coefficient of thermal conductivity	Btu per hour-foot-°R
K	flow resistance coefficient	dimensionless
L	length	feet
N	number of items	dimensionless
p	pressure	pounds per square foot, abs.
P	power	Btu per hour
PC	power-to-cooling ratio	dimensionless
Pr	Prandtl number	dimensionless
q	heat rate	Btu per hour
Re	Reynolds number	dimensionless
S	surface area	square feet
T	temperature	°R
u	flow velocity	feet per second
w	fluid flow rate	pounds per hour
α	area ratio	dimensionless

γ	specific weight	pounds per cubic foot
Δ	difference	

Subscript	Refers to
e	exit
E	equipment component
i	inlet
m	mean value

Superscript

o	total or stagnation conditions

Equipment Component Characteristics Requiring Specification for Cooling System Evaluation

Since, in general, it is not possible to specify the type and heat transfer and flow resistance characteristics of the equipment component, all characteristics of the equipment component required to conduct cooling system studies must be considered as independent variables of the cooling system. Thus, the cooling system studies should determine the effects these variables have on the system's performance and physical characteristics.

The general characteristics of the equipment component which should be specified are (1) the required cooling capacity, (2) the desired surface temperature, (3) the effectiveness of heat exchange, and (4) the flow resistance or the percentage of loss in total pressure of the fluid flowing over the heat transfer surface. These four characteristics are independent variables for the cooling system study. Practical limitations and approximate interrelations of the variables should be used whenever possible by the designer to avoid evaluation and design of systems operating under unrealistic conditions. Specification of the independent variables cooling capacity, percentage of loss in total pressure and the temperature rise of the fluid passing through the equipment component may be substituted for the above-mentioned group when it is not necessary to have specified the surface temperature associated with the heat exchange process. In general, it is believed that more practical limitations on the ranges of investigation may be maintained by using the former set.

The effectiveness of heat exchange of the equipment component is defined by

$$e_E = (T_{Ee} - T_{Ei})/(T_{Es} - T_{Ei}) \qquad \text{(IV-1)}$$

and represents the ratio of the actual temperature rise of the fluid passing through the equipment component to the maximum temperature rise theoretically possible. The cooling capacity in Btu per hour is related to the flow rate and fluid temperature rise by

$$q_E = w_E c_{pE} (T_{Ee} - T_{Ei}) \qquad \text{(IV-2)}$$

or

$$q_E = w_E c_{p_E} e_E (T_{Es} - T_{Ei}) \qquad \text{(IV-3)}$$

The percentage of total pressure loss is defined as the ratio of the drop in total pressure of the fluid across the equipment component to the total pressure of the fluid at inlet to the equipment component.

Analysis for the Equipment Component Simulated by a Tubular Heat Exchanger

The transfer or ultimate fluid flows through the tubes of the equipment component. Heat transfer between the tube surface and the fluid occurs by forced convection. The heat transfer coefficient is defined by the standard Nusselt expression

$$h\, d_j/k = 0.0225\, (Re)^{0.8}\, (Pr)^{0.4} \qquad \text{(IV-4)}$$

Effects of transitional flow in the vicinity of the tube entrance on the average heat transfer coefficient for the entire passage are ignored, which leads to conservative values of the heat transfer coefficient calculated from this equation. A more convenient form of equation (IV-4) is obtained by introduction of the friction factor f, which for smooth surfaces is related to the Reynolds number by the expression

$$f = 0.18/(Re)^{0.2} \qquad \text{(IV-5)}$$

Combining equations (IV-4) and (IV-5) yields

$$h = (f/8)(\gamma u\, c_p)/(Pr)^{0.4} \qquad \text{(IV-6)}$$

where γ represents the specific weight of the fluid in pounds per cubic foot and u the flow velocity of the fluid while passing through the tubes.

The heat dissipated to the fluid by forced convection is defined by

$$q_E = (h\, S\, \Delta T_m)_E \qquad \text{(IV-7)}$$

where S represents the inside surface area of all tubes in the equipment component and ΔT_m represents the mean temperature differential of heat transfer between the fluid and the tube surface. With the tube surface specified to be at constant temperature, the mean temperature differential is defined by

$$\Delta T_{mE} = (T_{Ee} - T_{Ei}) \Big/ \ln \left[(T_{Es} - T_{Ei})/(T_{Es} - T_{Ee}) \right] \qquad \text{(IV-8)}$$

The surface area of heat transfer is defined by

$$S_E = \pi d_{Ei} L_E N_E \qquad (IV-9)$$

with L_E representing the tube length and N_E the number of tubes in the equipment component. Also, by heat balance, the heat received by the transfer fluid is related to the flow area, velocity and fluid temperature rise by the equation

$$q_E = 0.785 N_E (d_{Ei})^2 (\gamma u c_p)_E (T_{Ee} - T_{Ei}) \qquad (IV-10)$$

By combining equations (IV-6), (IV-7), (IV-8), (IV-9) and (IV-10), one obtains

$$(f L_E/2d_i)_E = (Pr_E)^{0.6} \ln\left[(T_{Es} - T_{Ei})/(T_{Es} - T_{Ee})\right] \qquad (IV-11)$$

which relates the length parameter of the tubes in the equipment component to the inlet and exit temperatures of the fluid passing through and to the surface temperature of the equipment component. Then, by use of equation (IV-1), equation (IV-11) may be expressed in the form

$$(f L_E/2d_i)_E = (Pr_E)^{0.6} \ln\left[1/(1 - e_E)\right] \qquad (IV-12)$$

This equation serves to define the interrelation of effectiveness of heat exchange and tube length-to-diameter ratio when the heat exchange surfaces are at constant and uniform temperature.

The effectiveness of the equipment component is used extensively as an independent variable of analysis for evaluation of cooling system performance and physical characteristics. In general, high values of effectiveness, above about 0.90, imply equipment cooling design having considerable heat transfer surface in series with the flow, which creates near-maximum heat exchange for the available inlet temperature differential. The effectively long heat transfer passages also result in considerable resistance to flow. Low effectiveness of heat exchange implies relatively short flow passages having low flow resistance and reduced heat transfer capacity. Aircraft equipment items have effectivenesses ranging from 0.2 to, occasionally, above 0.9.

The pressure loss of the fluid across the equipment component is the result of frictional resistance of the flow passages and abrupt contraction and expansion at their entrance and exit, respectively. Assuming the flow to be incompressible, the loss in total pressure across the heat exchanger is defined by

$$(\Delta p^o/\gamma)_E = (u_E^2/2g)\left[K_{Ei} + (1 - \alpha_E)^2 + (fL/d_i)_E\right] \qquad (IV-13)$$

where u_E represents the flow velocity of the fluid during passage through the tubes, K_{Ei} the entrance loss coefficient and $(1-\alpha_E)^2$ the exit loss coefficient, where α_E represents the ratio of the cross-sectional area of flow in the tubes to that in the headers. Typically, K_{Ei}

and α_E have values of 0.25 to 0.35 and 0.4 to 0.5, respectively, so that the sum of the entrance and exit loss coefficients is about 0.6. Equations (IV-13) and (IV-12) may be combined to relate the flow resistance of the equipment component to the effectiveness of heat exchange.

$$(\Delta p^o/\gamma)_E = (u_E^2/2g)\left\{K_{Ei} + (1-\alpha_E)^2 + 2(Pr_E)^{0.6} \ln\left[1/(1-e_E)\right]\right\} \quad \text{(IV-14)}$$

With liquids as the transfer fluid flowing through the equipment component in indirect systems the entrance and exit losses represent a smaller percentage of the flow resistance than for air used in direct systems because of their higher Prandtl number. Typically, for an effectiveness of 80% the entrance and exit losses are about 10 and 20% of the total flow resistance for water and air, respectively.

The flow velocity in the tubes, u_E, is in the above pressure drop relationship basically an independent variable of analysis. Increasing the flow velocity results in heat exchangers of proportionally smaller frontal area and volume but greater flow resistance. Hence, the selection of the flow velocity involves a compromise in design between size and flow resistance. This phase of design must be approached from the equipment design viewpoint with the results being integrated with the effects on cooling system performance, and indicates the importance of integrating equipment cooling design with cooling system design.

The pumping power required to transport the fluid through the equipment component is related to the pressure drop by the equation

$$P_E = w_E(\Delta p^o/\gamma)_E \quad \text{(IV-15)}$$

The cooling capacity of the exchanger may be expressed as

$$q_E = (w\, c_p)_E(T_{Ee} - T_{Ei}) = (w\, c_p)\,(e_E)(T_{Es} - T_{Ei}) \quad \text{(IV-16)}$$

Thus, the power-cooling ratio of the exchanger is

$$PC_E = \Delta p_E^o \Big/ \left[J(c_p \gamma\, e)_E\,(T_{Es} - T_{Ei})\right]$$

or, by use of equation (IV-14)

$$PC_E = \frac{\left[K_{Ei} + (1-\alpha_E)^2 + 2(Pr_E)^{0.6} \ln \frac{1}{1-e_E}\right](u_E)^2}{2gJ(c_p\, e)_E\,(T_{Es} - T_{Ei})} \quad \text{(IV-17)}$$

or

$$(PC_E)\left[\frac{T_{Es}-T_{Ei}}{100}\right]\left[\frac{100}{u_E}\right]^2 = \frac{K_{Ei} + (1-\alpha_E)^2 + 2(Pr_E)^{0.6} \ln \frac{1}{1-e_E}}{501(c_p\, e)_E} \quad \text{(IV-18)}$$

An inspection of equation (IV-18) shows that for typical values of the entrance and exit loss coefficients, the power-cooling ratio of the exchanger is a minimum for effectivenesses in the range of 0.3 to 0.4 for liquids and 0.5 to 0.55 for gases. Although these conditions represent the minimum pumping power required for any required cooling capacity, the optimum condition refers only to the equipment component. The desirable effectiveness for the equipment component, from the standpoint of optimum cooling system design, would generally be greater than these values, since higher effectiveness reduces the required flow rate for the cooling system.

Equations defining the weight and spatial requirements of the equipment component are not included since these parameters are not included in the study of cooling systems. The equipment component is assumed to be an integral part of each equipment or group of equipment items and does not in effect constitute a part of the cooling system in the present study. The long-range integration of equipment cooling design and cooling system design would necessitate detailed consideration of these factors.

Equipment Component Interpretation for Groups of Equipment Items

As discussed in the previous sub-sections, the equipment component consists of a heat exchanger represented in regard to heat transfer by a surface temperature T_{ES} and an effectiveness of heat exchange e_E. Cooling systems, in general, would serve a number of equipment items so that the equipment component must be considered to represent the equivalent of all the individual equipment items. Since the procedure followed in this study is to evaluate cooling system characteristics in terms of equipment component surface temperature and effectiveness, it is necessary to be able to translate this information in terms of the heat transfer characteristics of any group or groups of equipment items. Thus, if the heat transfer characteristics of all equipment items are known, it would be necessary to translate this information in a manner such that an equivalent equipment component is defined having a specified surface temperature, effectiveness of heat exchange and cooling capacity. Oppositely, it would oftentimes be desirable to be able to specify the equivalent in terms of equipment items of any selected combination of equipment component surface temperature, effectiveness and cooling capacity.

Since, in general, the effective temperature for heat transfer varies considerably for different equipment items, a study of this problem has indicated only one general and reliable method for converting from a group of equipment items to an equivalent equipment component, or vice versa. This method is to convert from combinations of inlet temperature and coolant flow rates required to an equivalent combination of surface temperature, effective and inlet temperature. If the cooling requirements for each equipment item are specified by a plot of maximum permissible inlet temperature versus coolant flow rate, the overall mixed

mean temperature rise and required inlet temperature for any flow rate may be specified, since by equation (IV-1)

$$\Delta T_t = e_E (T_{Es} - T_{Ei}), \qquad \text{(IV-19)}$$

the arbitrary selection of any numerical value of either effectiveness or surface temperature will permit definition of the other. Stated in another way, knowledge of the required inlet temperature and the fluid temperature rise is sufficient to define the cooling system characteristics and any combination of effectiveness and surface temperature satisfying equation (IV-19) will suffice. Should all equipment items represented by an equipment component have the same surface temperature, then evaluation of the mixed mean temperature rise ΔT_t and the inlet temperature allows definition of the equipment component effectiveness directly by equation (IV-19), or selection of the effectiveness defines the fluid temperature rise. Best arrangement of the equipment items for any specified overall temperature rise and inlet temperature is not considered in the cooling system study.

Physical characteristics and performance of cooling systems presented in the subsequent sections treat the equipment component on the basis of surface temperature and effectiveness as independent variables. In order to interpret these data in terms of required inlet temperature and flow rates, values of the equipment component's inlet temperature are presented. Then, the mixed mean temperature rise may be defined by use of equation (IV-19), and the corresponding required flow rate by heat balance.

REFERENCES

VI-1 Report of Advisory Committee for Aircraft Equipment Cooling Systems, 2 March 1953 - 17 April 1953, R. O'Clock, Major, USAF, Chairman, Wright Air Development Center, Wright-Patterson Air Force Base, Ohio.

SECTION V

THE DISTRIBUTION COMPONENT

The distribution component of a direct cooling system represents the distribution lines for the supply of the ultimate coolant to equipment components. The distribution component of an indirect cooling system represents the flow system used for circulation of a transfer fluid between the equipment components and the intermediate component. In the present study, for the types of cooling systems considered and because of the use of the equipment component to represent the equipment items, the use of the distribution component is almost exclusively associated with indirect cooling systems. Thus, the use of a distribution component implies a cooling system consisting of an ultimate component, using either a liquid or air as the ultimate fluid, a heat exchanger serving as the intermediate component between the transfer and ultimate fluids, and a distribution component conveying the transfer fluid between the intermediate component and the equipment component representing the various equipment items.

The distribution component, when used as a flow system for circulation of a transfer fluid between equipment components and an intermediate component, may have physical characteristics of widely varying nature, depending upon cooling system variables such as (1) equipment heat load, (2) equipment surface temperature, (3) effectiveness of heat exchange at equipment heat transfer surfaces, (4) type of transfer fluid, (5) dispersion of heat loads throughout the aircraft, and (6) the piping arrangement selected for transfer of the fluid to and from the equipment components. Because of the multiplicity of possible flow arrangements of a transfer system and the operational conditions of the equipment components, and because of the influence the designer as an individual can have on the physical characteristics of a component of this type, it is desirable to simulate the distribution component by analytical models. The objective of constructing such models would be to reduce complex flow systems to simplified networks which are amenable to rational analysis. The simulating models should be analytically designed to permit the maximum generalization of all variables influencing the characteristics of the distribution component. The following generalizations, which are believed representative of real distribution components, can be made to permit this type of study.

All transfer lines (a transfer line consists of a supply header and a return header) can be visualized as consisting of starting sections and operating sections. A starting section in a transfer line serves to transport the cooling fluid between the intermediate component and the general vicinity within the aircraft at which the cooling fluid is used for cooling of equipment items. Within the starting section, fluid is not removed from or returned to either supply or return headers. Hence, the physical characteristics remain essentially constant, regardless of the operational conditions or the distance necessary for transport of

the fluid. The operating section of the transfer line is defined as those parts of the distribution component where fluid is removed from the supply header, passes through heat exchangers simulating equipment items, and is received by the return header for transport to the intermediate component. The length of the starting section relative to the length of the operating section of any transfer line depends upon the relative location of the intermediate component and the dispersion of equipment items selected to be served by any cooling system, whether individualized or centralized in basic design.

The operating section of a transfer line is generalized by introducing as an independent variable the gradient with respect to flow distance of the local cooling capacity divided by the product of the local effectiveness of heat exchange and the local difference in temperature of the equipment heat transfer surfaces and the transfer fluid. This gradient then serves to define the local gradients of flow output from the supply header and flow input to the return header. The gradient may be assigned various functional relationships with respect to distance, which thereby permits simulation of any type continuous liquid removal rates that would be required of arbitrarily arranged cooling loads along the transfer line. Furthermore, the assigned gradient can be interpreted to represent any combination of cooling capacity, effectiveness and surface-to-fluid temperature differential that might be associated with an equipment item.

With an analytical model so constructed, the general characteristics of the operating and starting section may be defined, and the results would be employed to define the characteristics of the transfer system serving any arbitrarily selected group of equipment items. The methods for selecting optimum transfer line sizes in relation to the overall penalty imposed on the aircraft must be defined. Thereafter, the penalty on aircraft performance resulting from the distribution component may be defined.

Nomenclature

Symbol	Concept	Dimensions
A	flow area	square feet
B	a parameter	dimensionless
c_p	specific heat at constant pressure	Btu per pound-^{o}R
Dr	drag	pounds
e	effectiveness of heat exchange	dimensionless
f	Darcy friction factor	dimensionless
K	flow resistance coefficient	dimensionless
kw	cooling rate	kilowatts
L	length	feet
Lf	lift of aircraft	pounds
p	pressure	pounds per square foot, abs.
P	power	Btu per hour

Symbol	Concept	Dimensions
q	heat rate	Btu per hour
Re	Reynolds number	dimensionless
SFC	thrust specific fuel consumption	pounds per hour-pound thrust
sg	specific gravity, referred to 62.4 pounds per cubic foot	dimensionless
t	thickness	feet
T	temperature	^{o}R
u	flow velocity	feet per second
V	volume	cubic feet
w	fluid flow rate	pounds per hour
W	weight	pounds
x	distance along tube	feet
X	ratio of fuel load at take-off to gross weight of aircraft	dimensionless
y	length parameter	dimensionless
α	area ratio or parameter	dimensionless
β	parameter	dimensionless
γ	specific weight	pounds per cubic foot
μ	viscosity, absolute	pound-seconds per square foot
η	component efficiency	dimensionless
φ	parameter	

Subscript	Refers to
d	constant-diameter header
D	distribution component
dp/dx	constant-pressure-gradient header
E	equipment component
ex	external
F	fitting
g	gross weight
i	inlet or internal
I	intermediate component
op	operating section
opt	optimum value
p-sy	power supply system
ref	reference value
s	surface
sh	shaft power
st	starting section
sy	cooling system
t	transfer fluid
u	constant-velocity header
U	ultimate component
o	base value or inlet station of operating section
1	exit of supply header in operating section
2	inlet of return header in operating section
3	exit of return header in operating section

Superscript	Refers to
"	unit of inches
o	total or stagnation conditions
'	power in horsepower or to partial value of any parameter
m	exponent
n	exponent
p	exponent

Physical Characteristics of Transfer Lines

When employing liquid transfer fluids in cooling systems it would not be desirable to pressurize the fluid more than is required to overcome the frictional resistance of the flow circuit. Hence, the maximum internal line pressure for most transfer systems would be in the range from a few pounds per square inch to several hundred pounds per square inch. Within this pressure range, medium and low pressure hydraulic tubing probably would be employed to convey the liquid transfer fluid.

Standards of wall thickness of aluminum, steel and copper hydraulic tubing were surveyed to determine variations with standard tube size, defined by external diameter. A maximum internal pressure of 500 pounds per square inch was considered. Wall thicknesses were defined on the basis of Class I use, according to the Joint Industrial Committee for Hydraulic Standards and on the basis of standard Class A aircraft service in which a working safety factor of four is utilized. The results of this survey are shown in Figure V-1, where wall thickness is plotted as a function of external tube diameter for standard sizes in various materials. It is intended that the curve shown on this graph be used for evaluation purposes to define wall thickness as a function of tube external diameter. Inasmuch, however, as results of cooling system studies have yielded optimum line diameters of less than 1 inch for nearly all design conditions, it is assumed in the following that the wall thickness is constant and equal to 0.038 inch for the general range of tube sizes from 1/8 to 1 inch. The wall thickness variation with diameter described by the curve in Figure V-1 is defined by the equation

$$t_D^{"} = 0.03\left[1 + (1/3)(d_{D-ex}^{"})^2\right] \qquad (V-1)$$

so that the internal diameter is defined by

$$d_{Di}^{"} = d_{D-ex}^{"}\,(1 - 0.02\, d_{D-ex}^{"}) - 0.06 \qquad (V-2)$$

and the weight per foot of tubing by

$$W_{D\text{-tubing}}/L_D = (\text{constant})\left[d_{D-ex}^{"} - 0.03 - 0.02(d_{D-ex}^{"})^2 + (1/3)(d_{D-ex}^{"})^3(1 - 0.01\, d_{D-ex}^{"})\right] \qquad (V-3)$$

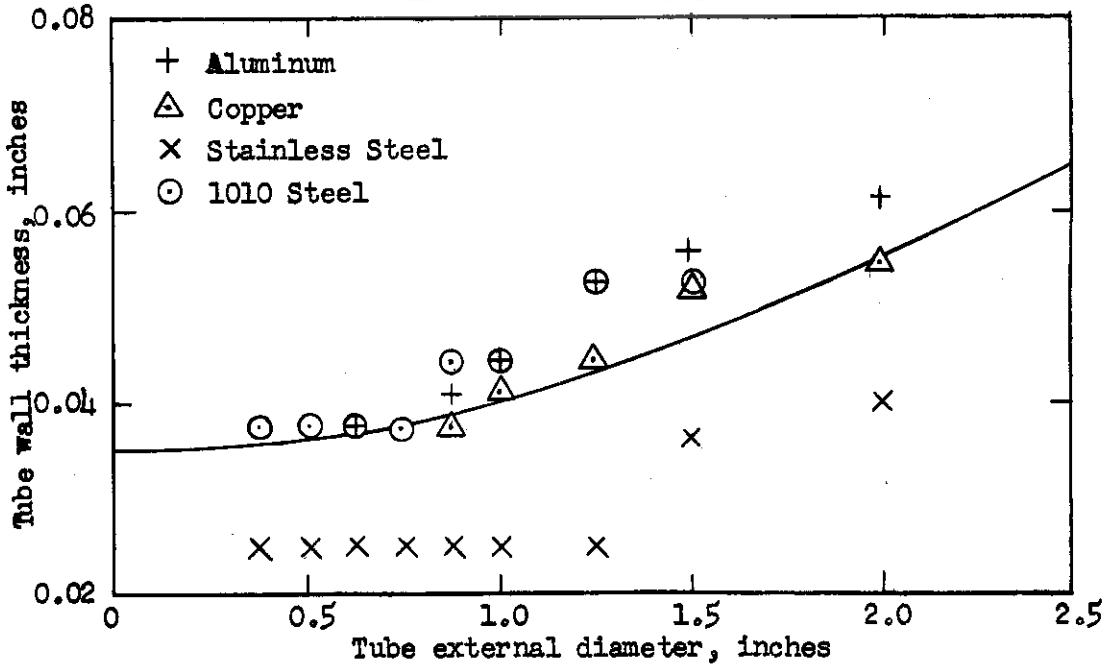

Figure V-1. Wall thickness of medium- and low-pressure tubing.

where the constant is equal to 0.110 for aluminum, 0.318 for steel and 0.363 for copper. If a constant wall thickness of 0.038 inch is assumed for the tube diameter range below about 1 inch, then the weight per foot of aluminum tubing is defined by

$$W_{D\text{-tubing}}/L_D = 0.140(d''_{D\text{-ex}} - 0.038) = 0.140(d''_{Di} + 0.038) \qquad (V\text{-}4)$$

The weight of standard aircraft fittings has been studied to establish their weight variation with size. The results are illustrated in Figure V-2 for aluminum fittings. In the general study of distribution components it is not possible to specify the number and various types of fittings used. Therefore, it is assumed that the weight of fittings is 25% of the line weight, which for an average line diameter of 0.50 inch is the equivalent of about one fitting to every 3 feet of line. Probably, this factor of 25% would be somewhat low for most operating sections and high for starting sections of distribution components, but may be considered as a representative value for an average distribution component. The weight of the distribution component per foot is defined, therefore, by

$$W_D/L_D = 0.175(d''_{D\text{-ex}} - 0.038) = 0.175(d''_{Di} + 0.038) \qquad (V\text{-}5)$$

based on aluminum as the material and a constant value for the wall thickness of 0.038 inch.

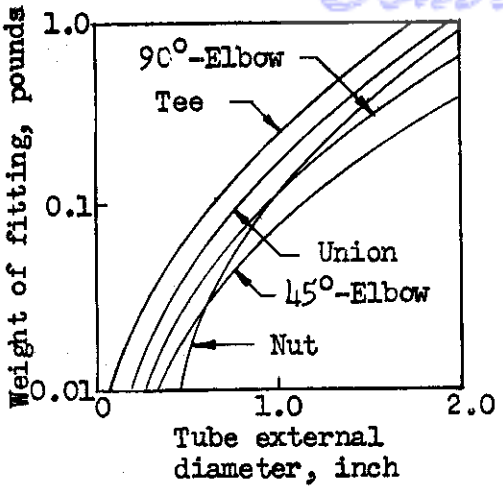

Figure V-2. Weight of standard aluminum aircraft fittings.

Energy Balance and Circulation Rate of Transfer Fluid

The flow circuit of the distribution component serving an indirect system between the equipment and intermediate components is illustrated schematically in Figure V-3. For purposes of simplifying analysis and evaluation, all equipment items are assumed to have their individual equipment heat exchangers represented by a single exchanger having a surface temperature T_{ES} and an effectiveness of heat exchange e_E, as discussed in Section IV. The transfer fluid is circulated through the distribution component by a pump. The location of the pump does not appear to be critical. In respect to heat transfer, the pump is best lo-

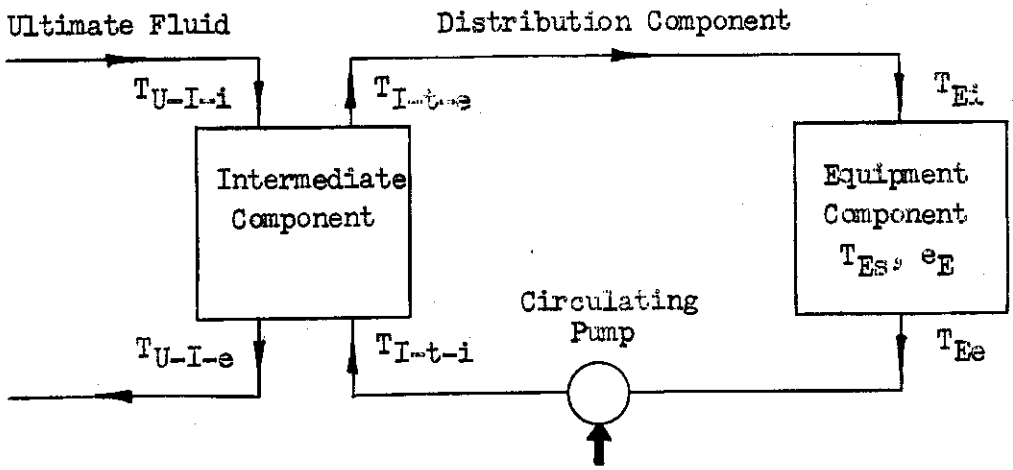

Figure V-3. Schematic arrangement of the distribution component in relation to equipment and intermediate components for indirect cooling systems.

cated immediately ahead of the intermediate component since any temperature rise of the fluid created by the pump would increase the temperature potential of the exchanger and, thereby, serve to minimize the effect of this temperature rise on the average temperature level of the transfer fluid in the distribution component. Oppositely, however, from the viewpoint of minimizing the required base pressure level of the transfer fluid, the pump would be best located immediately ahead of the equipment component. This would provide a pressure level sufficient to prevent boiling of the transfer fluid in the high-temperature region of the system, while operating the system at the lowest base pressure possible. Ordinarily, neither of these effects have been found to be important and are ignored in the evaluation procedures for the distribution component.

The transfer fluid enters the equipment component at the temperature T_{Ei}, which is assumed equal to the temperature of the transfer fluid at exit of the intermediate component, T_{I-t-e}, and leaves the equipment component at the mixed mean temperature T_{Ee}. Since any temperature rise of the transfer fluid across the circulation pump is assumed to be negligible, the temperature of the transfer fluid at entrance to the intermediate component, T_{I-t-i}, is equal to the mixed mean temperature T_{Ee}. Assuming no heat loss or gain in the distribution component between the equipment and intermediate components, the heat transfer rate in the intermediate component from the transfer fluid to the ultimate fluid is equal to the heat transfer rate in the equipment component and represents the cooling capacity of the system. The temperature of the ultimate fluid at inlet to the intermediate component is represented by T_{U-I-i} and at exit by T_{U-I-e}. The overall temperature potential for the equipment, distribution and intermediate components is the difference between the equipment component surface temperature, T_{Es}, and the temperature of the ultimate fluid at inlet to the intermediate component, T_{U-I-i}. By establishing analytically the distribution component characteristics as a function of this overall temperature difference, the physical characteristics and performance requirements of the distribution component may be integrated conveniently into the overall evaluation of cooling systems.

Since the transfer fluid flow rate through the equipment component is equal to that through the intermediate component, and the heat transfer rates in both components are assumed equal, heat balance between the two components yields

$$c_{p-t-E}(T_{Ee} - T_{Ei}) = c_{p-t-I}(T_{I-t-i} - T_{I-t-e}) \qquad (V-6)$$

The mean temperature level of the transfer fluid is the same for both components and the pressure level is essentially the same so that the numerical values of c_{p-t-E} and c_{p-t-I} are extremely close to being equal. Thus,

$$T_{Ee} - T_{Ei} = T_{I-t-i} - T_{I-t-e} \qquad (V-7)$$

The effectiveness of the equipment component is defined by

$$e_E = (T_{Ee} - T_{Ei})/(T_{Es} - T_{Ei}) \qquad (V-8)$$

and the effectiveness on the transfer fluid side of the intermediate component by

$$e_{I-t} = (T_{I-t-i} - T_{I-t-e})/(T_{I-t-i} - T_{U-I-i}) \qquad (V-9)$$

The temperature rise of the transfer fluid in the equipment component is, then

$$T_{Ee} - T_{Ei} = e_E(T_{Es} - T_{Ei})$$

and in the intermediate component

$$T_{I-t-i} - T_{I-t-e} = e_{I-t}(T_{I-t-i} - T_{U-I-i})$$

so that

$$\left[(T_{Ee}-T_{Ei})/e_E\right] + \left[(T_{I-t-i}-T_{I-t-e})/e_{I-t}\right] = T_{Es}-T_{Ei}+T_{I-t-i}-T_{U-I-i}$$

which by use of equation (V-7) reduces to

$$(T_{Ee} - T_{Ei})\left[(1/e_E) + (1/e_{I-t}) - 1\right] = T_{Es} - T_{U-I-i} \qquad (V-10)$$

and defines the temperature rise of the transfer fluid across the equipment component, or the temperature drop of the transfer fluid across the intermediate component, as a function of the overall temperature differential for the equipment distribution and intermediate components. The ratio of the temperature change of the transfer fluid to the maximum temperature change theoretically possible is defined by equation (V-10) as

$$(T_{Ee} - T_{Ei})/(T_{Es} - T_{U-I-i}) = 1\Big/\left[(1/e_E) + (1/e_{I-t}) - 1\right] \qquad (V-11)$$

Numerical values of this ratio are presented in Figure V-4 for a range of effectiveness of the equipment component and the transfer fluid side of the intermediate component. Effectivenesses of 70% for both components result in only a little more than one-half of the temperature potential actually being used for heat dissipation purposes. Effectivenesses of 90% result in about 82% of the temperature potential being used.

The required circulation rate of the transfer fluid may be defined by heat balance, which for the equipment component is

$$3413 \text{ kw} = w_{Dt}\, c_{p-t}\, (T_{Ee} - T_{Ei}) \qquad (V-12)$$

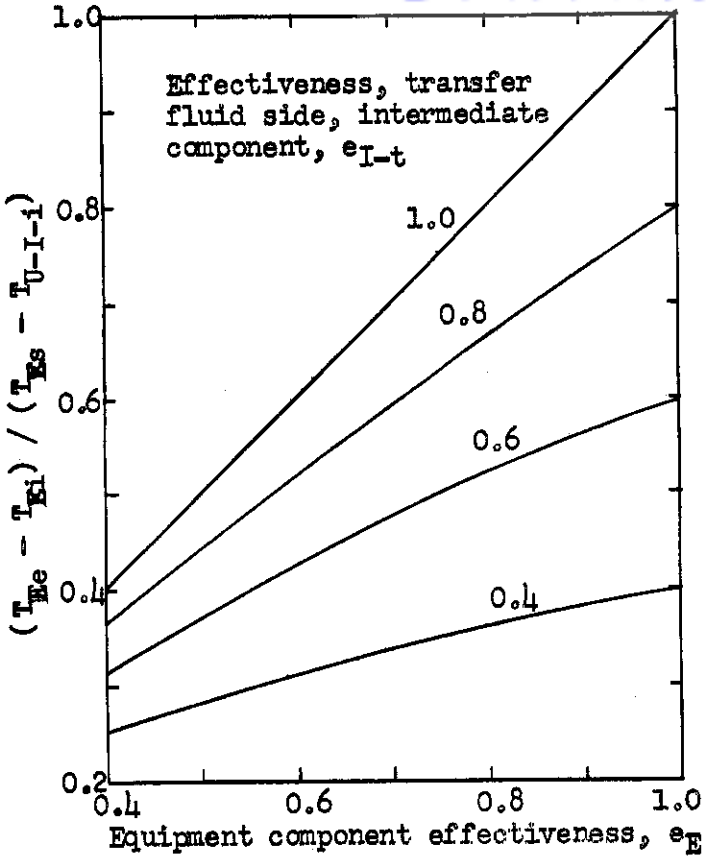

Figure V-4. Fraction of overall temperature potential used by transfer fluid for heat dissipation purposes.

where kw represents the cooling capacity of the system expressed in kilowatts and w_{Dt} the transfer fluid flow rate in pounds per hour. A generalization of equation (V-12) may be obtained by combining it with equation (V-11). This yields

$$w_{Dt}/kw = 3413 \left[(1/e_E) + (1/e_{I-t}) - 1\right] \Big/ \left[c_{p-t}(T_{Es} - T_{U-I-i})\right] \qquad (V-13)$$

or,

$$\frac{w_{Dt}}{kw} (c_{p-t}) \frac{T_{Es} - T_{U-I-i}}{100} = 34.13 \left[(1/e_E) + (1/e_{I-t}) - 1\right] \qquad (V-14)$$

The bracketed term on the right-hand side of this equation is equal to the reciprocal of the ordinate in Figure V-4, so that the required circulation rate for the transfer fluid may be estimated readily by use of this relationship.

Flow Resistance and Pumping Power

Pressure loss of the transfer fluid flowing in the distribution component proper results from flow resistance imposed by the transfer line and its fittings. The overall pressure loss for the entire distribution component circuit results from the transfer line, the fittings, the transfer fluid side of the intermediate component and the equipment component. The pressure gradient in the transfer line proper may be evaluated by application of the standard Darcy head-loss equation.

$$dp^{o}_{Dt}/dL_D = (f\gamma)_{Dt} (u^2_{Dt})/2g\, d_{Di} \qquad (V\text{-}15)$$

Since, by continuity

$$w_{Dt} = 3600\, (A\gamma u)_{Dt} \qquad (V\text{-}16)$$

and the specific gravity of the transfer fluid is

$$sg_{Dt} = \gamma_{Dt}/62.4 \qquad (V\text{-}17)$$

equation (V-15) may be rearranged to the form

$$dp^{o}_{Dt}/dL_D = f_{Dt}(w_{Dt}/100)^2/(12.9\, d^{m5}_{Di}\, sg_{Dt}) \qquad (V\text{-}18)$$

For constant-diameter transfer lines and when the transfer fluid is a liquid, equation (V-18) may be integrated directly since the pressure gradient will be constant along the tube. The resulting equation where pressure drop is expressed in pounds per square inch is

$$\Delta p^{om}_{Dt} = f_{Dt} L_D (w_{Dt}/1000)^2/(18.6\, d^{m5}_{Di}\, sg_{Dt}) \qquad (V\text{-}19)$$

The Darcy friction factor f_{Dt} is a function of the Reynolds number of flow and, if the flow is turbulent, also of the relative roughness of the tube surface. The Reynolds number of flow is defined by

$$Re = \gamma u\, d/(g\mu)$$

which may be rearranged to the more convenient form

$$Re_{Dt} = 0.132(w_{Dt}/1000)/(d^{m}_{Di}\, \mu_{Dt}) \qquad (V\text{-}20)$$

where the viscosity of the transfer fluid μ_{Dt} is expressed in the units of pound-seconds per square foot. The relative roughness of the tubing would be, typically, defined by 0.6×10^{-4} divided by the internal diameter of the tube expressed in inches. The Darcy friction factor for any combination of Reynolds number and relative roughness is defined by use of the standard Moody friction factor chart. In most distribution components it appears that the Reynolds number varies approximately in the range from 5000 to 100,000. Within this range the friction factor is

defined quite accurately by

$$f_{Dt} = 0.18/Re_{Dt}^{0.2} \tag{V-21}$$

or by use of equation (V-20)

$$f_{Dt} = 0.270(d_{Di}^{m}\,\mu_{Dt})^{0.2}/(w_{Dt}/1000)^{0.2} \tag{V-22}$$

Flow resistance of tube fittings, such as elbows, unions and tees, were studied and have been correlated by the following equations.

For a 90°-elbow,

$$\Delta p_{Dt}^{om} = 0.0058(sg_{Dt}/d_{D-ex}^{m\,3.95})(7.2w_{Dt}/sg_{Dt})^{(1.75-0.0074/d_{D-ex}^{m\,2.4})} \tag{V-23}$$

For a union,

$$\Delta p_{Dt}^{om} = 0.00021(sg_{Dt}/d_{D-ex}^{m\,5})(7.2w_{Dt}/sg_{Dt})^{(1.8+0.17d_{D-ex}^{m})} \tag{V-24}$$

For straight-through flow in a tee,

$$\Delta p_{Dt}^{om} = 0.00064(sg_{Dt}/d_{D-ex}^{m\,5})(7.2w_{Dt}/sg_{Dt})^{(1.8+0.17d_{D-ex}^{m})} \tag{V-25}$$

For 90°-flow in a tee,

$$\Delta p_{Dt}^{om} = 0.0046(sg_{Dt}/d_{D-ex}^{m\,4.4})(7.2w_{Dt}/sg_{Dt})^{(1.83+0.19d_{D-ex}^{m})} \tag{V-26}$$

For evaluation of cooling systems in general it is not practical to specify the type and number of fittings. Thus, the procedure in the general study has been to increase the line pressure loss by 25% to account for the loss due to fittings.

The pumping power in horsepower required to transport the fluid through the distribution component is related to the overall distribution component pressure drop expressed in pounds per square inch, transfer fluid specific gravity and flow rate in pounds per hour by the equation

$$P_{Dt}' = (w_{Dt}/1000)(\Delta p_{Dt}^{om})/(858\ sg_{Dt}) \tag{V-27}$$

This relationship defines the output power required of the circulation pump in the distribution component, assuming an incompressible fluid as the transfer fluid.

Power Supply System

The power supply system includes all equipment, such as lines, controls and power transmission equipment in general, necessary to transmit power from the aircraft's propulsion plant or an auxiliary powerplant

to the point of power application in the cooling system. Shaft power for cooling systems is needed for circulation of transfer fluids in the distribution component, for driving blowers, or for driving the compressor in vapor cycle refrigeration machines. A general review of power supply systems for aircraft indicates that, for those systems utilizing shaft power extraction from a main powerplant, the weight per delivered horsepower to a driving device is in the range of from 5 to 10 pounds. On this basis of weight definition it is not assumed that a separate power supply system would be installed for the cooling system, but rather that the power would be supplied through a power supply system, or systems, for the aircraft in general. An estimation of the weight of a pneumatic power supply system is placed in the range of from 1 to 6 pounds per shaft horsepower delivered by the air turbine.

For the distribution component, the power supply system must provide to the transfer fluid the pumping power necessary to circulate the transfer fluid at the specified flow rate. Inasmuch as the power requirements for this purpose are normally relatively low, it is assumed that the weight of the power supply system for circulating the transfer fluid is defined by

$$W_{p-sy} = 20\, P'_{Dt} \quad \text{for} \quad P'_{Dt} > 0.25 \tag{V-28}$$

and

$$W_{p-sy} = 5 \quad \text{for} \quad P'_{Dt} < 0.25 \tag{V-29}$$

The weight is assumed to be 20 pounds per output horsepower of the driving device for powers greater than 0.25 horsepower, which would correspond to the previously stated weight of 10 pounds per horsepower delivered to the driving device if the overall efficiency of the driving device is 50%. For power requirements below 0.25 horsepower, equation (V-29), it is assumed that a minimum representative weight for the entire power supply system, which includes the pump and drive motor, would be about 5 pounds. The pumping power P'_{Dt} for the distribution component in equations (V-28) and (V-29) is defined by equation (V-27). The procedure established by equations (V-28) and (V-29) is recommended for use only when the power requirements are relatively small and is not employed, for example, in connection with vapor cycle refrigeration systems.

The shaft power extraction from the aircraft powerplants P'_{sh} necessary to provide a pumping power P'_{Dt} is defined by

$$P'_{sh} = P'_{Dt} / \eta_{p-sy} \tag{V-30}$$

where η_{p-sy} represents the overall efficiency of the power supply system from the point of extraction from the powerplant to the point of delivery to the transfer fluid. In the analysis of distribution components it is assumed, because of the relatively low power requirements, that the efficiency of the power supply system is about 33.3%, so that

$$P'_{sh} = 3\,P'_{Dt} \qquad (V\text{-}31)$$

Generalized Representation of Operating Section

The operating section of the distribution component consists of the transfer line from the point of initial fluid removal to the point of final fluid return. It is assumed that within the operating section the distribution component is arranged in the form of supply and return headers and cross-over lines, the latter permitting fluid removed from the supply header to pass through equipment items to the return header. A schematic arrangement of the operating section is shown in Figure V-5. Each equipment item or group of equipment items connected in series is served by a cross-over line interconnecting the supply and return headers. The supply and return headers are assumed to be of equal length L.

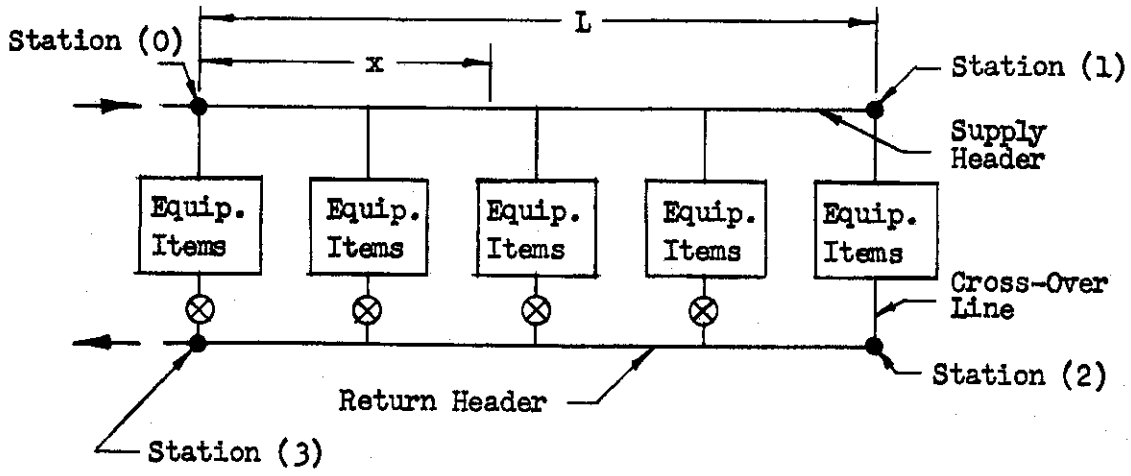

Figure V-5. Schematic arrangement of the operating section assumed for general analysis of the flow and physical characteristics of the distribution component.

The distance to any point along the supply header, measured from the point of initial fluid removal, is designated by x. It is assumed that the pressure differential between adjacent points of the supply and return headers is greater than the flow resistance of the equipment items placed between these points, so that the overall pressure drop of the operating section equals the pressure drop in the supply and return headers plus the pressure drop of the last group of equipment items and cross-over line.

The actual fluid removal rate at various points along the supply header is a function of the required cooling capacity, the effectiveness of heat exchange and the desired temperature level of the equipment component, and the initial temperature of the transfer fluid. In an effort to simulate the actual rate of fluid removal and return to the headers by a working model amenable to rational analysis, it is assumed for purposes of analysis that the fluid is continuously removed and returned at

all points of the supply and return headers. There exists, then, at all points along the headers a gradient of fluid removal and return with respect to the flow distance. The gradient of fluid removal and return at any point along the headers is defined by the gradient, with respect to distance, of the local cooling capacity divided by the product of the local effectiveness of heat exchange, specific heat and the local difference in temperature of the equipment heat transfer surfaces and the transfer fluid. In equation form the fluid removal and fluid return gradient is defined by

$$\frac{dw_{Dt}}{dx} = \frac{d}{dx}\left[\frac{q_E}{c_{p-t}\, e_E (T_{E-s} - T_{D-t-i})}\right] \qquad (V-32)$$

The gradient may be assigned various functional relationships with respect to flow distance to permit simulation of any type of continuous liquid removal rate that would be required by arbitrarily arranged cooling loads along the transfer line.

In order to develop the assumed generalization of fluid removal rate into a working equation which may be employed for general analysis of the operating section, the case of constant gradient of fluid removal is first considered. Suppose the groups of equipment items served by the operating section are all thermally equivalent so that each group requires the same flow rate of transfer fluid to accomplish the desired cooling. Therefore, the rate of fluid removal and return will be the same at all points along the headers and the gradient of fluid removal with respect to flow distance will be constant. The total flow rate which has been removed from the supply header at any distance x relative to the total flow rate removal for the entire supply header is, then

$$(w_{D-t-o} - w_{D-t-x})/(w_{D-t-o} - w_{D-t-l}) = x/L \qquad (V-33)$$

where w_{D-t-o} represents the transfer fluid flow rate at entrance to the operating section and w_{D-t-l} the transfer fluid flow rate at the end of the supply header. By rearrangement of equation (V-33), the ratio of the flow rate remaining in the header at any distance x relative to the initial flow rate for the case of constant gradient of fluid removal is defined by

$$(w_x/w_o)_{D-t} = 1 - \left[1 - (w_1/w_o)_{D-t}\right](x/L).$$

Since, in general, the characteristics of the equipment items may not dictate the use of a constant gradient of fluid removal and return, the equation may be modified to the more general form of

$$(w_x/w_o)_{D-t} = 1 - \left[1 - (w_1/w_o)_{D-t}\right](x/L)^n \qquad (V-34)$$

where the exponent n may be assigned various values to characterize various types of fluid removal along the header. The flow rate ratio

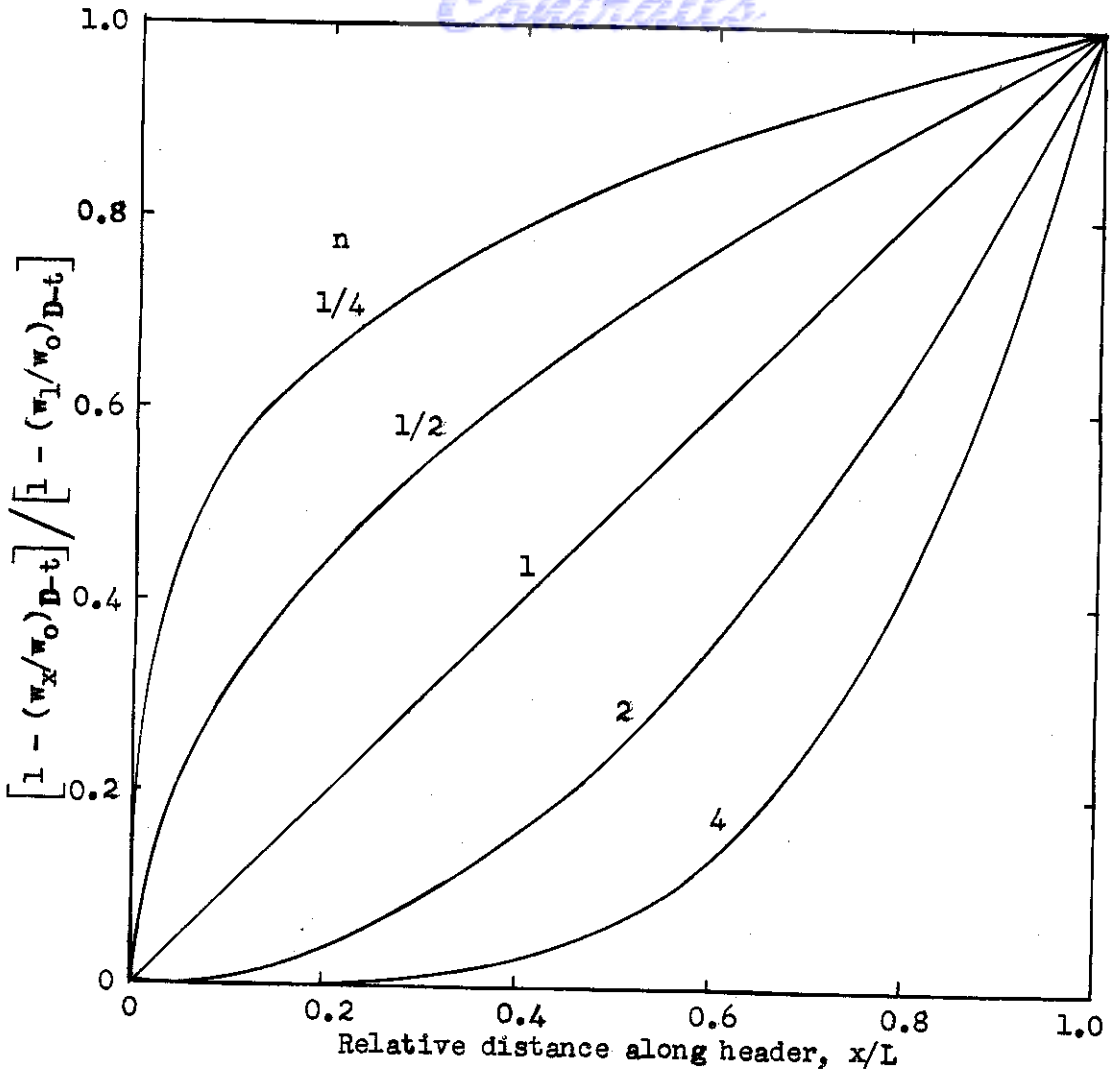

Figure V-6. Generalized representation of fluid extraction and return in the supply and return headers of the operating section in a distribution component. Equation (V-34).

$(w_1/w_o)_{Dt}$ is referred to as the terminal flow rate ratio of the operating section. Various types of fluid removal gradients are shown in Figure V-6, which represents a generalized plot of equation (V-34). The ordinate of the plot defines the fraction of the total fluid removed at any distance along the header. The difference of the ordinate value from unity defines the fraction of the total fluid removed which remains in the header at any distance. For example, with an exponent n of 2 and at a point midway along the supply header, i.e., x/L is 0.5, 25% of the total fluid removal has occurred. Between the middle and end of the supply header the remaining 75% of the total fluid extraction will occur. Thus, in general it would be possible to select an appropriate value of the exponent n to characterize the actual fluid removal gradients existing with any given set of equipment items and locations.

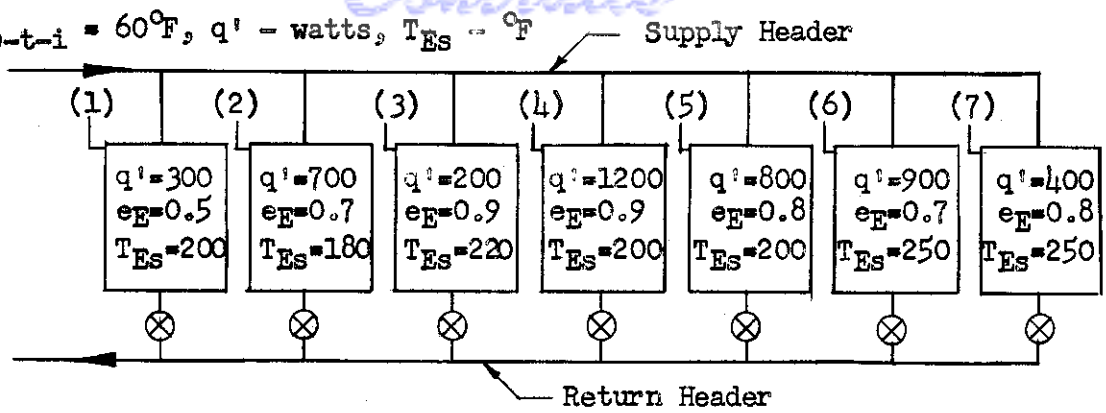

Figure V-7. An assumed group of equipment items served by the operating section of a distribution component, illustrating the selection of the characteristic exponent n. See equation (V-34).

The use of this generalized procedure may be illustrated by assuming a group of equipment items as shown in Figure V-7. The required cooling capacity, required temperature level, and effectiveness of heat exchange are specified for each equipment item. It is assumed that the equipment items are equally spaced along the headers and that the initial transfer fluid temperature is 60°F. By application of energy balance to the transfer fluid passing through an equipment component, the flow rate required by an equipment item is defined by

$$w_{D-t-E} = \text{const. } q' \Big/ \left[e_E (T_{E-s} - T_{D-t-i}) \right]$$

or, the total fluid removal up to any distance x along the header is defined by

$$w_{D-t-o} - w_{D-t-x} = \text{const. } \Sigma q' \Big/ \left[e_E (T_{E-s} - T_{D-t-i}) \right]$$

where the summation process is carried out for all equipment items served by the header up to the point along the header under consideration. From the data shown in Figure V-7, the total flow rate removal along the header may be calculated. The resulting distribution of flow rate removal is presented in Figure V-8 on a generalized basis as defined by equation (V-34). The terminal flow rate $(w_1/w_o)_{Dt}$ is assumed to be zero. The solid line in Figure V-8 corresponds to an exponent n of unity, and is seen to be representative of the fluid extraction gradients. Thus, it might be assumed for these data that the operating section can be described or represented by continuous linear fluid removal and return from the supply header to the return header.

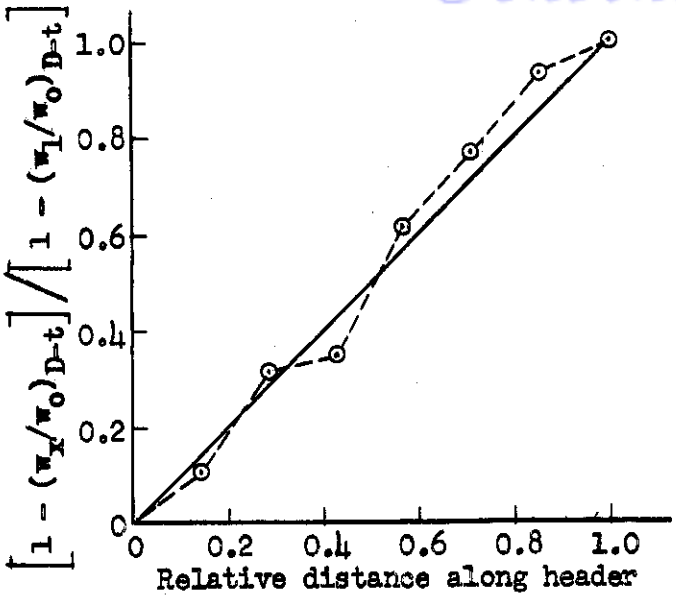

Figure V-8. Generalized representation of fluid extraction and return for selection of the characteristic exponent n.

Generalized Analysis of Flow Resistance and Weight of Operating Section

Since the fluid extraction and return in the headers is assumed continuous, the flow within the header is related to the flow velocity and flow area by the continuity equation for incompressible flow.

$$w_{D-t-x} = \gamma_{D-t}\, u_{D-t-x}\, A_{D-t-x} \tag{V-35}$$

or, by use of equation (V-34)

$$1 - By^n = (u_{D-t-x}/u_{D-t-o})(A_{D-t-x}/A_{D-t-o}) \tag{V-36}$$

where

$$B = 1 - (w_1/w_o)_{D-t} \tag{V-37}$$

and

$$y = x/L. \tag{V-38}$$

The parameter B defines the fractional removal of the total flow, equal to the difference of unity and the terminal flow rate ratio, and the parameter y defines the relative distance along the supply header.

Assume, for purposes of convenience in analysis, that the velocity distribution is defined by

$$(u_{D-t-x}/u_{D-t-o}) = (1 - By^n)^{1-m} \tag{V-39}$$

where m is a parameter of analysis having a numerical value dependent upon the type of header design. Thus, by combining equations (V-36) and (V-39), a generalized flow area equation is obtained, which is

$$(A_x/A_o)_{D-t} = (1 - By^n)^m. \qquad (V-40)$$

The total pressure gradient due to flow resistance at any point along the header is defined by the Darcy head-loss equation

$$(dp^o/dx)_{D-t} = -(\gamma f u_x^2/2gd_{x-i})_{D-t} \qquad (V-41)$$

which may be rearranged to the form

$$(dp^o/dx)_{D-t} = -(u_o^2 f_o/2gd_{o-i})_{D-t}(u_x/u_o)^2_{D-t}\left[\frac{d_{o-i}}{d_{x-i}}\right]_{D-t}\left[\frac{f_x}{f_o}\right]_{D-t} \qquad (V-42)$$

By use of equations (V-39) and (V-40), equation (V-42) reduces to

$$(dp^o/dx)_{D-t} = -(\gamma u_o^2 f_o/2gd_{o-i})_{D-t}(f_x/f_o)_{D-t}(1 - By^n)^{2-2.5m}$$

or,

$$(p_o^o - p_1^o)_{D-t} = \left[\frac{\gamma u_o^2 f_o}{2gd_{o-i}}\right]_{D-t} \int_o^L \left(\frac{f_x}{f_o}\right)_{D-t}(1 - By^n)^{2-2.5m}\, dx \qquad (V-43)$$

Letting

$$\alpha_o = \gamma u_o^2 f_o/2g \qquad (V-44)$$

and introducing equation (V-38), the generalized flow resistance equation for the supply header becomes

$$(p_o^o - p_1^o)_{D-t} = \frac{\alpha_o L_{o-1}}{d_{D-i-o}} \int_o^1 (f_x/f_o)_{D-t}(1 - By^n)^{2-2.5m}\, dy \qquad (V-45)$$

Experience in evaluating the flow characteristics of distribution components has shown that the optimum flow rates in the transfer lines are within the turbulent region for every case considered. Thus, the variation of the friction factor, f_x, along the header is never great. The internal surfaces of the transfer lines may be assumed to be hydraulically smooth, so that the variation of the friction factor may be expressed by the relationship

$$(f_x/f_o)_{D-t} = (Re_o/Re_x)^{0.2}_{D-t} \qquad (V-46)$$

Introducing into this expression the generalized equations for header flow area and flow rate, equations (V-34) and (V-40), yields

$$(f_x/f_o)_{D-t} = (1 - By^n)^{-0.2+0.1m} \qquad (V-47)$$

and the generalized flow resistance equation (V-45) for smooth tubes may be rearranged to the form

$$(p_o^o - p_1^o)_{D-t} = \frac{\alpha_o L_{o-1}}{d_{D-i-o}} \int_o^1 (1 - By^n)^{1.8-2.4m}\, dy \qquad (V-48)$$

The generalized flow resistance equation for the case of constant friction factor reduces from equation (V-45) to

$$(p_o^o - p_1^o)_{D-t} = \frac{\alpha_o L_{o-1}}{d_{D-i-o}} \int_o^1 (1 - By^n)^{2-2.5m}\, dy \qquad (V-49)$$

Thus, the flow characteristics are generalized in terms of the exponents n and m. Various values of the exponent n characterize various fluid removal gradients from the header while values of the exponent m characterize the type of header design. Table V-1 summarizes the types of header design dependent upon the selection of the value of the exponent m.

Table V-1. Relation of Type of Header Design to Exponent m.

Type of header design	Exponent m
Constant diameter	0
Constant flow velocity	1.0
Constant pressure gradient	0.75 (smooth tubes), 0.80 (constant friction factor)
Increasing diameter, $d(d_{x-i})/dx = (+)$	< 0
Increasing flow velocity, $du_x/d_x = (+)$	> 1

It is assumed, rather arbitrarily, that because of the flow disturbances due to fluid removal or return and because of the increasing relative roughness of the tube surface along the header when the diameter is reduced, a constant friction factor, rather than the variation defined for smooth tubes, is more realistic and should be used to define flow resistance of the headers. Hence, equation (V-49) is used for analysis in preference to equation (V-48). Integration of equation (V-49) for various values of the exponents n and m is obtained by either series formation or by the following transformation. Let

$$\int_o^1 (1 - By^n)^{2-2.5m}\, dy = \int_o^1 (1 - By^n)^p\, dy$$

and then let

$$y = (\sin \theta)^{2/n}/(B)^{1/n}$$

so that by the transformation

$$\int_o^1 (1 - By^n)^p = \frac{2}{n(B)^{1/n}} \int_o^{\sin^{-1}\sqrt{B}} (\cos \theta)^{2p+1} (\sin \theta)^{(2/n)-1} d\theta \qquad (V\text{-}50)$$

The transformation by equation (V-50) permits closed analytic solutions in many instances, while for others the method of series formation is employed.

Solutions to equation (V-49) for various values of n and m are presented in Table V-2. The pressure drop of the fluid through a header is generalized as a function of the initial flow conditions, the header length, and the terminal flow rate ratio $(w_1/w_o)_{D-t}$. The functions of $(w_1/w_o)_{D-t}$ shown in Table V-2 for the various values of n and m are equal to the generalized pressure drop parameter.

$$(p_o^o - p_1^o)_{D-t} (d_{D-i-o})/\alpha_o L_{o-1}$$

where α_o is defined by equation (V-44). The pressure drop for both the supply and return headers will be twice that defined by equation (V-49) since the drop in the supply header is equal to the drop in the return header, on the basis of the assumption that the fluid output gradient in the supply header equals the fluid input gradient to the return header at adjacent points along the header. Therefore, the overall pressure drop for the operating section of the distribution component is equal to twice the pressure drop of the supply header plus the pressure drop across the last group of equipment items served by the headers.

The volume of fluid within a header, which must be evaluated to determine the weight of the operating section, is defined by evaluation of

$$V_{t-o-1} = \int_o^L A_{x-D-t}\, dx \qquad (V\text{-}51)$$

where by substitution of equations (V-38) and (V-40), the generalized form becomes

Table V-2. Generalized Header Pressure Drop Relationships.

$(w_1/w_o)_{D-t}$ represented by w_1/w_o. $B = 1 - (w_1/w_o)_{D-t}$.

n \ m	0	0.4	0.8	1.0
0.25	$\frac{1}{15}\left[1+4\left(\frac{w_1}{w_o}\right)+10\left(\frac{w_1}{w_o}\right)^2\right]$	$\frac{1}{5}\left[1+4\left(\frac{w_1}{w_o}\right)\right]$	1.0	$\frac{8}{7B^4}\left\{\frac{16}{5}-\sqrt{\frac{w_1}{w_o}}\left[7-7\left(\frac{w_1}{w_o}\right)+\frac{21}{5}\left(\frac{w_1}{w_o}\right)^2-\left(\frac{w_1}{w_o}\right)^3\right]\right\}$
0.50	$\frac{1}{6}\left[1+2\left(\frac{w_1}{w_o}\right)+3\left(\frac{w_1}{w_o}\right)^2\right]$	$\frac{1}{3}\left[1+2\left(\frac{w_1}{w_o}\right)\right]$	1.0	$\frac{4}{3B^2}\left\{2-\sqrt{\frac{w_1}{w_o}}\left[3-\left(\frac{w_1}{w_o}\right)\right]\right\}$
1.0	$\frac{1}{3}\left[1+\left(\frac{w_1}{w_o}\right)+\left(\frac{w_1}{w_o}\right)^2\right]$	$\frac{1}{2}\left[1+\left(\frac{w_1}{w_o}\right)\right]$	1.0	$2\Big/\left[1+\sqrt{\frac{w_1}{w_o}}\right]$
2	$\frac{8}{15}\left[1+\frac{1}{2}\left(\frac{w_1}{w_o}\right)+\frac{3}{8}\left(\frac{w_1}{w_o}\right)^2\right]$	$\frac{2}{3}\left[1+\frac{1}{2}\left(\frac{w_1}{w_o}\right)\right]$	1.0	$\sin^{-1}\sqrt{1-\frac{w_1}{w_o}}\Big/\sqrt{1-\frac{w_1}{w_o}}$
4	$\frac{32}{45}\left[1+\frac{1}{4}\left(\frac{w_1}{w_o}\right)+\frac{5}{32}\left(\frac{w_1}{w_o}\right)^2\right]$	$\frac{4}{5}\left[1+\frac{1}{4}\left(\frac{w_1}{w_o}\right)\right]$	1.0	$1 + 0.1B + 0.0416B + + 0.0240B + 0.016B + + 0.0117B + 0.0090B + + 0.0072B + 0.0059B + + 0.005B + \ldots\ldots$ for $\lvert By^n\rvert < 1$

$$V_{t-o-1}/A_{D-t-o}\,L_{o-1} = \int_0^1 (1 - By^n)^m\,dy. \qquad (V\text{-}52)$$

Solutions to equation (V-52) are obtained for various values of n and m by use of the transformation equation (V-50) or by infinite series. Solutions for representative values of n and m are presented in Table V-3.

Table V-3. Generalized Fluid Volume Relationships for Header.

$(w_1/w_o)_{D-t}$ represented by w_1/w_o. $B = 1 - (w_1/w_o)_{D-t}$.

n \ m	0	0.4	0.8	1.0
0.25	1.0	$\frac{8}{B^4}\left\{0.06 - \left(\frac{w_1}{w_o}\right)\left[0.357\left(\frac{w_1}{w_o}\right)^{0.4} - 0.625\left(\frac{w_1}{w_o}\right)^{1.4} + 0.441\left(\frac{w_1}{w_o}\right)^{2.4} - 0.113\left(\frac{w_1}{w_o}\right)^{3.4}\right]\right\}$	$\frac{8}{B^4}\left\{0.033 - \left(\frac{w_1}{w_o}\right)^{1.8}\left[0.278 - 0.535\left(\frac{w_1}{w_o}\right) + 0.395\left(\frac{w_1}{w_o}\right)^{2} - 0.104\left(\frac{w_1}{w_o}\right)^{3}\right]\right\}$	$\frac{1}{5}\left[1 + 4\left(\frac{w_1}{w_o}\right)\right]$
0.5	1.0	$\frac{2}{B^2}\left[\frac{25}{84} + \frac{5}{12}\left(\frac{w_1}{w_o}\right)^{2.4} - \frac{5}{7}\left(\frac{w_1}{w_o}\right)^{1.4}\right]$	$\frac{5}{7B^2}\left[\frac{5}{9} - \frac{14}{9}\left(\frac{w_1}{w_o}\right)^{1.8} + \left(\frac{w_1}{w_o}\right)^{2.8}\right]$	$\frac{1}{3}\left[1 + 2\left(\frac{w_1}{w_o}\right)\right]$
1.0	1.0	$\frac{5}{7B}\left[1 - \left(\frac{w_1}{w_o}\right)^{1.4}\right]$	$\frac{5}{9B}\left[1 - \left(\frac{w_1}{w_o}\right)^{1.8}\right]$	$\frac{1}{2}\left[1 + \left(\frac{w_1}{w_o}\right)\right]$
2	1.0	Series	Series	$\frac{2}{3}\left[1 + \frac{1}{2}\left(\frac{w_1}{w_o}\right)\right]$
4	1.0	Series	Series	$\frac{4}{5}\left[1 + \frac{1}{4}\left(\frac{w_1}{w_o}\right)\right]$

The data shown in Figure V-1 indicate that for the internal diameter range of about 1/8 to 1 inch it is reasonable to assume that the tube wall thickness is constant and equal to 0.038 inch. Thus, the external diameter of the tubing is defined by

$$d^n_{D-e} = d^n_{D-i} + 0.076$$

and the cross-sectional area of metal by

$$A^n_{D-metal} = 0.5\ \pi\ (0.038)(d^n_{D-e} + d^n_{D-i})$$

Table V-4. Generalized Header Metal Volume Relationships.

$(w_1/w_o)_{D-t}$ represented by w_1/w_o. $B = 1 - (w_1/w_o)_{D-t}$.

n \ m	0	0.4	0.8	1.0
0.25	1.0	Series	$\frac{8}{B^4}\left\{0.06 - \left(\frac{w_1}{w_o}\right)\left[0.357\left(\frac{w_1}{w_o}\right)^{0.4} - 0.625\left(\frac{w_1}{w_o}\right)^{1.4} + 0.441\left(\frac{w_1}{w_o}\right)^{2.4} - 0.113\left(\frac{w_1}{w_o}\right)^{3.4}\right]\right\}$	$\frac{8}{9B^4}\left\{\frac{16}{35} - \sqrt{\frac{w_1}{w_o}}\left[3\left(\frac{w_1}{w_o}\right) - \frac{189}{35}\left(\frac{w_1}{w_o}\right)^2 + \frac{27}{7}\left(\frac{w_1}{w_o}\right)^3 - \left(\frac{w_1}{w_o}\right)^4\right]\right\}$
0.50	1.0	Series	$\frac{7}{5B^2}\left[\frac{5}{9} - \frac{14}{9}\left(\frac{w_1}{w_o}\right)^{1.8} + \left(\frac{w_1}{w_o}\right)^{2.8}\right]$	$\frac{4}{15B^2}\left\{2 + \left(\frac{w_1}{w_o}\right)^{1.5}\left[3\left(\frac{w_1}{w_o}\right) - 5\right]\right\}$
1.0	1.0	$\frac{5}{6B}\left[1 - \left(\frac{w_1}{w_o}\right)^{1.2}\right]$	$\frac{5}{7B}\left[1 - \left(\frac{w_1}{w_o}\right)^{1.4}\right]$	$\frac{2}{3B}\left[1 - \left(\frac{w_1}{w_o}\right)^{1.5}\right]$
2	1.0	Series	Series	$\frac{1}{2}\sqrt{\frac{w_1}{w_o}} + \frac{\sin^{-1}\sqrt{1-(w_1/w_o)}}{2\sqrt{1-(w_1/w_o)}}$
4	1.0	Series	Series	Series

or

$$A^{m}_{D\text{-metal}} = 0.019\,\pi\,(2d^{m}_{D-1} + 0.076).$$

The volume of metal in the header is defined by

$$V_{D\text{-metal}} = \int_0^{L_{o-1}} A_{D\text{-metal}}\,dx = L_{o-1}\int_0^1 A_{D\text{-metal}}\,dy$$

so that

$$V_{D\text{-metal}} = \frac{L_{o\text{-}1}}{144} \int_0^1 0.019\,\pi\,(2d_{D\text{-}i}^{m} + 0.076)dy.$$

By introducing the square root of equation (V-40) in the above equation to define the internal diameter variation of the header, the generalized equation for header metal volume is

$$\frac{V_{D\text{-metal}}(31{,}800)}{L_{o\text{-}1}} = 1 + 26.4\, d_{D\text{-}i\text{-}o}^{m} \int_0^1 (1 - By^n)^{m/2}\, dy \qquad (V\text{-}53)$$

Equations defining the term

$$\int_0^1 (1 - By^n)^{m/2}\, dy$$

are presented in Table V-4 for various values of n and m as a function of the terminal flow rate ratio $(w_1/w_o)_{D\text{-}t}$.

The header weight, equal to the weight of tubing and transfer fluid, is defined by combining equations (V-52) and (V-53) with the specific gravities of the fluid and metal.

$$(W_{metal} + W_t)_D/L_{o\text{-}1} = 0.34(sg)_t(d_{D\text{-}i\text{-}o}^{m})^2 \int_0^1 (1 - By^n)^m\, dy +$$

$$+ (sg)_{metal}\left[0.00196 + 0.052(d_{D\text{-}i\text{-}o}^{m}) \int_0^1 (1 - By^n)^{m/2}\, dy\right] \qquad (V\text{-}54)$$

Distribution Component Pressure Drop and Pumping Power for the Transfer Fluid

For a distribution component of the type illustrated in Figure V-5 the flow resistance is defined by the resistances of the starting section, the operating section, the last crossover line and equipment group in the operating section, and the transfer fluid side of the intermediate component. A generalized representation of the distribution component pressure drop is

$$\Delta p_{D\text{-}t}^{o} = \frac{\alpha_o L_{o\text{-}1}}{d_{o\text{-}i\text{-}o}}\left\{2\int_0^1 (1 - By^n)^{2-2.5m} dy + \right.$$

$$\left. + \beta_{1\text{-}2}\left(\frac{L_{1\text{-}2}}{L_{o\text{-}1}}\right) + \frac{L_{st}}{L_{o\text{-}1}}\left[2(1 + K_F) + \beta_I\left(\frac{L_I}{L_{st}}\right)\right]\right\} \qquad (V\text{-}55)$$

where the first term in the equation defines the pressure drop due to the operating section, the second term that due to the last crossover line in the operating section, the third that due to the starting section of the distribution component and the last term that due to the transfer fluid side of the intermediate component. The parameter β_{1-2} is used to convert the flow resistance of the last crossover line and equipment group into an equivalent straight run of tubing. The parameter K_F is introduced to allow for resistance of fittings in the starting section. Flow resistance of fittings within the operating section is not included since it is assumed that the pressure differential existing at adjacent points along the operating section is more than sufficient to overcome any resistances of this type. The parameter β_I is introduced to convert the resistance of the transfer fluid side of the intermediate component into an equivalent straight run of tubing.

The pumping power required to circulate the transfer fluid through the distribution component is defined by equation (V-27).

Comparison of Flow Resistance and Weight of the Operating Section for Various Types of Header Design

The pressure drop of the operating section of the distribution component for various types of header design is presented in Figure V-9. The flow resistance is compared to that for constant-pressure-gradient headers. The constant-diameter header, described by an exponent m equal to zero, has the least flow resistance. Constant-velocity header design, described by m equal to unity, results in the greatest flow resistance because of the rapidly decreasing diameter of the header as the terminal flow rate ratio $(w_1/w_o)_{D-t}$ is decreased. The header diameter reduction for constant pressure gradient is less than for constant velocity, so that the flow resistance is lower, but the reduction in the header diameter creates a flow resistance significantly above that for constant diameter.

The fluid removal gradient is characterized by the exponent n, with relative flow resistances presented in Figure V-9 for values of n of 0.5, 1.0 and 2.0. With reference to Figure V-6, low values of n define appreciable fluid removal rates along the beginning portion of the operating section, while high values of the exponent n characterize cases of relatively little fluid removal near the beginning of the operating section and appreciable rates of fluid removal toward the end of the section. The effect of the type of fluid removal gradient on the flow resistance, illustrated in Figure V-9, depends greatly upon the type of header design. With constant-pressure-gradient header design, the flow resistance is independent of the type of fluid removal gradient. Constant-diameter header design is affected to the greatest extent by the type of fluid removal gradient. An increase in the value of the exponent n tends to decrease the flow resistance with constant-velocity design, since late removal of appreciable portions of the fluid results in a larger average diameter of the header. When a large percentage of the total fluid removal occurs early along the header, such as with n of 0.50, or less, the

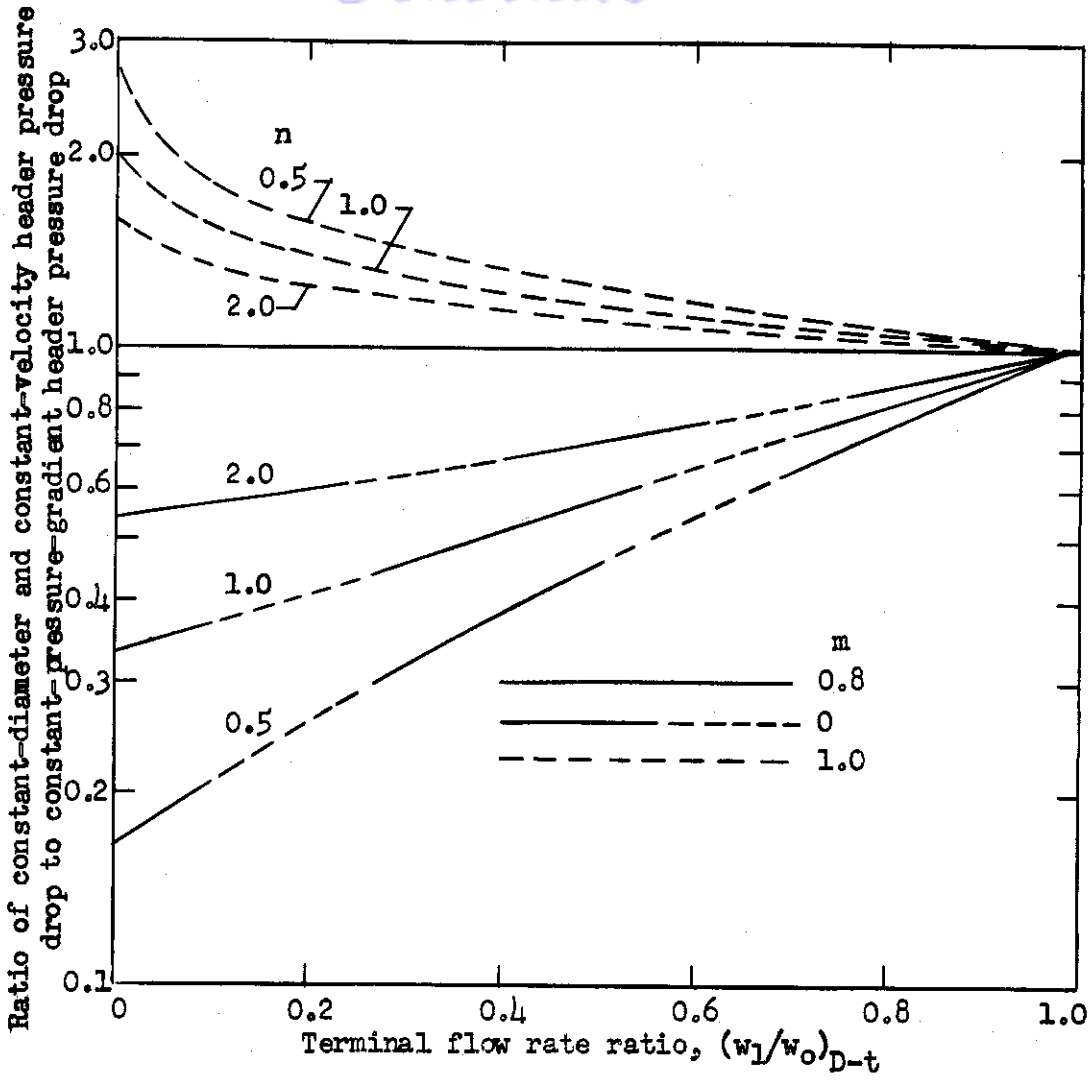

Figure V-9. Comparison of pressure drop or flow resistance for the operating section of a distribution component. Pressure drop for constant-diameter (m = 0) and constant-velocity (m = 1) header design referred to that for constant-pressure-gradient (m = 0.8) header design.

header diameter becomes quite small near the end of the fluid removal section. With constant-diameter header design, however, the effect of a decrease in the value of the exponent n is a reduction of the flow resistance, because, with constancy of flow area for this type of design, the average velocity of flow along the header is greatly reduced with appreciable fluid removal early along the header. With constant-diameter headers, and a terminal flow rate ratio of 0.10, the data of Figure V-9 illustrate that should rearrangement of the equipment items served by the operating section be possible so that n is decreased from 2.0 to 0.5, the flow resistance is reduced by a ratio of nearly 3 to 1. Oppositely, with constant-velocity header design, a decrease of the exponent n from 2.0 to

0.5 at a terminal flow rate ratio of 0.1 results in about 35% increase in flow resistance.

The importance of different types of header design and fluid removal gradients is not nearly so great with high values of the terminal flow rate ratio. The magnitude of the terminal flow rate ratio employed in a distribution component depends upon the arrangement of the equipment items and the compromise in design of a system between the penalty of power supply for overcoming flow resistance and the penalty due to weight of the distribution component. If more than one group of equipment items is being served by a distribution component, then the terminal flow rate ratio for the first operating section may be quite high so as to provide considerable subsequent fluid removal for other groups of equipment items. The compromise in aircraft penalty between pumping power and weight must be studied from the viewpoint of minimizing the gross weight penalty imposed on the aircraft.

The effect of different types of header design and fluid removal gradients on the weight of the operating section is presented in Figures V-10 and V-11. In Figure V-10, the weight of the transfer fluid and metal in the operating section for constant-pressure-gradient design is presented as the fraction of that for constant-diameter header design. Figure V-11 presents a similar comparison for constant-velocity-header design. The type of fluid removal gradient, characterized by the value of the exponent n, has no effect on the weight of fluid and metal for constant-diameter-header design. An increase in the value of the exponent n always results in greater weight of the header whenever the exponent m is greater than zero. Thus, for both constant-pressure-gradient and constant-velocity design the weight of the header is reduced for low values of the exponent n, i.e., early fluid removal along the header. Constant-pressure-gradient header design always results in greater weight of fluid and metal than constant-velocity header design. The difference is not particularly significant, except for relatively low values of the terminal flow rate ratio. For an initial header diameter of 0.75 inch and a terminal flow rate ratio of 0.10, the operating section of a constant-pressure-gradient header is about 9% greater in weight than for a constant-velocity-header for linear fluid removal, i.e., an exponent n equal to unity. The greater the initial diameter of the header, i.e., the larger the diameter of the starting section of the distribution component, the greater is the possible weight saving with constant-velocity or constant-pressure-gradient header design. This effect is due to the fact that with small tubes the weight of the metal becomes a greater portion of the total weight.

Comparison of Aircraft Weight Penalty for Various Types of Header Design

Comparison of the weight data of Figures V-10 and V-11 with the flow resistance data of Figure V-9 shows that for all conditions of design the various types of header design and fluid removal gradients produce opposite effects on weight and flow resistance of the operating

section of a distribution component. Thus, from the previous data and analysis it is not possible to define which type of header design produces the minimum gross weight penalty of a cooling system. Although, in general, a complete analysis and evaluation of a cooling system would be required to define the optimum type of header design, considerable

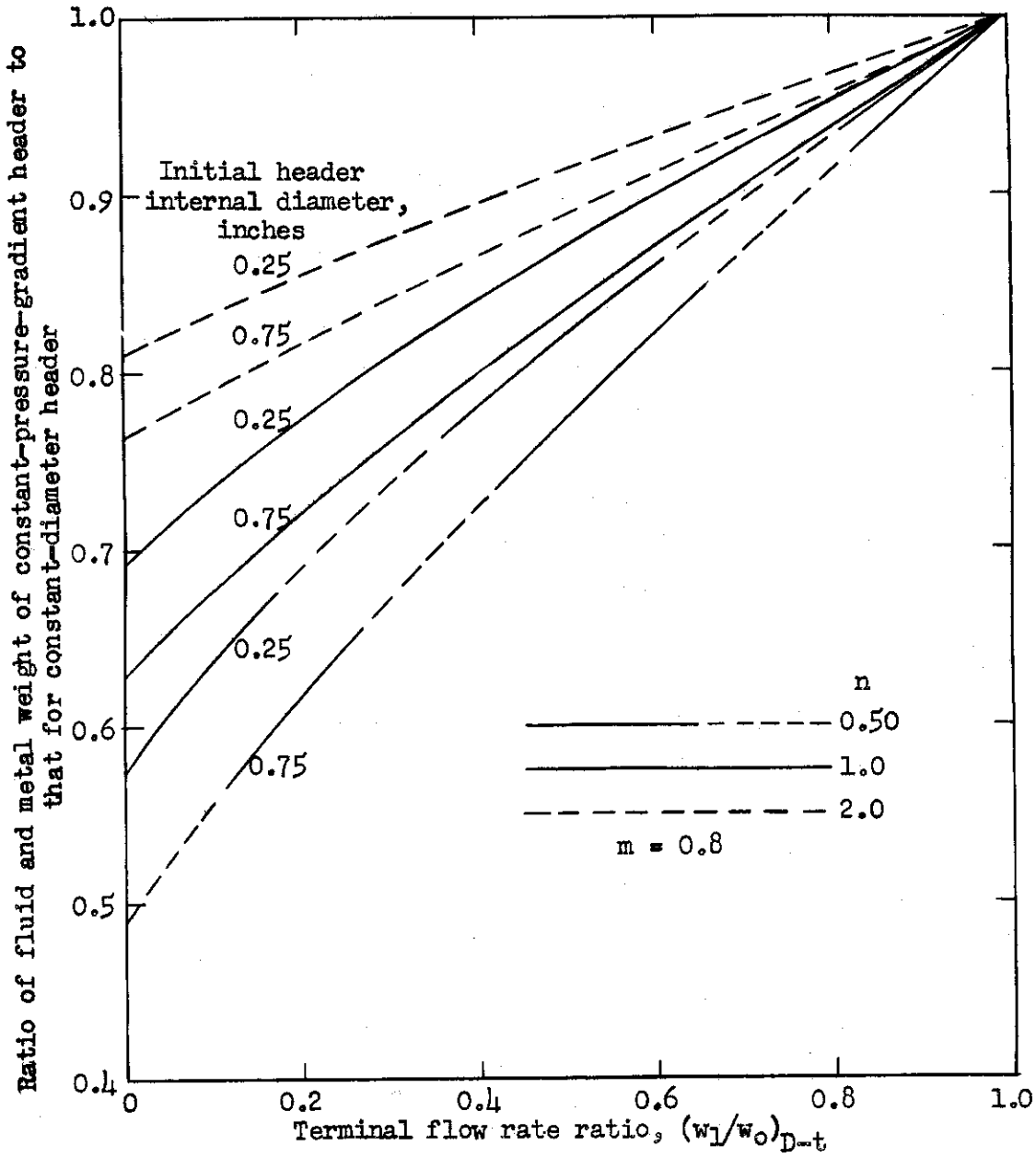

Figure V-10. Comparison of the weight of fluid and metal in the operating section of a distribution component for constant-pressure-gradient header design (m = 0.80) with constant-diameter header design (m = 0). Specific gravity of fluid, 0.88. Specific gravity of metal, 2.7.

insight as to the relative penalties involved for the different designs can be obtained by evaluation of the aircraft's gross weight penalty due to the operating section alone. Since the supply and return headers of the operating section have the same characteristics, it is necessary to consider only one header. The basic independent variable of analysis

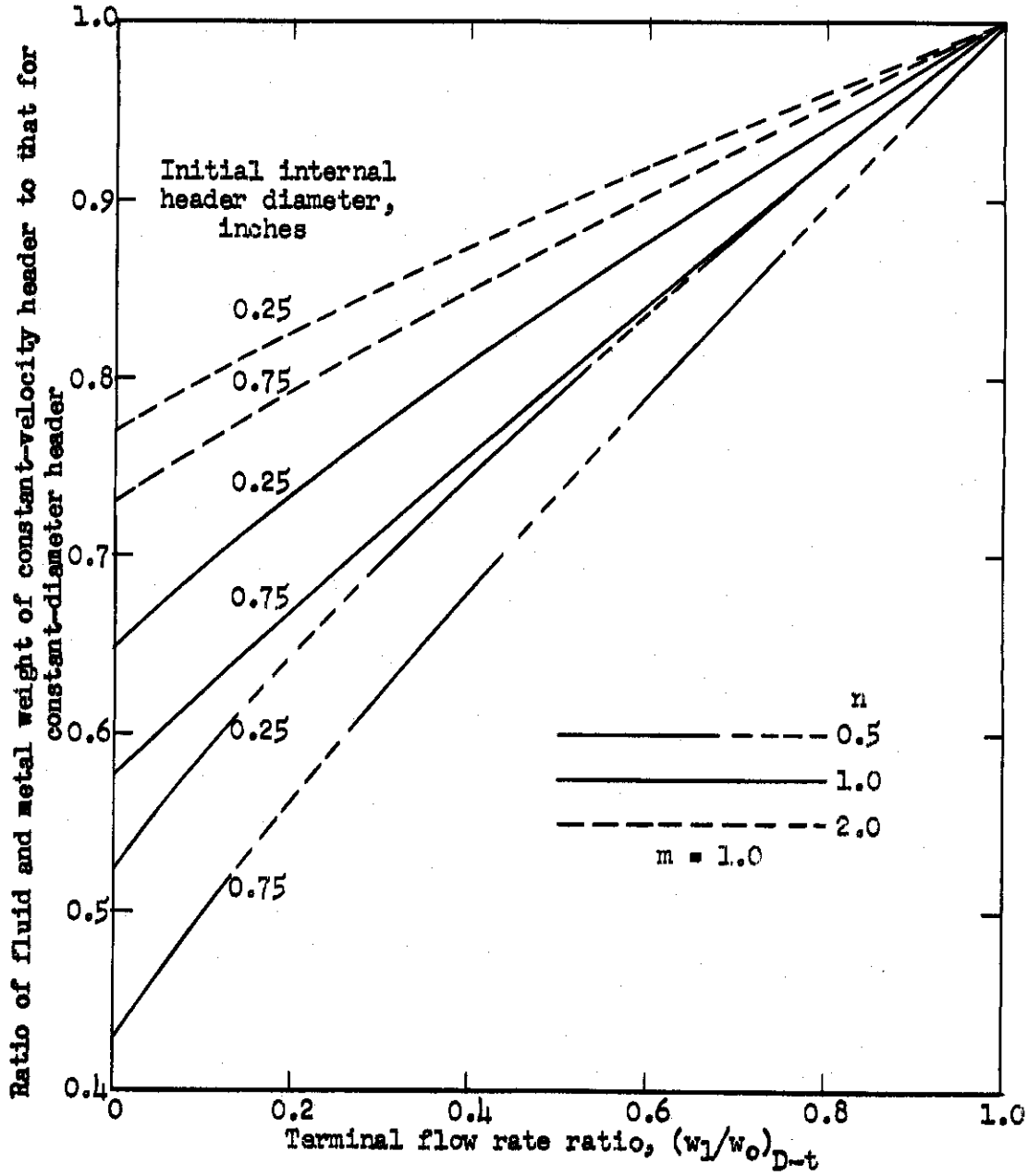

Figure V-11. Comparison of the weight of fluid and metal in the operating section of a distribution component for constant-velocity header design (m = 1) with constant-diameter-header design (m = 0). Specific gravity of fluid, 0.88. Specific gravity of metal, 2.7.

is the type of header design, characterized by the exponent m.

With reference to equation (III-14a), the increase in gross weight of an aircraft having constant range and payload due to system weight and drag is defined by

$$(1 - X_{ref})\,\Delta W_g = W_{sy} + \left[(1 - X_{ref})\,\ln \frac{1}{1-X_{ref}}\right](Lf/Dr)(Dr_{sy}).$$

The system for this analysis is the operating section of the distribution component and the power supply system associated with providing the required pumping power for the operating section. Thus,

$$W_{sy} = (W_{metal} + W_t)_{D-op} + W_{p-sy} \qquad (V-56)$$

The drag of the system, Dr_{sy}, would be the potential loss in propulsive thrust equivalent to the required increase in fuel flow rate to the powerplant for constant propulsive thrust, when shaft power is extracted for the power supply system. Thus,

$$Dr_{sy} = \Delta w_{fuel}/SFC_{ref}$$

or

$$Dr_{sy} = (\Delta w_{fuel}/P'_{sh})(P'_{sh}/SFC_{ref})$$

which by use of equation (V-30) becomes

$$Dr_{sy} = (\Delta w_{fuel}/P'_{sh})(P'_{Dt-op}\,\eta_{p-sy}\,SFC_{ref}) \qquad (V-57)$$

The parameter $\Delta w_{fuel}/P'_{sh}$, the increase in fuel flow per hour for each shaft horsepower extracted from the powerplant, is defined by equation (III-25). Suppose the parameter φ is defined as

$$\varphi = (\Delta w_{fuel}/P'_{sh})(Lf/Dr)\left[(1-X_{ref})\,\ln \frac{1}{1-X_{ref}}\right]\Big/(SFC_{ref}) \qquad (V-58)$$

Then, by introducing equations (V-56), (V-57) and (V-58) into equation (III-14a) one obtains

$$(1-X_{ref})\,\Delta W'_g = (W_{metal} + W_t)_{D-op} + W_{p-sy} + \varphi P'_{Dt-op}/\eta_{p-sy} \qquad (V-59)$$

Assuming the weight of the power supply system is defined by equation (V-28) and the overall efficiency of the power supply system is 33.3%, a working form of equation (V-59) is

$$(1-X_{ref})\,\Delta W'_g = (W_{metal} + W_t)_{D-op} + (20 + 3\varphi)P'_{Dt-op} \qquad (V-60)$$

where $\Delta W'_g$ represents the gross weight increase of the aircraft due to the operating section of the distribution component. The parameter φ

could vary from roughly 0.4 to 5, but typically would have a value of about 1 to 3.

By use of the generalized pressure drop equation (V-49) and equation (V-27) defining the relation between flow rate of fluid, pressure drop, and pumping power, the following generalized expression for the pumping power required to transport the fluid through the supply header is obtained.

$$P'_{Dt}/L_{o-1} = 0.1155 d^{m}_{D-i-o}\, \alpha' \int_{o}^{1} (1 - By^{n})^{2-2.5m}\, dy \qquad (V-61)$$

where the parameter α' is defined by

$$\alpha' = f_o (u_{D-t-o}/10)^3 (sg_{Dt}) \qquad (V-62)$$

Also, since the integral term of equation (V-61) has a value of unity for a constant-pressure-gradient header, the generalized pumping power equation may be re-expressed as

$$P'_{Dt}/(P'_{D})_{dp/dx} = \int_{o}^{1} (1 - By^{n})^{2-2.5m}\, dy \qquad (V-63)$$

and

$$(P'_{Dt})_{dp/dx} = 0.1155\, d^{m}_{D-i-o}\, \alpha' \qquad (V-64)$$

The weight of the fluid and metal in the header is defined by the general equation (V-54). For a constant-diameter the integral terms of this equation have values of unity, so that the generalized weight equation becomes

$$(W_{metal} + W_t)_D/L_D = \left[0.34(sg_{Dt})(d^{m}_{D-i-o})^2 + 0.052(sg_{metal})(d^{m}_{D-i-o}) + 0.00196(sg_{metal})\right] \left[\frac{(W_{metal} + W_t)}{(W_{metal} + W_t)_d}\right] \qquad (V-65)$$

where the right-hand term of the equation represents the ratio of weight of fluid and metal for any type of header design to that for constant-diameter design. Numerical values of this ratio for various conditions of design are presented in Figures V-10 and V-11.

The combination of equations (V-60), (V-63) and (V-65) yields an expression which may be used to define the gross weight increase for the various types of header design. As previously mentioned, it is not possible to analyze generally the effect of various types of header design without giving consideration to the entire cooling system. This is illustrated specifically by the parameter α', which is a function of the

Darcy friction factor and the transfer fluid flow velocity. In particular, the optimum value of the flow velocity cannot be determined except by an overall evaluation of the entire cooling system. In order to circumvent this basic difficulty, a study of the flow velocity in the distribution component of previously optimized cooling system designs employing constant-diameter headers has been conducted. The results have shown that for a rather wide range of operational conditions of cooling systems the flow velocity in the distribution component varies from about 8 to 15 feet per second. When this range of flow velocity is com-

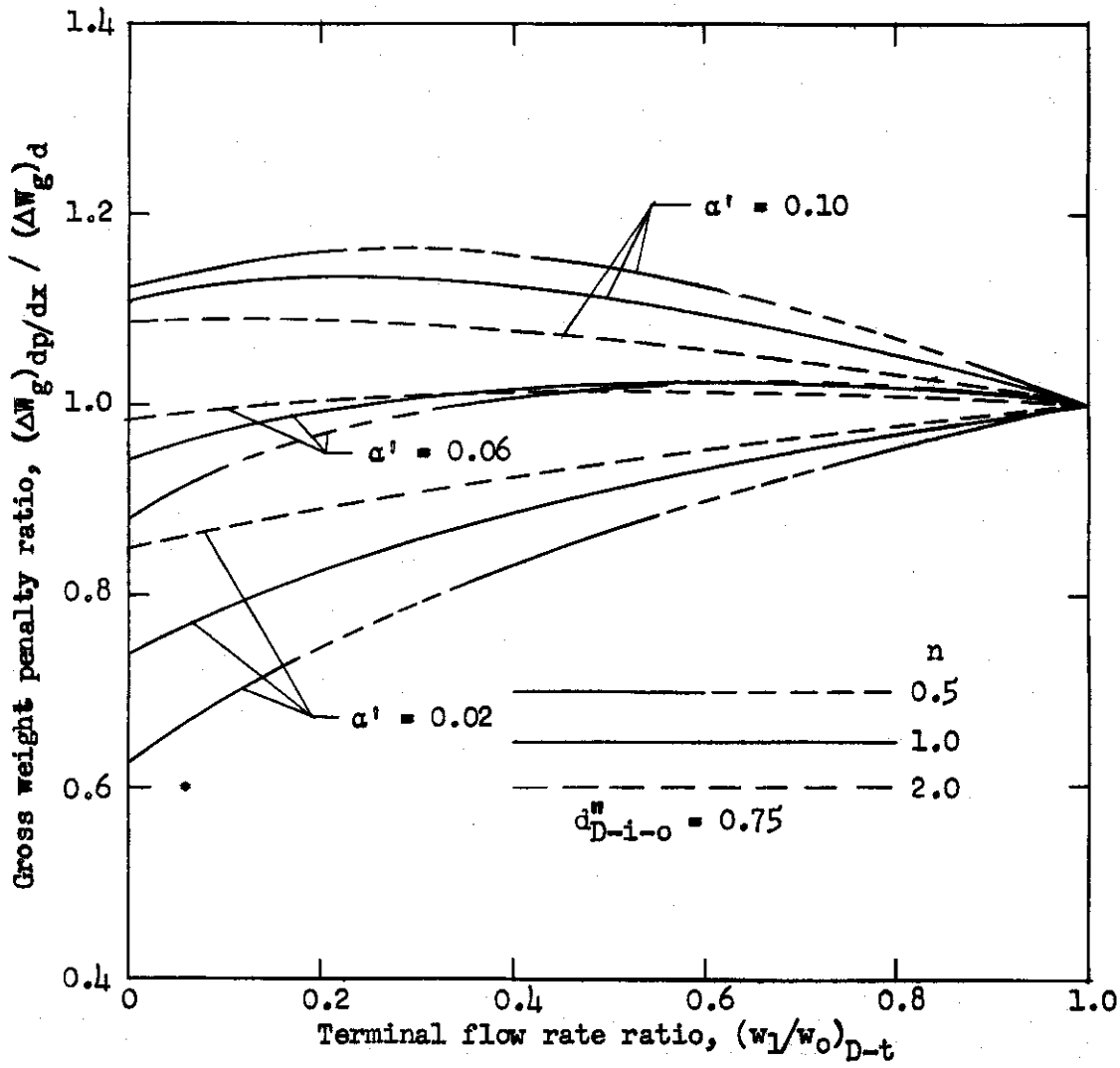

Figure V-12. Comparison of gross weight penalty of constant-pressure-gradient header design to constant-diameter header design for various operational conditions of the operating section and an initial internal diameter of the transfer line of 0.75 inch. Specific gravity of fluid, 0.88. Specific gravity of metal, 2.7. $\varphi = 3.0$.

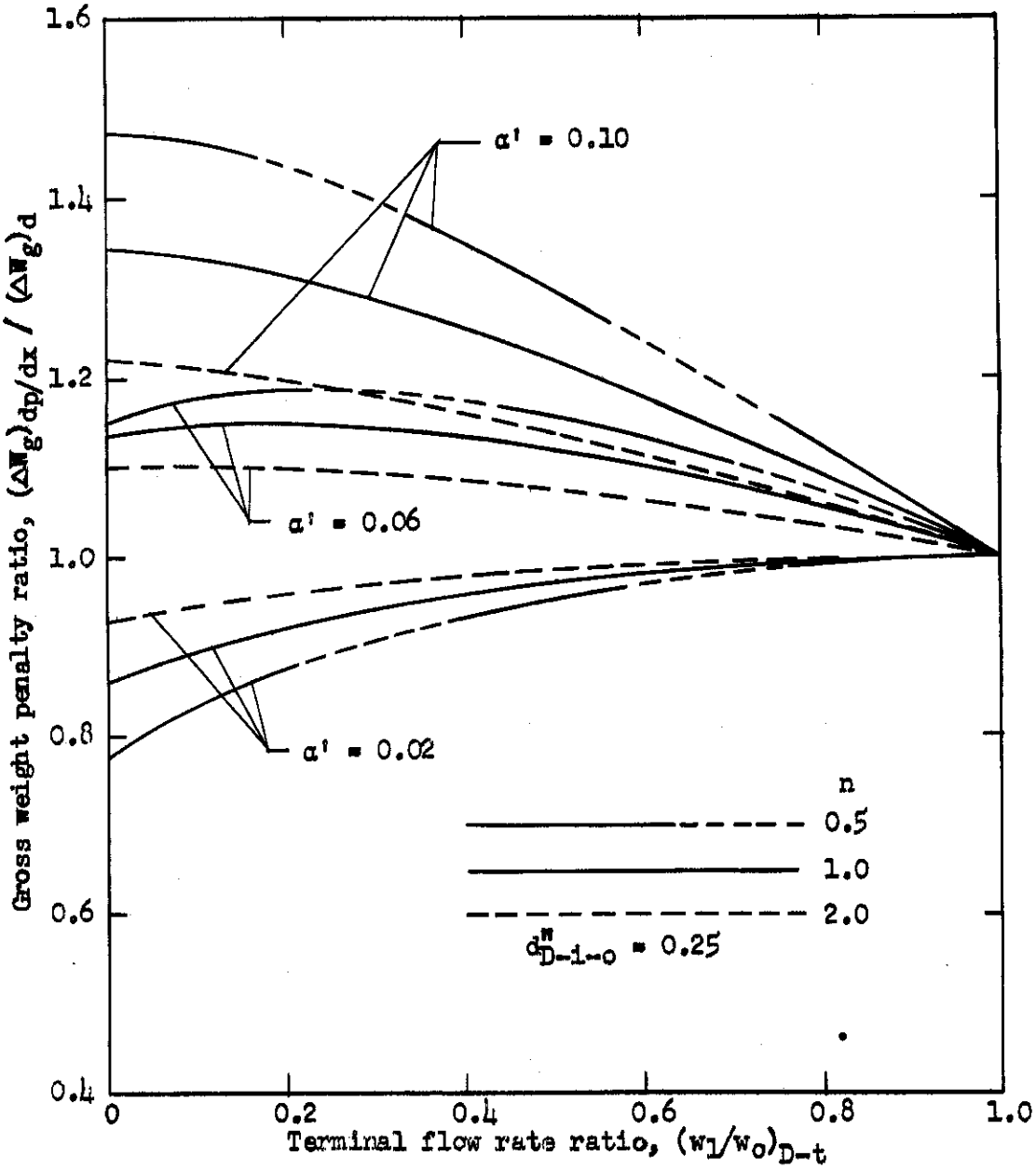

Figure V-13. Comparison of gross weight penalty of constant-pressure-gradient-header design to constant-diameter header design for various operational conditions of the operating section and an initial diameter of the transfer line of 0.25 inch. Specific gravity of fluid, 0.88. Specific gravity of metal, 2.7. φ = 3.0.

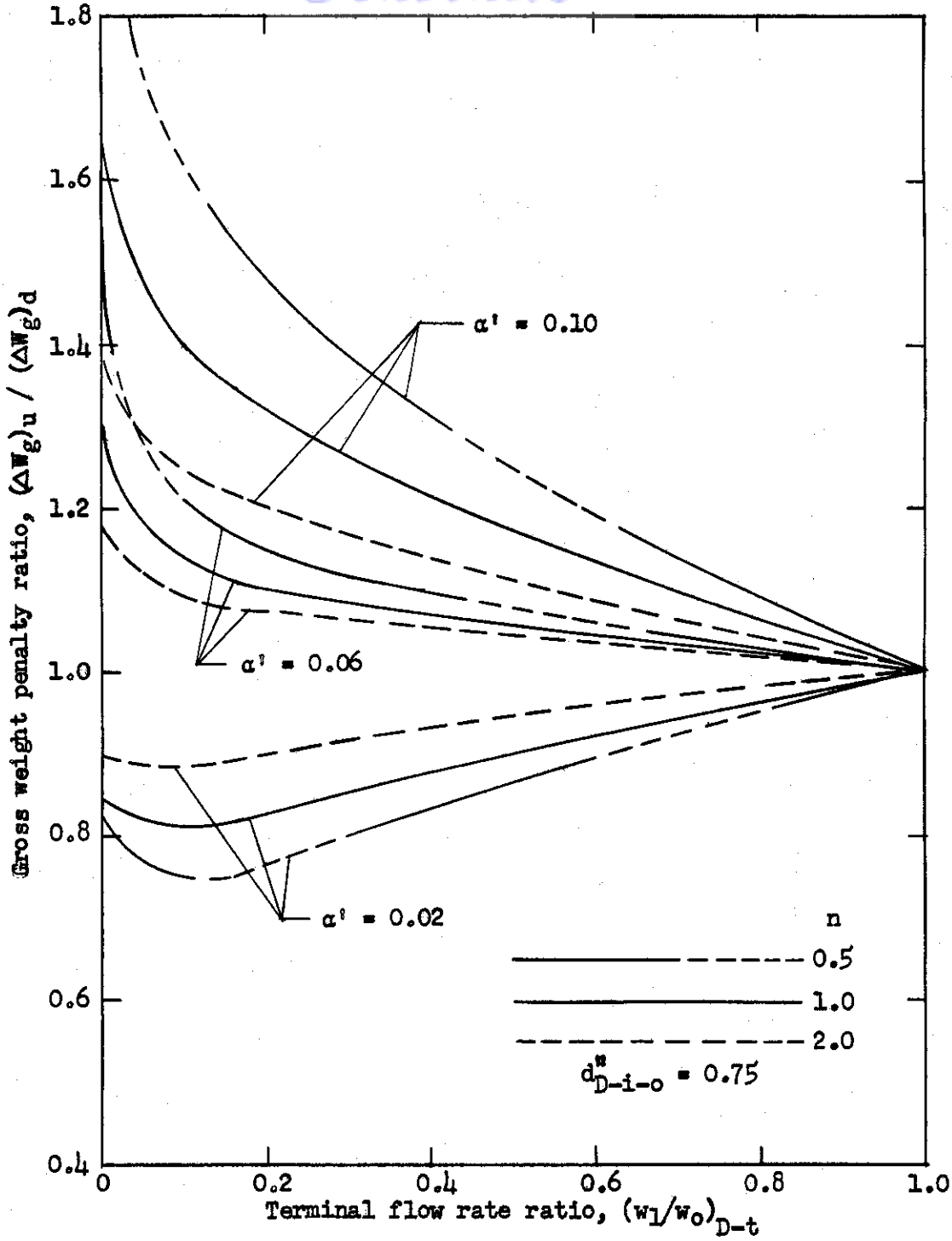

Figure V-14. Comparison of gross weight penalty of constant-velocity header design to constant-diameter header design for various operational conditions of the operating section and an initial diameter of the transfer line of 0.75 inch. Specific gravity of fluid, 0.88. Specific gravity of metal, 2.7. $\varphi = 3.0$.

bined with a typical range of values for the Darcy friction factor, it is found that a representative range of values for the parameter α' would be from about 0.01 to 0.12. Thus, the general effects of various types of header design are studied by including α' as an independent variable of analysis having values within this range.

A comparison of the gross weight penalty for constant-pressure-gradient headers to the penalty for constant-diameter headers is presented in Figure V-12 for an initial line diameter of 0.75 inch and in Figure V-13 for an initial line diameter of 0.25 inch. The data are presented for a value of the parameter φ of 3.0 and values of the parameter α' of 0.02, 0.06 and 0.10. Also included in the plots are data for three values of the exponent n, of 0.5, 1.0 and 2.0, to characterize various types of fluid removal gradients of the header. A high value of α' denotes relatively high flow velocity and/or friction factor. The results show that when the frictional effects are low, the use of a constant-pressure-gradient header results in a gross weight saving compared to a constant-diameter header. However, for the initial diameter range of 0.25 to 0.75 inch (the most commonly encountered diameters of liquid distribution components are usually less than 0.75 inch) the use of a constant-pressure-gradient header rather than a constant-diameter header shows no significant savings in weight for values of α' above about 0.04. For an initial line diameter of 0.25 inch (see Figure V-13) the constant-diameter header appears superior to the constant-pressure-gradient header for nearly all operational conditions which might be encountered.

In comparison with the constant-pressure gradient header, a constant-velocity header has the advantage of less volume and, thereby, less weight, but has the disadvantage of appreciably greater flow resistance. Thus, in comparison with a constant-diameter header, the constant-velocity header will show still greater gross weight penalty than the constant-pressure-gradient header. This is illustrated in Figure V-14 for an initial line diameter of 0.75 inch. The constant-diameter header will appear more favorable relative to a constant-velocity header as the initial line diameter is reduced. It is apparent by inspection of Figure V-14 that the constant-velocity header has a small weight advantage over the constant-diameter header only when the frictional effects are reduced to a minimum.

On the basis of this study it is concluded that in general the use of a constant-diameter operating section of a distribution component is superior to other possible types of design for typical operational characteristics of distribution components and for all arrangements of the equipment items served by an operating section. Thus, the simplification in evaluation procedures for determining cooling system penalty made possible by assuming constant-diameter headers for the distribution component appears entirely justifiable. The assumption of constant-diameter headers will only rarely introduce a slightly greater weight penalty than other types of header design. Also, since in most types of cooling systems the weight of the operating section is a relatively

small percentage of the total system weight, the effects on gross weight herein illustrated are of considerably less importance on the overall aircraft penalty introduced by the cooling system.

Evaluation of Optimum Line Diameter for the Distribution Component

In any indirect cooling system, considering all variables fixed, except the diameter of the transfer lines, it is apparent that an increase in this diameter reduces the pumping power required to circulate the transfer fluid and, thereby, the extra fuel load and dead weight of the power supply system, but increases the weight of the transfer lines. Consequently, there exists an optimum transfer line diameter for any selected set of operational conditions of the cooling system. The optimum line diameter may be determined by evaluating the variation in gross weight penalty of the cooling system with line diameter, while maintaining all system variables fixed. On the basis of the conclusions of the preceding sub-section, it is assumed that a constant line diameter would be used in both the operating and starting section of the distribution component. The analysis may be conducted on the basis of the starting section only, where no fluid removal occurs, since the flow resistance of any operating section may be represented as a certain fraction of the resistance for an equivalent length of starting section. Flow resistance of the equipment and intermediate components need not be considered since these resistances would remain essentially constant as the transfer line diameter is varied.

For aluminum tubing and a constant diameter, equation (V-65) becomes

$$(W_{metal} + W_t)_D/L_D = 0.34(sg_{Dt})(d''_{Di})^2 + 0.14d''_{Di} + 0.0053 \qquad (V-66)$$

The required pumping power is defined by equation (V-61) as

$$P'_{Dt}/L_D = 0.1155\, d''_{Di}\, \alpha'(1 + K_F) \qquad (V-67)$$

where the factor $(1 + K_F)$ is added to account for flow resistance of fittings. The continuity equation defines the flow rate as

$$w_{Dt} = 3600(u_{Dt})(62.4\, sg_{Dt})(0.785\, d''_{Di})/144 \qquad (V-68)$$

Combining equation (V-67) with equations (V-62) and (V-68) yields

$$P'_{Dt}/L_D = f_{Dt}(1 + K_F)(w_{Dt}/1000)^3 \Big/ \left[(sg^2_{Dt})(d''^5_{Di})(15{,}900)\right]$$

Then, assuming smooth tubing, and introducing the friction factor relationship of equation (V-22), the pumping power equation becomes

$$P'_{Dt}/L_D = (1 + K_F)(\mu^{0.2}_{Dt})(w_{Dt}/1000)^{2.8} \Big/ \left[(sg^2_{Dt})(d''^{4.8}_{Di})(59{,}100)\right] \qquad (V-69)$$

The effect of line diameter on the gross weight penalty of the distribution component may now be established by substituting equations (V-66) and (V-69) into equation (V-59) to yield

$$(1-X_{ref})\,\Delta W'_g/L_D = 0.34(sg_{Dt})(d''_{Di})^2 + 0.44d''_{Di} + 0.0053 + \frac{\left[\frac{W_{p-sy}}{P_{Dt}} + \frac{\varphi}{\eta_{p-sy}}\right](\mu_{Dt}^{0.2})(1+K_F)\left[\frac{w_{Dt}}{1000}\right]^{2.8}}{59{,}000\,(sg_{Dt}^2)(d''^{4.8}_{Di})} \qquad (V-70)$$

Differentiation of this equation with respect to the line diameter allows derivation of an expression for the optimum internal diameter of the transfer line in the distribution component. The resulting relationship is

$$d''_{Di-opt} = \frac{0.275(1+K_F)^{0.158}\left[\frac{W_{p-sy}}{P_{Dt}} + \frac{\varphi}{\eta_{p-sy}}\right]^{0.158}(\mu_{Dt}x10^5)^{0.0316}\left[\frac{w_{Dt}}{1000}\right]^{0.442}}{1 + 0.667\,sg_{Dt}} \qquad (V-71)$$

which permits definition of the optimum line diameter for any type of transfer fluid, weight and efficiency characteristics of the power supply system and flow rate of transfer fluid. For the specific weight and efficiency characteristics of the power supply system defined by equations (V-28) and (V-31), i.e., 20 pounds per pumping horsepower and 33.3% overall efficiency, and K_F equal to 0.25 to account for fitting flow resistance, equation (V-71) may be reduced to the form

$$d''_{Di-opt} = \frac{0.457(1+0.02\varphi)(\mu_{Dt}x10^5)^{0.0316}(w_{Dt}/1000)^{0.442}}{1 + 0.667\,sg_{Dt}} \qquad (V-72)$$

Examination of equation (V-71) or (V-72) shows that the optimum line diameter is controlled or affected principally by the flow rate of the transfer fluid. For example, doubling the transfer fluid flow rate increases the optimum diameter by 36%. The specific gravity of the transfer fluid also is of considerable importance. An increase in the specific gravity of the transfer fluid from 1.0 to 1.5, for example, would decrease the optimum line diameter by 25%. The effect of the viscosity on the optimum line diameter is almost negligible. For example, a tenfold increase in viscosity increases the optimum line diameter by only about 7.5%. The effect of the power supply system weight and efficiency characteristics are not of major importance, since the simultaneous doubling of the weight per horsepower and reducing the efficiency by one-half increases the optimum diameter only 12%. The variation of optimum line diameter with transfer fluid flow rate and specific gravity

is presented in Figure V-15. The most common range of tube diameter has been found to be from about 1/8 to 3/8 inch, although with some systems the line diameter may be 0.75 inch.

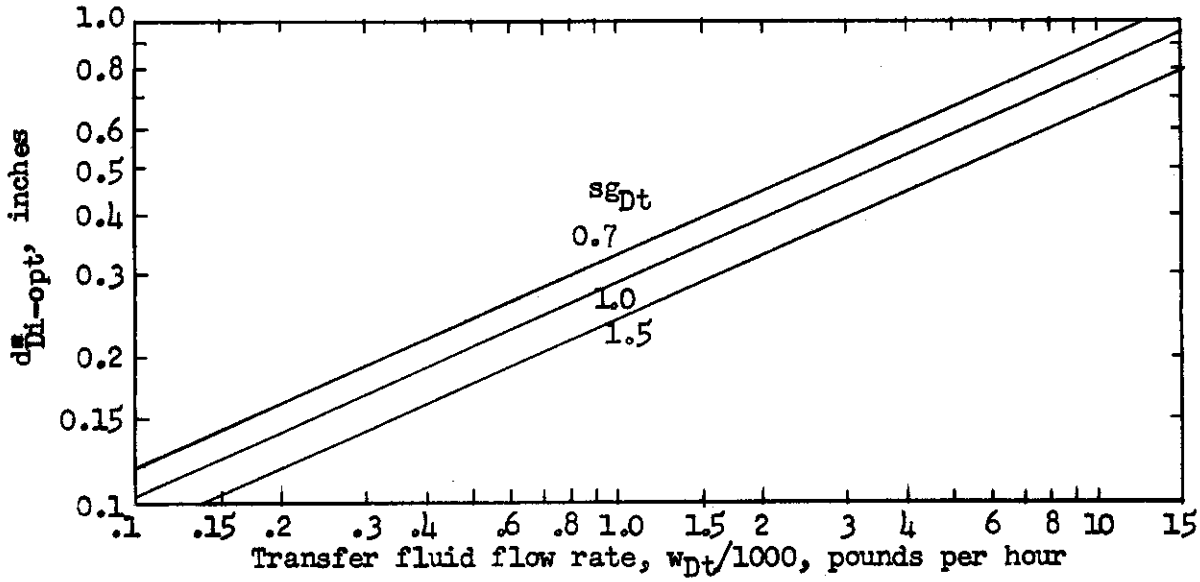

Figure V-15. Variation in the optimum line diameter of the distribution component with transfer fluid flow rate and specific gravity. $\varphi = 2.5$. $\mu = 10^{-5}$ lb-sec per ft^2. $W_{p-sy}/P'_{Dt} = 20$ lbs per hp. $\eta_{p-sy} = 33.3\%$. $sg_{metal} = 2.7$.

SECTION VI

THE INTERMEDIATE COMPONENT

The intermediate component serves in all aircraft cooling systems whenever the ultimate fluid does not pass through the equipment component. In these cases a transfer fluid flows through the equipment component wherein energy is absorbed by the transfer fluid at a rate sufficient to cool the equipment item or items. The transfer fluid carries the heat rejected by the equipment component to some point in the cooling system where it must be transferred to an ultimate fluid. The component of the cooling system which permits this energy transfer is termed the intermediate component. The average temperature level within the intermediate component will always be lower than in the equipment component, so that the temperature level at which heat is rejected to the ultimate fluid in an indirect system will always be lower than for the same operational conditions in a direct system. Thus, it is apparent that the design of indirect systems will be more critical in terms of aircraft penalty, not only because of the lower average temperature at which heat is rejected to the ultimate fluid, but also because of the weight and pumping power requirement introduced by the intermediate component.

The intermediate component in an indirect ram air cooling system would be either an air-to-liquid or air-to-gas heat exchanger. Since the transfer fluid will, most commonly, be a liquid, the air-to-liquid heat exchanger is considered to be the principal type of intermediate component for the indirect ram air cooling system. The heat transfer process will be forced convection between the fluids and the heat exchanger surface and conduction through the separator plates forming the surface in the exchanger, since neither the air nor the liquid transfer fluid would normally undergo any change in phase. For the evaluation of the performance and physical characteristics of the indirect ram air system, it is necessary to define working methods whereby the physical characteristics and nearly optimum design of this type exchanger may be determined.

The ultimate fluid in the expanded ram-air cooling system is also air, so that the design of this type of cooling system as an indirect system would require an intermediate component which is an air-to-liquid or air-to-gas heat exchanger. Here again, the most likely transfer fluid would be a liquid so that the air-to-liquid heat exchanger represents the principal type for this cooling system.

Similar considerations apply to bleed air cooling systems with the exception that precoolers or other auxiliary heat exchangers are oftentimes employed in the cycle. Thus, for example, with the simple bleed air cooling system an air-to-air heat exchanger would serve as the precooler since ram air is used as the thermal sink. The characteristics of air-to-air and air-to-liquid heat exchangers should be defined,

therefore, for study of bleed air cooling systems.

With indirect blower cooling systems either air-to-liquid or air-to-gas heat exchangers would most likely serve as the intermediate component. Fuel cooling systems are considered to be principally of the indirect type and, therefore, with a liquid transfer fluid, the liquid-to-liquid heat exchanger is considered to be the most important type of intermediate component. The refrigeration machine proper represents the intermediate component in vapor cycle cooling systems. For this reason, the details of the intermediate component are covered in Section XIV dealing with the performance and physical characteristics of vapor cycle cooling systems. An indirect expendable cooling system requires a heat exchanger to serve as the intermediate component wherein forced convection heat transfer occurs on the transfer-fluid side and evaporation or boiling occurs on the ultimate fluid side. Thus, the principal type of intermediate component for indirect expendable systems is a boiling liquid-to-liquid heat exchanger.

The following sub-sections present the analyses and development of evaluation methods for liquid-to-liquid, air-to-air, air-to-liquid and boiling liquid-to-liquid heat exchangers.

Nomenclature

Symbol	Concept	Dimensions
A	cross-sectional area of flow	square feet
b	plate spacing	feet
c_p	specific heat at constant pressure	Btu per pound-^{o}R
C	coefficient	variable
d	diameter	feet
e	effectiveness	dimensionless
f	friction factor	dimensionless
g	dimensional constant	32.2 pounds per slug
G	mass velocity	pounds per hour-square foot
h	heat transfer coefficient	Btu per hour-square foot-^{o}R
j	heat transfer correlation factor	dimensionless
k	coefficient of thermal conductivity	Btu per hour-foot-^{o}R
K	flow resistance coefficient	dimensionless
kw	cooling capacity	kilowatts
l	length parameter	dimensionless
L	length	feet
m	parameter	dimensionless
n	number of tube rows or laminations	dimensionless
N	number of items	dimensionless
NTU	number of transfer units	dimensionless
p	pressure	pounds per square foot, abs.
PC	power-to-cooling ratio	dimensionless
Pr	Prandtl number	dimensionless
q	heat rate	Btu per hour
r_h	hydraulic radius	feet

Symbol	Concept	Dimensions
R	thermal resistance and gas constant	^{o}R-hour per Btu and feet per ^{o}R
Re	Reynolds number	dimensionless
s	pitch of tubes in heat exchanger	dimensionless
S	surface area	square feet
t	thickness	feet
T	temperature	^{o}R
u	absolute velocity	feet per second
U	overall coefficient of heat transfer	Btu per hour-square foot-^{o}R
V	volume	cubic feet
w	fluid flow rate	pounds per hour
W	weight	pounds
β	heat transfer parameter	
γ	specific weight	pounds per cubic foot
δ	ratio of absolute pressure to standard sea level pressure (2115 pounds per square foot)	dimensionless
ζ	crossflow factor	dimensionless
η	temperature effectiveness	dimensionless
θ	ratio of absolute temperature to standard sea level absolute temperature (519^{o}R)	dimensionless
μ	absolute viscosity	pounds per foot-hour
ρ	density	slugs per cubic foot
φ	parameter	variable
Φ	thermal resistance ratio	dimensionless

Subscript	Refers to
c	combined value
core	core of heat exchange
e	exit
f	frictional factor or coefficient
F	fin
fl	fuel
h	heat transfer coefficient
hη	coefficient associated with the product hη
i	inlet or internal
I	intermediate component
j	heat transfer correlation coefficient
m	mean value
max	maximum value
min	minimum value
nf	no-flow dimension
o	overall value
s	surface or separator plate
t	transfer fluid
th	thermodynamic value

Subscript	Refers to
U	ultimate component
X	heat exchanger
1,2	sides of heat exchanger

Superscript

"	dimension in inches
'	power in horsepower or watts
o	total or stagnation values
a,m,n,r	exponents

Liquid-to-Liquid Heat Exchanger

The indirect fuel cooling system requires a liquid-to-liquid heat exchanger to transfer the heat dissipated by the equipment items from the transfer fluid to the fuel acting as the thermal sink. It is assumed that the heat exchanger consists of a tube bundle and shell with the fuel flowing through the tubes and the transfer fluid flowing in crossflow over the tubes. The transfer fluid side may be baffled for multi-pass flow. A schematic diagram of the general flow arrangement assumed is shown in Figure VI-1. The dimension L_1 represents the fuel flow length, L_2 the transfer fluid flow length for one pass and L_3 the no-flow dimension.

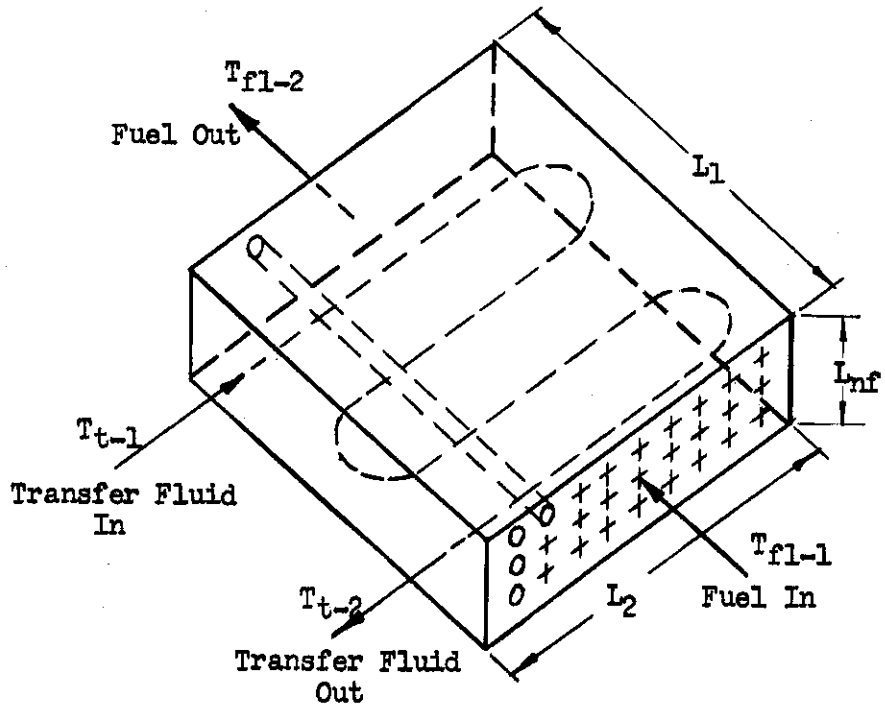

Figure VI-1. Assumed general flow arrangement for liquid-to-liquid heat exchanger.

1. Fuel-Side Heat Transfer Coefficient and Flow Resistance

With the fuel flowing through the tubes, the heat transfer coefficient of forced convection between the inside surface of the tubes and the fuel may be defined by

$$h_{fl} = \frac{0.023\, k_{fl}}{d_i} (Re_{fl})^{0.8} (Pr_{fl})^{0.4} \qquad \text{(VI-1)}$$

where k_{fl}, Re_{fl} and Pr_{fl} represent the coefficient of thermal conductivity, Reynolds number and Prandtl number of the fuel during flow through tubes of inside diameter d_i. The heat transfer coefficient h_i defined by equation (VI-1) represents an average value for established flow in fairly long tubes, and will therefore define values somewhat on the conservative side, when applied to tubes of relatively short length. The Reynolds number of the fuel flow may be re-expressed in the following manner.

$$Re_{fl} = \rho_{fl}\, u_{fl}\, d_i/\mu_{fl} = (d_i/\mu_{fl})(w_{fl}/A_{fl}) \qquad \text{(VI-2)}$$

where

$$A_{fl} = (\pi/4)(d_i^2)(N_{tubes}) = 0.785 d_i^2 (L_2 L_{nf}/s^2 d_o^2) \qquad \text{(VI-3)}$$

assuming a square pitch. Letting the parameter l_3 be defined by

$$l_3 = L_2/L_{nf} \qquad \text{(VI-4)}$$

equation (VI-2) may be rearranged to the form

$$Re_{fl} = d_o^2\, w_{fl}\, l_3\, s^2/(0.785\, L_2^2\, \mu_{fl}\, d_i) \qquad \text{(VI-5)}$$

Assuming the inside and outside diameters of the tubes to be 0.20 and 0.25 inch, respectively, and substituting equation (VI-5) into (VI-1) yields for the fuel-side heat transfer coefficient

$$h_{fl} = 1200\, \beta_{fl} \left[\frac{s}{L_2} \sqrt{l_3} \sqrt{\frac{w_{fl}}{1000}} \right]^{1.6} \qquad \text{(VI-6)}$$

where the parameter β_{fl} is defined by

$$\beta_{fl} = k_{fl}\, Pr_{fl}^{0.4}/\mu_{fl}^{0.8} \qquad \text{(VI-7)}$$

The flow resistance of the fuel-side of the heat exchanger is due to tube entrance and exit losses and the resistance of the tube section proper. Since the flow is incompressible, the loss in total pressure of the fuel due to the flow resistance may be defined by

$$\Delta p''_{f1} = \left[K_i + K_e + f_{f1} L_1/d_i\right] (\gamma_{f1} u_{f1}^2/288g) \qquad \text{(VI-8)}$$

where f_{f1} represents the standard Darcy friction factor. The inlet and exit loss coefficients K_i and K_e remain nearly constant for fixed pitch of the tubes. In this analysis it is assumed that

$$K_i + K_e = 0.75 \qquad \text{(VI-9)}$$

which corresponds to a pitch in the vicinity of 1.3. Then, by use of the continuity equation

$$u_{f1} = w_{f1}/(A_{f1} \gamma_{f1} 3600)$$

and equations (VI-3) and (VI-4) and the tube diameters of 0.20 and 0.25 inch, equation (VI-8) may be rearranged to the form

$$(\Delta p''_{f1})(\gamma_{f1}) = 0.684(0.75 + 5 f_{f1} L''_1) \left[\frac{s}{L''_2} \sqrt{l_3} \sqrt{\frac{w_{f1}}{1000}}\right]^4 \qquad \text{(VI-10)}$$

The fuel-side heat transfer coefficient h_{f1} may now be expressed as a function of the fuel-side pressure drop by equating the fuel-side flow parameter $(s/L''_2)(\sqrt{l_3})(\sqrt{w_{f1}/1000})$ which appears in equations (VI-6) and (VI-10). This yields

$$h_{f1} = 1400 \beta_{f1} (\Delta p''_{f1} \gamma_{f1})^{0.4}/(0.75 + 5 f_{f1} L''_1)^{0.4} \qquad \text{(VI-11)}$$

and illustrates the interrelationship of the heat transfer coefficient with permissible pressure drop of the fuel. Doubling the pressure drop increases the fuel-side heat transfer coefficient by about 32%.

2. Transfer-Fluid-Side Heat Transfer Coefficient and Flow Resistance

The forced convection coefficient of heat transfer for the transfer fluid on the outside surface of a tube bank, with the tubes having in-line arrangement, is closely defined by

$$h_t = 0.26(k_t/d_o)(Re_t)^{0.6}(Pr_t)^{0.33} \qquad \text{(VI-12)}$$

where the Reynolds number is defined by

$$Re_t = d_o w_t/\mu_t A_{min} \qquad \text{(VI-13)}$$

The minimum area of flow used in defining the Reynolds number is the area of flow between two in-line tubes.

$$A_{min} = \left[L_1(s - 1)d_o\right] (L_3/Nsd_o) \qquad \text{(VI-14)}$$

or

$$A_{min} = \left[(s-1)/s\right](L_1 L_3/N) \qquad \text{(VI-15)}$$

where N represents the number of passes through the exchanger made by the transfer fluid. Thus,

$$w_t/A_{min} = \left[s/(s-1)\right](N)(w_t/L_1 L_{nf})$$

Let the parameter l_2 be defined by

$$l_2 = L_2 N/L_1 \qquad \text{(VI-16)}$$

then, by use of equations (VI-4) and (VI-16)

$$w_t/A_{min} = \left[s/(s-1)\right](l_3\, l_2)(w_t/L_2^2)$$

or

$$w_t/A_{min} = 1.44 \times 10^5 (w_t/1000)\left[s/(s-1)\right](l_2\, l_3/L_2^{"2}) \qquad \text{(VI-17)}$$

Combining equation (VI-17) with (VI-13) and (VI-12) and introducing d_o equal to 0.25 inch and a pitch of 1.3 yields

$$h_t = 3670\, \beta_t \left[(l_2\, l_3)(w_t/1000)/L_2^{"2}\right]^{0.6} \qquad \text{(VI-18)}$$

where $\beta_t = Pr_t^{0.33} k_t/\mu_t^{0.6}$, for the heat transfer coefficient of forced convection during flow of the transfer fluid over the tube bank.

The pressure loss of the transfer fluid during passage through the exchanger may be evaluated by use of the tube-bank equations presented in Reference VI-1. The pressure loss equation for incompressible flow is

$$\Delta p_t^o/\gamma_t = 4\, f_t\, n\, u_{max}^2/2g \qquad \text{(VI-19)}$$

where n represents the total number of tube rows encountered by the fluid and f_t is a friction factor defined by

$$f_t = \left[0.044 + 0.08\, s/(s-1)^a\right]/Re_t^{0.15} \qquad \text{(VI-20)}$$

where $a = 0.43 + 1.13/s$.

The friction factor f_t is seen to be relatively insensitive to the Reynolds number of flow, so that by assuming a typical average value of 10,000 for the Reynolds number and using a pitch s equal to 1.3, the friction factor is equal to 0.136. Thus, by equation (VI-19)

$$\Delta p_t^o/\gamma_t = 0.272\, n\, u_{max}^2/g$$

The number of tube rows is defined by the number per pass multiplied by the N passes. Thus,

$$n = NL_2''/sd_o'' = NL_2''/1.3x0.25 = 3.08\ NL_2'' \qquad \text{(VI-21)}$$

By continuity,

$$u_{max} = w_t/(3600\ \gamma_t\ A_{min})$$

so that by use of equation (VI-17)

$$u_{max} = 40(w_t/1000)\left[s/(s-1)\right](l_2\ l_3/L_2''^2\ \gamma_t) \qquad \text{(VI-22)}$$

and

$$\Delta p_t''' \gamma_t = 6.75(NL_2'')\left[(l_2 l_3/L_2''^2)(w_t/1000)\right]^2 \qquad \text{(VI-23)}$$

The interrelation of the heat transfer coefficient and pressure drop on the transfer-fluid-side of the exchanger is defined by combining equations (VI-18) and (VI-23); the combination yields

$$h_t = 2065\ \beta_t\left[\Delta p_t''' \gamma_t/NL_2''\right]^{0.3} \qquad \text{(VI-24)}$$

Doubling the pressure drop across the heat exchanger on the transfer-fluid-side increases the heat transfer coefficient by about 23%.

3. Mean Temperature Difference for Heat Transfer

So as to permit algebraic reduction of the heat transfer relationships to yield equations defining directly the volume, weight and fluid pressure drop for the heat exchanger, it was found necessary to simplify existing methods for defining the mean temperature difference of heat transfer. The general arrangement of the heat exchanger is a single pass for the fuel and multipass on the transfer-fluid-side. With a single pass on the transfer-fluid-side, the heat exchanger becomes one of conventional crossflow, for which data are well known to define the mean temperature difference for heat transfer. Also, the mean temperature difference may be defined by the equivalent of counterflow when a large number of passes on the transfer-fluid-side are employed. Since this exchanger commonly will have several passes on the transfer-fluid-side, it is assumed that the mean temperature difference will be between the two extremes. A study of crossflow and counterflow data indicates that a reasonably good approximation to the mean temperature difference for several passes on one side and a single pass on the other is defined by the equation

$$\Delta T_{mX}/(T_{t-1} - T_{f1-1}) = 1 - 0.55(e_t + e_{f1}) \qquad \text{(VI-25)}$$

where e_t represents the effectiveness parameter for the transfer-fluid-

side defined by

$$e_t = (T_{t-1} - T_{t-2})/(T_{t-1} - T_{f1-1}) \qquad \text{(VI-26)}$$

and e_{f1} represents the effectiveness parameter for the fuel-side defined by

$$e_{f1} = (T_{f1-2} - T_{f1-1})/(T_{t-1} - T_{f1-1}) \qquad \text{(VI-27)}$$

Equation (VI-25) does not represent a good approximation to the mean temperature difference when the effectivenesses on both sides of the exchanger are high. Thus, the following limitations on the use of equation (VI-25) are introduced. The effectiveness on either side shall not exceed 0.70 and the sum of the effectiveness ($e_t + e_{f1}$) shall not exceed 1.1.

4. Overall Coefficient of Heat Transfer and Energy Balance

The transfer of heat from the transfer fluid to the fuel involves flow through three thermal resistances: that due to forced convection heat transfer between the transfer fluid and the outside surface of the tubes, that due to conduction of heat through the tube walls and that due to forced convection heat transfer between the inside surface of the tubes and the fuel. A study of the relative magnitudes of the three thermal resistances indicates that the thermal resistance of the tube wall is less than 5% of the total thermal resistance, and, therefore, will be ignored in the definition of the overall coefficient of heat transfer in order to simplify the resulting algebraic relationships.

The overall coefficient of heat transfer based on the inside tube surface area is

$$U_i = \frac{1}{(1/h_{f1}) + (d_i/d_o)(1/h_t)} \qquad \text{(VI-28)}$$

or, based on the assumed internal and external diameters of 0.2 and 0.25 inch for the tubes,

$$U_i = (1.25\ h_t)/(1 + 1.25\ h_t/h_{f1}) \qquad \text{(VI-29)}$$

By use of equations (VI-24) and (VI-11)

$$h_t/h_{f1} = 1.477 \left[\frac{\beta_t}{\beta_{f1}}\right]\left[\frac{\Delta p_t^o \gamma_t}{\Delta p_{f1}^g \gamma_{f1}}\right]^{0.4} \frac{(0.75 + 5 f_{f1} L_1'')^{0.4}}{(\Delta p_t^g \gamma_t)^{0.1} (N L_2'')^{0.3}} \qquad \text{(VI-30)}$$

Also, the inside surface area A_i is defined by

$$S_i = (\pi\ d_i\ L_1)(L_2\ L_{nf}/s^2\ d_o^2) \qquad \text{(VI-31)}$$

or,

$$S_i = 0.0414\, L_1'' L_2'' L_{nf}'' = 0.0414\, L_2''^3 N / l_2 l_3 \qquad \text{(VI-32)}$$

where the diameter of 0.2 inch and pitch of 1.3 is assumed. Then, by use of equation (VI-16), which defines the parameter l_2 as the flow length on the transfer-fluid-side to the flow length on the fuel-side, equation (VI-32) becomes

$$S_i = 0.0414\, (L_1'')^3 (l_2/N)^2 / l_3 \qquad \text{(VI-33)}$$

so that the product of overall heat transfer coefficient and surface area is

$$U_i S_i = \frac{107 \beta_t (\Delta p_t^{o''} \gamma_t / N L_2'')^{0.3} (l_2/N)^2 (L_1''^3/l_3)}{1 + 1.845 \left[\frac{\beta_t}{\beta_{f1}}\right] \left[\frac{\Delta p_t^o \gamma_t}{\Delta p_{f1}^o \gamma_{f1}}\right]^{0.4} \frac{(0.75 + 5 f_{f1} L_1'')^{0.4}}{(\Delta p_t^o \gamma_t)^{0.1} (L_1'' l_2)^{0.3}}} \qquad \text{(VI-34)}$$

The rate of heat transfer in the exchanger is related to the overall heat transfer coefficient and the mean temperature difference by

$$q_X = U_i S_i \Delta T_{mX} \qquad \text{(VI-35)}$$

Thus, by equation (VI-25)

$$q_X = U_i S_i \left[1 - 0.55(e_t + e_{f1})\right] (T_{t-1} - T_{f1-1}) \qquad \text{(VI-36)}$$

where $U_i S_i$ is defined by equation (VI-34). By energy balance,

$$q_X = w_{f1} c_{p-f1} (T_{f1-2} - T_{f1-1}) \qquad \text{(VI-37)}$$

and

$$q_X = w_t c_{pt} (T_{t-1} - T_{t-2}) \qquad \text{(VI-38)}$$

so by equations (VI-36), (VI-37) and (VI-38)

$$U_i S_i \left[1 - 0.55(e_t + e_{f1})\right] = w_{f1} c_{p-f1} e_{f1} = w_t c_{pt} e_t \qquad \text{(VI-39)}$$

which relates the product of the overall heat transfer coefficient and surface area to the two effectivenesses of heat exchange and the fuel and transfer fluid flow rates.

5. Physical Characteristics of Heat Exchanger

The following derivation presents the methods by which the working equations are established which are used to define the flow and no-flow dimensions, volume and weight of the fuel-to-transfer-fluid heat

exchanger. In an effort to establish practical working equations for use in cooling system evaluation and study, various assumptions are introduced during the process of equation derivation. These assumptions are indicated at the points in the analysis at which they are first used.

Equations (VI-23) and (VI-16) may be combined and solved for the transfer fluid flow rate. This yields

$$w_t = 384(\Delta p_t^{o''} \gamma_t)^{0.5}(l_2)^{0.5}(L_1'')^{1.5}/(N^2 l_3) \qquad \text{(VI-40)}$$

Then by direct combination of this expression with equations (VI-34) and (VI-39) one obtains

$$3.6c_{p_t}\left\{1 + 1.845(\beta_t/\beta_{f1})\left[\frac{\Delta p_t^{o''}\gamma_t}{\Delta p_{f1}^{o''}\gamma_{f1}}\right]^{0.4}\left[\frac{(0.75 + 5f_{f1}L_1'')^{0.4}}{(\Delta p_t^{o''}\gamma_t)^{0.1}(L_1''l_2)^{0.3}}\right]\right\} =$$

$$= \beta_t(l_2)^{1.2}(L_1'')^{1.2}(\Delta p_t^{o''}\gamma_t)^{-0.2}\left[\frac{1 - 0.55(e_t + e_{f1})}{e_t}\right] \qquad \text{(VI-41)}$$

Numerical evaluation of the various terms within the bracketed quantity on the left-hand side of this equation has indicated that the term

$$(0.75 + 5f_{f1}L_1'')^{0.4}/(L_1'')^{0.3}$$

may be roughly approximated by a constant value of 0.75. Then it becomes possible to solve equation (VI-41) explicitly for the heat exchanger dimension L_1, which represents the length of the tubes through which the fuel flows.

$$L_1'' = 2.88\left[\frac{c_{pt}}{\beta_t}\right]^{5/6}\frac{(\Delta p_t^{o''}\gamma_t)^{1/6}}{l_2}\left[\frac{e_t}{1 - 0.55(e_t + e_{f1})}\right]^{5/6} x$$

$$x\left\{1 + 1.4\left[\frac{\beta_t}{\beta_{f1}}\right]\left[\frac{\Delta p_t^{o''}\gamma_t}{\Delta p_{f1}^{o''}\gamma_{f1}}\right]^{0.4}\frac{1}{(\Delta p_t^{o''}\gamma_t)^{0.1}(l_2)^{0.3}}\right\}^{5/6} \qquad \text{(VI-42)}$$

Next, it is assumed that an average value of the specific gravity of the fuel is 0.77. As a representative transfer fluid a mixture of water and methyl alcohol (43% water by weight, -65°F freezing point) is assumed, having an average specific gravity of 0.87 in the temperature range encountered in this study. Thus, the value of $(\gamma_t/\gamma_{f1})^{0.4}$ is 1.04. The physical properties of the transfer fluid in that temperature range are such as to permit the approximation

$$(c_{pt}/\beta_t)^{5/6} = 3.31\left[1 - 0.156(T_{t-m}/100)\right] \qquad \text{(VI-43)}$$

The ratio β_t/β_{f1} has a typical numerical value of about 2.25. In equation (VI-42) the specific gravity of the transfer fluid raised to the 1/6-power is taken equal to 0.975. Lastly, in the same equation the term $(\Delta p_t^{o''} \gamma_t)^{0.1}$ is represented by the assumption that $(\Delta p_t^{o''} sg_t)^{0.1} = 1.11$. Introducing these constants into equation (VI-42) yields

$$L_1'' = (18.5/l_2)(\varphi_1)(\varphi_3)^{5/6}(\Delta p_t^{o''})^{1/6}(e_t/\varphi_2)^{5/6} \qquad \text{(VI-44)}$$

where

$$\varphi_1 = 1 - 0.156\ (T_{t-m}/100) \qquad \text{(VI-45)}$$

$$\varphi_2 = 1 - 0.55\ (e_t + e_{f1}) \qquad \text{(VI-46)}$$

and

$$\varphi_3 = 1 + (1.96/l_2^{0.3})(\Delta p_t^{o''}/\Delta p_{f1}^{o''})^{0.4} \qquad \text{(VI-47)}$$

The parameter l_2 requires evaluation for definition of the heat exchanger length in the direction of the transfer fluid flow. By equations (VI-10), (VI-23) and (VI-39) and assuming typical average values for the specific heat and specific weight of the fuel and transfer fluid, one obtains by direct solution

$$l_2 = \left[(0.75 + 5f_1 L_1'')/L_1''\right]^{1/3}(e_t/e_{f1})^{2/3}(\Delta p_t^o/\Delta p_{f1}^o)^{1/3} \qquad \text{(VI-48)}$$

The variation in the friction factor f_1 may be expressed as a function of the Reynolds' number, which in turn may be expressed as a function of the fuel-side pressure drop. The rearrangement of this type yields, then

$$l_2 = 0.9\left[\frac{1}{L_1''} + \frac{0.173}{(\Delta p_{f1}^{o''})^{0.1}}\right]^{1/3}\left[\frac{e_t}{e_{f1}}\right]^{2/3}\left[\frac{\Delta p_t^o}{\Delta p_{f1}^o}\right]^{1/3} \qquad \text{(VI-49)}$$

The parameter l_3 used to define the no-flow dimension L_3 is evaluated by solving equation (VI-23) for l_3. The length L_2 may be expressed as a function of L_1, N and l_2 by equation (VI-16). The transfer fluid flow rate is related to the heat transfer rate by

$$3.413\ q' = (w_t/1000)\ c_{pt}\ e_t(T_{t-1} - T_{f1-1}) \qquad \text{(VI-50)}$$

so that by assuming an average value for c_{pt} of 0.86 Btu per pound-^oR

$$w_t/1000 = 3.97\ q'/e_t(T_{t-1} - T_{f1-1}) \qquad \text{(VI-51)}$$

where q' represents the heat transfer rate in kilowatts. Introducing this relationship into the equation defining l_3 yields

$$l_3 = 0.72 \left[\frac{\sqrt{\Delta p_t^{o''} (L_1'')^3 l_2}}{N^2}\right] \left[\frac{e_t (T_{t-1} - T_{f1-1})}{q'}\right] \qquad \text{(VI-52)}$$

which may be used to define the no-flow dimension L_3.

The general procedure of evaluation for defining the dimensions of the heat exchanger core is to first assume a value of the parameter l_2. Then, by equation (VI-44) evaluate L_1'', which then permits evaluation of l_2 by use of equation (VI-49). The better value of l_2 would be used in equation (VI-44) to define a better value of L_1'', etc., with the trial-and-error process being continued until agreement is reached. Thereafter, for any selected value of N, representing the number of flow passes on the transfer fluid side, the dimension L_2'' may be evaluated by use of equation (VI-16) and the dimension L_3'' by equations (VI-52) and (VI-4).

During the evaluation of cooling systems employing heat exchangers of this type attention is directed more to the weight and spatial requirements of the heat exchanger than to the configuration of the core. Convenience in evaluation of weight and volume is obtained by combining the previously defined relationships and simplifying. This yields for the core volume

$$\frac{V_{X\text{-core}}'' (T_{t-1} - T_{f1-1})}{q'} = 111 \left[1 - 0.156 \frac{T_{t-m}}{100}\right]^{1.5} (e_t)^{0.25} \times \times \frac{\left[1 + 2.3 (\Delta p_t^o / \Delta p_{f1}^o)^{0.3} (e_{f1}/e_t)^{0.2}\right]^{1.25}}{(\Delta p_t^{o''})^{0.25} \left[1 - 0.55 (e_t + e_{f1})\right]^{1.25}} \qquad \text{(VI-53)}$$

When accurate evaluation of the core volume is required for relatively high effectiveness of heat exchange, e_t and e_{f1}, the term $1 - 0.55(e_t + e_{f1})$ in the denominator of equation (VI-53) may be replaced with a more accurate definition of the crossflow factor ζ, the ratio of the mean temperature difference to the inlet temperature difference $T_{t-1} - T_{f1-1}$. This procedure, in general, however, requires the use of tabular or graphical data and does not permit analytical combination of the heat exchanger characteristics with other components in the cooling system to permit evaluation of optimum operational conditions. Table VI-1 contains values of crossflow factors for ranges of effectiveness e_1 and e_2, representative, in general, of sides (1) and (2) of the heat exchange surface.

The total volume of the heat exchangers, i.e., core and headers, is assumed to be defined by

$$V_X'' = 1.25\, V_{X\text{-core}}'' \qquad \text{(VI-54)}$$

Table VI-1. Values of crossflow factor f, fluids unmixed (Reference VI-8)

e_2 \ e_1	0	0.1	0.2	0.3	0.4	0.5	0.6	0.7	0.8	0.9	1.0
0	1.000	0.947	0.893	0.838	0.781	0.721	0.657	0.586	0.502	0.388	0
0.1	0.947	0.893	0.840	0.786	0.729	0.670	0.605	0.533	0.448	0.338	0
0.2	0.893	0.840	0.785	0.734	0.677	0.617	0.552	0.480	0.398	0.292	0
0.3	0.838	0.786	0.734	0.682	0.625	0.565	0.502	0.430	0.348	0.247	0
0.4	0.781	0.729	0.677	0.625	0.569	0.513	0.449	0.378	0.300	0.206	0
0.5	0.721	0.670	0.617	0.565	0.513	0.456	0.394	0.326	0.251	0.167	0
0.6	0.657	0.605	0.552	0.502	0.449	0.394	0.334	0.271	0.201	0.128	0
0.7	0.586	0.533	0.480	0.430	0.378	0.326	0.271	0.213	0.151	0.089	0
0.8	0.502	0.448	0.398	0.348	0.300	0.251	0.201	0.151	0.100	0.052	0
0.9	0.388	0.338	0.292	0.247	0.206	0.167	0.128	0.089	0.052	0.022	0
1.0	0	0	0	0	0	0	0	0	0	0	0

The total weight of the heat exchanger, which includes the stored liquid, tubes, shell, headers, etc., is defined by

$$W_X = 0.0362\ V_{X\text{-core}}^{in^3} \qquad \text{(VI-55)}$$

or

$$W_X = 0.029\ W_X^{in^3} \qquad \text{(VI-56)}$$

where the weight is expressed in pounds with the volume in cubic inches. The weight-volume equations represent the average results of a fairly extensive weight analysis of a number of commercial liquid-to-liquid heat exchangers.

Air-to-Air Heat Exchanger

Certain cooling systems would employ air-to-air or gas-to-gas heat exchangers. Many cooling systems would require this type of heat exchanger if the system is indirect and the transfer fluid a gas. One of the common requirements for the use of air-to-air exchangers is with air cycle refrigeration systems, where, for example, in the bleed air

system it is normal to precool the bleed air by ram air before the bleed air passes through the turbine. The following material presents the basic relationships for forced convection heat transfer and flow resistance, and the application of these relationships to the establishment of working methods for defining the general characteristics of gas-to-gas heat exchangers in aircraft cooling systems.

The overall heat transfer process is considered to be: forced convection heat transfer between a flowing gas and a surface, conduction to an opposite surface through a metallic wall and forced convection heat transfer from this opposite surface to another flowing gas. In order to first present the equations in a general manner, the heat exchanger is considered as having two sides, referred to as side (1) and side (2), with the two sides separated by the metallic wall. The state of the gas at inlet on either side is denoted by use of the subscript (i) and at exit by the subscript (e). Figure VI-2 illustrates the flow system, inlet and exit temperatures and the definition of the dimensions L_1, L_2 and L_{nf}. The dimension L_1 represents the length of the flow path for the fluid on side (1), L_2 the comparable dimension for side (2) and L_{nf} the no-flow dimension of the heat exchanger.

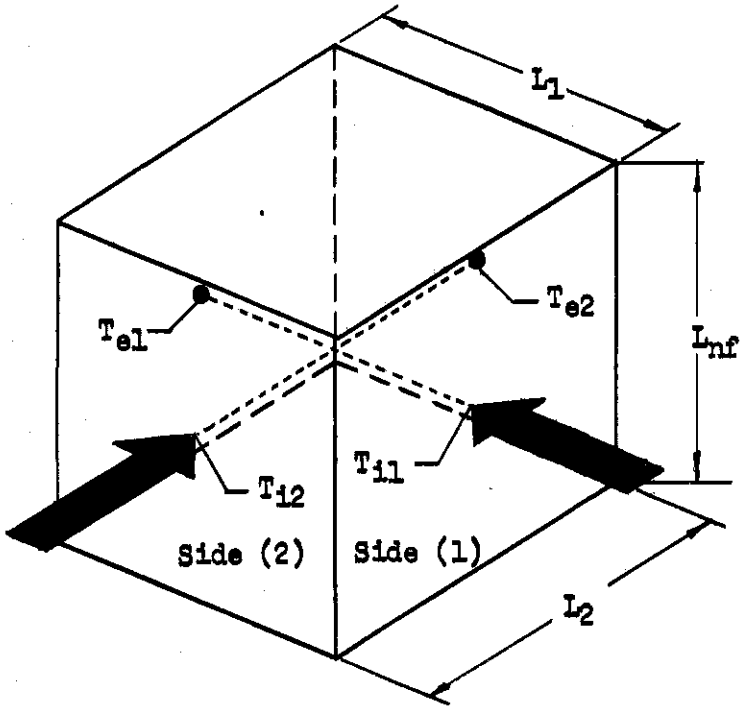

Figure VI-2. Schematic illustration of heat exchanger flow system and definition of dimensions.

1. Basic Relationships for Heat Transfer and Flow Resistance in Forced Convection

A common method of reporting heat transfer data in graphical form is with a plot of the factor

$$j = (h/G\,c_p)(Pr)^{2/3} \qquad \text{(VI-57)}$$

as a function of the Reynolds number Re, where h represents the heat transfer coefficient in Btu per hour-square foot-^{o}F, G the mass velocity in pounds per hour-square foot and Pr the Prandtl number of the fluid. Many examples of data of this type are found in Reference VI-2. It is often possible to represent such graphical data by an empirical equation of simple form, such as

$$j = C_j\,(Re)^{-r} \qquad \text{(VI-58)}$$

since the factor j is commonly a power-function of the Reynolds number for some ranges of values of the Reynolds number. For turbulent flow in circular channels the coefficient C_j has the generally accepted value of 0.023 and r the value of 0.20, and defines, therefore, the Darcy friction factor divided by a factor of 8 for turbulent flow over hydraulically smooth surfaces.

In order to determine or prescribe the pressure drop or power loss of fluids in a heat exchanger, it is necessary to have data describing the friction characteristics of heat exchanger surfaces. These friction characteristics are normally expressed by use of a friction factor f, defined by the equation

$$\Delta p = \gamma\,(fL/4r_h)(u^2/2g) \qquad \text{(VI-59)}$$

where the hydraulic radius r_h is defined as

$$r_h = AL/S \qquad \text{(VI-60)}$$

with A representing the cross-sectional area of flow, L the length of the flow passage and S the wetted surface. For a circular tube,

$$A = (\pi/4)d^2$$

and

$$S = \pi dL$$

whence

$$r_h = d/4 \qquad \text{(VI-61)}$$

For a hydraulically smooth tube the friction factor may be approximated by the equation

$$f = 0.184(Re)^{-0.2} \qquad \text{(VI-62)}$$

and applies quite accurately for values of the Reynolds number from 5000 to 200,000. For heat transfer surfaces other than tubes, friction factor data are usually presented in graphical form, as plots of the factor f versus the Reynolds number Re. Such data can often be expressed by an empirical equation of the form

$$f = C_f(Re)^{-m} \qquad \text{(VI-63)}$$

of which equation (VI-62) would be a special case.

The process of transferring heat from one fluid to another through an intermediate separating surface may be visualized as the transfer of heat through thermal resistances. In the fundamental equation for heat transfer between a fluid and a surface,

$$q = h S \Delta T_{mX} \qquad \text{(VI-64)}$$

where h is the coefficient of heat transfer, S is the surface area, and ΔT_{mX} is the temperature difference between surface and fluid, the product (hS) can be considered as a thermal conductance, or its reciprocal (1/hS) as a thermal resistance. The resistance equation of the heat transfer process may be written as

$$R_c = R_1 + R_s + R_2 \qquad \text{(VI-65)}$$

where the combined or overall thermal resistance is equal to the sum of the resistance (reciprocal of conductance) on the side of the first fluid, plus the resistance of the separating surface, plus the resistance on the side of the second fluid. Since the resistance to heat flow through the separating surface is usually quite small due to high metal thermal conductivities, it is neglected in this analysis. Equation (VI-65) may therefore be rewritten as,

$$R_c = (1/h_1 S_1 \eta_1) + (1/h_2 S_2 \eta_2) \qquad \text{(VI-66)}$$

where the factors η_1 and η_2 are the temperature effectiveness of the heat transfer surfaces. This concept pertains to extended surfaces, such as fins, where due to the thermal resistance of the fin material itself, all of the fin surface is not at the same temperature as the parent surface to which it is attached. The temperature effectiveness of a straight fin η_F with constant cross section is given by the equation

$$\eta_F = \left[\tanh (m L_F)\right] \Big/ m L_F \qquad \text{(VI-67)}$$

where

$$m = \sqrt{(2h)/(k t_F)} \qquad \text{(VI-68)}$$

In these equations, L_F represents the projective length of the fin, h the heat transfer coefficient between the surrounding fluid and the fin, k the thermal conductivity of the fin material and t_F the thickness of the fin. With the fin surface area represented by S_F and the total heat transfer surface area by S, the overall temperature effectiveness of a surface η is related to the temperature effectiveness of a fin η_F by the relationship

$$\eta = 1 - (S_F/S)(1 - \eta_F) \qquad \text{(VI-69)}$$

For heat exchanger surfaces which do not have extended surface, such as simple flat plates or plain tubes, the temperature effectiveness is unity, since S_F is zero.

If the ratio of R_1 to R_2 is denoted by ϕ, equation (VI-65) may be written as

$$\phi/R_1 = (1 + \phi)/R_c \qquad \text{(VI-70)}$$

It is convenient to introduce a concept discussed at some length in Reference VI-2, whereby the overall thermal resistance is defined by

$$R_c = 1/\left[(NTU)(w\ c_p)_{min}\right] \qquad \text{(VI-71)}$$

Reference VI-2 gives values of the factor NTU for a large number of heat exchanger flow arrangements. This factor may be thought of as the ratio of the temperature rise of the fluid having the smallest thermal capacity rate $(w\ c_p)_{min}$ to the effective temperature potential for heat transfer between the two fluids. Thus,

$$NTU = (T_e - T_i)_{max}/\Delta T_{mX} \qquad \text{(VI-72)}$$

where the meaning of the terms may be clarified by examination of the defining equation

$$q = \Delta T_{mX}/R_c = (w\ c_p)_{min}(T_e - T_i)_{max} \qquad \text{(VI-73)}$$

Equation (VI-70) may then be rewritten in the form

$$h_1 S_1 \eta_1 = \left[(1 + \phi)/\phi\right](NTU)(w\ c_p)_{min} \qquad \text{(VI-74)}$$

Substitution of equations (VI-57) and (VI-60) in equation (VI-74), rearranging and simplifying yields

$$(j\eta)_1(wc_p)_1(Pr)_1^{-2/3}(L/r_h)_1 = \left[(1+\phi)/\phi\right](NTU)(wc_p)_{min} \qquad \text{(VI-75)}$$

This equation will be used later in the development of a general relationship for the flow resistance characteristic of a heat exchanger expressed in terms of its thermal performance characteristics.

Equation (VI-54) is now considered to develop an expression for the resistance characteristic of a heat exchanger. In addition to the pressure loss required to pump a fluid through a heat exchanger core, there are additional losses associated with entrance and exit of the fluid to and from the core. These are conveniently treated in the manner of a minor loss such as occur due to abrupt expansions and contractions in pipe lines. A suitable equation for these losses is, Reference VI-3,

$$\Delta p = \gamma K (u^2/2g) \tag{VI-76}$$

The overall pressure loss of a fluid entering, traversing, and leaving the core of a heat exchanger is then given by

$$\Delta p = \gamma(u^2/2g)\left[(fL/4r_h) + K\right] \tag{VI-77}$$

which is obtained by adding equations (VI-59) and (VI-76). Thus, the coefficient for the total loss is defined by

$$K_o = \left[(fL/4r_h) + K\right] \tag{VI-78}$$

for use in the equation

$$\Delta p = \gamma K_o(u^2/2g) \tag{VI-79}$$

Equation (VI-78) may be solved for the ratio (L/r_h), and then this quantity may be substituted into equation (VI-75). The result, after rearranging, is

$$K_{o1} = K_1 + \left[\frac{(Pr)_1^{2/3}}{4(j\eta/f)_1}\right]\left[\frac{(1+\phi)(NTU)(wc_p)_{min}}{\phi(wc_p)_1}\right] \tag{VI-80}$$

Equation (VI-80) expresses the flow resistance characteristic of the heat exchanger on side (1) in terms of the entrance and exit loss coefficient K, the thermal resistance ratio ϕ, the fluid flow rates w_{min} and w_1, the physical properties Pr and c_p, and the parameter $(j\eta/f)$. The quantity NTU appearing in the equation is a function of the flow rates $(wc_p)_1$ and $(wc_p)_2$, the flow arrangement (crossflow, single or multiple pass, counterflow, etc.) and of the thermodynamic effectiveness, to be discussed later. An analogous derivation for the overall loss coefficient on side (2), K_{o2}, gives the result,

$$K_{o2} = K_2 + \left[\frac{(Pr)_2^{2/3}}{4(j\eta/f)_2}\right]\left[\frac{(1+\phi)(NTU)(wc_p)_{min}}{(wc_p)_2}\right] \tag{VI-81}$$

The appearance of the parameter $(j\eta/f)$ in equations (VI-80) and (VI-81) is of special interest. If the heat exchanger surface consists

of plain tubes through which the fluid flows, where $\eta = 1$, the parameter has a numerical value of 0.125, so that the parameter, as appearing in equations (VI-80) and (VI-81) is a constant, for this geometry, although the factors j and f are functions of the Reynolds number. This condition also holds approximately for many other useful heat exchanger surfaces, including many of the compact surfaces described in Reference VI-2. For surfaces having extensions, or fins, a complication is introduced by the fact that the temperature effectiveness of the surface η_F is a function of both the Reynolds number and the temperature level of the fluid. Calculation studies have shown, however, that the effect of temperature level on the parameter $(j\eta/f)$ is small, so that it is possible to approximate its value with a single, constant value for any surface type which is appropriate for a wide range of Reynolds numbers and fluid temperatures.

Another important parameter in the design of heat exchangers is the power-to-cooling ratio, defined as the ratio of the power required to pump the fluid through the exchanger to the heat transferred in the exchanger. This parameter is mathematically defined by the equation,

$$(PC) = (w/\gamma)(\Delta p/778q) \qquad \text{(VI-82)}$$

Substituting equation (VI-79) into equation (VI-82), with substitution of

$$u = w/(3600\gamma A)$$

gives

$$(PC) = (w^3/\gamma^2 A^2)\left[\frac{1}{2g \times 778 \times 3600^2\, q}\right] K_o \qquad \text{(VI-83)}$$

By use of equation (VI-60), equation (VI-83) becomes

$$(PC) = (w^3/\gamma^2)(L/S)^2\left[\frac{1}{2g \times 778 r_h^2 \times 3600^2\, q}\right] K_o \qquad \text{(VI-84)}$$

where K_o may be defined by either equation (VI-80) or (VI-81) depending as the quantities of equation (VI-84) are applicable to side (1) or side (2) of the exchanger.

It is now of interest to combine certain of the foregoing equations into a form which will describe the frontal area requirements of the heat exchanger. Solving equation (VI-84) for $S/L = A/r_h$, substituting K_{o1} from equation (VI-80), and rearranging gives

$$A_1 = \left[\frac{r_h S}{L}\right]_1 = \left[\frac{w}{\gamma}\right]_1 \sqrt{\frac{w_1}{q(PC)_1}} \left[\frac{1}{3600\sqrt{2g \times 778}}\right] \times$$

$$\sqrt{K_1 + \left[\frac{(Pr)_1^{2/3}}{4(j\tau/f)}\right]\left[\frac{(1+\phi)(NTU)(wc_p)_{min}}{\phi(wc_p)_1}\right]} \qquad \text{(VI-85)}$$

Subsequent use will be made of this equation in the discussion of the effect of flow arrangement and other factors on heat exchanger shape.

A parameter commonly used to describe the performance of a heat exchanger is the effectiveness. In the case of an exchanger transferring heat between two fluids, there are two values of the effectiveness which may be defined, one for each side. These are as follows,

$$e_1 = \frac{q}{(wc_p)_1(T_{i2} - T_{i1})} = \frac{(T_e - T_i)_1}{(T_{i2} - T_{i1})} \qquad \text{(VI-86)}$$

and,

$$e_2 = \frac{q}{(wc_p)_2(T_{i2} - T_{i1})} = \frac{(T_e - T_i)_2}{(T_{i2} - T_{i1})} \qquad \text{(VI-87)}$$

In addition, there is a significant parameter called the thermodynamic effectiveness of an exchanger, defined as the ratio of maximum actual temperature rise of either fluid to the maximum temperature rise possible. This is given by

$$e_{th} = \frac{q}{(wc_p)_{min}(T_{i2} - T_{i1})} = \frac{(T_e - T_i)_{max}}{(T_{i2} - T_{i1})} \qquad \text{(VI-88)}$$

From equations (VI-86), (VI-87) and (VI-88), it is apparent that the thermodynamic effectiveness is equal to whichever effectiveness is the larger, i.e., either e_1 or e_2. In this connection it is noteworthy that combining equations (VI-86) and (VI-87) gives,

$$e_1/e_2 = (wc_p)_2/(wc_p)_1 \qquad \text{(VI-89)}$$

whereby it is observed that the side having the largest effectiveness value is that side which has the least thermal capacity rate $(wc_p)_{min}$.

With the inlet temperatures T_{i2} and T_{i1}, the heat transfer rate q, and the thermal capacity rates $(wc_p)_1$ and $(wc_p)_2$ specified, equation (VI-88) may be used to calculate the thermodynamic effectiveness. This value of e_{th} is then used, together with the ratio $(wc_p)_{min}/(wc_p)_{max}$, to obtain the value of NTU from charts for the various flow arrangements as given in Reference VI-2. The factor NTU is then applied in equation

(VI-85) for finding the frontal flow area of the exchanger.

It is next desired to derive an expression for the length required of the heat exchanger core. Equation (VI-78) may be solved for L to give

$$L = (K_o - K)(4r_h/f) \tag{VI-89}$$

But by equation (VI-63)

$$L = (K_o - K)(4r_h)\left[4r_h \gamma (3600\ u)/\mu\right]^m / C_f \tag{VI-90}$$

and from equation (VI-83)

$$u = \left[2g \times 778\ q(PC)/(w\ K_o)\right]^{1/2} \tag{VI-91}$$

Thus, by substitution,

$$L = \left[\frac{K_o - K}{K_o^{m/2}}\right]\left[\frac{\gamma}{\mu}\right]^m\left[\frac{q(PC)}{w}\right]^{m/2}\left[\frac{(4r_h)^{1+m}}{C_f}\ (2g \times 778)^{m/2}(3600)^m\right] \tag{VI-92}$$

Equation (VI-92) gives the flow length of the exchanger for either the side associated with fluid (1) or that associated with fluid (2). The required surface area for heat transfer may now be defined by use of the relationship

$$S = AL/r_h \tag{VI-93}$$

As previously indicated, the equations for K_o, L, A and S are appropriate for either side (1) or side (2) of the exchanger. Unfortunately, however, it is not possible to design each side of the exchanger using these relationships, since once these quantities are established for one side, there are physical and thermal limitations which must be satisfied by the other side. For example, in a heat exchanger of established core surface, there is a fixed relationship between S_1 and S_2, the surface areas wetted by each fluid. It is therefore necessary, once the first side has been designed, to make the second side furnish a sufficient heat transfer coefficient that the relationship

$$\phi = R_1/R_2 = (h_2\ \eta_2 S_2)/(h_1\ \eta_1 S_1) \tag{VI-94}$$

is satisfied, where ϕ is the same value as selected for the design of the first side of the exchanger. If equations (VI-80), (VI-85), (VI-92) and (VI-93) are used to obtain K_{o1}, A_1, L_1 and S_1, the design requirements are satisfied if L_2 is determined from

$$L_2/L_1 = (r_{h2}/r_{h1})(S_2/S_1)(A_1/A_2) \tag{VI-95}$$

which is derived from the definition of the hydraulic radius, equation (VI-60). In equation (VI-95) the ratios r_{h2}/r_{h1} and S_2/S_1 would be known by the type of core structure used, thus making it necessary only to give special attention to the method of determining the flow areas A_1 and A_2. The value of the flow area A_1 is determined from the continuity relationship

$$A_1 = w_1/(3600\,\gamma u_1) \tag{VI-96}$$

where the velocity u_1 is defined by use of equation (VI-91). In order to establish the flow area A_2, it is necessary to examine the relationships which govern the heat transfer coefficient on the second side. By combining equations (VI-57) and (VI-58) and expressing the mass velocity G by means of the Reynolds number of flow defined by

$$Re = 4r_h G/\mu \tag{VI-97}$$

one obtains for the heat transfer coefficient

$$h = C_j(c_p\mu/4r_h)(Pr)^{2/3}(Re)^{(1-r)} \tag{VI-98}$$

which, for a particular core surface structure, is a function of the Reynolds number and the fluid temperature. Since the overall fin temperature effectiveness η_F of a given surface is a function of the heat transfer coefficient h, and since the variation of the effectiveness is small compared to that of the coefficient h, it follows that a satisfactory approximation for the product $h_2\,\eta_2$ is,

$$h_2\,\eta_2 = C_{h\eta}\,(Re)^n \tag{VI-99}$$

In this equation both $C_{h\eta}$ and the exponent n are assumed to be strictly a function of temperature. It has been found possible, however, to define an average value of n suitable for a wide temperature range (such as -100° to $+500^\circ$F for air), and correlate data for the $h\eta$ product as a function of the Reynolds number by assuming that only $C_{h\eta}$ varies with temperature. It is therefore convenient to write

$$G_2 = (\mu/4r_h)(h_2\,\eta_2/C_{h\eta})^{1/n} \tag{VI-100}$$

But from equations (VI-70) and (VI-71)

$$\phi(h_1\,\eta_1 S_1) = (1+\phi)(NTU)(wc_p)_{min} = h_2\,\eta_2 S_2 \tag{VI-101}$$

Thus,

$$h_2\,\eta_2 = (1+\phi)(NTU)(wc_p)_{min}/S_2 \tag{VI-102}$$

Using the continuity equation in the form

$$A_2 = w_2/G_2$$

and equations (VI-96), (VI-100) and (VI-101) substituted in equation (VI-95) yields the flow length on side (2) as

$$L_2 = L_1\left[\frac{r_{h2}}{r_{h1}}\right]\left[\frac{S_2}{S_1}\right]\left[\frac{w_1}{\gamma_1}\right]\left[\frac{q(PC)}{w_1 K_o}\right]^{-1/2}\left\{\frac{\left[(1+\phi)(NTU)(wc_p)_{min}\right]^{1/n}}{w_2(S_1)^{1/n}}\right\}x$$

$$x\left[\frac{\mu_2}{3600\, r_{h2}\sqrt{2g\times 778}\, 4(C_{h\eta})^{1/n}}\right] \qquad \text{(VI-103)}$$

The only remaining dimension of the heat exchanger is L_{nf}, the no-flow dimension. Since this dimension is a function of the core surface geometry as well as the flow arrangement of the exchanger, it is not discussed at this point. Examples of determining the no-flow dimension of an exchanger are given later in cases of designs for which the core surface geometry and the flow arrangement have been selected.

The power-to-cooling ratio of the second side of the heat exchanger is similar to the length L_2, in that it is a dependent variable which must satisfy the conditions resulting from the design of the first side of the heat exchanger. Using equation (VI-84) and the definition of the hydraulic radius to eliminate the flow areas A_1 and A_2, the second side power-to-cooling ratio is given by,

$$\frac{(PC)_2}{(PC)_1} = \left[\frac{w_2}{w_1}\right]^3\left[\frac{\gamma_1}{\gamma_2}\right]^2\left[\frac{K_{o2}}{K_{o1}}\right]\left[\frac{r_{h1}}{r_{h2}}\right]^2\left[\frac{S_1}{S_2}\right]^2\left[\frac{L_2}{L_1}\right]^2 \qquad \text{(VI-104)}$$

The relationships developed to this point are generally applicable to the design of heat exchangers transferring heat between two fluids in forced convection. They are suitable for fluids, either gas or liquid, so long as basic data for j factors and friction factors can be suitably correlated in the forms shown.

Thus far there has been no consideration given to the questions of selecting core surfaces or flow arrangements. Consideration is next given to these factors, after which it will be possible to show the application of the equations developed here to the design of a number of particular types of heat exchangers.

2. Heat Exchanger Flow Arrangements and Core Surfaces

There are a number of flow arrangements used in heat exchanger construction. The heat exchanger designer must select a flow arrangement suitable to the design problem, where in general the basis of selection includes both physical arrangement and thermal performance con-

siderations. From a thermal performance standpoint, the best flow arrangement for an exchanger is the counterflow arrangement, since this type always requires the least surface area and the smallest size for a given heat transfer rate and temperature potential. However, there are physical difficulties encountered in the construction of a counterflow exchanger, since the problem of suitably manifolding the two fluids can be complicated. Therefore, in many cases it is practical to use some form of crossflow exchanger. Although the manifolding of a crossflow exchanger is less involved, the size is somewhat greater than in counterflow for comparable operating conditions, and the maximum attainable values of thermodynamic effectiveness are not as high as with the counterflow arrangement. This latter difficulty can be partially overcome by the use of multipass crossflow, where the greater the number of passes, the more closely the counterflow performance is approached. In penalty for this, however, the multipass arrangements require return headers, adding to the complexity of construction and imposing additional resistance to flow of the heat transfer fluids.

For purposes of cooling systems studies, it is desired to select a flow arrangement which is generally applicable to a wide variety of physical situations, but which still gives heat exchanger designs which represent reasonably the order of size that any flow arrangement would require under the same conditions. In order to do this, the effect of flow arrangement on size is now considered.

Referring to equation (VI-85), the only variable determined by flow arrangement that affects the heat exchanger size is the factor NTU, for fixed conditions of specified thermodynamic effectiveness, pressure level, and flow rates of the two fluids. Reference VI-2 presents a chart showing the effect of various flow arrangements on the value of NTU. These data show that the maximum ratio of the NTU for a single-pass crossflow arrangement (fluids unmixed) to the NTU for a counterflow arrangement is of the order of 2:1 within the practical range of values of NTU. From equation (VI-85) it is therefore apparent that the flow area would vary by $(2)^{0.5}$ or in a ratio of about 1.4:1. Since the frontal dimensions are approximately proportional to the square root of the area **A**, it follows that the frontal dimensions would vary by roughly 20%. It follows, therefore, that the frontal dimensions of an exchanger would not be reduced by more than about 20% by use of any flow arrangement superior in performance to single-pass crossflow with fluids unmixed. The arrangement using a single-pass crossflow exchanger with one fluid mixed is on the opposite side from the counterflow, so that the frontal dimensions for this case would be larger, and to a similar extent. Therefore, single-pass crossflow with fluids unmixed appears to be a reasonably representative flow arrangement, and is neither the smallest nor largest heat exchanger that will fit a specified performance condition. Furthermore, it appears to be physically suited to many applications because of its simple manifolding, thus making it ideal for a general comparative study of cooling systems.

The next item to be considered is the selection of the type of

core surface for a heat exchanger. The surface selected should afford the best available characteristics of heat transfer rate per unit volume of core, at a specified temperature potential and per unit of power expended to pump the fluids. The core, for aircraft service, should also have the least weight compatible with pressure-safety or reliability requirements. Data are available in Reference VI-2 describing the characteristics of a large number of surfaces in a form convenient for comparing their performance on the basis of heat transfer rate, size, and power requirements. A study of these data has indicated that the surface shown in Figure VI-3 is well suited for use in aircraft heat exchangers. Reference VI-4 indicates that this surface should be suitable for working pressures up to 450 psi for the temperature range -350° to +300°F, and up to 200 psi for the temperatures up to 600°F, when the core is assembled by brazing aluminum plates and fin structures together. The separator plates, which sandwich the fin structure, are 0.032 inch thick.

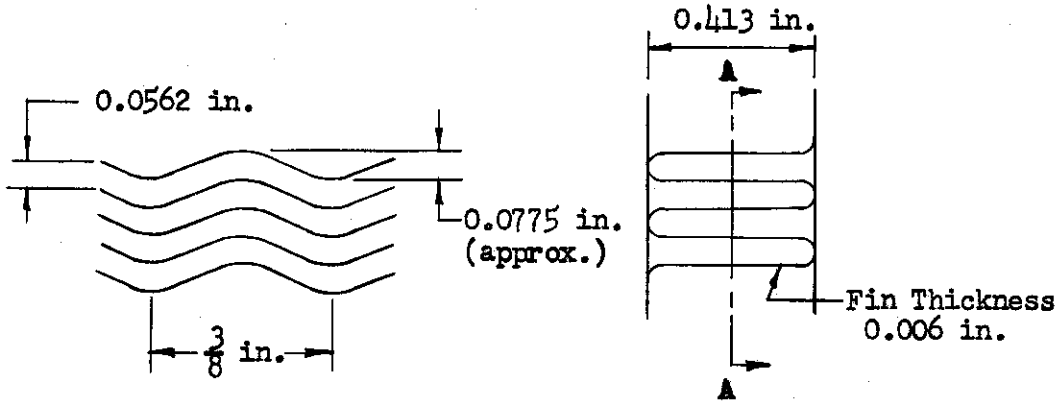

Section A-A

Figure VI-3. Ruffled plate-fin surface. Surface designation, 17.8-3/8-R, Reference VI-2.

A surface of the type shown in Figure VI-3 is well suited to heat exchanger construction, since the core can be built up of layers, or laminae, consisting of the corrugated fin stampings and the separator plates alternated and brazed together. A core so fabricated requires very little by way of external pressure casing, since it is a pressure-tight unit of itself when manifolds are attached and when small end pieces are brazed in to close off those areas otherwise closed off only by the outermost fin.

With the development of the basic relationship governing dimensions and performance of forced convection heat exchangers, together with the selection of flow arrangement and core surface, it is possible to proceed to the development of design procedures for air-to-air heat exchangers.

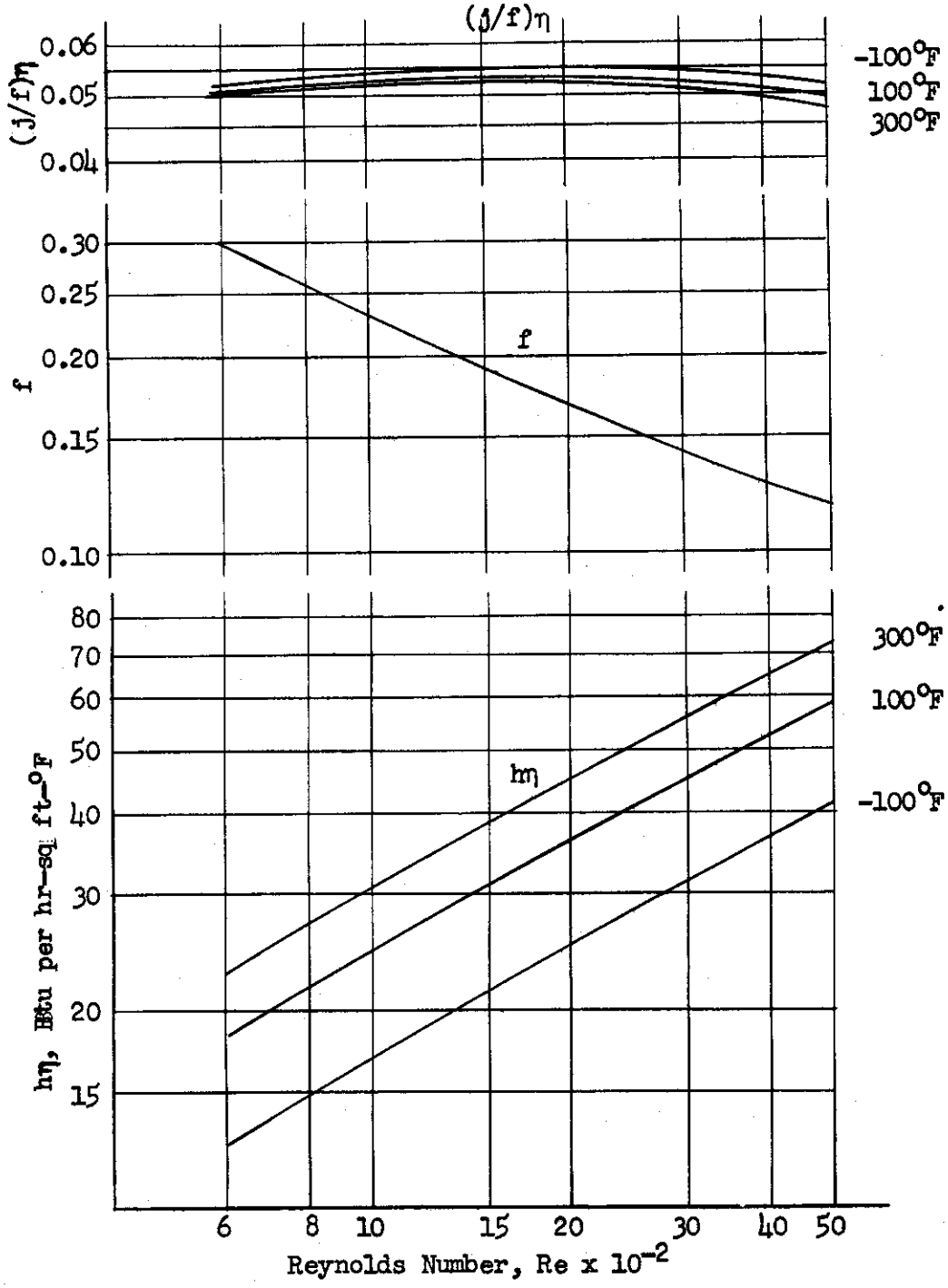

Figure VI-4. Plots of the design factors $(j/f)\eta$ and $h\eta$ for an air-to-air crossflow exchanger with surface 17.8-3/8-R.

3. Design Procedures

The air-to-air heat exchanger is considered in the form of a single-pass crossflow arrangement with the core surface of the type illustrated in Figure VI-3. The construction of this surface is such that it is impossible for the air to mix, during flow through the exchanger, so the condition of the fluids being unmixed pertains. The same core surface is used for each side.

Figure VI-4 presents the information which must be prepared for the method of heat exchanger design to be used. The data shown are based on those presented for this surface in Reference VI-2. From Figure VI-4 it may be seen that the friction factor data can be represented in the form of a power function, as indicated for equation (VI-63). A suitable equation for these data has been determined to be

$$f = 4.73(Re)^{-0.434} \qquad \text{(VI-105)}$$

The plots of the parameter $j\eta/f$ shown in Figure VI-4 are calculated from the j-factor data of Reference VI-2, by selecting a range of air temperatures and using equations (VI-67), (VI-68) and (VI-69) to evaluate the temperature effectiveness η. It is apparent from Figure VI-4 that the parameter $j\eta/f$ is substantially constant for this application. A value of $j\eta/f$ of 0.051 has been selected as suitable to represent the parameter in the range -100° to 500°F, and for Reynolds numbers from 500 to 5000, or for reasonable extrapolations of this range. As explained in Reference VI-2, for the selected surface, the fin length is one-half the spacing between separator plates, i.e., 0.206 inch.

An evaluation of the product $h\eta$ for this surface and for the temperature range from -100° to 500°F was conducted and thereby determined that a fairly accurate representation of this variation is described by the equation

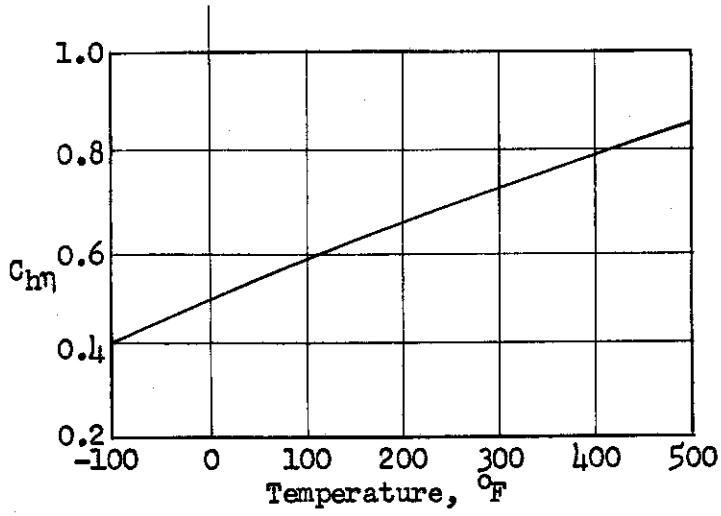

Figure VI-5. Variation of the coefficient $C_{h\eta}$ (equation VI-106) with temperature.

$$h\eta = C_{h\eta}(Re)^{0.542} \qquad \text{(VI-106)}$$

where the coefficient $C_{h\eta}$ is a function of the air temperature as shown in Figure VI-5.

It is next desired to calculate the values of the loss coefficients K_1 and K_2 as applied to a core of the selected 17.8-3/8-R surface. For one lamination the ratio of free frontal area available for fluid flow to gross frontal area is 0.82. However, one lamination constitutes only one-half of the total gross frontal area for that lamination, since each such lamination is matched by another for flow of the other fluid. Since the entire area occupied by the other lamination is blocked, the true area ratio α for flow of either fluid is only 0.41. This area ratio defines an abrupt expansion loss coefficient of 0.35 (Reference VI-3). The coefficient for entrance loss is difficult to determine in the absence of any data or information on the sharpness of the entrance corners. A value on the order of 0.35 is reasonably representative, so

$$K_1 + K_2 = 0.35 + 0.35 = 0.70 \qquad \text{(VI-107)}$$

With the selection of flow arrangement and surface, it is now possible to derive an equation for the no-flow dimension L_{nf} of the exchanger. The flow frontal area of the exchanger, from geometrical considerations, is given by

$$A_1 = L_{nf} L_2 \alpha$$

or

$$L_{nf} = A_1/L_2 \alpha \qquad \text{(VI-108)}$$

where α is the ratio of free flow to gross frontal area, as calculated above to be 0.41. Therefore,

$$L_{nf} = 2.44 A_1/L_2 \qquad \text{(VI-109)}$$

which, together with the equations developed in the basic analysis makes it possible to completely design the core of the air-to-air heat exchanger.

In Figure VI-6 are shown physical properties of air appearing in the design equations, namely, specific heat c_p, viscosity μ, and standard specific weight γ/δ. The figure also contains a plot of $Pr^{2/3}/(4j\eta/f)$ for $j\eta/f = 0.051$ and a plot of $\mu_2 C_{h\eta}^{-1/n}$, appearing in equation (VI-103), based on the variation of $C_{h\eta}$ with temperature shown in Figure VI-5 and the value for n of 0.542 indicated by equation (VI-106). Thus

$$\varphi_1 = \mu_2(C_{h\eta})^{-1.846} \qquad \text{(VI-110)}$$

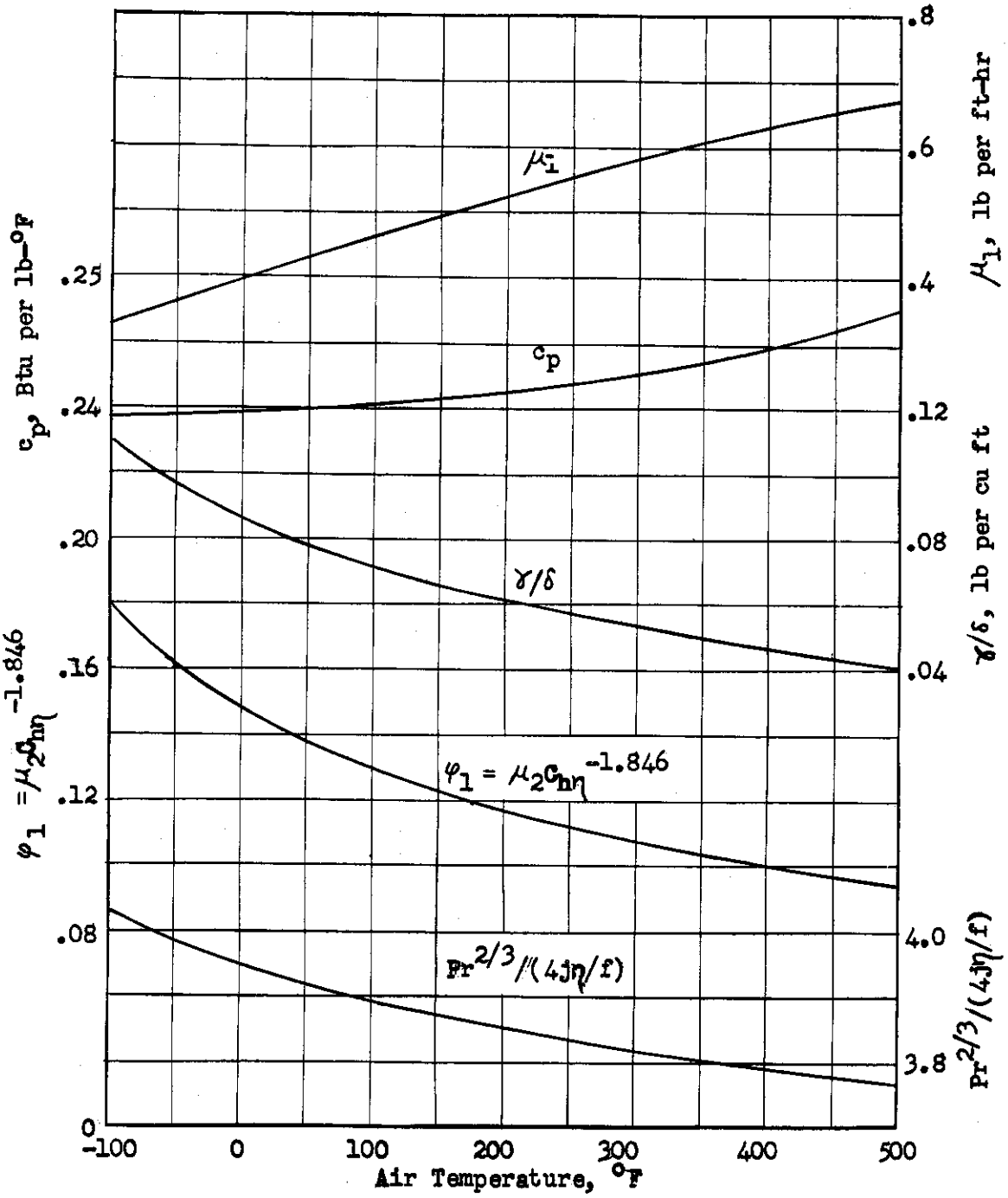

Figure VI-6. Properties of air and design parameters for air-to-air heat exchanger.

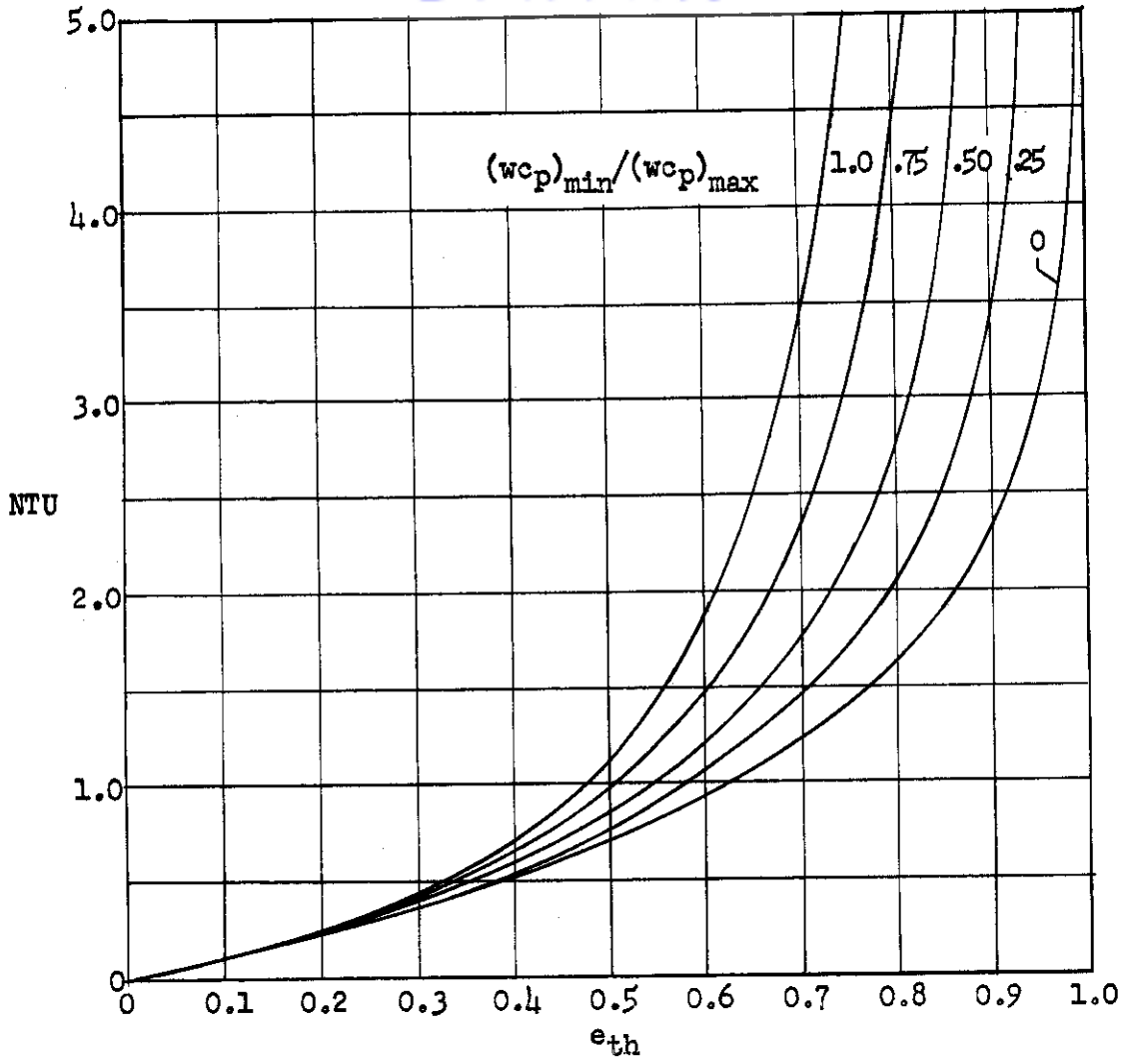

Figure VI-7. NTU-effectiveness relationships for crossflow of unmixed fluids.

Figure VI-7 contains curves defining the parameter NTU as a function of the thermodynamic effectiveness e_{th} and the ratio of thermal capacity rates for crossflow and unmixed fluids (Reference VI-2).

The methods may be used to illustrate the design of an air-to-air heat exchanger for the following conditions:

$w_1 = w_2 = 1000$ lb/hr
$S_1 = S_2 = 1.0$ sq ft
$q = 10{,}000$ Btu/hr

$T_{i1} = 0°F$
$T_{i2} = 100°F$
$(\overline{PC})_1 = 0.10$
$\Phi = 1.0$
$p_{i1} = 14.7$ psia
$p_{i2} = 14.7$ psia

The hydraulic radius r_h of the selected surface is 0.00174 feet. The parameter $j\eta/f$ has the selected average value of 0.051, the exponent m is 0.434, the exponent n=0.542 and the coefficient C_f=4.73, the coefficients K_1 and K_2 are each 0.7. The exit temperatures of the air on sides (1) and (2) are defined by heat balance, i.e.,

$$q = w_1 c_{p-1}(T_{e1} - T_{i1})$$

or

$$10{,}000 = 1000 \times 0.239(T_{e1} - 0)$$

$$T_{e1} = 41.7°F$$

where the factor 0.239 represents the specific heat c_p (Figure VI-6) for the average air temperature at side (1) of 20.8°F. Also,

$$q = w_2 c_{p-2}(T_{e2} - T_{i2})$$

or

$$-10{,}000 = 1000 \times 0.240 (T_{e2} - 100)$$

$$T_{e2} = 58.4°F$$

where the factor 0.240 represents the specific heat c_p (Figure VI-6) for the average air temperature at side (2) of 79.2°F. For these average temperatures, Figure VI-6 gives

$$Pr_1^{2/3}/(4j\eta/f)_1 = 3.94$$

$$\mu_1 = 0.041 \text{ lb/ft-hr}$$

$$Pr_2^{2/3}/(4j\eta/f)_2 = 3.90$$

$$\varphi_1 = 0.133$$

The specific weights of the air based on inlet pressure and average temperature are by Figure VI-6 ($\delta_1 = \delta_2 = 1$)

$$\gamma_1 = 0.0825 \text{ lb/cu ft}$$

$$\gamma_2 = 0.0738 \text{ lb/cu ft}$$

The thermodynamic effectiveness is, by equation (VI-88)

$$e_{th} = 10{,}000/(1000 \times 0.24 \times 100) = 0.416$$

since $(wc_p)_{min} = (wc_p)_1$. The ratio $(wc_p)_{max}/(wc_p)_{min}$ is 240/239 = 1.00. The parameter NTU may then be found in Figure VI-7. It has a value of 0.76. Thus, by equation (VI-81)

$$K_{o1} = 0.70 + (3.94)(0.76)(2)(1) = 6.7$$

and, therefore, by use of equation (VI-92)

$$L_1 = 0.334 \text{ ft}$$

The surface area on side (1) is defined by equation (VI-85) as

$$S_1 = 7.46 \text{ sq ft}$$

and the length L_2 by equation (VI-103)

$$L_2 = 0.338 \text{ ft}$$

Then, by use of equation (VI-109)

$$L_{nf} = 0.288 \text{ ft}$$

The equivalent loss coefficient for side (2) is defined by equation (VI-81) as $K_{o2} = 6.7$, so that by equation (VI-104)

$$(PC)_2/(PC)_1 = 1.28$$

The pressure drop of the air on both sides may then be evaluated from the PC-ratios. By equation (VI-82)

$$PC_1 = 0.1 = 1000\,\Delta p_1/(778 \times 0.0825 \times 10{,}000)$$

$$\Delta p_1 = 64 \text{ psf} = 0.445 \text{ psi}$$

or,

$$\Delta p_1/p_{i1} = 0.445/14.7 = 0.03$$

Then,

$$PC_2 = 0.1 \times 1.28 = 1000\,\Delta p_2/(778 \times 0.0738 \times 10{,}000)$$

$$\Delta p_2 = 73.5 \text{ psf} = 0.51 \text{ psi}$$

or,

$$\Delta p_2/p_{i2} = 0.51/14.7 = 0.035$$

A check on the accuracy of this design by using the evaluated dimensions and then determining the power-to-cooling ratio for the two sides by the detailed method without any approximations indicates a value of 1.33 versus the example value of 1.28. In general, the agreement is quite good.

It is of interest to note from this example that there are nine variables which may be specified for the design of a heat exchanger. Among them the thermal resistance ratio $\phi = (R_1/R_2)$ is of special interest. Its value is an important factor in determining the shape and overall volume and weight of the exchanger core. An increase of ϕ decreases the flow length L_1, increases the flow length L_2, and decreases the no-flow length L_{nf}. Since these lengths can vary widely, it is usually necessary to determine the range of the resistance ratio which will give reasonable heat exchanger configuration. These effects are illustrated in Figure VI-8. It may be noted that the resistance ratio ϕ also affects the volume and weight of the heat exchanger, as indicated by the variation of the surface area S, to which both are directly proportional. As the thermal resistance ratio ϕ increases, the volume and weight decrease, but at the expense of an increased power requirement to pump the air through the second side, as evidenced by the increase in $(PC)_2/(PC)_1$. This is because the increase of ϕ requires a larger product of heat transfer coefficient and surface area h_2S_2 on the second side.

The dimensions and ratio $(PC)_2/(PC)_1$ of a heat exchanger for specified operating conditions of heat transfer capacity, flow rates, inlet temperatures, pressure levels and power-cooling ratio of side (1) and various resistance ratios ϕ can be determined on the basis of a reference design of known resistance ratio ϕ_{ref}. The exchanger characteristics are related by the following equations to the reference characteristics.

$$(1+\phi)/\phi = F \tag{VI-111}$$

$$\frac{L_1}{L_{1\text{-ref}}} = \frac{F}{F_{ref}} \left\{ \frac{0.7}{K_{o1\text{-ref}}} \left[1 - \frac{F}{F_{ref}} \right] + \frac{F}{F_{ref}} \right\}^{-0.217} \tag{VI-112}$$

$$\frac{K_{o1}}{K_{o1\text{-ref}}} = \frac{0.70}{K_{o1\text{-ref}}} \left[1 - \frac{F}{F_{ref}} \right] + \frac{F}{F_{ref}} \tag{VI-113}$$

$$\frac{K_{o2}}{K_{o2\text{-ref}}} = \frac{0.70}{K_{o2\text{-ref}}} \left[1 - \frac{1+\phi}{1+\phi_{ref}} \right] + \frac{1+\phi}{1+\phi_{ref}} \tag{VI-114}$$

$$\frac{S_1}{S_{1\text{-ref}}} = \frac{L_1}{L_{1\text{-ref}}} \left[\frac{K_{o1}}{K_{o1\text{-ref}}} \right]^{0.5} \tag{VI-115}$$

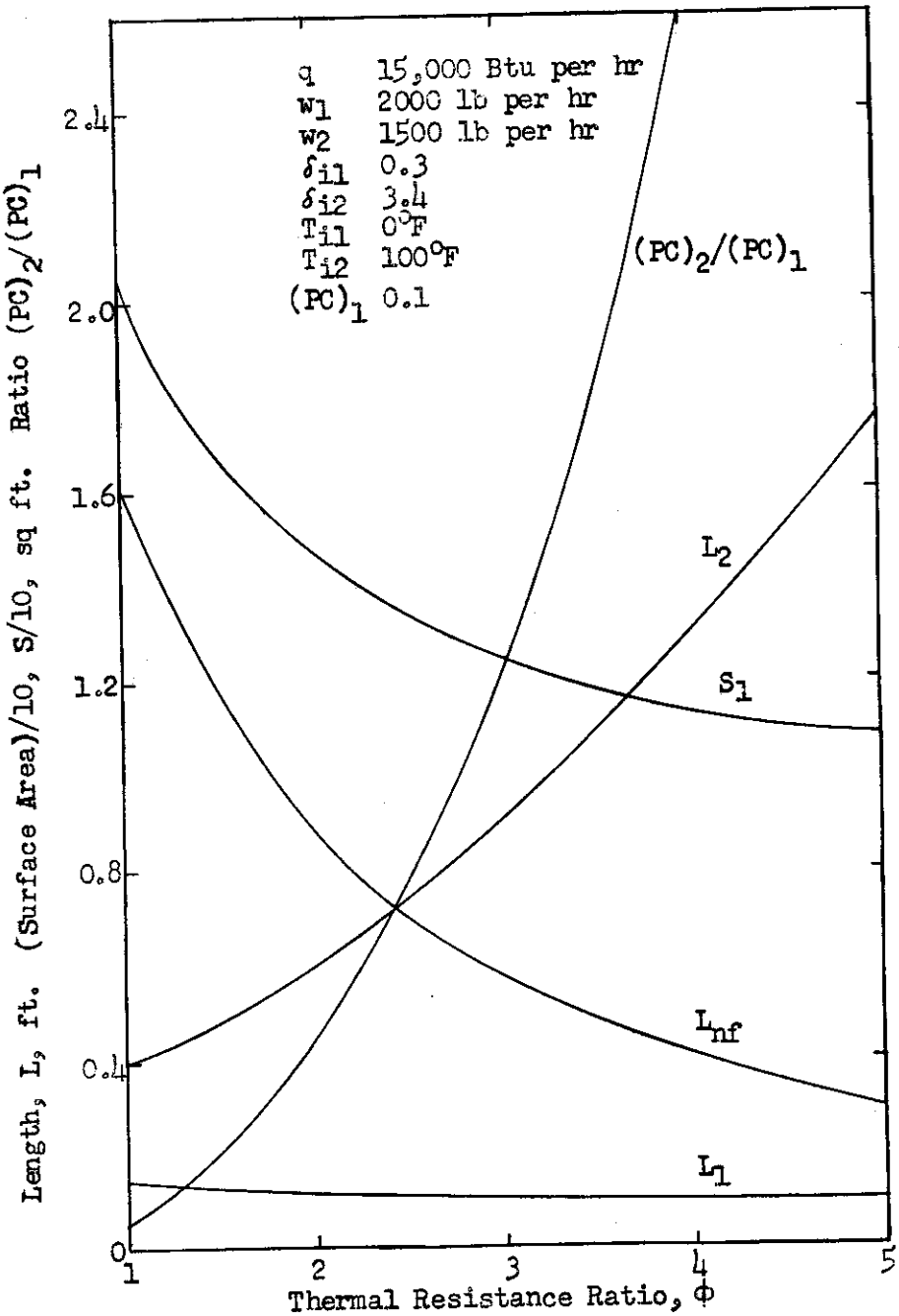

Figure VI-8. Effect of thermal resistance ratio Φ on characteristics of air-to-air heat exchanger.

$$\frac{L_2}{L_{2\text{-ref}}} = \left[\frac{S_1}{S_{1\text{-ref}}}\right]^{-0.846}\left[\frac{1+\phi}{1+\phi_{ref}}\right]^{1.846} \qquad \text{(VI-116)}$$

$$\frac{L_{nf}}{L_{nf\text{-ref}}} = \left[\frac{K_{o1}}{K_{o1\text{-ref}}}\right]^{0.5} \Big/ \left[\frac{L_2}{L_{2\text{-ref}}}\right] \qquad \text{(VI-117)}$$

$$\frac{\left[\frac{(PC)_2}{(PC)_1}\right]}{\left[\frac{(PC)_2}{(PC)_1}\right]_{ref}} = \frac{\left[\frac{K_{o2}}{K_{o2\text{-ref}}}\right]}{\left[\frac{K_{o1}}{K_{o1\text{-ref}}}\right]} \frac{\left[\frac{L_2}{L_{2\text{-ref}}}\right]^2}{\left[\frac{L_1}{L_{1\text{-ref}}}\right]^2} \qquad \text{(VI-118)}$$

The use of above relationships in design work is greatly facilitated by representing them graphically. This is done most conveniently on logarithmic coordinates.

It is also possible to determine readily the effects of changing the pressure levels δ_{i1} and δ_{i2} and the power-cooling ratio of side (1) on the heat exchanger dimensions, required surface area and power-cooling ratio of side (2). The following proportionalities are derived from the basic equations.

$$L_1 \propto (PC)_1^{0.217} \qquad \text{(VI-119)}$$

$$L_2 \propto (PC)_1^{0.239} \qquad \text{(VI-120)}$$

$$L_{nf} \propto (PC)_1^{-0.739} \qquad \text{(VI-121)}$$

$$S_1 \propto (PC)_1^{-0.283} \qquad \text{(VI-122)}$$

$$(PC)_2 \propto (PC)_1^{1.044} \qquad \text{(VI-123)}$$

Similarly,

$$L_1 \propto (\delta_{i1})^{0.434} \qquad \text{(VI-124)}$$

$$L_2 \propto (\delta_{i1})^{0.478} \qquad \text{(VI-125)}$$

$$L_{nf} \propto (\delta_{i1})^{-1.479} \qquad \text{(VI-126)}$$

$$S_1 \propto (\delta_{i1})^{-0.566} \qquad \text{(VI-127)}$$

$$(PC)_2 \propto (\delta_{i1})^{2.088} \qquad \text{(VI-128)}$$

$$(PC)_2 \propto (\delta_{i2})^{-2.00} \qquad \text{(VI-129)}$$

It should be noted that the pressure level of the air on side (2), δ_{i2},

has no effect on any of the heat exchanger dimensions, but affects only the power requirement on this side.

The use of the above relationships in design work is facilitated by expressing them graphically in relation to a set of reference values. Straight-line plots are obtained on logarithmic coordinates.

4. Simplified Approximate Method

For the evaluation of the performance and physical characteristics of cooling systems employing heat exchangers of this type it is very desirable to use methods which are considerably simpler in evaluation form than those presented in the preceding sub-sections in order to permit analytical combination of the various components in a cooling system. By means of a simplification method it may be possible to establish analytically optimum design conditions for a cooling system, without resorting to extensive computations.

For the selected core construction, the previously determined constant values are used; namely, r_h is 0.00174 ft, C_f is 4.73, exponent m is 0.434, exponent n is 0.542, $j\eta/f$ is 0.051. The parameter φ_1 is as shown in Figure VI-6. Furthermore, it is assumed that the entrance and exit losses may be neglected. Thus, the factors K_1 and K_2 in equations (VI-80) and (VI-81) are dropped out. Then, by introducing the perfect gas equation of state into equation (VI-82), one obtains

$$(PC)_1 q/w_1 = 35.6(\theta_{i1})(\Delta p_1^o/p_{i1}) \qquad \text{(VI-130)}$$

Substituting in equation (VI-92), the flow dimension on side (1) is given by

$$L_1 = 0.164(\delta_{i1})^{0.434}(\Delta p_1^o/p_{i1})^{0.217}(K_{o1})^{0.783}/(\theta_{i1})^{0.217} \qquad \text{(VI-131)}$$

where the viscosity on side (1) has been assigned a typical average value since its effect on this dimension has been found to be small. Following a similar procedure for the flow dimension on side (2), one obtains

$$L_2 = 1.62\,\varphi_1\left[\frac{e_2}{e_1}\right](K_{o1})^{0.758}(\delta_{i1})^{0.48}\left[\frac{\Delta p_1^o}{p_{i1}}\right]^{0.24}(\phi)^{1.846}/(\theta_{i1})^{0.24} \qquad \text{(VI-132)}$$

The ratio of the two flow dimensions L_2/L_1 becomes, therefore,

$$\frac{L_2}{L_1} = 9.92\,\varphi_1\left[\frac{e_2}{e_1}\right](\delta_{i1})^{0.046}\left[\frac{\Delta p_1^o}{p_{i1}}\right]^{0.023}(\phi)^{1.846}\Big/\left[(K_{o1})^{0.025}(\theta_{i1})^{0.023}\right] \qquad \text{(VI-133)}$$

and because of the small variation of the flow length ratio L_2/L_1 with pressure level, pressure drop, temperature level and the resistance coefficient, indicated by their small exponents, equation (VI-133) may be simplified to the form

$$L_2/L_1 = 10\varphi_1(e_2/e_1)(\phi)^{1.846} \qquad \text{(VI-134)}$$

The no-flow dimension L_{nf} is obtained by combination of equations (VI-109), (VI-85), (VI-131) and (VI-134). This gives

$$L_{nf} = \frac{w_1(\theta_{i1})^{0.74}(e_1/e_2)}{244{,}000(\delta_{i1})^{1.48}(\Delta p_1^o/p_{i1})^{0.74}(\varphi_1)(K_{o1})^{0.258}(\phi)^{1.846}} \qquad \text{(VI-135)}$$

Then, the volume of the heat exchanger core is obtained by the product of equations (VI-131), (VI-132) and (VI-135)

$$V''_{core} = \frac{1.88(\theta_{i1})^{0.283}(K_{o1})^{1.283}(w_1/1000)}{(\delta_{i1})^{0.566}(\Delta p_1^o/p_{i1})^{0.283}} \qquad \text{(VI-136}$$

The ratio of the pressure drops on sides (2) and (1) is defined by use of equation (VI-76).

$$\Delta p_2^o/\Delta p_1^o = (\gamma_2/\gamma_1)(K_{o2}/K_{o1})(u_2^2/u_1^2) \qquad \text{(VI-137)}$$

Then, by use of the equation of continuity and the assumption that the Prandtl number on side (2) equals the Prandtl number on side (1) so that by equations (VI-80) and (VI-81)

$$K_{o2}/K_{o1} = \phi(e_2/e_1) \qquad \text{(VI-138)}$$

equation (VI-137) reduces to the form

$$(\Delta p_2^8/p_{i2})/(\Delta p_1^o/p_{i1}) = (\delta_{i1}/\delta_{i2})^2(\theta_2/\theta_1)(\phi)^{4.7}(e_2/e_1)(10\varphi_1)^2 \qquad \text{(VI-139)}$$

Also, the resistance coefficient K_{o1} is defined by

$$K_{o1} = 3.86(NTU)(e_1/e_{max})(1 + \phi)/\phi \qquad \text{(VI-140)}$$

The final working equations are (VI-136), (VI-139) and (VI-140). The assumed independent variables are the effectivenesses on sides (1) and (2), e_1 and e_2, the inlet pressure and temperatures on sides (1) and (2) and the permissible percentage of pressure drop on sides (1) and (2). From these data the resistance ratio ϕ may be evaluated from equation (VI-139), then the resistance coefficient K_{o1} from equation (VI-140) and lastly the core volume from equation (VI-136). For any particular application of this heat exchanger to a cooling system it is possible, normally, by examining the ranges on the variables involved, to further simplify these equations so that heat exchanger volume may be evaluated directly from a single equation.

The weight of the heat exchanger, including the headers, is defined by

$$W_X = 0.0214\ V''_{core} \qquad \text{(VI-141)}$$

or, assuming that

$$V''_X = 1.25\ V''_{core} \qquad \text{(VI-142)}$$

then

$$W_X = 0.0171\ V''_X \qquad \text{(VI-143)}$$

Liquid-to-Air Heat Exchanger

The liquid-to-air heat exchangers are considered to be of the single-pass crossflow type. On the air side of the exchanger, the 17.8-3/8-R surface is used, Figure VI-3. From exploratory calculations, it has been found that this type of surface cannot generally be used on the liquid side, because the volumetric flow rate ordinarily encountered on the liquid side is considerably smaller and it would be necessary to employ a very small frontal area for the liquid side to produce liquid velocities high enough that the liquid-film heat transfer coefficients may contribute in any measure to the overall thermal conductance between the two fluids. The resulting low frontal areas lead to very great flow lengths on the liquid side, and therefore require unreasonable configurations for the heat exchanger core. In order to avoid this, the liquid-side surface is assumed to consist simply of flat plate areas, furnished by the separator, or sandwiching plates of the 17.8-3/8-R surfaces. These flat plates would be closely spaced, and, thereby, furnish a parallel-boundary channel through which the liquid flows in laminar or viscous flow.

1. Design Equations and Evaluation Procedure

The heat transfer coefficient for laminar flow of a liquid between two plane walls is given approximately (Reference VI-5) by

$$hb/k = 3.75 \qquad \text{(VI-144)}$$

where b denotes the plate spacing in feet. This equation applies to fully developed laminar flow, such as exists in the case of passages of considerable length and small hydraulic radius. Thus, in neglecting the entrance effect, the relationship is conservative for use in heat exchanger design, since the entrance effect tends to give larger average values of the heat transfer coefficient than would exist for fully developed laminar flow. Equation (VI-144) will be used in developing the design relationships for the liquid-to-air heat exchanger. In deriving the equations which govern heat transfer on the air side of the liquid-to-air exchanger, it is possible to use those derived for the air-to-air case with but minor alterations.

The entrance and exit loss allowance for the liquid-to-air exchanger would vary slightly from one design to another, since the plate

spacing b would vary, and thus cause variation of the expansion and contraction ratios at entrance and exit of the core. Assuming that the plate spacing is of the order of 0.040 inch, a suitable allowance for entrance and exit losses would be defined by a value of K equal to about 0.54. Thus, by equation (VI-80)

$$K_{o1} = 0.54 + \left[\frac{(Pr)_1^{2/3}}{4(j\eta/f)_1}\right](NTU)\left[\frac{1+\phi}{\phi}\right]\frac{(wc_p)_{min}}{(wc_p)_1} \qquad (VI\text{-}145)$$

and from equation (VI-92)

$$L_1 = \left[\frac{K_{o1}-0.54}{K_{o1}^{m/2}}\right]\left[\frac{\gamma_1}{\mu_1}\right]^m\left[\frac{q(PC)_1}{w_1}\right]^{m/2}\left[\frac{(4r_{h1})^{1+m}(3600)^m(2gx778)^{m/2}}{C_f}\right] \qquad (VI\text{-}146)$$

where side (1) represents the air side of the exchanger. Then, by use of equation (VI-85)

$$S_1 = L_1\left[\frac{w_1}{\gamma_1}\right]\left[\frac{q(PC)_1}{w_1}\right]^{-1/2}(K_{o1})^{1/2}\left[\frac{1}{3600\, r_{h1}\sqrt{2gx778}}\right] \qquad (VI\text{-}147)$$

The heat transfer relationships governing the second side or liquid side of the exchanger are next derived. From the definition of the thermal resistance ratio ϕ and equation (VI-74)

$$h_2 S_2 = (1+\phi)(NTU)(wc_p)_{min} \qquad (VI\text{-}148)$$

so that by combining equations (VI-144) and (VI-148)

$$b = \frac{3.75\, k\, S_1}{(1+\phi)(NTU)(wc_p)_{min}}\left[\frac{S_2}{S_1}\right] \qquad (VI\text{-}149)$$

The surface on the air side has 514 square feet per cubic foot of space between plates. The surface on the liquid side has 2/b square feet per cubic foot of space between the plates. Thus, since the air-side surface has a spacing of 0.413 inch, the ratio of the surface areas

$$S_2/S_1 = \left[(2/b)/514\right](12b/0.413) = 0.113 \qquad (VI\text{-}150)$$

and by equation (VI-149)

$$b = 0.425\, k\, S_1 \Big/ \left[(1+\phi)(NTU)(wc_p)_{min}\right] \qquad (VI\text{-}151)$$

The number of laminations in an exchanger of this type will be defined by

$$n = L_{nf}/(b + 0.0397) \qquad (VI\text{-}152)$$

since the spacing is 0.413 inch and the separator plates are 0.032 inch in thickness. Thus, for one lamination, the thickness is

$$b + (0.413/12) + (2 \times 0.032/12) = b + 0.0397$$

Let l_3 denote the ratio of the liquid flow dimension to the no-flow dimension

$$l_3 = L_2/L_{nf} \qquad \text{(VI-153)}$$

Then, since

$$L_2 = r_{h2}\, S_2/A_2, \qquad \text{(VI-154)}$$

by combining this relationship with equations (VI-152) and (VI-150) there results

$$L_2 = 0.239(\, l_3\, S_1/L_1)^{0.5}(b + 0.0397)^{0.5} \qquad \text{(VI-155)}$$

The no-flow dimension L_{nf} will be defined by (VI-153) and (VI-155) for any selected value of the ratio l_3.

The equation defining the pressure drop of an incompressible fluid flowing in laminar motion between parallel plates is

$$\Delta p_2 = 12\, \mu_2\, L_2\, u_2/(3600\, g\, b^2) \qquad \text{(VI-156)}$$

and by use of the continuity equation

$$w_2 = 3600\, \gamma_2\, u_2\, n\, b\, L_1 \qquad \text{(VI-157)}$$

equation (VI-156) becomes

$$\Delta p_2 = (\mu_2 w_2\, L_2)/(1.08 \times 10^6\, g\, b^3\, \gamma_2\, n\, L_1) \qquad \text{(VI-158)}$$

2. Simplified Evaluation Procedure

The evaluation procedures presented in the preceding sub-section may be shortened considerably by making several simplifying assumptions and by assuming a specific transfer fluid. As for the liquid-to-liquid heat exchanger, a mixture of water and methyl alcohol is assumed.

The simplified methods herein presented are believed to give accurate values of weight and volume within 8 to 10%. Referring to equation (VI-145), detailed computations have indicated that no great error will be introduced by neglecting the entrance and exit loss coefficient of 0.54 and using an average value for air of 3.75 for the parameter

$$(Pr^{2/3})/(4j\eta/f) = 3.75 \qquad \text{(VI-159)}$$

It is estimated that either of these approximations would rarely introduce an error in excess of 3%. Also, the parameter in equation (VI-146) involving the power-cooling ratio PC may be re-expressed in terms of the fractional pressure drop of the air.

$$q\ PC_1/w_1 = 35.6\ \theta_{m1}(\Delta p_1^o/p_{m1}^o) \qquad \text{(VI-160)}$$

Then, introducing equations (VI-159) and (VI-160) into (VI-146) yields

$$L_1 = \text{const.}(NTU)^{0.783}\left[(1+\phi)/\phi\right]^{0.783}\left[\frac{\gamma_{il}}{\mu_{il}}\right]^{0.434}\left[\theta_{m1}^o\,\frac{\Delta p_1^o}{p_{m1}^o}\right]^{0.217} \qquad \text{(VI-161)}$$

Next, by assuming that

$$p_{m1}^o = p_{i1}^o$$

and

$$\theta_{m1}^o = \theta_{i1}^o$$

and, because of the small variation of $\mu_{il}^{0.434}$ over the required temperature range, using for it a constant value, equation (VI-161) reduces to

$$L_1 = 0.484(NTU)^{0.783}\left[\frac{(1+\phi)}{\phi}\right]^{0.783}(\delta_{il}^o)^{0.434}(\theta_{il}^o)^{-0.528}\left[\frac{\Delta p_1^o}{p_{il}^o}\right]^{0.217} \qquad \text{(VI-162)}$$

By a similar procedure starting with equation (VI-147) it may be shown that

$$S_1 = 1.5\times10^{-3}\ w_1(NTU)^{1.283}\left[\frac{1+\phi}{\phi}\right]^{1.283}\Big/\left\{(\delta_{il}^o)^{0.566}\left[\frac{\Delta p_1^o}{p_{il}^o}\right]^{0.283}\right\} \qquad \text{(VI-163)}$$

Using an average value of the coefficient of thermal conductivity k for the water-alcohol transfer fluid, equation (VI-149) may be reduced to

$$b = 0.0005(NTU)^{0.283}(1+\phi)^{0.283}\Big/\left\{(\phi)^{1.283}(\delta_{il}^o)^{0.566}\left[\frac{\Delta p_1^o}{p_{il}^o}\right]^{0.283}\right\} \qquad \text{(VI-164)}$$

Inspection of this equation reveals that a typical maximum value of b is about 0.0085 feet. Further, a detailed study indicates that an average value for b of about 0.004 feet would rarely introduce an error in excess of 5%. Thus, the plate spacing b on the liquid side is assumed equal to a constant value of 0.004 feet.

Next, it is assumed that the liquid flow length L_2 is equal to

the no-flow dimension L_{nf}, making l_3 equal to unity and presenting a square frontal area to the air. Then, by equations (VI-155), (VI-163) and (VI-162) one obtains

$$L_2 = \frac{2.78 \times 10^{-3}(w_1)^{0.5}(NTU)^{0.25}\left[(1+\phi)/\phi\right]^{0.25}(\theta^o_{i1})^{0.264}}{(\delta^o_{i1})^{0.5}(\Delta p^o_1/p^o_{i1})^{0.25}} \quad \text{(VI-165)}$$

The volume of the core is defined by

$$V_{core} = L_1 L_2 L_{nf} = L_1 L_2^2 \quad \text{(VI-166)}$$

since l_3 is unity. By use of equations (VI-162) and (VI-165), equation (VI-166) becomes

$$V_{core} = 3.47\times10^{-3}\left[\frac{w_1}{1000}\right]\left[(NTU)\,\frac{1+\phi}{\phi}\right]^{1.283}\Bigg/\left\{(\delta^o_{i1})^{0.566}\left[\frac{\Delta p^o_1}{p^o_{i1}}\right]^{0.283}\right\} \quad \text{(VI-167)}$$

The only remaining difficulty in the use of equation (VI-167) is the selection of the resistance ratio ϕ. An increase in ϕ results in decreased weight and volume but greater pressure drop and pumping power. A study of the size of this type heat exchanger as affected by the resistance ratio ϕ indicates that a value in the vicinity of four represents a good balance between size and flow resistance. The plate spacing b with this value of ϕ would be quite small and somewhat impractical, which indicates that in all probability the exchanger would not actually be constructed on the flat plate basis but would use fairly widely spaced flat tubes for the liquid flow. This would yield a relatively high value for ϕ and allows the air side to be the principal factor in defining the required surface of the exchanger. Thus, for ϕ of 4 the volume defined by equation (VI-167) is expected to be quite representative of that defined by detailed design procedures. For ϕ of 4, equation (VI-167) reduces to

$$V_{core} = 4.63\times10^{-3}(NTU)^{1.283}(w_1/1000)\Bigg/\left\{(\delta^o_{i1})^{0.566}\left[\frac{\Delta p^o_1}{p^o_{i1}}\right]^{0.283}\right\} \quad \text{(VI-168)}$$

which is the final form for the core volume equation. The volume of the exchanger is assumed to be defined by

$$V_X = 1.30\, V_{core} \quad \text{(VI-169)}$$

A study of the weight of the exchanger, including headers and the water-alcohol transfer fluid indicates that

$$W_X = 60\, V_{core} \quad \text{(VI-170)}$$

or

$$W_X = 0.0348\, V^n_{core} \quad \text{(VI-171)}$$

Boiling Liquid-to-Liquid Heat Exchanger

With indirect expendable cooling systems a heat exchanger must serve as the intermediate component between the transfer and ultimate fluids. The heat received by the ultimate fluid is absorbed in the process of a change in phase. Thus, boiling may be assumed to occur on the ultimate side. Heat transfer occurs by forced convection between the transfer fluid and the heat exchanger surface. The heat exchanger is assumed to be of the shell-and-tube type with the ultimate fluid located outside the tubes and the transfer fluid flowing through the tubes. The tubes are assumed to be standard aluminum tubing, 1/4 inch outside diameter and 0.025 inch wall thickness. In order to provide sufficient space for vapor rise between tube rows, a square pitch equal to twice the external tube diameter is employed. This arrangement of the tubes provides 37.8 square feet external heat transfer surface per cubic foot of exchanger core.

The cooling capacity of the exchanger is defined by

$$q = h_U S_{IU} \Delta T_{IU} \qquad \text{(VI-172)}$$

where h_U represents the heat transfer coefficient on the ultimate side, S_{IU} the surface for heat transfer on the ultimate side of the intermediate component and ΔT_{IU} the difference in temperature between the ultimate-side surface and the ultimate fluid. It is assumed that the surface temperature is uniformly the same over the entire external surface of the tubes. For the specified tube arrangement,

$$S_{IU}/V_{core} = 37.8 \text{ sq ft/cu ft} \qquad \text{(VI-173)}$$

so

$$q/V_{core} = 37.8\, h_U \Delta T_{IU} \qquad \text{(VI-174)}$$

By this procedure the definition of volume and weight for this type exchanger becomes quite direct and simple. When applying the exchanger to a cooling system it is then necessary to start from the tube surface temperature and define the forced convection heat transfer and flow resistance on the transfer side in a manner identical to that presented for the equipment component in Section IV. The heat exchanger may be adapted to any ultimate fluid by introducing into equation (VI-174) the appropriate relationship for the boiling heat transfer coefficient.

With water as the ultimate fluid, a study of boiling heat transfer coefficients indicates that the following derived empirical relationship may be employed with reasonably good accuracy.

$$h_{U\text{-}H_2O} = 3(\Delta T_{IU})^{1.5}\left[1 + 4(T_U/100)\right] \qquad \text{(VI-175)}$$

This expression attempts to account for the variation of the coefficient with pressure, since the temperature of the water in ^{o}F is included in

the equation. Introducing equation (VI-175) in (VI-174) yields

$$q/V''_{core} = 20.7(\Delta T_{IU}/10)^{2.5}\left[1 + 4(T_U/100)\right] \qquad \text{(VI-176)}$$

or

$$V''_{core}/kw = 165/(\Delta T_{IU}/10)^{2.5}\left[1 + 4(T_U/100)\right] \qquad \text{(VI-177)}$$

The overall volume of the exchanger is assumed to be defined by

$$V''_X = 1.21\ V''_{core} \qquad \text{(VI-178)}$$

and the weight of the exchanger for aluminum construction and water as the ultimate and transfer fluids by

$$W_X = 0.042\ V''_X \qquad \text{(VI-179)}$$

or

$$W_X = 0.05\ V''_{core} \qquad \text{(VI-180)}$$

The physical characteristics for this type exchanger with other fluids may be defined starting from equation (VI-174). Examples for other fluids are presented in Section XIII dealing with expendable cooling systems.

REFERENCES

VI-1 Brown, A. I. and Marco, S. M., Introduction to Heat Transfer, Second Edition, McGraw-Hill Book Company, Inc., New York, 1951.

VI-2 Kays, W. M., London, A. L., and Johnson, D. W., Gas Turbine Plant Heat Exchangers, A.S.M.E., 29 W. 39th St., New York 18, N. Y., April 1951.

VI-3 Vennard, J. K., Elementary Fluid Mechanics, Second Edition, John Wiley and Sons, Inc., New York, 1949.

VI-4 Bulletin D-378A, The Trane Company, LaCrosse, Wisconsin, October, 1951.

VI-5 Eckert, E. R. G., Introduction to the Transfer of Heat and Mass, First Edition, McGraw-Hill Book Company, Inc., New York, 1950.

VI-6 Dodge, R. A., and Thompson, M. J., Fluid Mechanics, First Edition, McGraw-Hill Book Company, Inc., New York, 1937.

VI-7 McAdams, W. H., Heat Transmission, Second Edition, McGraw-Hill Book Company, Inc., New York, 1942.

VI-8 Nusselt, W., Eine neue Formel fuer den Waermedurchgang im Kreuzstrom, Technische Mechanik und Thermodynamik, Vol. 1, No. 12, December 1930, pp. 417-422.

SECTION VII

THE ULTIMATE COMPONENT

The ultimate component of aircraft cooling systems consists of all the physical components associated with the supply, storage, discharge and conditioning of the ultimate fluid before and after receiving heat, rejected by the equipment items, in the equipment component of direct systems and in the intermediate component of indirect systems. The ultimate component provides conveyance of the ultimate fluid to and from the equipment or intermediate components, depending upon whether the cooling system is direct or indirect. Storage facilities for an ultimate fluid would be part of the ultimate component in expendable cooling systems. Conditioning equipment for the ultimate fluid prior to receiving heat rejected by the equipment items, such as diffusers for raising the static pressure level of the ultimate fluid or expansion turbines for lowering the total temperature level, are part of the ultimate component in many cooling systems utilizing atmospheric air as the ultimate fluid.

The ultimate component in ram air cooling systems consists of the air intake, which includes any internal diffuser, the duct or ducts conveying the air to the intermediate or equipment component, the duct or ducts conveying the air to the point of discharge and the air outlet, when provided. The flight performance penalty imposed on the aircraft by the ultimate component of ram air cooling systems is the result of the weight of the ducts, inlets and outlets and the momentum and external drags introduced by the atmospheric air being taken on board and subsequently ejected. The momentum drag, which may be thrust for some operational conditions of the aircraft and cooling system, represents the net propulsive force of the influx and outflux of momentum of the atmospheric air. A flight velocity greater than the final relative velocity of the air issuing from the outlet of the system represents a momentum drag, since the aircraft must expend a greater propulsive force in taking the air on board than is derived by the aircraft from the air ejection process. If the momentum of the cooling air stream is increased from inlet to exit of the ultimate component, a negative momentum drag or thrust is derived by the aircraft. The external drag of the ultimate component represents the increased parasitic drag of the aircraft because of skin protuberances, such as air intakes and outlets. The air intake for ram air cooling systems might be of the leading-edge, the fully-protruding or scoop type, semi-protruding, flush, or might be designed in some instances to handle only low-energy boundary-layer air. The type of intake which would be utilized for a ram air cooling system depends upon many aerodynamic and general design factors of the aircraft and cannot, therefore, be fully prescribed by considerations of the cooling system design alone. There are, however, several compromise design features of the ultimate component which can be studied from the standpoint of optimum ram air cooling system design. In general, increasing the pressure recovery characteristics of ram intakes results

in increased external drag and quite often greater momentum drag. The additional pressure recovery could be employed to reduce the size of the internal air ducts in the ultimate component, or to reduce the size of the intermediate component, or to permit an increase in the effectiveness of heat exchange of the intermediate or equipment components so as to reduce the flow rate of ultimate air required, or to change simultaneously several of these system design features. Once the performance and physical characteristics of the various parts of the ultimate component are defined, it is generally possible to study the effects of compromise in design of the ultimate component on the overall performance and physical characteristics of the entire cooling system.

The ultimate component of the expanded ram air cooling system consists of the same general components as for the ram air cooling systems with the addition of an expansion turbine, its loading device and any precooling heat exchanger which might be employed. Since, in general, the flight performance penalty introduced by cooling systems of this type is appreciable and the expansion in the turbine depends upon the degree of intake diffusion, it is desirable to employ air intakes having fairly good pressure recovery characteristics. As with the ram air systems, compromise in the design of the ultimate component, such as the size versus pressure loss of ducting, or the amount of total temperature reduction in the turbine versus the pressure level at exit of the turbine, must be studied in relation to the overall performance and physical characteristics of the entire cooling system in order to determine optimum design conditions.

The ultimate component in bleed air cooling systems consists of all bleed air ducts, ram air ducts, the expansion turbine and its loading device and any precooling heat exchangers. The physical components of the aircraft's powerplants are not included as parts of the ultimate component, since the penalty of bleeding air from the powerplants as a required increase in fuel flow is charged to the ultimate component. For the type of bleed air cooling system considered in this study, the ultimate component consists of the bleed air duct from the point of bleed on the powerplant to the precooling heat exchanger, the precooling heat exchanger, the turbine, its loading device which is a compressor, the ram air intake, the ram air ducts from intake, through the precooler, through the compressor and to the ram air outlet, and any ducts conveying bleed air to and from the intermediate or equipment components. The penalty due to the ultimate component in bleed air cooling systems represents a very large percentage of the entire cooling system penalty. Consequently, the physical characteristics and performance of the different parts must be defined to permit evaluation of optimum system design.

The ultimate component for cooling systems relying on blowers as the source of air flow consists of the blowers, their driving devices, the power supply system within the aircraft serving the driving devices, air ducts to and from the blowers and intermediate or equipment components and any air intakes and outlets. The increased fuel flow to the powerplants necessary to supply power to the power supply system for

driving the blowers must be charged as part of the overall penalty imposed on the aircraft by the ultimate component. External and momentum drags may also occur, depending upon the source of the cooling air. When blowers are used for cooling in compartments having a natural ventilation rate greater than the cooling air rate required, air intakes and outlets for the cooling air need not be provided and external and momentum drags associated with the natural ventilation should not be charged to the cooling system. With compartments having no natural ventilation, air intakes and outlets must be provided and any momentum and external drags so introduced must be included.

With fuel cooling systems the ultimate component is of minor importance in terms of aircraft penalty due to weight and power requirements. The ultimate component probably would consist of a few relatively short fuel by-pass lines leading to and from the intermediate component, where the intermediate component would be expected to be located relatively close to a main fuel line. Other than the weight of these lines and any associated flow control equipment, the penalty on the aircraft would only be due to the pumping power required to transfer the fuel through the lines.

The ultimate fluid in expendable cooling systems is the expendable fluid used as the thermal sink and must, therefore, be stored within the aircraft. The ultimate component consists of the storage facilities and any associated control equipment, the flow lines, if any, for transferring the fluid to the intermediate or equipment components and the physical facilities for rejecting the ultimate fluid from the aircraft. In general, the penalty of the ultimate component is a relatively small portion of overall penalty of the entire cooling system; including, of course, the weight of the ultimate fluid.

The ultimate fluid in vapor cycle refrigeration systems is atmospheric air, taken on board the aircraft through an air intake, delivered by ducting to the condenser of the refrigeration machine, the refrigeration machine being a part of the intermediate component, and then being delivered by ducting to an air outlet. Thus, the ultimate component for vapor cycle systems is physically equivalent in all respects to the ultimate component in ram air cooling systems.

In summary, the physical parts of the ultimate component in the various types of cooling systems are air intakes, air outlets, ducting, blowers, compressors, turbines, heat exchangers and power supply systems. The heat exchangers in ultimate components are precoolers located in the flow circuit ahead of the intermediate or equipment component and have physical characteristics essentially the same as the comparable type of intermediate component. For this reason, the physical characteristics of heat exchangers used in the ultimate component have been presented in Section VI. The physical characteristics of the power supply system have been presented in Section V and the penalties chargeable to air bleed and shaft power extraction from the aircraft's powerplants in Section III. The following material presents the fluid dynamics,

thermodynamics and the physical characteristics of ducting, air intakes, outlets, blowers, compressors and turbines as used as a basis for evaluating the performance and physical characteristics of the ultimate component in aircraft cooling systems.

Nomenclature

Symbol	Concept	Dimensions
a	velocity of sound	feet per second
A	flow area	square feet
b	ratio of impeller width to diameter	dimensionless
c_p	specific heat at constant pressure	Btu per pound-^oF
C	constant	
d	diameter	feet
Dr	drag	pounds
f	Darcy friction factor	dimensionless
F	correction factor	dimensionless
g	dimensional constant	32.2 pounds per slug
H	head of fluid	feet
J	mechanical equivalent of heat	foot pounds per Btu
k	ratio of specific heat at constant pressure to specific heat at constant volume	dimensionless
L	length	feet
M	Mach number	dimensionless
n	rotational speed	revolutions per minute
N	number of stages	
p	pressure	pounds per square foot,abs.
P	power	Btu per hour
R	gas constant	feet per ^oR
Re	Reynolds number	dimensionless
sg	specific gravity	dimensionless
T	temperature	^oR
u	absolute velocity	feet per second
U	relative velocity	feet per second
v	volume rate of flow	cubic feet per minute
V	volume	cubic feet
w	fluid flow rate	pounds per hour
W	weight	pounds
y	distance measured normal to a surface	feet
β	Mach number parameter $1 + [(k-1)/2]\ M^2$	dimensionless
γ	specific weight	pounds per cubic foot
Γ	angle	degrees
δ	ratio of absolute pressure of fluid to standard sea level pressure (2115 pounds per square foot)	dimensionless
ϵ	absolute roughness	feet
η	component efficiency	dimensionless

Symbol	Concept	Dimensions
θ	ratio of absolute temperature to standard sea level absolute temperature ($519^{\circ}R$)	dimensionless
λ	diameter ratio	dimensionless
μ	absolute viscosity	pound-seconds per square foot
ν	hub-to-tip diameter ratio	dimensionless
σ	ratio of air density to standard air density at sea level (0.0765 lb/cu ft)	dimensionless
φ	flow coefficient	dimensionless
ϕ	ratio of turbine tip speed to spouting velocity	dimensionless
χ	power coefficient	dimensionless
ψ	pressure coefficient	dimensionless

Subscript	Refers to
a	axial component of velocity
A	axial unit
B	blower
bl	boundary layer
C	compressor
d	diameter
D	distribution component
df	diffuser
e	exit
ex	external
i	inlet
I	impeller
mh	mechanical
mom	momentum
n	nozzle
pt	pitch section
R	radial unit
Re	Reynolds number
ref	reference value
rt	root section
sh	shaft
st	stage
tp	tip section
wh	whirl component
η	efficiency
λ	diameter ratio
τ	turbine
∞	free stream conditions

Superscript	Refers to
o	total or stagnation conditions
t	power in horsepower
w	dimension of inches

Ducting

Ducts transporting air at low pressure would probably be of lightweight metal ducting or fabric ducting in combination with flexible corrugated sections for bends, elbows, expansion and flexing joints, wherever an absolutely leak-proof flow system is not required. The internal pressure range applicable for these types of low-pressure ducting would be from less than 1 to about 75 pounds per square inch. Straight runs of low-pressure metal ducting would probably be of the thin-wall stainless steel type, having single-ply construction and annular corrugations in the duct wall for purposes of reinforcement which are spaced at a distance roughly equal to the duct diameter. Wall thickness of this type ducting may be from 0.005 to above 0.010 inch. Internal pressures up to 30 or 40 pounds per square inch are permitted with duct diameters greater than about 3 inches, and up to 60 to 80 pounds per square inch for ducts of smaller diameter. Two-ply construction permits doubling of the allowable internal pressure. The external diameter of this type ducting is defined as the outer diameter of the corrugations and is related to the internal diameter of the duct by

$$d_{ex}^{w} = 0.1 + 1.12\, d_{i}^{w} \qquad \text{(VII-1)}$$

The external diameter of the duct wall proper is from 0.01 to 0.02 inch greater than the internal diameter. The volume occupied by the ducting, expressed in cubic inches per foot, is defined on the basis of the external diameter of the corrugations and is expressed by

$$V^{w}/L = 2.1\, d_{i}^{w}(1 + 5.6\, d_{i}^{w}) \qquad \text{(VII-2)}$$

Weight of this thin-walled stainless ducting expressed in pounds per foot is defined by the equation

$$W/L = 0.058\, (d_{i}^{w})^{1.4} \qquad \text{(VII-3)}$$

Elbows, bends and flexure and alignment connections for this type of metal ducting would be of construction similar to that for the straight-run ducting, except for the annular corrugations which have a spacing of 6 to 7 per lineal inch. External diameter and volume for this part of the ducting would be defined by equations (VII-1) and (VII-2). Weight would be evaluated by equation (VII-3) multiplied by a factor of 1.4.

Fabric ducting, of which ducts made of commercially available rubber-impregnated fiberglass cloth are typical, might be used with certain

systems for transportation of air at relatively low pressures. Straight runs of the ducting probably would be of semi-rigid construction with convolutions spaced at intervals along the duct for added rigidity. Permissible internal pressure may be as high as 15 pounds per square inch, but ordinarily the ducting would be employed for internal pressures of 5 pounds per square inch and less. Wall thickness would be in the range 0.035 to 0.04 inch for duct internal diameters up to 6 inches. The external diameter of the convolutions varies with the duct internal diameter approximately as

$$d''_{ex} = 0.2 + 1.1\, d''_i \qquad \text{(VII-4)}$$

The volume occupied by the ducting is expressed by

$$V''/L = 4.25\, d''_i(1 + 2.7\, d''_i) \qquad \text{(VII-5)}$$

Weight of this type ducting for low pressures is expressed by

$$W/L = 0.075\, d''_i \qquad \text{(VII-6)}$$

and for pressures of about 15 pounds per square inch by

$$W/L = 0.09\, d''_i \qquad \text{(VII-7)}$$

These equations have been derived from data giving physical characteristics of commercially available ducting. Elbows, bends and flexure and alignment connections would be of the fully convoluted type having wire-supported construction. External diameters and volumes would be defined by equations (VII-4) and (VII-5). Weight would be evaluated by equation (VII-7) multiplied by a factor of 1.5. Leakage rates typical of straight-run fabric ducting are expressed by the equation

$$v/L = 0.001\, p''\, d''_i \qquad \text{(VII-8)}$$

where v defines the leakage rate expressed in cubic feet per minute. For fabric ducting employed in elbows, bends, etc., as described in the previous paragraphs, the leakage rate averages about 4 times that given by equation (VII-8).

For low-pressure metal ducting which is not corrugated, the Darcy friction factor used in evaluating flow resistance may be defined by the relationship

$$f = 0.18/Re^{0.2} \qquad \text{(VII-9)}$$

where the Reynolds number Re is defined by

$$Re = \gamma u\, d_i/g \qquad \text{(VII-10)}$$

The friction factor defined by equation (VII-9) would be increased by

about one-third when the duct has corrugations which are spaced at distances approximately equal to the duct diameter. The frictional characteristics of low-pressure fabric ducting of the fully-convoluted type have been studied using manufacturers' data. Results of this study are shown in Figure VII-1, where the Darcy friction factor is plotted as a function of the Reynolds number. The results are based on three series of tests on tubing of similar physical characteristics, with flow being well within the turbulent region for all tests. The friction factor is

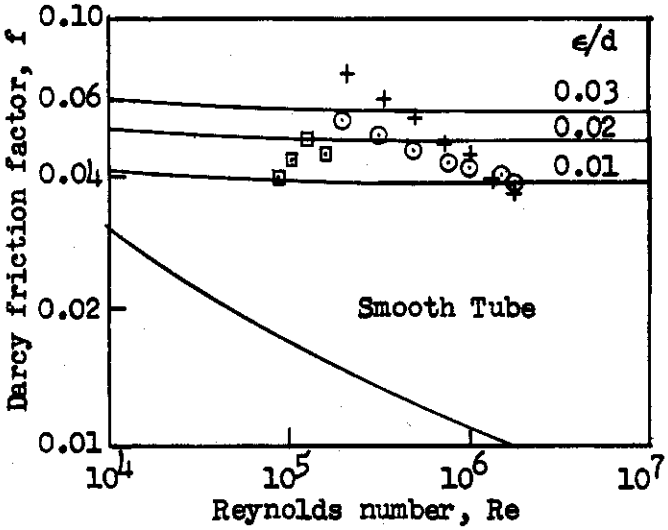

Figure VII-1. Friction factor of fully convoluted low pressure fabric ducting.

compared with friction factors as defined by various values of the relative roughness on the Moody chart. This comparison indicates that the equivalent relative roughness for the fully convoluted fabric ducting is in the range of 0.01 to 0.03. For evaluation of the physical characteristics of cooling systems employing this type of ducting, the use of a friction factor of about 0.05 to 0.06 for all conditions of flow within the turbulent region appears reasonable. Test data on flow resistance of bends for this type of ducting indicate that for the ratio of the radius of curvature of the bend to the diameter of the ducting within the range of 3 to 6, the flow resistance of an equivalent length of straight ducting multiplied by a factor of about 11 yields a good average value for the flow resistance of the bend. Thus, the equivalent Darcy friction factor would be about 0.60.

In many instances for internal ducting in the ultimate component it is convenient and practical to evaluate the loss in total pressure of the air because of the flow resistance by the incompressible-flow relationship

$$\Delta p^o = (fL/d)(\gamma u^2/2g) \qquad \text{(VII-11)}$$

which may be rearranged to the form

$$\Delta p^o/p_i = (fL/d)(kM_1^2/2) \qquad \text{(VII-12)}$$

where M_i represents the Mach number of flow at inlet to the duct. Using k for air equal to 1.4 and solving equation (VII-12) for the Mach number M_i yields

$$M_i = 2.9(d/fL)^{0.5}(\Delta p^o/p_i)^{0.5} \qquad \text{(VII-13)}$$

The equation of continuity

$$w = 3600 \gamma u A$$

for flow through the duct may be rearranged, assuming air, to the form

$$w\sqrt{\theta_i^o}/\delta_i^o = 1674\, M_i\, d''^2 \qquad \text{(VII-14)}$$

by assuming that the inlet Mach number of flow never exceeds about 0.20. By combining equations (VII-13) and (VII-14) and solving for the duct diameter, one obtains

$$d'' = 0.0782(fL)^{0.2}(w\sqrt{\theta_i^o}/\delta_i^o)^{0.4}\Big/\left[1 - (p_e^o/p_i^o)\right]^{0.2} \qquad \text{(VII-15)}$$

This relationship permits evaluation of the required duct size for any selected flow rate, temperature and pressure of the air, duct length, permissible pressure loss and overall equivalent friction factor for the duct run. By introducing into equation (VII-15) a typical average value for the friction factor f of 0.02,

$$d'' = 0.036(L)^{0.2}(w\sqrt{\theta_i^o}/\delta_i^o)^{0.4}\Big/\left[1 - (p_e^o/p_i^o)\right]^{0.2} \qquad \text{(VII-16)}$$

and defines the relationship which has been used quite frequently for evaluating required duct size. When the flow Mach numbers are found to be in the vicinity of 0.20 and above, an equation relating total pressure loss to the duct length, diameter and friction factor is used in place of the incompressible relationship defined by equation (VII-11).

Air Intakes

Many cooling systems, whether centralized or individualized, utilize atmospheric air for the ultimate heat sink. Atmospheric air would be taken aboard an aircraft through an intake which may be one of four general types: (1) leading-edge, (2) scoop, (3) skin, (4) internal. Leading-edge intakes normally have the best pressure recovery characteristics because of the absence of boundary layer flow ahead of the entrance section of the intake, but they cannot always be employed, since in many instances leading edge surfaces are not available in the general vicinity of the equipments to be cooled, or aerodynamic considerations of the aircraft in general would preclude their use. Scoop intakes are inlets located on a surface of an aircraft which protrude outwardly from the surface into an airstream flowing parallel to the aircraft's surface. The protuberance of the intake generally serves to define whether the intake is handling principally free-stream or boundary-layer flow. Pressure

recovery and flow capacity characteristics depend greatly upon the relative amount of boundary layer flow handled by the intake. Well-designed scoop intakes handling essentially free-stream flow provide ram pressure recovery nearly as good as for leading-edge intakes, but with higher overall drag imposed on the aircraft. Intakes of small relative protuberance have inferior pressure recovery characteristics due to the handling of low-energy boundary layer flow, but aid in reducing the overall drag imposed on the aircraft for any required flow rate of cooling air.

Skin intakes are flush openings in the aircraft's skin, and may be arranged to provide inflow of air in any direction from tangential to normal entry. External drag of this type intake generally is low in comparison with the scoop-type intake. Pressure recovery and flow characteristics for skin intakes having tangential entry can be as good as with well-designed scoop intakes, but must operate in a region of thin boundary layer, or in conjunction with boundary layer bleed. Skin intakes in supersonic flow are generally believed to be inferior to scoop intakes. Internal intakes are principally openings or scoops located in the main air ducts supplying ram air to the aircraft's powerplants. Pressure recovery would be high since the powerplants require well-designed air inlets. The use of an inlet of this type has the basic disadvantage that equipments to be cooled are commonly located quite remote to the powerplants and air ducts of considerable length may be required to transfer the cooling air to equipment or intermediate components of cooling systems.

1. Pressure Recovery and Flow Capacity of Leading-Edge Intakes

A leading-edge intake is illustrated schematically in Figure VII-2, with station (∞) defining the undisturbed free-stream state of the air, station (i) the state at entrance to the diffuser and station (e) the state at exit of the diffuser and entrance to the distribution component. Free-stream diffusion occurs ahead of the diffuser. For subsonic flight speeds it may be considered to occur isentropically. Within the diffuser, the stream is diffused to the maximum permissible flow velocity at the exit of the diffuser. The diffuser is assumed to

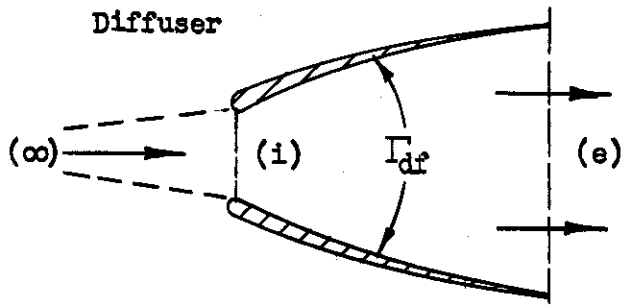

Figure VII-2. Schematic of a leading-edge air intake.

be conical. The rate of variation of its cross-sectional flow area is defined by the total included angle Γ_{df}. Within the supersonic flight Mach number range considered in this study, i.e., 1.0 to 1.8, the diffuser is assumed to operate subsonically at all times, so that a bow wave would be formed ahead of the inlet section, thus permitting spillage of the free-stream air over the leading edge of the inlet. The bow wave is assumed to possess the characteristics of a normal shock within the flow region defined by the inlet area of the diffuser. The selection of the diffuser with external normal shock for supersonic flight speeds is based on a general study of supersonic diffusers applicable to the flight Mach number range from unity to 1.8. This type of supersonic intake is generally considered superior to the full-flow oblique-wave diffusers for flight Mach numbers less than 1.5. For this study, the preference for the normal-shock diffuser is assumed to extend to the maximum Mach number of 1.8 for the purpose of simplifying evaluation procedures. The performance of an external-normal-shock diffuser at a flight Mach number of 1.8 apparently does not differ significantly from that of an oblique-wave diffusion system.

A review of existing methods of design for subsonic leading-edge intakes indicates that a well-proportioned intake operates in level flight with a diffuser inlet velocity u_{df-i} of approximately 70% of the flight velocity. Reduction of the design inlet velocity has the advantages of increasing the overall efficiency of diffusion and reducing the spatial requirements of the diffuser proper. It has the disadvantages of increasing the frontal area and, correspondingly, the external drag attributable to the intake. An inlet velocity of 70% of the flight velocity tends to emphasize minimization of external drag and of leading-edge surface required for the intake opening. The minor penalties of lowered overall efficiency of diffusion and greater spatial requirements are justifiable for most cooling systems, since the absolute size of intakes for cooling systems would normally be relatively small. On this basis, for subsonic flight Mach numbers,

$$T_{df-i}/T_{\infty} = 1 + 0.102\, M_{\infty}^2 \qquad \text{(VII-17)}$$

and

$$p_{df-i}/p_{\infty} = (1 + 0.102\, M_{\infty}^2)^{3.5} \qquad \text{(VII-18)}$$

The pressure recovery of the diffuser proper is defined by the diffuser efficiency and the flow conditions at entrance to the diffuser. The relation between pressure recovery and diffuser efficiency is defined by

$$\eta_{df} = (p^{o}_{df-e} - p_{df-i})/(p^{o}_{df-i} - p_{df-i}) \qquad \text{(VII-19)}$$

This, combined with the relationship

$$p^{o}_{\infty}/p_{\infty} = p^{o}_{df-i}/p_{\infty} = (1 + 0.2\, M_{\infty}^2)^{3.5} \qquad \text{(VII-20)}$$

yields

$$\frac{p^{o}_{df-e}}{p_{\infty}} = (1 + 0.102\ M^{2}_{\infty})^{3.5}\left\{1 + \eta_{df}\left[\left(\frac{1 + 0.2\ M^{2}_{\infty}}{1 + 0.102\ M^{2}_{\infty}}\right)^{3.5} - 1\right]\right\} \qquad \text{(VII-21)}$$

For known values of the diffuser efficiency and flight Mach number, the total pressure of the air at exit of the diffuser is defined in terms of the atmospheric pressure by equation (VII-21).

The efficiency of the diffuser η_{df} is a function of the required area change and the included angle of the conical section. The required area change from inlet to exit of the diffuser depends upon the permissible flow velocity at entrance to the ducting. Increasing the flow velocity at exit of the diffuser increases the efficiency of the diffuser and, correspondingly, the pressure recovery, but would also increase the pressure loss in the ducting. Hence, the exit velocity of the diffuser must remain as an independent variable of analysis. Any selected value must be based upon a compromise indicated by the results of a design study of the entire cooling system. The included angle of the diffuser Γ_{df} normally would be within the range from 8^{o} to roughly 25^{o}. A reduction in the spatial requirements of the diffuser would be obtained by increasing the included angle, which, however, would reduce the efficiency and pressure recovery. Included angles in the range from 10^{o} to 15^{o} would be considered as the most likely design values for aircraft cooling systems.

Based on a study of subsonic diffusers to determine the interrelation of included angle and area change with diffuser efficiency, the following empirical equation is proposed to correlate the efficiency with fairly good accuracy for a range of included angles from 5^{o} to about 35^{o} and area ratios up to roughly 10.

$$\eta_{df} = 1 - 0.014(\Gamma_{df})^{1.33}\left\{\left[\sqrt{\frac{A_{df-e}}{A_{df-i}}} - 1\right]\Big/\left[\sqrt{\frac{A_{df-e}}{A_{df-i}}} + 1\right]\right\} \qquad \text{(VII-22)}$$

The area ratio of the diffuser A_{df-e}/A_{df-i} may be defined by application of the equation of continuity from inlet to exit of the diffuser, i.e.,

$$(\gamma A u)_{df-i} = (\gamma A u)_{df-e} \qquad \text{(VII-23)}$$

which may be rearranged to yield

$$\frac{A_{df-e}}{A_{df-i}} = \frac{0.7 M_{\infty}(1 + 0.102 M^{2}_{\infty})^{2.5}(1 + 0.2 M^{2}_{\infty})^{0.5}(1 + 0.2 M^{2}_{df-e})^{3}}{M_{df-e}(p^{o}_{df-e}/p_{\infty})} \qquad \text{(VII-24)}$$

The required area ratio of the diffuser is a function of the selected permissible flow Mach number at the diffuser exit.

Equations (VII-21), (VII-22) and (VII-24) define the basic relationships for evaluation of pressure recovery and area ratio for lead-

ing-edge intakes in the subsonic flight region. For evaluation of pressure recovery, a trial-and-error solution is required. In general, the procedure would be to assume a value for the diffuser efficiency, calculate the recovery pressure ratio by equation (VII-21), then the required area ratio by equation (VII-24), and lastly evaluate the diffuser efficiency by equation (VII-22) to check the accuracy of the initially assumed value.

The inlet area of the diffuser required for taking aboard the aircraft air at a specified rate may be evaluated by application of the equation of continuity to the inlet section. In order to account for boundary layer effects, the actual flow capacity of the opening is assumed to be 95% of that evaluated on the basis of one-dimensional flow. The resulting expression is

$$w_{df}\sqrt{\theta_{\infty}}/(\delta_{\infty}A''_{df-i}) = 1420\, M_{\infty}(1 + 0.102\, M_{\infty}^2)^{2.5} \qquad \text{(VII-25)}$$

For the subsonic flight Mach number range of 0.6 to 1.0 the required area ratio of the diffuser is defined quite accurately by $0.56\, M_{\infty}^{0.76}/M_{df-e}$. Thus, the required area ratios would normally be within the range of about 2 to 5. Typical ratios of diffuser length to inlet diameter are in the range 1.5 to 5, and have approximately the same magnitude as the required area ratio. The volume of a diffuser having an area ratio of 5, corresponding to an exit Mach number of about 0.10, is roughly twice that of a diffuser having an area ratio of 2, which corresponds to an exit Mach number of about 0.25. The volume varies roughly in direct proportion with the corrected air rate raised to the 1.5-power. Thus, for example, at an altitude of 60,000 feet, the diffuser volume would be about 45 times that for standard sea level atmospheric conditions.

Within the supersonic flight range, a normal shock wave is assumed to exist ahead of the diffuser inlet. The Mach number at entrance to the diffuser is assumed equal to the Mach number downstream of the normal shock, so as to prevent any expansion or recompression of the stream between the standing wave and the diffuser entrance. On this basis, and using the flow properties characteristic of a normal shock wave, the ratio of the total pressure at exit of the diffuser to the free stream pressure is defined by

$$p''_{df-e}/p_{\infty} = \left[(7M_{\infty}^2 - 1)/6\right]\left\{1 + \eta_{df}\left[\left\langle 7.2M_{\infty}^2/(7M_{\infty}^2 - 1)\right\rangle^{3.5} - 1\right]\right\} \qquad \text{(VII-26)}$$

The diffuser efficiency is defined by equation (VII-22) since subsonic flow exists at all times within the diffuser section proper. The ratio of exit to inlet flow area of the diffuser is defined by

$$A_{df-e}/A_{df-i} = (p_{\infty}/p''_{df-e})(M_{\infty})\sqrt{1+(M_{\infty}^2/5)}\;(1+0.2M_{df-e}^2)^3/M_{df-e} \qquad \text{(VII-27)}$$

and the flow capacity by

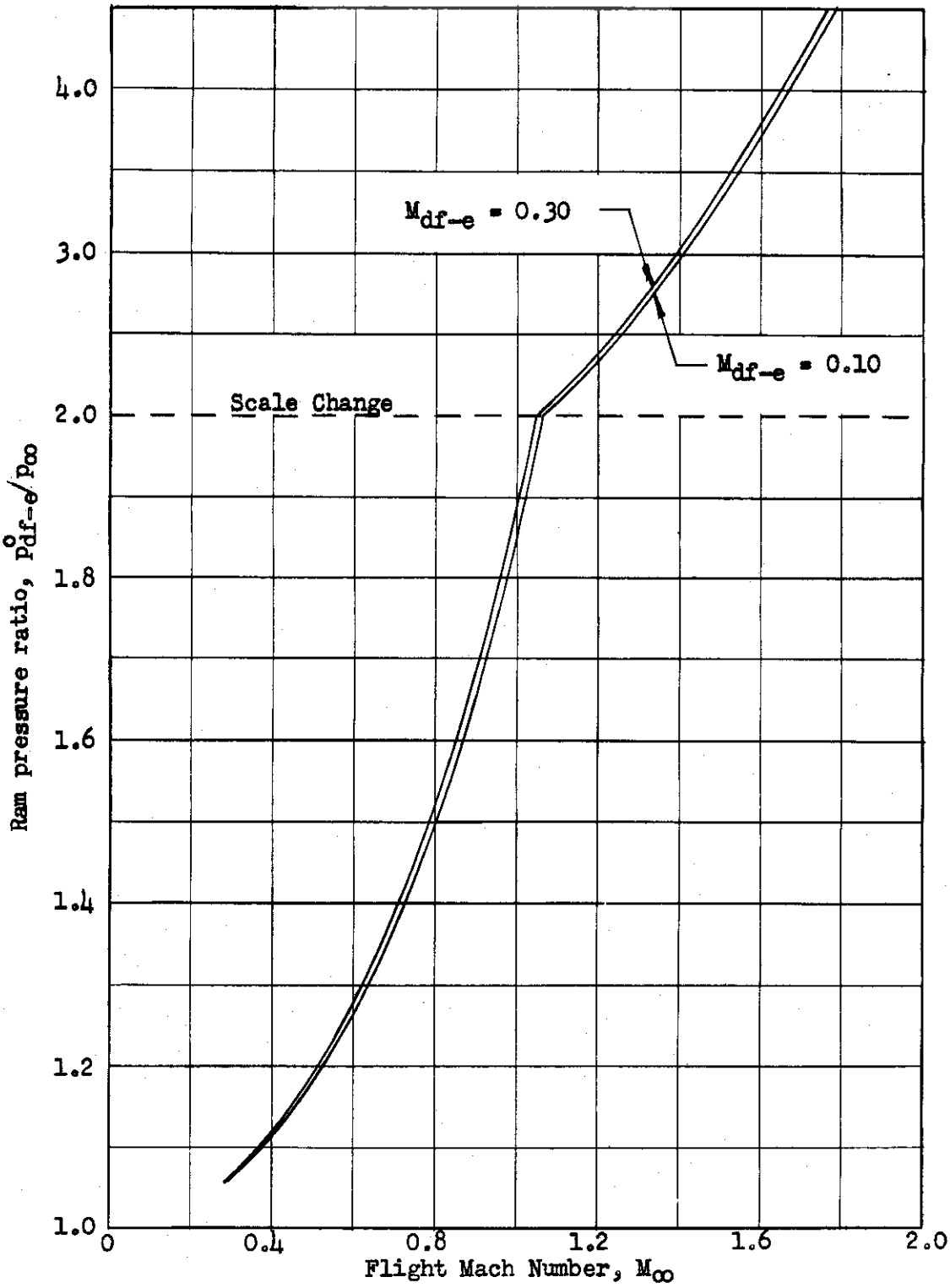

Figure VII-3. Pressure recovery characteristics of leading-edge intakes.

$$w\sqrt{\theta_\infty}/(\delta_\infty A_i'') = 2030\, M_\infty \qquad \text{(VII-28)}$$

The required inlet flow area of the diffuser would be evaluated by equation (VII-28). The procedure for evaluation of performance and physical characteristics of leading-edge intakes for supersonic flight speeds is identical to that outlined for subsonic speeds.

Simplified evaluation procedures for leading-edge intakes may be employed in many instances. If the included angle for the diffuser is assumed to be within the range of 10° to 12°, the ram pressure ratio may be evaluated as a function of the flight Mach number and the Mach number of flow at exit of the diffuser. The results of this evaluation

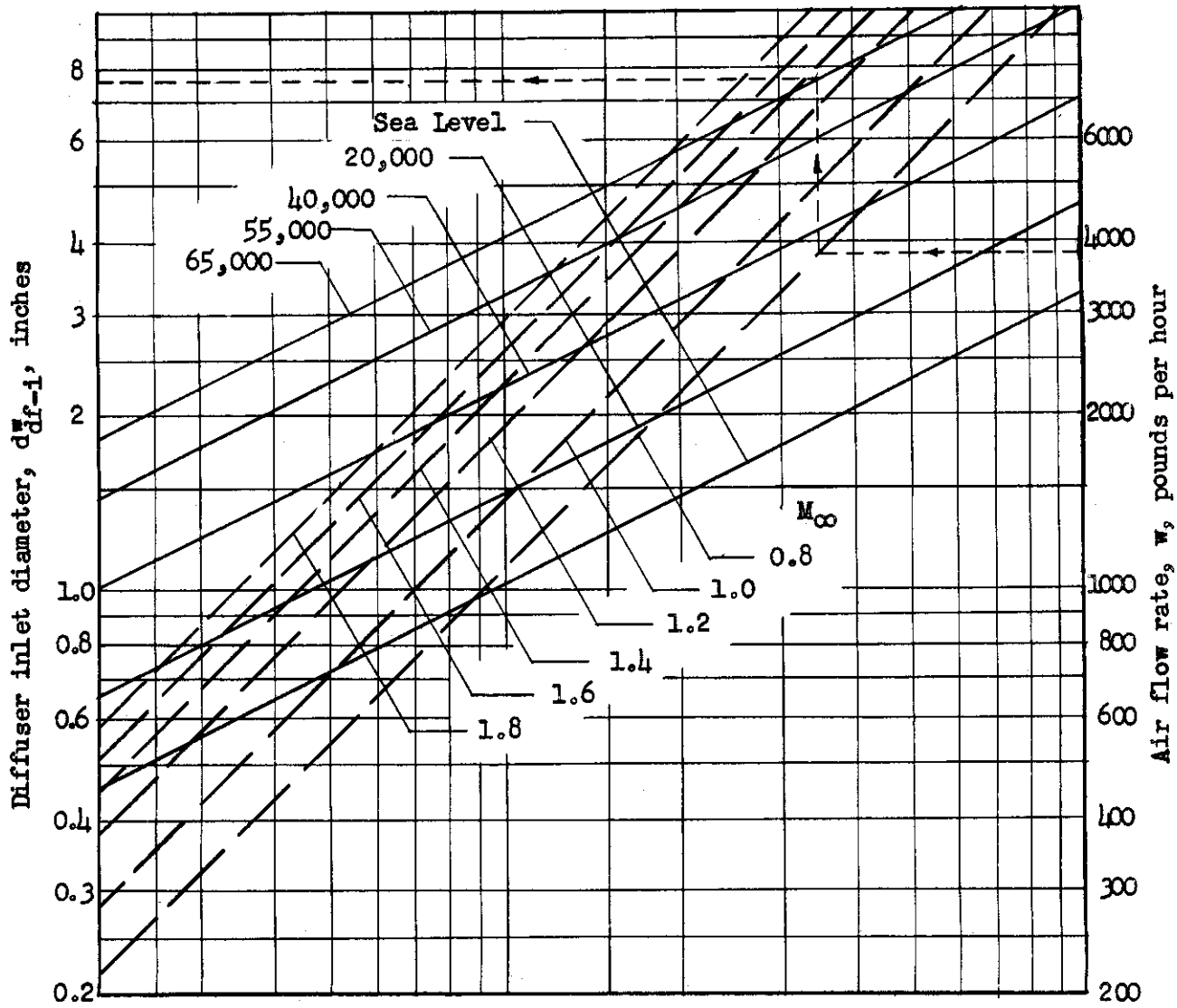

Figure VII-4. Working chart for evaluation of inlet diameter of leading-edge intakes.

are shown in Figure VII-3, and it may be observed that the Mach number of flow at exit of the diffuser has no major effect on the pressure recovery of the intake. For the flight Mach number range of 1.2 to 1.8 the ram pressure ratio may be represented quite accurately by the equation

$$p^{s}_{df-e}/p_{\infty} = 1.6\, M_{\infty}^{1.8} \qquad \text{(VII-29)}$$

For the subsonic range of flight Mach numbers from 0.4 to 1.0, an equation which quite accurately defines the ram pressure ratio is

$$p^{s}_{df-e}/p_{\infty} = 1 + 0.85\, M_{\infty}^{2.2} \qquad \text{(VII-30)}$$

The required inlet flow area of the diffuser is defined by equation (VII-25) for subsonic flight Mach numbers and by (VII-28) for supersonic flight Mach numbers. A graphical solution to the evaluation of the required inlet area is presented in Figure VII-4.

2. Pressure Recovery and Flow Capacity of Scoop Intakes

Scoop intakes have performance and physical characteristics which vary widely with the purpose of use, location on the aircraft outer surface, type and configuration of the intake and aircraft flight conditions. It has not been found practical to develop a working method capable of evaluating the effects on performance and physical characteristics of the intakes for the wide variety of operational and design conditions possible. Methods are presented in the following paragraphs which are not rigorous for all applications and flight conditions, but are designed to evaluate approximately the performance and physical characteristics of scoop intakes. If during any cooling system analysis it should occur that the characteristics of a scoop intake play a key role in establishing the criteria of design, it would be necessary to consider the design and performance evaluation of the scoop intake in considerably more detail.

For purposes of analysis, scoop intakes are separated in three general groups: (1) those having a height, as measured by the normal projection of the scoop into the air stream, equal to or less than the thickness of the boundary layer, (2) those having a height in the range of one- to four times the boundary layer thickness, and (3) those handling essentially free stream air, such that the boundary layer air represents a small percentage of the total inflow to the scoop.

The velocity profile within the boundary layer is assumed to be represented by the conventional one-seventh power variation, with a flow velocity of zero at the aircraft's surface and free stream velocity at the outer edge of the boundary layer. Also, it is assumed that no diffusion of the air occurs before entrance to the scoop intake. For scoops having a height equal to or less than the thickness of the boundary layer, the mean temperature of the boundary layer is assumed to be

the arithmetic average of the free stream and adiabatic wall temperatures, the latter defined on the basis of a recovery factor equal to 0.9. The resulting expression defining the flow capacity of the scoop, when $(y_{df-i}/y_{bl}) < 1$, may be shown to be

$$w_{df}\sqrt{\theta_\infty}/(\delta_\infty A''_{df-i}) = \frac{1870\, M_\infty (y_{df-i}/y_{bl})^{0.143}}{1 + 0.09\, M_\infty^2 (2 - y_{df-i}/y_{bl})} \qquad \text{(VII-31)}$$

The thickness of the boundary layer is assumed to be defined by

$$y''_{bl} = 0.19(L_{bl})^{0.8}\, \theta_\infty^{0.24}/(\delta_\infty M_\infty)^{0.2} \qquad \text{(VII-32)}$$

where L_{bl} represents the distance from the scoop intake to the leading edge of the aerodynamic surface on which the intake is mounted. The integrated mean total pressure at the entrance section of the diffuser, when $(y_{df-i}/y_{bl}) < 1$, is defined in terms of the free-stream pressure by the expression

$$p^\circ_{df-i}/p_\infty = \left[1 + 0.16\, M_\infty^2 (y_{df-i}/y_{bl})^{0.286}\right]^{3.5} \qquad \text{(VII-33)}$$

The scoop must provide internal diffusion of the air from the mean flow velocity at entrance of the diffuser to the required flow velocity at exit of the diffuser and entrance to the ducting. The mean flow velocity at entrance of the diffuser is defined by

$$u_{df-i}/u_\infty = 0.875(y_{df-i}/y_{bl})^{0.143} \qquad \text{(VII-34)}$$

The area ratio required of the diffuser is defined by application of the equation of continuity from inlet to exit, which yields

$$\frac{A_{df-e}}{A_{df-i}} = 0.875(p_\infty/p^\circ_{df-e})(\beta^{3.5}_{df-e})(M_\infty/M_{df-e})(y_{df-i}/y_{bl})^{0.143} \qquad \text{(VII-35)}$$

where the total pressure at exit of the diffuser is related to the inlet total pressure by

$$p^\circ_{df-e}/p_\infty = 1 + \eta_{df}\left[(p^\circ_{df-i}/p_\infty) - 1\right] \qquad \text{(VII-36)}$$

The efficiency of the internal diffusion process is assumed to be defined by equation (VII-22). For scoop intakes having a ratio of (y_{df-i}/y_{bl}) much less than unity, the mean flow velocity would be relatively low and no internal diffusion is required. An area ratio A_{df-e}/A_{df-i} less than unity would indicate that the boundary-layer flow must be accelerated within the scoop to reach the specified flow velocity at exit of the diffuser. As for evaluation of the leading-edge intake, a trial-and-error process is required to define the pressure recovery of this type intake.

With the second general type of scoop intake, where the boundary layer thickness is within the range of 25 to 100% of the scoop height, the equation defining the flow capacity of the inlet section is

$$w_{df}\sqrt{\theta_\infty}/(\delta_\infty A''_{df-i}) = 1870\, M_\infty\left\{(8/7)\left[1-\frac{y''_{bl}}{y''_{df-i}}\right]+\frac{y''_{bl}/y''_{df-i}}{(1+0.09M_\infty^2)}\right\} \quad \text{(VII-37)}$$

The thickness of the boundary layer is defined by equation (VII-32). The mean total pressure of the air at entrance to the diffuser is defined by

$$p^o_{df-i}/p_\infty = \left\{1+0.2M_\infty^2\left[(y''_{df-i}/y''_{bl})-0.3\right]\Big/\left[(y''_{df-i}/y''_{bl})-0.125\right]\right\}^{3.5} \quad \text{(VII-38)}$$

The pressure recovery during diffusion within the intake is evaluated by equations (VII-22) and (VII-36), with the internal area ratio of the intake defined by

$$\frac{A_{df-e}}{A_{df-i}} = \left[1-0.125(y''_{bl}/y''_{df-i})\right](p_\infty/p^o_{df-e})(\beta^3_{df-e}/M_{df-e})(M_\infty\sqrt{\beta_\infty}) \quad \text{(VII-39)}$$

When the height of a scoop intake is more than five times the thickness of the boundary layer, it is assumed that the required inlet flow area and external pressure recovery may be evaluated independent of the boundary layer characteristics. The scoop acts essentially as a leading-edge intake. The external pressure recovery is quite high over the range of inlet velocity ratio u_{df-i}/u_∞ from about 0.4 to 1.2. In order to permit a compromise in design between inlet flow area and overall pressure recovery, the following equations are presented as a function of the inlet velocity ratio, and are valid for a range of inlet aspect ratios from 1 to 5. The flow capacity of the scoop is defined by

$$w\sqrt{\theta_\infty}/(\delta_\infty A''_{df-i}) = 2030 M_\infty \frac{u_{df-i}}{u_\infty}\left\{1+0.2M_\infty^2\left[1-(u_{df-i}/u_\infty)^2\right]\right\}^{2.5} \quad \text{(VII-40)}$$

The external total pressure recovery is assumed independent of the inlet velocity ratio and is defined therefore, by the equation

$$p^o_{df-i}/p_\infty = \left[1+0.195\, M_\infty^2\right]^{3.5} \quad \text{(VII-41)}$$

The internal pressure recovery is evaluated by equations (VII-19) and (VII-22), with the internal area ratio defined by

$$\frac{A_{df-e}}{A_{df-i}} = \frac{p_\infty}{p^o_{df-e}}\,\frac{u_{df-i}}{u_\infty}\,\frac{M_\infty}{M_{df-e}}\,\beta^3_{df-e}\sqrt{\beta_\infty}\left\{1+0.2M_\infty^2\left[1-\left(\frac{u_{df-i}}{u_\infty}\right)^2\right]\right\}^{2.5} \quad \text{(VII-42)}$$

Inlet velocity ratios in the range 0.7 to 1.0 would be considered most typical for subsonic flight speeds.

With scoop intakes and supersonic flight speeds, the following assumptions are made. A normal-shock wave precedes the flow at the entrance to the diffuser, and the free-stream flow conditions ahead of the inlet are defined as those downstream of the normal shock. Thereafter, the scoop intakes are evaluated in the manner outlined in the preceding paragraphs. This method of analysis yields only approximate results.

3. Pressure Recovery and Flow Capacity of Skin Intakes

The performance of skin intakes depends greatly upon the boundary layer conditions at entrance to the intake, the aspect ratio of the intake and the relative amount of boundary layer bleed employed. Details of general design procedures for high-performance skin intakes have not been compiled. Specific procedures yielding designs with good pressure recovery should be utilized when a high-performance skin intake is required for a cooling system.

Typically, a flush recessed opening in the skin of an aircraft would yield a pressure recovery defined by

$$p^{o}_{df-e}/p_{\infty} = \left[1 + 0.06\, M^{2}_{\infty}\right]^{3.5} \qquad \text{(VII-43)}$$

when the flow velocity u_{df-e} at the exit of the intake is within 10 to 70% of the flight velocity. The required flow area at exit of the diffuser is defined by

$$w\sqrt{\theta_{\infty}}/(A''_{df-e}\,\delta_{\infty}) = 2030(M_{\infty}/\beta_{\infty})(u_{df-e}/u_{\infty})(p^{o}_{df-e}/p_{\infty})/(\beta_{df-e})^{2.5} \qquad \text{(VII-43)}$$

4. Pressure Recovery and Flow Capacity of Internal Intakes

An internal intake located on the surface of any main air duct acts essentially as a scoop intake. Pressure recovery and flow capacity for this type intake would be evaluated by the procedures outlined in the preceding sub-section (2).

5. Drag of Air Inlets

The total drag imposed on an aircraft by use of an air inlet may be evaluated as the sum of the momentum and external drags. Momentum drag accounts for drag on the aircraft resulting from change in the absolute or relative air velocity between inlet and exit of the flow system. External drag includes all parasitic drag originating from added surfaces, edges and protuberances in general.

External drag of leading-edge inlets having the general design features as presented in sub-section (1) would be, on the average, defined approximately by

$$Dr_{ex} = 0.5\,\delta_{\infty}\,A''_{df-i}\,M^{2}_{\infty} \quad \text{for } M_{\infty} < 1 \qquad \text{(VII-44)}$$

over the subsonic flight range.

Within the supersonic flight range of the study, i.e., for Mach numbers up to 1.8, the external drag would be roughly 1.5 times that defined by equation (VII-44) when the inlet is operating at its design flight speed. Under off-design operation, if the inlet handles less air than the swept-volume of flow, so that spillage of air over the leading edge of the intake exists, a drag increase results which must be added to 1.5 times the drag defined by equation (VII-44). The total external drag under these conditions is defined approximately by

$$Dr_{ex} = 14.7\,\delta_\infty A''_{df-i}\left[\frac{P_{df-i}}{P_\infty} - 1\right] + \frac{w_{df}(u_{df-i} - u_\infty)}{3600\,g} + \delta_\infty A''_{df-i} M_\infty^2 \qquad \text{(VII-45)}$$

where, in general, the diffuser inlet pressure and flow velocity can only be defined from considerations of the flow characteristics of the entire cooling system. When the inlet operates under off-design conditions with the shock located within the diffuser proper, so that the inflow of air is defined by the swept-volume of flow, the external drag would be evaluated approximately by 1.5 times the drag defined by equation (VII-44).

The momentum drag with subsonic or supersonic leading-edge intakes is defined by

$$Dr_{mom} = 0.00915\, w_{df}\, M_\infty \sqrt{\theta_\infty} \qquad \text{(VII-46)}$$

which for subsonic design reduces to

$$Dr_{mom} = 13\,\delta_\infty A''_{df-i}\, M_\infty^2 (1 + 0.102\, M_\infty^2)^{2.5} \qquad \text{(VII-47)}$$

and for supersonic design to

$$Dr_{mom} = 19.6\,\delta_\infty\, A''_{df-i}\, M_\infty^2 \qquad \text{(VII-48)}$$

The external drag of scoop inlets operating over the subsonic flight speed range is approximately defined by

$$Dr_{ex} = 1.25\,\delta_\infty\, A''_{df-i}\, M_\infty^2 \qquad \text{(VII-49)}$$

For the supersonic speed range, the external drag of a scoop would be defined by equation (VII-49) multiplied by a factor of 2, except under conditions where the boundary layer extends beyond the maximum protuberance of the scoop. For the latter case, the external drag would be defined by equation (VII-49).

The momentum drag of boundary layer scoops for both sub- and supersonic flight speeds is defined by

$$Dr_{mom} = 16\,\delta_\infty M_\infty^2\, A''_{df-i}(y_{df-i}/y_{bl})^{2/7} \qquad \text{(VII-50)}$$

when the diffuser inlet height y_{df-i} is less than or equal to the boundary layer thickness y_{bl}; or by

$$Dr_{mom} = 16\,\delta_\infty M_\infty^2 A''_{df-i}\,\frac{y_{bl}}{y_{df-i}} + 0.00915 w_{df}\,M_\infty\sqrt{\theta_\infty}\left[1 - \frac{y_{bl}}{y_{df-i}}\right] \qquad \text{(VII-51)}$$

when the diffuser inlet height y_{df-i} is from 1 to 4 times the boundary layer thickness, or by equation (VII-46) when the ratio of inlet height to boundary layer thickness is greater than 4.

Air Outlets

The general practice in the cooling system study has been to ignore external drag of air outlets and to define their weight and space on the basis of an equivalent length of ducting. The thrust which may be derived from expansion and ejection of the air has been included in some systems and ignored in others. When the flow circuit is such that pressure drop at the outlet is available, in general the thrust is included. The cooling system studies presented in subsequent sections specify when the thrust is included or ignored. With some systems there is no practical benefit to be derived by raising the back pressure throughout the flow circuit so as to have a pressure drop available in the outlet of the system for development of thrust. The thrust resulting from an exit velocity of the outlet, u_{n-e}, is defined by

$$\text{thrust} = -Dr_{mom} = 0.863 \times 10^{-5}\, w\, u_{n-e} \qquad \text{(VII-52)}$$

where w represents the flow rate of air in pounds per hour and the u_{n-e} the exit velocity in feet per second. The net momentum drag is defined by the sum of the inlet and outlet momentum drags.

Blowers

Evaluation of cooling systems employing blowers as the source of air motion requires working procedures which permit convenient definition of size, weight, speed and power for any specified air flow rate and system flow resistance. Studies of the performance of low and medium pressure centrifugal and axial blowers have been conducted to establish evaluation methods for determining physical characteristics and performance. Low and medium pressure blowers are arbitrarily classified as those having pressure producing ability up to about 10 to 15 inches of water at standard density.

1. Centrifugal Blowers

The study of low and medium pressure centrifugal blowers has been restricted to blowers employing forward curved multiple vanes of shallow radial depth. Centrifugal blowers employing backward curved vanes have not been considered for aircraft application because of their inherently small pressure-producing ability. The performance of 55 units

of the forward-curved multi-vaned type, representing products of five manufacturers, have been studied to define representative performance. Impeller diameters ranged from 3 to 36 inches, and rotational speed from 280 to 5000 revolutions per minute.

Performance of each unit was studied and correlated by assuming the blowers to be homologous, i.e., assuming the fan or blower laws to apply. On this basis three parameters may be defined to correlate the volumetric capacity, the pressure-producing ability and the input power

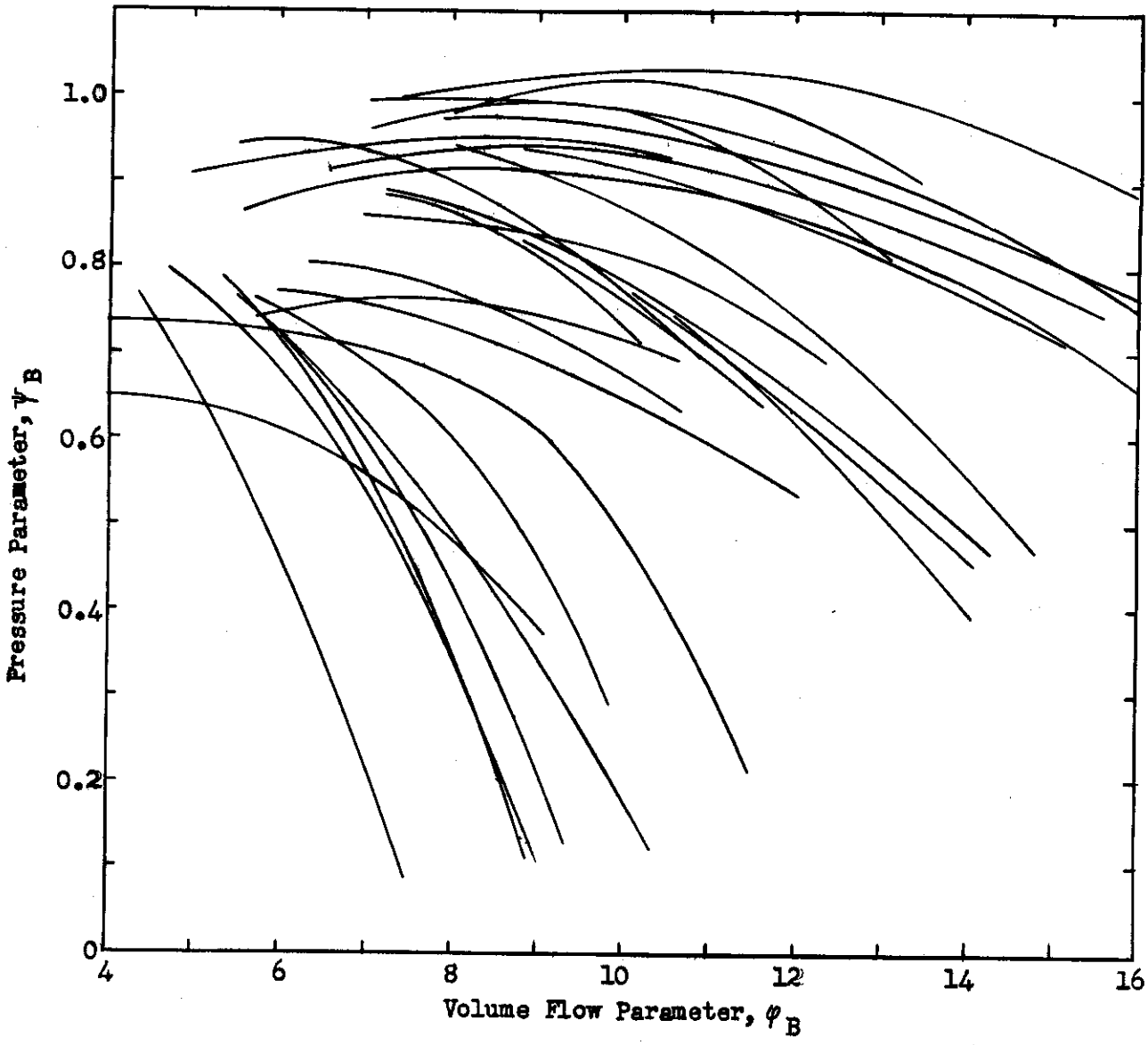

Figure VII-5. Generalized pressure and volume flow characteristics of low- and medium-pressure centrifugal blowers.

requirements. The relative volumetric capacity of the blowers was correlated by using a parameter equivalent to the standard flow coefficient for compressors and blowers. The parameter is defined by

$$\varphi_B = (v_B/100)(0.5/b_B)/[(n_B/1000)(d_{BI}^{w}/10)^3] \qquad \text{(VII-53)}$$

which assumes that for homologous blowers the flow rate is directly proportional to the rotational speed and to the cube of the impeller diameter when all impeller widths are first corrected to a comparable percentage of the impeller diameter. The standard geometry of the impeller is selected as a width ratio b_B of 0.5, i.e., an impeller width equal to one-half the tip diameter. A practical design range for the width ratio would be considered as from about 0.3 to about 0.7. The volume flow

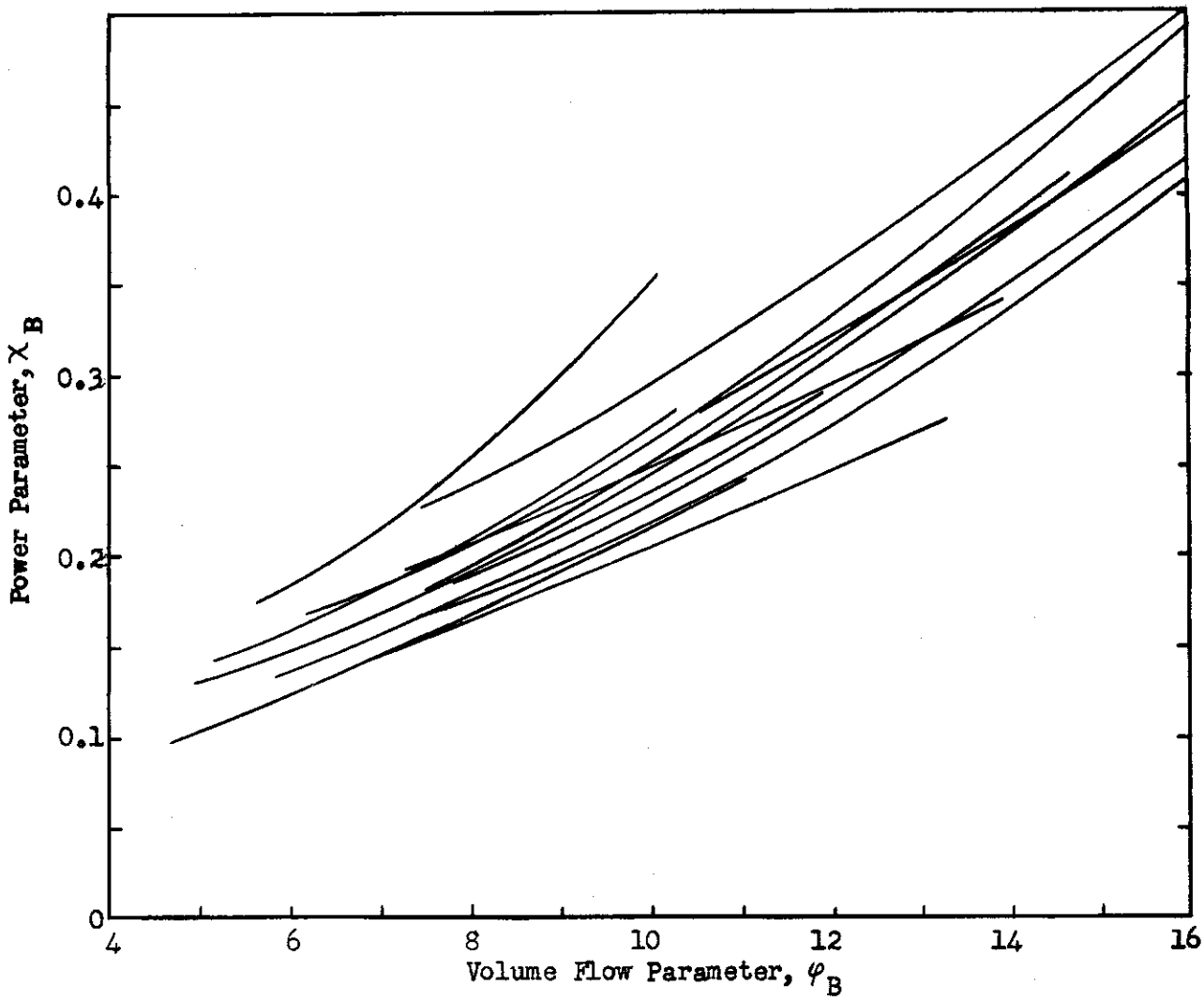

Figure VII-6. Generalized shaft power requirements of low- and medium-pressure centrifugal blowers.

parameter for any blower would vary from zero, i.e., shut-off operating condition, to a value corresponding to the maximum flow handling capacity of the unit, defined as the operational condition where the outlet static pressure equals the inlet total pressure. The pressure-producing ability of the various units has been correlated by the parameter

$$\psi_B = (\Delta p_B^{o''}/\sigma_{Bi})/\left[(n_B/1000)^2(d''_{BI}/10)^2\right] \qquad \text{(VII-54)}$$

which is basically equivalent to the definition of the standard pressure coefficient employed in compressor design theory. The denominator of equation (VII-54) is proportional to the square of the impeller tip speed. The numerator of equation (VII-54) is proportional to the head produced by the blower, where σ_{Bi} represents the ratio of the air density at inlet to the blower to standard air density. Data on shaft power required to drive the blower were evaluated and correlated by the power parameter

$$\chi_B = (P'_B/\sigma_{Bi})(0.5/b_B)/\left[(n_B/1000)^3(d''_{BI}/10)^5\right] \qquad \text{(VII-55)}$$

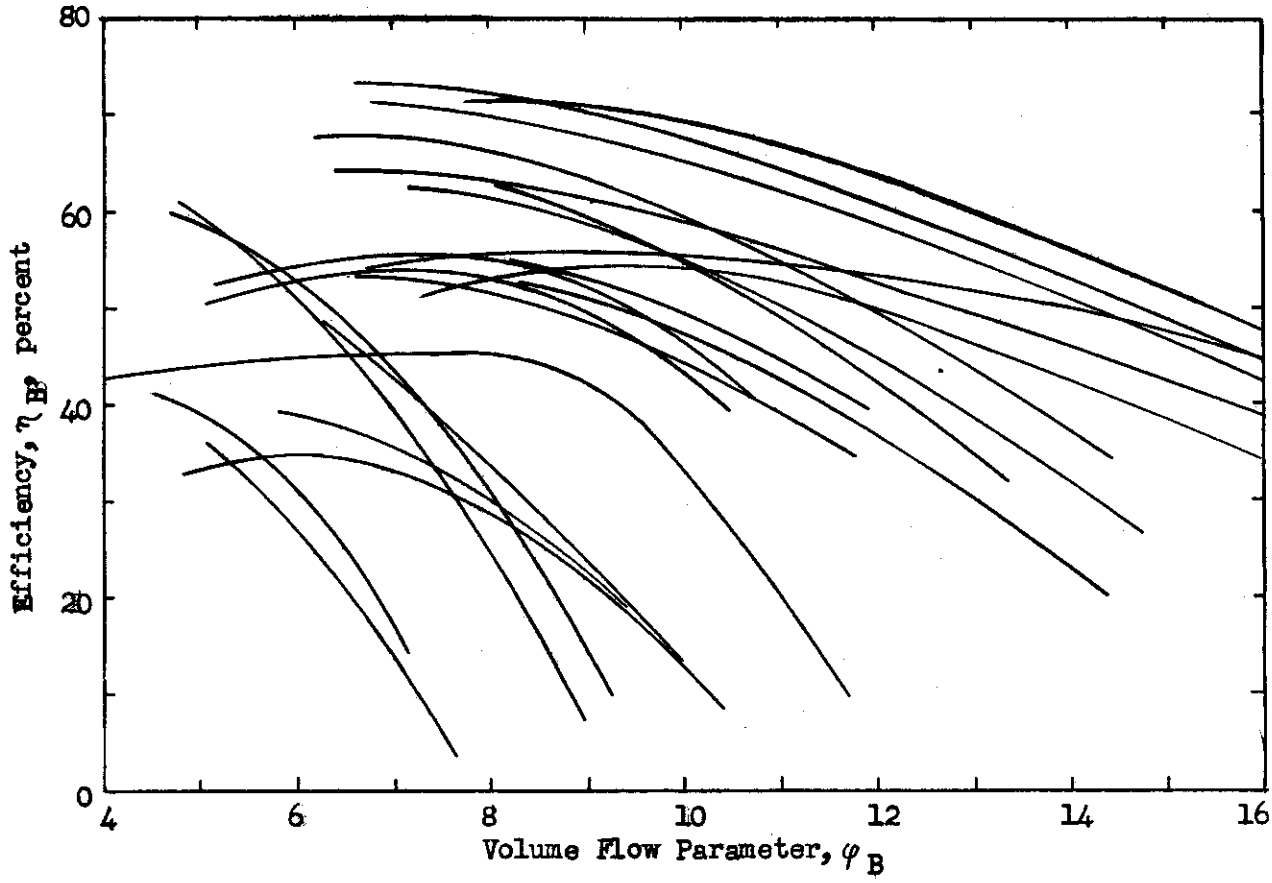

Figure VII-7. Generalized efficiency of low- and medium-pressure centrifugal blowers.

where P_B'/σ_{Bi} defines the corrected shaft horsepower required by the blower.

The blower efficiency is defined by the generalized parameters and was calculated from

$$\eta_B = \varphi_B \psi_B/(63.5\chi_B) \qquad \text{(VII-56)}$$

The results obtained in correlating centrifugal blower performance by the parameters φ_B, ψ_B and χ_B are shown in Figures VII-5, VII-6 and VII-7. Representative generalized performance for this type of blower may be selected from average performance shown in Figures VII-5 and VII-6, as illustrated schematically in Figure VII-8. These

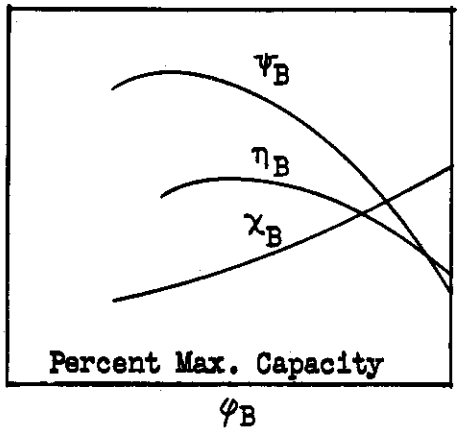

Figure VII-8. Representative generalized performance of low and medium pressure centrifugal blower.

generalized characteristics are used for selection of required impeller diameter and rotational speed of a blower. The criteria for selection are obtained by combining equations (VII-53) and (VII-54) to yield explicit definitions of required diameter and speed. The resulting expressions are

$$d''_{BI}/10 = \left[0.707\,\psi_B^{0.25}/\varphi_B^{0.5}\right]\left\{(v_B/100)^{0.5}/\left[(b_B)^{0.5}(\Delta p_B^{o''}/\sigma_{Bi})^{0.25}\right]\right\} \qquad \text{(VII-57)}$$

$$n_B/1000 = \left[\varphi_B^{0.5}/0.707\,\psi_B^{0.75}\right]\left[(\Delta p_B^{o''}/\sigma_{Bi})^{0.75}(b_B)^{0.5}/(v_B/100)^{0.5}\right] \qquad \text{(VII-58)}$$

These relationships illustrate that for any volumetric capacity and total pressure rise required of the blower, the diameter and rotational speed are defined explicitly by selection of the width ratio of the impeller and the efficiency level or percent maximum capacity at which the blower would operate.

Generalization of bulk volume and weight for low and medium pressure centrifugal blowers has been obtained from a study of existing designs representing 31 units and 5 manufacturers. Impeller diameters

of these units ranged from 3 to 11 inches. Blower volume is correlated as a function of the diameter and axial width of the impeller by the parameter $b_B(d''_{BI})^3$, where b_B is the ratio of the axial width to tip diameter of the impeller. Results of this type correlation are shown in Figure VII-9. For any specific blower type, as for example blowers of varying size but built by the same manufacturer, the volume is found to vary linearly with the parameter $b_B(d''_{BI})^3$. However, a range in blower volume is found at any fixed value of the abscissa in Figure VII-9 due to variations among the designs of the various manufacturers. For purposes of evaluation of blower volume required for aircraft equipment cooling systems it is assumed that the effort would be directed toward practical minimization of physical size, so that the solid line indicated in Figure VII-9 would be representative of blower designs suitable for cooling system applications. This line may be described by the equation

$$V''_B = 3500\, b_B(d''_{BI}/10)^3 \qquad \text{(VII-59)}$$

and would be used to define spatial requirements of low and medium pressure centrifugal blowers.

A study of the weight of various low and medium pressure centrifugal blowers indicates that weight may be correlated with volume.

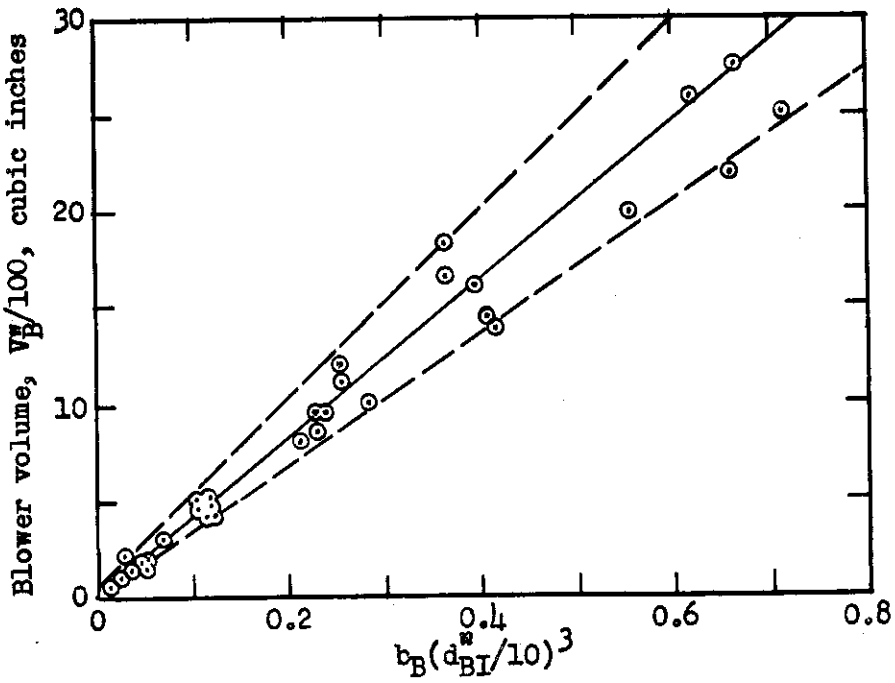

Figure VII-9. Results of correlation of volume for low and medium pressure centrifugal blowers as function of impeller dimensions.

The representative weight variation is defined by

$$W_B = 1.28(V_B''/100)^{0.8} \qquad \text{(VII-60)}$$

The flow velocity of the air at the blower discharge is defined by the flow rate and the exit area. In order that the exit velocity may be defined for any selected low and medium pressure centrifugal blower, a study of exit areas of existing blowers was made in an effort to correlate this area as a function of the impeller dimensions. The results obtained from this study of 36 commercially available units having impeller diameters in the range 3 to 12 inches define the variation of exit area with the abscissa parameter by the equation

$$A_{Be}'' = 100\, b_B(d_{BI}''/10)^2 \qquad \text{(VII-61)}$$

External dimensions of the scroll for low and medium pressure centrifugal blowers were studied for 34 units having impeller diameters in the range from 3 to 15 inches. Dimensions of the scroll were found to vary about in direct proportion with the diameter of the impeller.

2. Axial Blowers

A study of low and medium pressure axial blowers was conducted to define generalized performance and physical characteristics in a manner similar to that used for low and medium pressure centrifugal blowers. The purpose of determining performance and physical characteristics has been to allow evaluation of rotational speed, power, weight and volume of a typical blower employed as a source of air movement in an aircraft equipment cooling system. Physical characteristics and performance of low and medium pressure axial blowers were determined from the characteristics of existing designs, in order to define typical average values. No attempt was made to study effects of details in design, such as rotor or stator blade angle and solidity.

The results are based on the study of 17 single-stage units, which have rotor diameters in the range from 3.5 to 21 inches and rotational speeds from 3600 to 14,000 revolutions per minute. Generalized performance is defined in terms of the flow coefficient φ_B, the pressure coefficient ψ_B and the power coefficient χ_B. The flow coefficient for axial blowers is defined as

$$\varphi_B = (v_B/100)\left[0.51/(1-\nu_B^2)\right] \Big/ \left[(n_B/1000)(d_{BI}''/10)^3\right] \qquad \text{(VII-62)}$$

which is identical to that used for centrifugal blowers except that a correction factor is introduced to allow for variation in the hub-to-tip diameter ratio of the impeller ν_B, whereas with centrifugal units a correction factor b_B is included to allow for variation in the axial width of the impeller relative to the tip diameter. For axial units, a reference hub-to-tip diameter ratio is selected as 0.70, which defines the constant of 0.51 equal to $(1-\nu^2)$ in equation (VII-62). It is as-

sumed that some variation in the hub-to-tip diameter ratio for blower selection or design is possible without affecting to any appreciable extent the pressure-producing ability or power requirements of the blower, and that the volumetric capacity of a unit would be proportional to the factor $(1-\nu^2)$, as indicated by equation (VII-62). Actually, performance of axial blowers would be affected to some extent when this ratio is varied, principally due to radial flow when the ratio is low and to high relative skin friction when

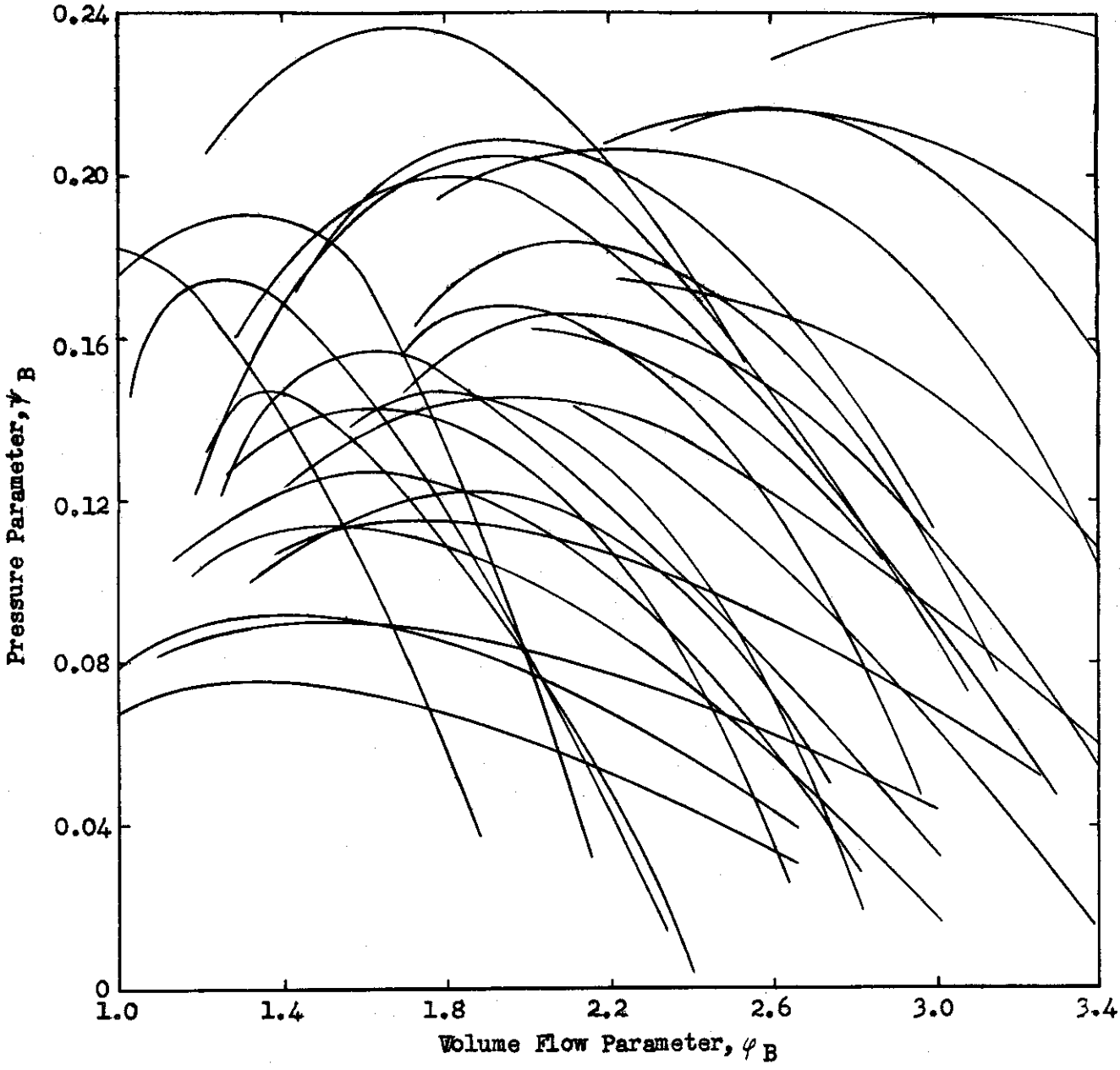

Figure VII-10. Generalized pressure and flow volume characteristics of low and medium pressure single stage axial blowers.

the ratio is high. A practical range of the hub-to-tip diameter ratio ν_B permitting correlation by the factor introduced in equation (VII-62) is estimated to be from about 0.60 to 0.80.

The pressure-producing ability of a single stage axial blower is correlated by the pressure coefficient, defined as

$$\psi_B = (\Delta p_B''/\sigma_{Bi}) \Big/ \left[(n_B/1000)^2 (d_{BI}''/10)^2\right] \qquad \text{(VII-63)}$$

which is identical in definition to that employed for centrifugal blowers. As previously pointed out, the pressure-producing ability is assumed to be independent of the hub-to-tip diameter ratio within a practical range of variation, such as 0.60 to 0.80. The effect of inlet air density on the actual air pressure rise is accounted for by the inlet air density ratio σ_{Bi}. This method of correction is fairly accurate as long as the flow pro-

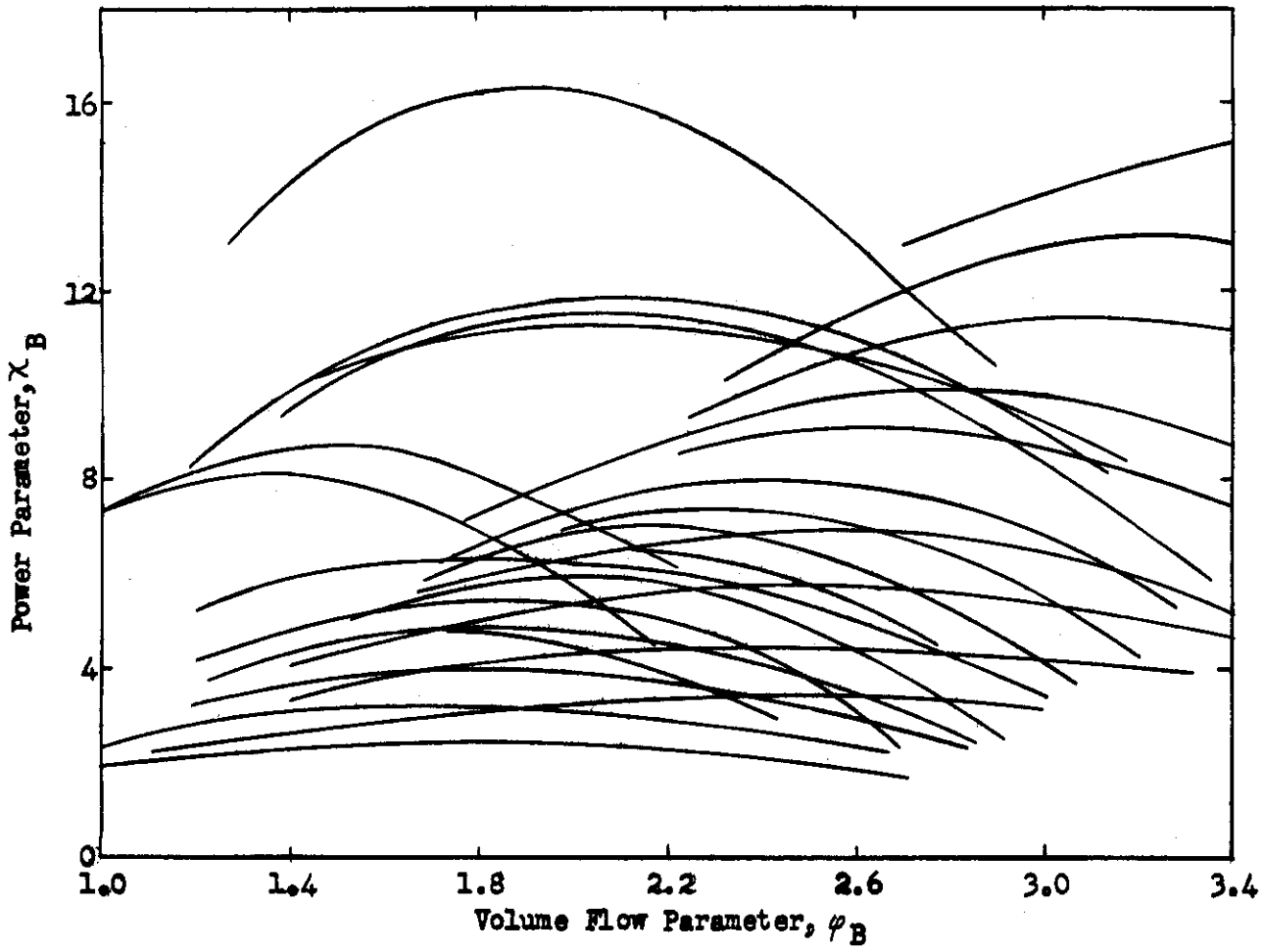

Figure VII-11. Generalized shaft power requirements of low and medium pressure single stage axial blowers.

cess is essentially incompressible, as would be the case for most single-stage axial blowers. Basically, equation (VII-63) defines the ratio of head development to the square of the impeller tip speed for one stage of a blower.

Shaft power required of axial blowers is correlated by the power coefficient, defined as

$$\chi_B = (P'_B/\sigma_{Bi}) \left[0.51/(1-\nu_B^2)\right] \Big/ \left[(n_B/1000)^3 (d''_{BI}/10)^5\right] \quad \text{(VII-64)}$$

which is basically equivalent to that employed for centrifugal blowers except for the factor including the hub-to-tip diameter ratio in place of the

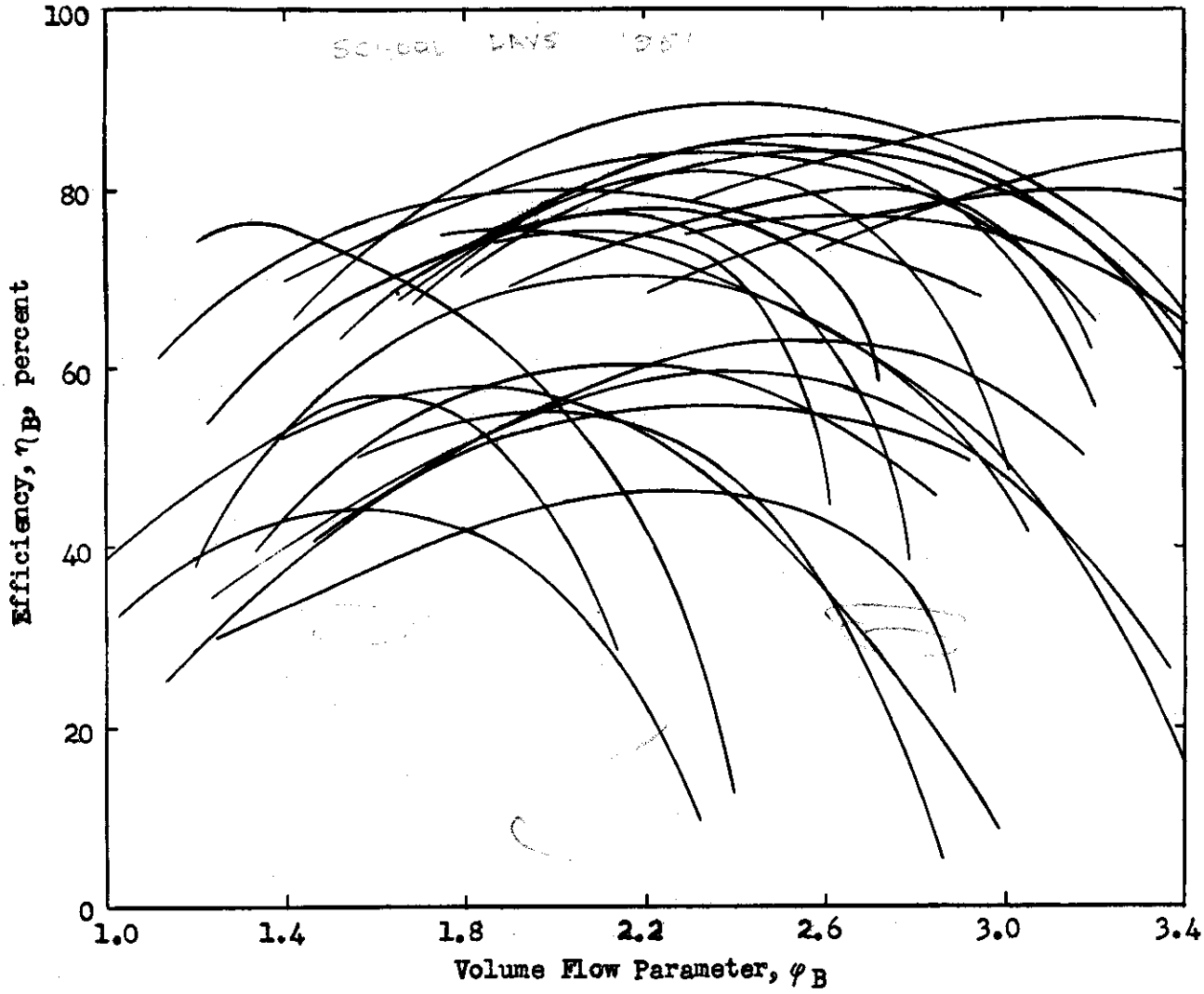

Figure VII-12. Generalized efficiency of low and medium pressure single stage axial blowers.

width-to-diameter ratio for centrifugal units. It is assumed that mechanical losses are included in defining shaft power required of any blower by use of the power coefficient defined in equation (VII-64).

Results obtained by correlation of performance of single-stage axial blowers in terms of flow, pressure and power coefficients are illustrated in Figures VII-10, VII-11 and VII-12. The variation in results may in part be attributed to differences of solidity, blade angle of rotor and stator and stator vane location.

Representative generalized performance for this type blower may be selected from average performance of Figures VII-10 and VII-11 is illustrated schematically in Figure VII-13. The generalized performance so defined would be employed to define typical operational characteristics of low and medium pressure axial blowers.

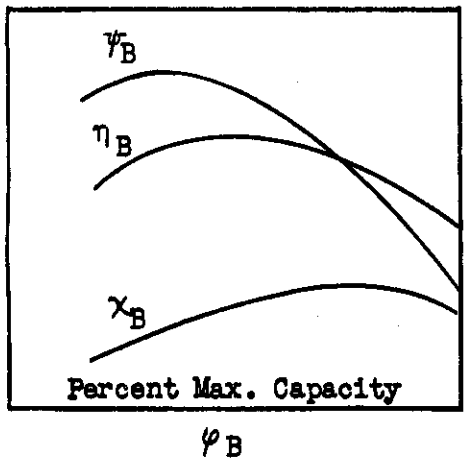

Figure VII-13. Representative generalized performance of low and medium pressure single-stage axial blower.

From the generalized performance of Figure VII-13 for any selected operational condition, usually defined by percent maximum capacity or percent maximum efficiency derived from required power level or control considerations, the required impeller diameter and rotational speed may be explicitly defined from the equations

$$d''_{BI}/10 = \left[0.714\psi_B^{0.25}/\varphi_B^{0.5}\right]\left[(v_B/100)^{0.5}/(1-\nu_B^2)^{0.5}(\Delta p''_B/\sigma_{Bi})^{0.25}\right] \quad \text{(VII-65)}$$

$$n_B/1000 = \left[\varphi_B^{0.5}/0.714\psi_B^{0.75}\right]\left[(\Delta p''_B/\sigma_{Bi})^{0.75}(1-\nu_B^2)^{0.5}/(v_B/100)^{0.5}\right] \quad \text{(VII-66)}$$

The procedures of selecting a blower and the determination of its performance are identical to those for the centrifugal blower.

The performance and physical characteristics of low and medium pressure axial blowers requiring more than one stage, i.e., more than one impeller, would be obtained by assuming that the performance of individual stages may be combined in series. A procedure of this type

would be approximately correct when only a few stages are required. Beyond this, the blower would have fairly great pressure-producing ability and would be evaluated as an axial-flow compressor.

Bulk volume and weight relationships for low and medium pressure axial blowers have been established, based on a limited quantity of information. The bulk volume of this type blower is defined by

$$V_B^{''} = 1.75(d_{BI}^{''})^{2.6} \qquad \text{(VII-67)}$$

and the weight by

$$W_B = 3.86(V_B^{''}/100). \qquad \text{(VII-68)}$$

Both expressions apply specifically to single stage units which include either inlet or exit stationary guide vanes for the impeller.

Compressors

A study of aircraft cooling systems in general requires knowledge of the performance and physical characteristics of small radial (centrifugal) and axial compressors. Radial compressors would be employed in certain types of air cycle refrigeration systems and as compression elements of a completely pneumatic power supply system and vapor cycle refrigeration systems. Axial compressors are employed rather extensively in many air cycle refrigeration systems.

1. Radial Compressors

A radial compressor is classified in this study as a radial-flow turbomachine producing in any one stage a total pressure ratio of the compressed fluid from 1.1 upwards. All units are considered to have radial vanes, i.e., units having impeller vanes inclined toward or away from the direction of impeller rotation at the outer diameter of the impeller are not considered. Lower values of required total pressure ratio would classify the machine as a low and medium pressure or high pressure centrifugal blower. The maximum total pressure ratio possible for development in any one stage of a radial compressor is limited to values in the vicinity of 4 to 1, primarily by mechanical strength limitations of the impeller and secondarily by an acceptable efficiency level for the machine.

Under normal conditions of application of this type compressor to an aircraft cooling system, the total temperature and pressure at inlet of the unit, the air rate to be handled by the unit, the rotational speed, and the shaft power available for driving the unit would be determined by performance of other components within the system. Hence, they may be considered as independent variables of analysis. In other instances, the rotational speed or the flow rate would not be known. Also, with some systems the total pressure ratio required to be developed by

the compressor may be an independent variable of analysis. Dependent variables to be determined when evaluating a radial compressor are (1) those affecting directly the performance of other components within a cooling system, such as outlet total temperature and pressure and rotational speed, and (2) those affecting merit considerations of the compressor and entire cooling system when compared to other systems producing an equivalent cooling effect, such as inlet, impeller and external diameters, axial length, efficiency and spatial and weight requirements.

Working methods to be used for evaluation of performance and physical characteristics of radial compressors are presented in the following sub-sections, derived on the basis of conventional thermodynamic and fluid dynamic principles and typical generalized performance characteristics for this type compressor. The approach is basically one of design or selection of radial-vaned units meeting specified performance requirements for the design conditions of the cooling system. "Off-design" performance of the compressor is not considered herein. Working methods are presented for design of units having maximum air capacity, i.e., minimum physical size for any specified air rate, and for design of units operating at or near peak efficiency. Compromise in selection between maximum capacity and maximum efficiency is discussed.

a. Flow Capacity

Two parameters useful for evaluation of compressor performance in general are the flow coefficient and the impeller tip Mach number. The flow coefficient, which characterizes the operational condition of the compressor, is defined as the ratio of the absolute axial flow velocity at inlet to the compressor to the tip speed of the impeller. In equation form, the flow coefficient is defined as

$$\varphi_{CR} = u_{CRi}/u_{CRI} \qquad \text{(VII-69)}$$

It is assumed in all instances that at the inlet the flow is uniform and in the axial direction only. Prerotation vanes are not considered, so that the inlet velocity of equation (VII-69) represents the actual average flow velocity for the fluid. The impeller tip Mach number of the compressor is a fictitious parameter used to relate the peripheral speed of the impeller to the total temperature of the fluid at the inlet of the compressor. It is defined in equation form as

$$M_{CRI} = u_{CRI}/\sqrt{kgRT^{o}_{CRi}} \qquad \text{(VII-70)}$$

Typical values of this parameter are in the range 0.3 to 1.4, the lower limit being defined by a total pressure ratio for the compressor of approximately 1.1, and the upper limit being defined by typical values of the maximum permissible peripheral speed of an impeller and the total temperature of the fluid at the inlet. Most commonly, in connection with aircraft cooling systems, the impeller tip Mach number would be in the range 0.5 to 1.2.

A general expression for the flow capacity of a radial compressor may be derived in terms of the flow coefficient and impeller Mach number by application of the steady-state equation of continuity to the inlet section of the compressor. The flow rate expressed in pounds per hour is related to the specific weight, the flow velocity and the flow area at inlet by

$$w_{CR} = 3600(\gamma A u)_{CRi} \qquad \text{(VII-71)}$$

The inlet flow area is defined in terms of the impeller diameter by the expression

$$A_{CRi} = (\pi/4)(d_{CRI})^2(\lambda^2_{CR} - 0.0625), \qquad \text{(VII-72)}$$

where it is assumed that the ratio of the hub and tip diameters is 0.25. Thus the available inlet flow area has an outer diameter, i.e., the eye diameter, equal to λ times the impeller diameter and an inner diameter equal to 0.25 times the impeller diameter. The specific weight of the fluid at the inlet plane may be defined in terms of the total temperature and pressure at inlet by the following expression, assuming the fluid to obey the equation of state for a perfect gas,

$$\gamma_{CRi} = (p/RT)_{CRi} = (p^o/RT^o)_{CRi}/(p_{CRi})^{1/(k-1)} \qquad \text{(VII-73)}$$

The actual Mach number of flow at the inlet of the unit is related to the flow factor and impeller Mach number by

$$M_{CRi} = (u/a)_{CRi} = \varphi_{CR} u_{CRI} / \sqrt{kgRT_{CRi}} \qquad \text{(VII-74)}$$

or, by combining equations (VII-70) and (VII-74),

$$M^2_{CRi} = \varphi^2_{CR} M^2_{CRI} \beta_{CRi} \qquad \text{(VII-75)}$$

which may be solved directly to yield

$$\beta_{CRi} = \frac{1}{1 - [(k-1)/2] \varphi^2_{CR} M^2_{CRI}} \qquad \text{(VII-76)}$$

Then, by combining equations (VII-73) and (VII-76) an expression for the inlet specific weight of the gas is determined as

$$\gamma_{CRi} = (p^o/RT^o)_{CRi} \left\{ 1 - \left[(k-1)/2\right] \varphi^2_{CR} M^2_{CRI} \right\}^{1/(k-1)} \qquad \text{(VII-77)}$$

and the general expression for flow rate is obtained by combining equations (VII-69), (VII-70), (VII-71), (VII-72) and (VII-77),

$$w_{CR} \sqrt{T^o_{CRi}}/(p^o_{CRi} d^2_{CRI}) = (900\pi \sqrt{kg/R})(\varphi_{CR} M_{CRI})(\lambda^2_{CR} - 0.0625) \times \left\{ 1 - \left[(k-1)/2\right] \varphi^2_{CR} M^2_{CRI} \right\}^{1/(k-1)} \qquad \text{(VII-78)}$$

or,

$$w_{CR}\sqrt{\theta^{o}_{CRi}}/(\delta^{o}_{CRi}d^{m2}_{CRI}) = 1680\varphi_{CR}M_{CRI}(\lambda^{2}_{CR}-0.0625)\left[1-0.2\varphi^{2}_{CR}M^{2}_{CRI}\right]^{2.5} \quad \text{(VII-79)}$$

for air with k and R equal to 1.4 and 53.3, respectively, and δ and θ defined as the ratio of pressure and temperature to standard sea level pressure and temperature of 2115 pounds per square foot and 519°F absolute, respectively.

A review of radial compressor performance as presented in the literature, References VII-5, VII-6 and VII-7, indicates that design for maximum efficiency requires the flow coefficient to be in the range 0.25 to slightly above 0.3, with the peak efficiency varying little over this range. Therefore, it is assumed in this analysis that radial compressors expected to operate at peak efficiency are designed for a flow coefficient of 0.3. Secondly, it is assumed that a well-proportioned impeller would be designed to have an eye diameter of about 62.5% of the impeller diameter, i.e., λ_{CR} is 0.625, as verified by conventional practice in compressor design as well as theoretical analyses. Reference VII-5 indicates that slightly higher efficiencies are possible with λ_{CR} of about 0.7. However, the use of larger eye diameters introduces additional mechanical problems in the design of the impeller inlet vanes or inducer. For this reason and the fact that in design practice somewhat lower ratios are employed, the value of λ_{CR} equal to 0.625 is maintained as the maximum value in design, for maximum efficiency. However, in the subsequent analysis dealing with design for maximum capacity, values of λ_{CR} up to 0.7 are used. With the flow coefficient maintained constant at a value of 0.3 for maximum-efficiency design, the absolute axial inlet velocity increases in direct proportion to the impeller Mach number. Thus, at high values of the impeller Mach number, corresponding to an appreciable total pressure rise of the air produced by the compressor, the flow velocity relative to the inlet vanes or inducer of the impeller becomes very great. Normally, an excessive relative inlet velocity is considered to exist when the Mach number of flow relative to the inlet vanes is within the transonic region, so that shock wave formations over the vanes may possibly create separation of the flow and consequent reduction in efficiency and capacity of the unit. Conventional practice is to limit the maximum Mach number of flow relative to the inlet vanes, occurring at the outer inlet diameter for pure axial entry, to a value of 0.9. Slightly higher efficiency of the compressor would be expected when this Mach number is limited to values in the range 0.7 to 0.8, as corresponding, for example, to the critical Mach number of simple aerodynamic shapes, but the flow capacity would be greatly reduced. In this analysis, the relative inlet Mach number is limited to 0.9.

The maximum impeller Mach number at which the relative inlet Mach number is not excessive for a flow coefficient of 0.3 is defined in the following manner. At the outer diameter of the inlet and for pure axial entry of the air in the approach section, the maximum relative velocity is

$$U^2_{CRi\lambda} = u^2_{CRi} + \lambda^2_{CR}\, u^2_{CRI} \qquad \text{(VII-80)}$$

or,

$$U^2_{CRi\lambda} / \left[(kgRT_{CRi})(\beta_{CRi})\right] = \varphi^2_{CR} M^2_{CRI} + \lambda^2_{CR} M^2_{CRI} \qquad \text{(VII-81)}$$

where

$$U^2_{CRi\lambda} / kgRT_{CRi} = (0.9)^2 = 0.81 \qquad \text{(VII-82)}$$

since the relative inlet Mach number is limited to 0.9. Hence, solving equation (VII-81) for the impeller Mach number, using the relationship of equation (VII-76) and k equal to 1.4, yields

$$M_{CRI} = 0.9 \Big/ \sqrt{1.16\,\varphi^2_{CR} + \lambda^2_{CR}} \qquad \text{(VII-83)}$$

For φ_{CR} and λ_{CR} of 0.3 and 0.625, respectively, the impeller Mach number is 1.28. Thus, whenever the impeller Mach number is less than 1.28, the relative Mach number at inlet of the vanes is everywhere less than 0.9, it is equal to 0.9 at an impeller tip Mach number of 1.28, and would exceed 0.9 for impeller Mach numbers greater than 1.28. With impeller Mach numbers greater than 1.28, either the flow coefficient or the eye diameter must be reduced. A study of this condition shows that from the standpoint of flow capacity reduction of the eye diameter is greatly superior to reduction of the flow coefficient. For example, at an impeller Mach number of 1.4 with a flow coefficient of 0.3, the required value of λ_{CR} would be 0.555 instead of 0.625, creating a loss in flow capacity of 25%. However, should λ_{CR} be maintained at the standard value of 0.625 and the flow coefficient be reduced to maintain the limiting relative Mach number of 0.9 at an impeller Mach number of 1.4, the flow coefficient would have to be reduced to 0.139 which, compared to the standard value of 0.3, represents a flow capacity drop of over 50%. Also, with the latter design the efficiency level would be appreciably lowered. Hence, for impeller Mach numbers greater than 1.28, design practice would be to reduce the eye diameter, i.e., reduce λ_{CR}, as required by equation (VII-83) for a flow coefficient of 0.3. It is to be emphasized that prerotation vanes within the inlet are not considered. Values of the flow coefficient and inlet diameter ratio for design at maximum efficiency as a function of the impeller Mach number are presented in Figure VII-14.

The flow capacity of radial compressors designed for operation at maximum efficiency may now be defined from the data of Figure VII-14 and equation (VII-79), which is valid for air. When the impeller Mach number is less than 1.28, which would be the usual condition, φ_{CR} and λ_{CR} are 0.3 and 0.625, respectively, and

$$w_{CR}\sqrt{\theta_{CRi}} / (\delta_{CRi} d^{*2}_{CRI}) = 165.5 M_{CRI} (1 - 0.018 M^2_{CRI})^{2.5} \qquad \text{(VII-84)}$$

When the impeller Mach number exceeds a value of 1.28, the flow capacity is defined by

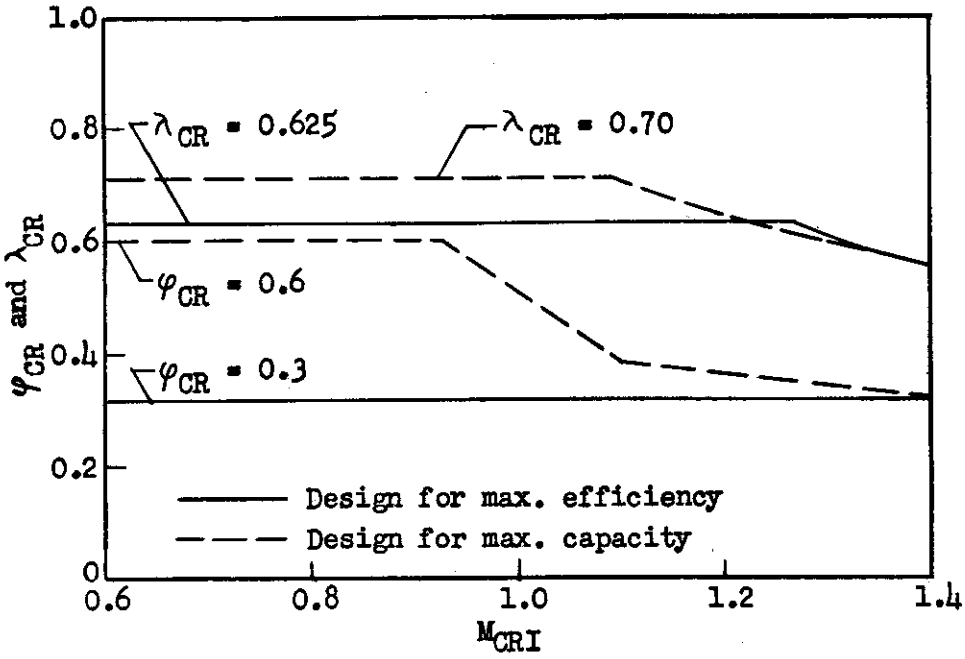

Figure VII-14. Flow coefficient and inlet diameter ratios for radial compressors.

$$w_{CR}\sqrt{\theta_{CRi}}/(\delta_{CRi}d_{CRI}^2) = 84.2M_{CRI}\left[(4.85/M_{CRI}^2)-1\right](1-0.018M_{CRI}^2)^{2.5} \quad \text{(VII-85)}$$

using λ_{CR} as defined by equation (VII-83) for $\varphi_{CR} = 0.3$. The variation in corrected flow capacity, pounds per hour per inch squared of impeller tip diameter, is illustrated in Figure VII-15. The maximum flow capacity exists at the impeller tip Mach number of 1.28, where the value of the ordinate is about 196 pounds per hour-inch squared.

Design for maximum flow capacity of a radial compressor is based upon the maximum flow rate the inlet section can handle without exceeding the selected maximum value of 0.9 for the relative Mach number of flow at the inlet and without prerotation vanes. A detailed study of the maximum flow capacity of radial compressors is presented in Reference VII-8. For a hub-to-tip diameter ratio of the impeller of 0.25, as herein used, and a limiting relative Mach number of 0.9, maximum flow capacity is achieved when

$$\lambda_{CR} = 0.778/M_{CRI} \quad \text{(VII-86)}$$

Substituting this relationship into equation (VII-83) defines the corresponding variation in the flow coefficient, which is

$$\varphi_{CR} = 0.42/M_{CRI} \quad \text{(VII-87)}$$

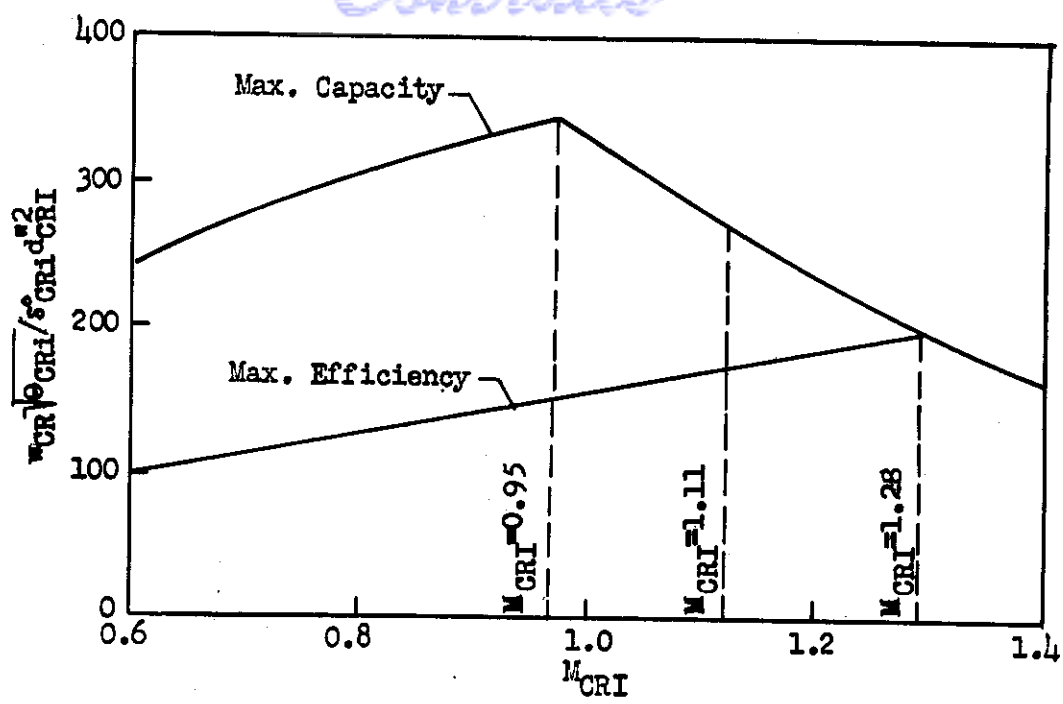

Figure VII-15. Flow capacity of radial compressors for design with maximum efficiency or maximum flow capacity.

Equation (VII-86) indicates that very high values of the inlet diameter ratio are required at low values of the impeller Mach number. For practical reasons of design, the maximum value of λ_{CR} is limited to 0.7, which corresponds to impeller Mach numbers below 1.11. Thus, when $M_{CRI} > 1.11$, λ_{CR} and φ_{CR} are defined by equations (VII-86) and (VII-87). When $M_{CRI} < 1.11$, λ_{CR} is 0.7 and φ_{CR} is defined from equation (VII-83) to be

$$\varphi_{CR} = 0.65\sqrt{(1.65/M^2_{CRI}) - 1} \qquad \text{(VII-88)}$$

Here again, a limit must be placed on φ_{CR} since at low impeller Mach numbers the flow coefficient would be very high, so that the efficiency and pressure-producing ability would be negligible. Hence, the maximum value of φ_{CR} is limited to 0.6, which occurs when M_{CRI} is about 0.95. The variations of flow coefficient and inlet diameter ratio with design for maximum flow capacity are presented in Figure VII-14.

The air flow rate with design for maximum capacity is defined by equation (VII-79) and the previously established conditions of the flow coefficient and inlet diameter ratio. For impeller Mach numbers greater than 1.11, equations (VII-86) and (VII-87) are substituted into equation (VII-79) to yield

$$w_{CR}\sqrt{\theta^{\circ}_{CRi}}/(\delta^{\circ}_{CRi}d^{\prime\prime 2}_{CRI}) = 40.3\left[(3.11/M_{CRI})^2 - 1\right] \qquad \text{(VII-89)}$$

For impeller Mach numbers greater than 0.95 and less than 1.11, equation (VII-88) and λ_{CR} equal to 0.7 are substituted into equation (VII-79) to yield

$$w_{CR}\sqrt{\theta^{o}_{CRi}}/(\delta^{o}_{CRi}d^{*2}_{CRI}) = 467\sqrt{1.65-M^{2}_{CRI}}\left[1-0.0845(1.65-M^{2}_{CRI})\right]^{2.5} \quad \text{(VII-90)}$$

Lastly, for impeller Mach numbers less than 0.95, φ_{CR} and λ_{CR} are restricted to 0.6 and 0.7, respectively, so that equation (VII-79) reduces to

$$w_{CR}\sqrt{\theta^{o}_{CRi}}/(\delta^{o}_{CRi}d^{*2}_{CRI}) = 431\, M_{CRI}(1-0.072M^{2}_{CRI})^{2.5} \quad \text{(VII-91)}$$

The variation in corrected air flow capacity with design for maximum capacity is presented in Figure VII-15 as a function of the impeller Mach number. At a value M_{CRI} of 1.4, the conditions of design for maximum efficiency coincide with those for maximum capacity. Design for maximum capacity with impeller Mach numbers less than unity results in from 2 to 2.5 times as much flow rate as with design for maximum efficiency, the impeller tip diameter being the same in both cases.

Compromise in design between maximum efficiency and maximum capacity is achieved by employing variations in the flow coefficient intermediate to those shown in Figure VII-14. As may be seen in the subsequent discussion dealing with the variation in efficiency with flow coefficients, the flow capacity at various prescribed efficiency levels may be established, which would then permit construction of additional curves on the plot in Figure VII-15 and allow direct selection for compromise in design of efficiency versus size of the machine.

b. Efficiency and Pressure Coefficient

The operational efficiency level of a radial compressor is primarily a function of the flow coefficient, impeller Mach number and machine Reynolds number, and secondarily of the inlet diameter ratio, clearances and general mechanical design features within the range of conventional design practice. A study of efficiency characteristics for this type compressor indicates that efficiency correlated as a function of flow coefficient, impeller Mach number, machine Reynolds number and inlet diameter ratio is satisfactory for predicting general performance and physical characteristics. Reynolds number and inlet diameter ratio are considered as secondary factors in the evaluation of efficiency.

Typical average efficiency variations as function of the flow coefficient and impeller Mach number are presented in Figure VII-16. All data in this plot are for a machine Reynolds number of 10^6 and an inlet diameter ratio of 0.625. Design for maximum efficiency based on a flow coefficient of 0.3, as used in the preceding sub-section for evaluation of flow capacity, may be seen to represent an average value for the range in flow coefficient corresponding to peak efficiency at various impeller Mach numbers. The selected variation of flow coefficient for design with maximum flow capacity, as shown in Figure VII-14, defines an

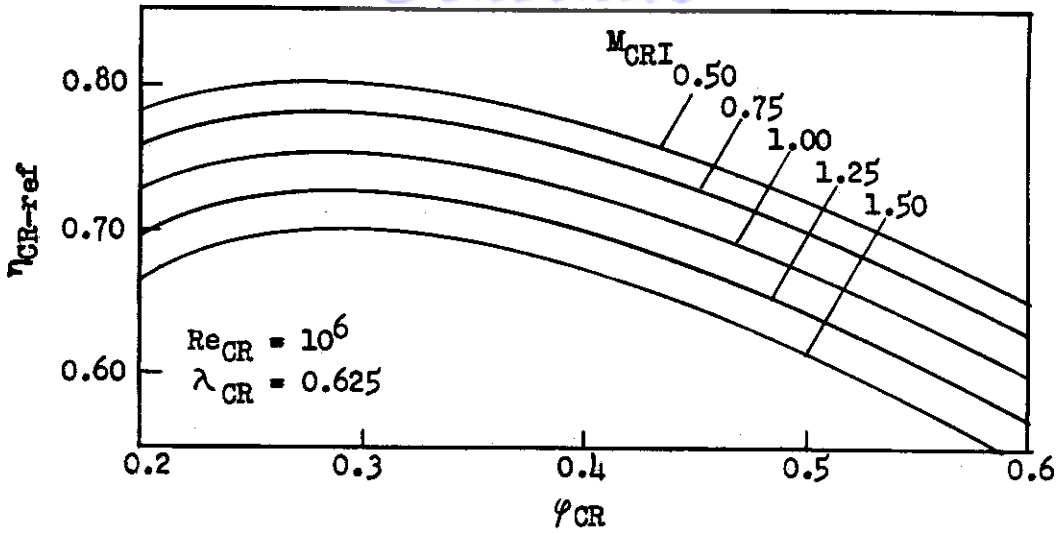

Figure VII-16. Reference efficiency of radial compressor as function of flow coefficient and impeller Mach number.

efficiency level of approximately 80% of that for a flow coefficient of 0.3.

Correction factors to be applied to the reference efficiency shown in Figure VII-16 for machine Reynolds numbers and inlet diameter ratios other than 10^6 and 0.625, respectively, are presented in Figures VII-17 and VII-18. Thus, for any values of flow coefficient, impeller Mach number, machine Reynolds number and inlet diameter ratio, the operating efficiency of a radial compressor is evaluated by

$$\eta_{CR} = (F_{CR-\eta-Re})(F_{CR-\eta-\lambda})(\eta_{CR-ref}) \qquad \text{(VII-92)}$$

The machine Reynolds number for any operational condition of the compressor is defined and evaluated in the following manner. The Reynolds number is defined as

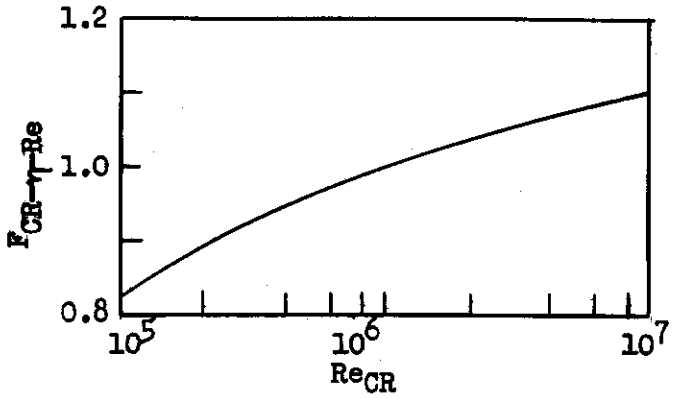

Figure VII-17. Correction factor for effect of machine Reynolds number on efficiency of radial compressor.

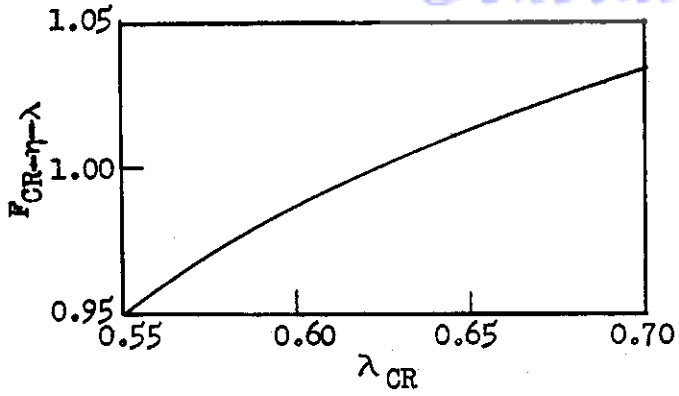

Figure VII-18. Correction factor for effect of inlet diameter ratio on efficiency of radial compressor.

$$Re_{CR} = \rho_{CRi}\, u_{CRI}\, d_{CRI}/\mu_{CRi} \qquad \text{(VII-93)}$$

The inlet density ρ_{CRi} is defined by equation (VII-77) when divided by the dimensional constant g equal to 32.2 pounds per slug. The absolute viscosity of air is a function of the inlet static temperature, and for the temperature range -100° to 1000°F its variation may be quite accurately expressed by the empirical equation

$$\mu = 4.16 \times 10^{-9}\, T^{0.72} \qquad \text{(VII-94)}$$

Combining equations (VII-70), (VII-77), (VII-93) and (VII-94), and introducing the definitions of corrected pressure δ and corrected temperature θ yields a generalized expression for the machine Reynolds number, which is for air

$$Re_{CR}(\theta^{o}_{CRi})^{1.22}/(\delta^{o}_{CRi} d^{m}_{CRI}) = 5.9 \times 10^{5} M_{CRI}\left[1-0.2(\varphi_{CR} M_{CRI})^{2}\right]^{2.5} \qquad \text{(VII-95)}$$

The pressure coefficient of a radial compressor is a parame-

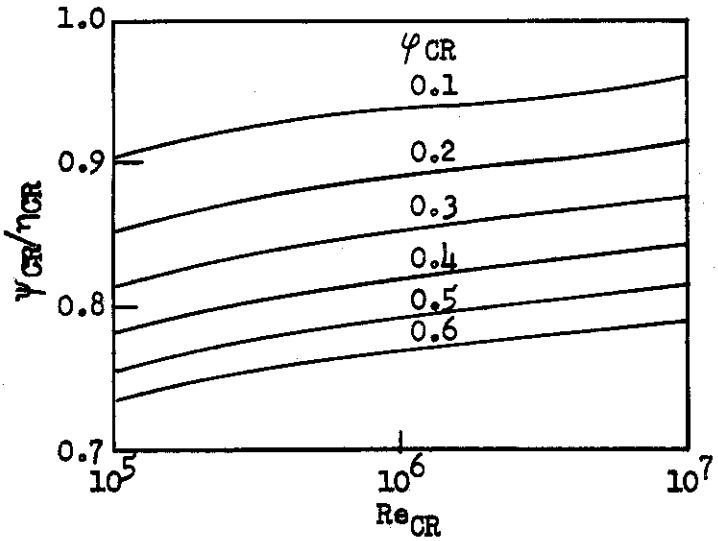

Figure VII-19. Chart for evaluation of pressure coefficient for radial compressors.

ter useful for evaluation of head production as a function of the impeller's peripheral speed. It is defined by

$$\psi_{CR} = gH^{o}_{CR}/u^{2}_{CRI} \qquad \text{(VII-96)}$$

The ratio of the pressure coefficient to the efficiency of a radial compressor is normally referred to as the slip or circulatory flow coefficient. A study of the pressure coefficient as affected by design conditions for the compressor indicates that the ratio of the pressure coefficient to efficiency may be correlated as a function of the flow coefficient and machine Reynolds number. This correlation is presented in Figure VII-19, which illustrates that evaluation of the pressure coefficient may be obtained directly once the efficiency of the compressor has been defined.

c. Pressure and Temperature Developed by Compressor

The ratio of the total pressure at the exit of the total pressure at the inlet of a compressor handling a perfect gas is related to the head produced by the compressor according to the expression

$$H^{o}_{CR} = Jc_{p}T^{o}_{CRi}\left[(p^{o}_{CRe}/p^{o}_{CRi})^{(k-1)/k} - 1\right] \qquad \text{(VII-97)}$$

Introducing this relationship into equation (VII-96), substituting for c_p its equivalent $Rk/[J(k-1)]$, and introducing the definition of impeller Mach number by equation (VII-70), yields

$$p^{o}_{CRe}/p^{o}_{CRi} = \left[1 + (k-1)\psi_{CR}M^{2}_{CRI}\right]^{k/(k-1)} \qquad \text{(VII-98)}$$

which for air at normal atmospheric temperatures reduces to

$$p^{o}_{CRe}/p^{o}_{CRi} = \left[1 + 0.4\,\psi_{CR}M^{2}_{CRI}\right]^{3.5} \qquad \text{(VII-99)}$$

The total pressure developed is defined directly by the impeller Mach number once the pressure coefficient is defined according to the procedures outlined in the previous sub-section.

Change in total temperature of the air from inlet to exit of the compressor may also be evaluated from the impeller Mach number. Assuming mechanical losses of the compressor to have no effect on the temperature change of the air and the specific heats for air to be constant from inlet to exit, the efficiency is defined by

$$\eta_{CR} = T^{o}_{CRi}\left[(p^{o}_{CRe}/p^{o}_{CRi})^{1/3.5} - 1\right]/(T^{o}_{CRe} - T^{o}_{CRi}) \qquad \text{(VII-100)}$$

which, when combined with equation (VII-99), reduces directly to

$$T^{o}_{CRe}/T^{o}_{CRi} = 1 + 0.4(\psi_{CR}/\eta_{CR})M^{2}_{CRI} \qquad \text{(VII-101)}$$

d. Shaft Power

The power required to drive the compressor equals the sum of the rates of energy addition to the air passing through the compressor and required to overcome mechanical losses. The latter portion of the energy addition is assumed to be received by a thermal sink other than the air passing through the compressor. The rate of energy addition to the air passing through the compressor is defined by temperature rise of the air according to the relationship

$$P_{CR-air} = w_{CR}\, c_p(T^o_{CRe} - T^o_{CRi}) \qquad \text{(VII-102)}$$

The mechanical efficiency of the compressor is defined by

$$\eta_{CR-mh} = P_{CR-air}/P_{CR-sh} \qquad \text{(VII-103)}$$

Thus, the rate of energy addition required to drive the compressor is

$$P_{CR-sh} = w_{CR}\, c_p(T^o_{CRe} - T^o_{CRi})/\eta_{CR-mh} \qquad \text{(VII-104)}$$

or,

$$P'_{CR-sh} = w_{CR}(T^o_{CRe} - T^o_{CRi})/(10{,}600\, \eta_{CR-mh}) \qquad \text{(VII-105)}$$

The shaft horsepower may also be expressed as a function of the impeller Mach number by introduction of equation (VII-101) into equation (VII-105), which, on a corrected basis, is

$$P'_{CR-sh}/(w_{CR}\theta^o_{CRi}) = (\psi_{CR}/\eta_{CR})M^2_{CRI}/(51.05\, \eta_{CR-mh}) \qquad \text{(VII-106)}$$

e. Rotational Speed

The rotational speed of the compressor is related to the peripheral speed and diameter of the impeller by the expression

$$u_{CRI} = \pi\, d^m_{CRI}\, n_{CR}/720 \qquad \text{(VII-107)}$$

which, when combined with equation (VII-70) and the definition of corrected temperature, yields

$$(n_{CR}/1000) = 256\, M_{CRI}\sqrt{\theta^o_{CRi}}/d^m_{CRI} \qquad \text{(VII-108)}$$

f. Physical Characteristics

Evaluation of radial compressors as a practical compression component in aircraft cooling systems requires knowledge of their size and weight. A study of existing practice in small compressor design indicates that approximate relationships may be established to define these characteristics. The maximum external diameter of a small radial compressor is approximately twice the impeller diameter,

$$d''_{CRex} = 2d''_{CRI} \qquad \text{(VII-109)}$$

and the maximum axial width, including the impeller housing, is about 0.3 of the impeller diameter, i.e.,

$$b_{CR} = 0.3 \qquad \text{(VII-110)}$$

The hub-to-tip diameter ratio of the impeller is selected as 0.25 and the inlet diameter ratio λ_{CR} is a function of the type of design. Evaluation of the inlet diameter ratio is discussed in the preceding subsection (1a).

Spatial requirements of radial compressors have been determined to be represented approximately by the expression

$$V''_{CR} = (d''_{CRI})^3 \qquad \text{(VII-111)}$$

The weight is defined approximately by

$$W_{CR} = C_{CR}(d''_{CRI})^3 \qquad \text{(VII-112)}$$

where C_{CR} represents an average bulk density and has been found to be from about 0.02 to 0.075 pound per cubic inch, depending upon the size and general design features of the unit. In general the larger the unit the lower will be the value of C_{CR}.

g. Evaluation Procedures

A general discussion of procedures for use of the previously presented evaluation methods is presented in the subsequent paragraphs. The intent is not to present details for calculation, but to indicate generally the procedures of evaluation which would be employed when a radial compressor is used in connection with an aircraft cooling system. Also, when used for evaluation, working charts may be used to permit reduction of the number of steps in the process.

With many applications for radial compressors, the performance characteristics of the driving device would be known or previously evaluated. Thus, the total pressure and temperature at inlet to the compressor, weight flow rate of air and driving power would be known and represent independent variables of analysis. The problem would be to determine, then, the performance and physical characteristics of a radial compressor operated with the specified driving power and handling the necessary air flow rate at the specified inlet total pressure and temperature. First, a value of the ratio $(\psi/\eta)_{CR}$ would be assumed, using the plot shown in Figure VII-19 as a guide to the selection of a typical value. The mechanical efficiency of the compressor is assumed next. Its value must be taken as representative for small radial compressors, commonly 95%, and cannot be verified as to its accuracy in the subsequent

evaluation steps. The required impeller Mach number may now be determined by equation (VII-106). The values of the flow coefficient φ_{CR} and inlet diameter ratio λ_{CR} are determined from a working chart, such as illustrated in Figure VII-14, based on the selected condition of design, i.e., either maximum efficiency or capacity, or any selected compromise between efficiency and capacity, and the value of the impeller Mach number. Then, the required impeller diameter is defined from the value of the parameter employed as the ordinate of the air capacity chart, Figure VII-15. Next, the machine Reynolds number would be evaluated, by equation (VII-95), which permits, thereafter, direct evaluation of the efficiency η_{CR} and the pressure coefficient ψ_{CR} by equation (VII-92) and the charts illustrated in Figures VII-16, VII-17, VII-18 and VII-19. At this point along the evaluation process, the accuracy of the value of $(\psi/\eta)_{CR}$ assumed at the beginning of the process would be checked. When the assumed value of this ratio and the value given by Figure VII-19 are not in agreement, it is necessary to assume a new value of the ratio and repeat the evaluation process. Once this trial-and-error procedure is completed, the total pressure and total temperature ratios of the air developed by the compressor are defined directly by equations (VII-99) and (VII-101). The rotational speed of the impeller is determined by equation (VII-108). External diameter, axial width, volume occupied and weight of the compressor would be evaluated by equations (VII-109), (VII-110), (VII-111) and (VII-112), respectively. Compromise in design between units operating at maximum efficiency or maximum capacity is obtained by selecting other combinations of inlet diameter ratio and flow coefficient between the limits indicated on the plot of Figure VII-14.

Should, in addition to inlet total pressure and temperature and shaft power, the rotational speed of the compressor be specified, as for example, when a driving device must operate at maximum efficiency and its rotational speed is, therefore, specified, the evaluation process would be identical to that previously outlined through the step defining the impeller Mach number. From values of the rotational speed and impeller Mach number, the impeller diameter is defined by equation (VII-108). Next, the ordinate parameter for the chart of Figure VII-15 would be evaluated from the known values for the air rate, impeller diameter and inlet total pressure and temperature. The value of this parameter and the value of the impeller Mach number locate a point on the flow capacity chart of Figure VII-15. If the point so defined falls above the line for maximum capacity and the impeller Mach number is greater than 0.95, the relative Mach number at the inlet of the impeller's vanes for this design would be excessive. Then, either the compressor would not be capable of handling the specified air rate because the required Mach number at inlet would be supersonic, or it would be within the transonic range where the expected efficiency would be low and the capacity somewhat reduced. Under these circumstances of design, the only alternatives would be (1) redesign of the driving device to allow reduction of the rotational speed so that the impeller diameter may be increased, hence, increasing the size of both compressor and driving device, (2) the use of stationary guide vanes at the inlet of the com-

pressor so as to prerotate the air in the direction of the impeller rotation and permit greater axial flow velocity without incurring excessive relative Mach numbers of flow over the inlet vanes, a design approach which can increase the flow capacity from 5 to 40% over the impeller Mach number range 0.6 to 1.4, but creates 7 to 8% loss in head-producing ability and several percent loss in efficiency of the unit, or (3) to actually employ the design even though the relative Mach number is within the transonic region and efficiency and flow capacity are reduced. If, with rotational speed specified, the design condition defines a point in Figure VII-15 above the maximum capacity line but the impeller Mach number is less than 0.95, the capacity may be increased by methods (1) and (2) described above, or by increasing the flow coefficient until the limiting inlet Mach number of 0.9 is reached. The latter method appreciably reduces the efficiency and pressure-producing ability of the compressor, but serves to define a compressor capable of handling the air flow at the specified rotational speed. The maximum permissible value for the flow coefficient is defined by equation (VII-88), and the flow capacity by equation (VII-79) using λ_{CR} equal to 0.7.

When design with rotational speed specified defines a point on the chart of Figure VII-15 between the lines of maximum capacity and maximum efficiency, the specified conditions dictate design based on compromise between capacity and efficiency. Figure VII-14 would be used as a guide in selecting an appropriate inlet diameter ratio and then the required flow coefficient may be calculated from equation (VII-79). Hereafter the procedure for evaluation would be identical to that outlined when the rotational speed is not specified. Should the point in Figure VII-15 fall below the line corresponding to maximum efficiency, it would indicate that the specified rotational speed dictates the use of a greatly oversized compressor and driving unit, and redesign of the driving unit would be desirable to increase the rotational speed.

For another type of application a radial compressor might be required to develop a specified total pressure ratio at specified values of the air rate and inlet total pressure and temperature, as for example, a pressurization unit. The procedure for design and evaluation would be to assume a value for the pressure coefficient ψ_{CR} and to determine from equation (VII-99) the required impeller Mach number. Next, for the selected condition of design, maximum efficiency, maximum capacity, or compromise between maximum efficiency and capacity, the required impeller diameter is defined from the working chart illustrated in Figure VII-15, after which the machine Reynolds number is evaluated by equation (VII-95). This permits evaluation of the efficiency and pressure coefficient by use of Figures VII-16, VII-17, VII-18 and VII-19 and equation (VII-92). The correctness of the assumed value of the pressure coefficient would then be checked to determine if the calculational process should be repeated. After the assumed and calculated values are in agreement, the evaluation process to define additional performance and the physical characteristics follows the general procedure outlined in the previous paragraphs, except for the required shaft power which would be defined by equation (VII-106).

2. Axial Compressors

The study of aircraft cooling systems in general requires knowledge of the performance and physical characteristics of axial compressors. In the following the relationships for evaluation of performance and physical characteristics for this type machine are described.

Because of its relatively high flow capacity and pressure-producing ability, the symmetric type of stage design will be employed. Symmetric design may be defined on the basis of the flow velocities at the pitch diameter of the compressor as follows: the relative flow velocity at the impeller inlet equals the absolute flow velocity at the impeller outlet, and the relative flow velocity at the impeller outlet equals the absolute flow velocity at the impeller inlet. In equation form,

$$U_{CAIi-pt} = u_{CAIe-pt} \qquad \text{(VII-113)}$$

and

$$U_{CAIe-pt} = u_{CAIi-pt} \qquad \text{(VII-114)}$$

In Figure VII-20 a schematic diagram of the blading arrangement is presented along with nomenclature and velocity diagrams.

The axial flow velocity is assumed constant throughout the stage. Since the absolute velocities at the impeller inlet and exit are equal to the absolute velocities at the stator exit and inlet, respectively, the analysis is conducted on basis of the flow velocities throughout the impeller. Further, the analysis is performed on basis of the pitch-diameter conditions of the first stage, and the remaining stages are assumed to have similar pressure-producing and efficiency characteristics.

a. Flow Capacity

The effective velocity with which the flow proceeds through the compressor may be defined as the axial component of the absolute velocity at the impeller entrance. This velocity may be defined in terms of the flow coefficient by the expression

$$u_{CAIi-a} = \varphi_{CA}\, u_{CAI-pt} \qquad \text{(VII-115)}$$

Maximum compressor efficiency occurs for values of the flow coefficient, φ_{CA}, in the vicinity of 0.5, with small change in efficiency occurring when the flow coefficient varies over the range of 0.3 to 0.75. In this study it is assumed that the flow coefficient is permitted to vary over the range of 0.3 to 0.75 for purposes of matching the compressor rotational speed to the rotational speed of the driving component. The effective flow area may be expressed by the equation

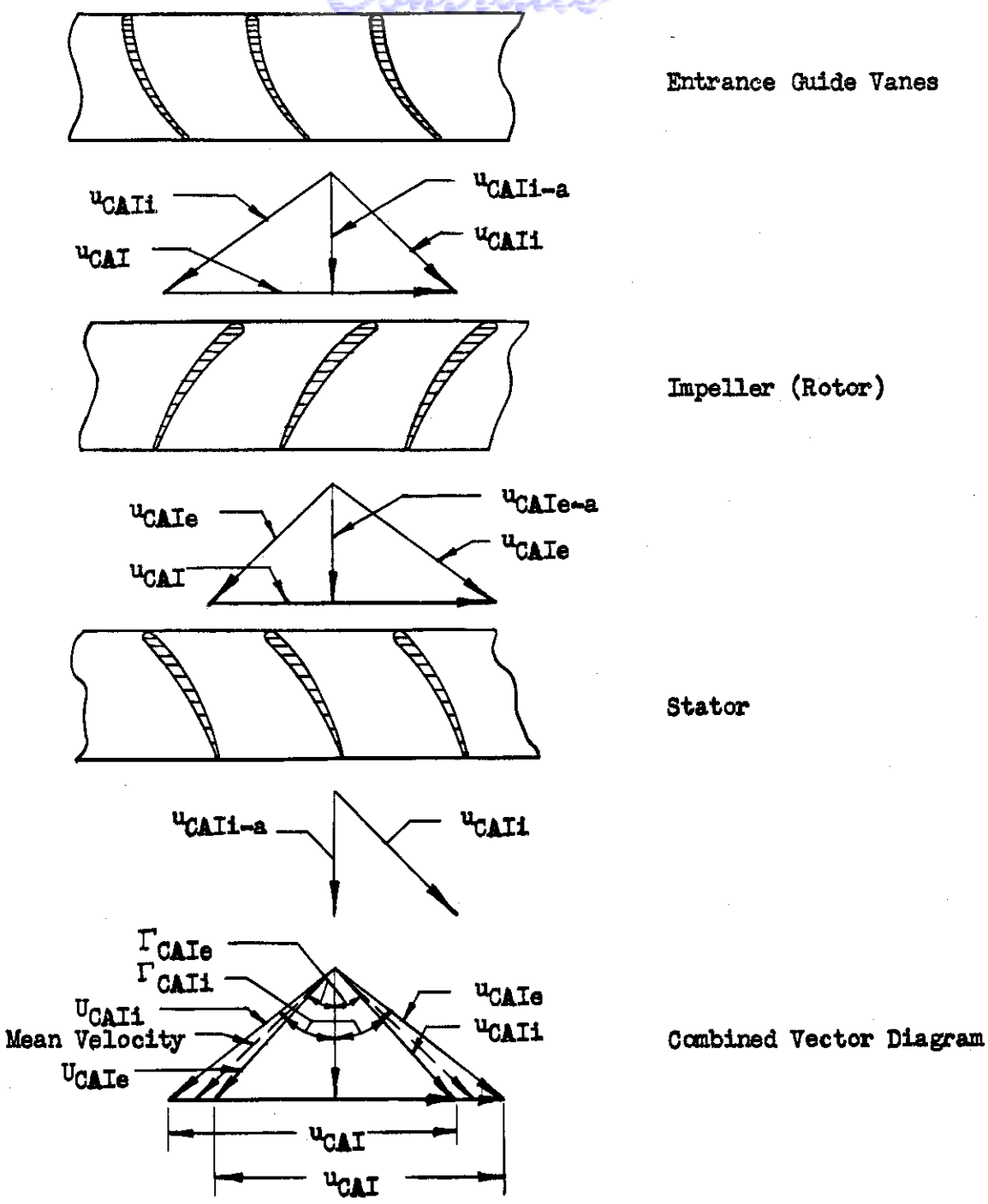

Figure VII-20. Schematic diagram of axial compressor blading, velocity diagrams and nomenclature.

$$A_{CA} = (\pi/4)(d^2_{CAI\text{-}pt})(1 - \nu_{CA}) \qquad \text{(VII-116)}$$

From conservation of energy, the static temperature of the air at entrance to the impeller may be expressed by

$$T_{CAIi\text{-}pt} = T^o_{CAi}\left[1 - \varphi^2_{CA} u^2_{CAIi\text{-}pt}/(2gJc_p T^o_{CAi} \cos^2 \Gamma_{CAIe\text{-}pt})\right] \qquad \text{(VII-117)}$$

Neglecting the small pressure loss caused by inlet guide vanes, the static pressure at entrance to the impeller may be expressed by

$$p_{CAIi\text{-}pt} = p^o_{CAi}\left[1 - \varphi^2_{CA} u^2_{CAI\text{-}pt}/(2gJc_p T^o_{CAi} \cos^2 \Gamma_{CAIe\text{-}pt})\right]^{3.5} \qquad \text{(VII-118)}$$

Hence, by combining equations (VII-117) and (VII-118), the specific weight at entrance to the impeller may be expressed by

$$\gamma_{CAIi\text{-}pt} = \frac{p^o_{CAi}}{RT^o_{CAi}}\left[1 - \varphi^2_{CA} u^2_{CAI\text{-}pt}/(2gJc_p T^o_{CAi} \cos^2 \Gamma_{CAIe\text{-}pt})\right]^{2.5} \qquad \text{(VII-119)}$$

The flow capacity of the axial compressor may then be defined by combining equations (VII-115), (VII-116) and (VII-119) with the equation of continuity to yield

$$\frac{w\sqrt{\theta^o_{CAi}}}{\delta^o_{CAi} d^{*2}_{CAI\text{-}pt}} = 3(1-\nu_{CA})\frac{\varphi_{CA} u_{CAI\text{-}pt}}{\sqrt{\theta^o_{CAi}}}\left[1 - \frac{\varphi^2_{CA}\, u^2_{CAI\text{-}pt}}{6.24\times10^6 \theta^o_{CAi} \cos^2 \Gamma_{CAI\text{-}pt}}\right]^{2.5} \qquad \text{(VII-120)}$$

With reference to Figure VII-20, the angle of the mean velocity relative to the axial direction is equal to the arc tan $(1/2\ \varphi_{CA})$. The turning angle of the air at the pitch diameter, i.e., $\Gamma_{CAIi\text{-}pt} - \Gamma_{CAIe\text{-}pt}$, normally has a maximum permissible value in the range of 20° to 30° to prevent stalling of the blades at the root section. Hence, the angle in equation (VII-120) may be evaluated, with negligible error on the flow rate, by the expression

$$\Gamma_{CAIe} = (\text{arc tan } 1/2\ \varphi_{CA}) - 15, \qquad \text{(VII-121)}$$

which corresponds to a blade turning angle of approximately 25°. By substituting equation (VII-121) into equation (VII-120) an expression for the flow handling capacity of the compressor is defined, where the flow parameter on the left of equation (VII-120) becomes a function of the corrected pitch line speed of the blades $u_{CAI\text{-}pt}/\sqrt{\theta^o_{CAi}}$, the flow coefficient φ_{CA} and the hub-to-tip diameter ratio ν_{CA}. Selection of a value for the ratio ν_{CA} is required, and the value selected normally would be the result of a compromise between flow capacity, efficiency and stress level of the compressor. Typical values of the diameter ratio ν_{CA} are within the range of 0.55 to 0.7, with a value of about 0.6 being commonly employed.

b. Rotational Speed

The rotational speed required of an axial compressor is related to the pitch diameter and pitch line speed of the blades by the expression

$$n_{CA} = 229\ u_{CAI\text{-}pt}/d^{m}_{CAI\text{-}pt} \qquad \text{(VII-122)}$$

By use of equation (VII-122) the impeller pitch diameter and pitch line blade velocity may be evaluated for any selected value of the flow factor and diameter ratio, when the inlet total temperature and pressure, the required rotational speed and the required flow rate are known.

c. Pressure Development

With reference to Figure VII-20, the increase in static temperature within the impeller equals the kinetic energy decrease from the relative velocity at entrance to exit of the impeller, and the static temperature increase within the stator equals the kinetic energy decrease from the absolute velocity at entrance to exit of the stator. Furthermore, these two energy changes are equal and the absolute air velocity leaving the stator is equal to the absolute air velocity entering the rotor. Hence, the increase of static temperature across the stage is equal to the increase in total temperature. Thus, by introducing equation (VII-115) the total temperature rise of the stage may be expressed by

$$T^{o}_{CAe\text{-}st} - T^{o}_{CAi\text{-}st} = \left[\varphi^{2}_{CA} u^{2}_{CAI\text{-}pt}/6010\right]\left[\tan^{2}\Gamma_{CAIi} - \tan^{2}\Gamma_{CAIe}\right] \qquad \text{(VII-123)}$$

From the geometry of the velocity diagram, it can be shown that

$$\varphi_{CA} \tan \Gamma_{CAIi} = 1 - \varphi_{CA} \tan \Gamma_{CAIe} \qquad \text{(VII-124)}$$

Combining equations (VII-123) and (VII-124) yields

$$T^{o}_{CAe\text{-}st} - T^{o}_{CAi\text{-}st} = \left[u^{2}_{CAI\text{-}pt}/6010\right]\left[1 - 2\,\varphi_{CA} \tan \Gamma_{CAIe}\right] \qquad \text{(VII-125)}$$

The total temperature ratio for the stage is related to the total pressure ratio developed by the stage by the expression

$$T^{o}_{CAe\text{-}st}/T^{o}_{CAi\text{-}st} = 1 + \left[\left(p^{o}_{CAe\text{-}st}/p^{o}_{CAi\text{-}st}\right)^{0.286} - 1\right]/\eta_{CA\text{-}st} \qquad \text{(VII-126)}$$

Combining equations (VII-125) and (VII-126) and solving for the pressure ratio yields

$$p^{o}_{CAe\text{-}st}/p^{o}_{CAi\text{-}st} = \left[\frac{u^{2}_{CAI\text{-}pt}\,\eta_{CA\text{-}st}}{3.12\text{x}10^{6}\,\theta^{o}_{CAi\text{-}st}}\left(1 - 2\,\varphi_{CA} \tan \Gamma_{CAIe}\right)\right]^{3.5} \qquad \text{(VII-127)}$$

Since the pressure ratio is assumed equal for all stages, the overall compressor pressure ratio is defined by

$$p^{\circ}_{CAe}/p^{\circ}_{CAi} = (p^{\circ}_{CAe-st}/p^{\circ}_{CAi-st})^{N_{CA-st}} \qquad \text{(VII-128)}$$

The maximum stage pressure ratio is limited by stalling of the blades at the root section and by the Mach number of flow relative to the blades at the tip section. Stalling of the blading is a function of the air turning angle. In this study the limiting turning angle will be represented by the limit of the air exit angle relative to the rotor as given by equation (VII-121). The Mach number relative to the blades at the tip section is limited to 0.7. This limit is used to define the maximum permissible tip speed of the impeller.

d. Temperature Ratio

The stage temperature ratio is defined by equation (VII-126), and since the pressure ratio and efficiency for all stages have been assumed equal, the total temperature ratio developed by (N) stages can be expressed by

$$T^{\circ}_{CAe}/T^{\circ}_{CAi} = \left\{1 + \left[(p^{\circ}_{CAe-st}/p^{\circ}_{CAi-st})^{0.286} - 1\right]/\eta_{CA-st}\right\}^{N_{CA-st}} \qquad \text{(VII-129)}$$

e. Power

The power required to drive the compressor equals the sum of the rates of energy addition to the air while passing through the compressor and the energy rate required to overcome mechanical losses. The latter portion of the energy addition is assumed to be received by a thermal sink other than the air passing through the compressor. The rate of energy addition to the air passing through the compressor is defined by the total temperature rise of the air according to the relationship

$$P_{CA-air} = w_{CA}\, c_p (T^{\circ}_{CAe} - T^{\circ}_{CAi}) \qquad \text{(VII-130)}$$

The mechanical efficiency is defined by

$$\eta_{CA-mh} = P_{CA-air}/P_{CA-sh} \qquad \text{(VII-131)}$$

Thus, the rate of energy addition required to drive the compressor is defined by

$$P_{CA-sh} = w_{CA}\, c_p (T^{\circ}_{CAe} - T^{\circ}_{CAi})/\eta_{CA-mh} \qquad \text{(VII-132)}$$

Equation (VII-132) may be reduced to the corrected horsepower required per pound of air per hour and assumes then the form

$$P'_{CA-sh}/(w_{CA}\theta^{\circ}_{CAi}) = 0.049\left[(T^{\circ}_{CAe}/T^{\circ}_{CAi}) - 1\right]/\eta_{CA-mh} \qquad \text{(VII-133)}$$

f. Stage Efficiency

The stage efficiency of the compressor is primarily a function of the machine Reynolds number and stage pressure ratio. The Reynolds number may be expressed by the equation

$$Re_{CA}/\delta^{o}_{CAi} = 500\, u_{CAI-tp}/\left[d''_{CAI-tp}\theta^{o}_{CAi}{}^{1.72}\right] \qquad \text{(VII-134)}$$

As the pressure ratio is increased, the air turning angle and/or the relative Mach number of the air at the tip section increases, either or both creating a decrease in the efficiency.

g. Physical Characteristics

Evaluation of axial compressors for application in aircraft cooling systems requires knowledge of their size and weight. A study of existing design practice indicates that approximate relationships may be established to define these characteristics. The maximum external dimension in the plane of rotation may be defined roughly by the equation

$$d''_{CAex} = 1.25\, d''_{CAI-tp} \qquad \text{(VII-135)}$$

Ordinarily, flow passages forming the inlet and outlet of the compressor will have an axial length roughly equal to the impeller tip diameter. Each stage of the compressor will have an axial length of approximately 20% of the tip diameter and the entrance guide vanes will have an axial length of roughly 10% of the tip diameter. Thus, the axial length of the compressor may be represented by the expression

$$L''_{CA-a} = (1.1 + 0.20\, N_{CA-st})d''_{CAI-tp} \qquad \text{(VII-136)}$$

The spatial requirements of the compressor may be approximated by combining equations (VII-135) and (VII-136) to yield

$$V''_{CA} = (1.35 + 0.25\, N_{CA-st})d''^{3}_{CAI-tp} \qquad \text{(VII-137)}$$

The bulk density of a typical unit is estimated to be approximately 0.02 pound per cubic inch. Hence, the weight is expressed by

$$W_{CA} = (0.027 + 0.005\, N_{CA-st})d''^{3}_{CAI-tp} \qquad \text{(VII-138)}$$

Turbines

Turbines are employed in cooling systems for reduction of the total temperature of cooling media, principally air, by expansion of the gas and transfer of energy from the gas as mechanical work. Also, turbines would be employed as a power source, such as an air turbine driving a circulation pump or a vapor cycle refrigeration machine. The principal association of a turbine with a cooling system, however, would be as a

mechanical device for transferring energy from air as work, when it is less practical to transfer the energy as heat. In the following, working methods are presented for evaluation of the performance and physical characteristics of radial inflow and axial turbines.

1. Radial Turbines

Radial turbines of the inward-flow type and with straight radial vanes are considered. Figure VII-21 illustrates schematically the arrangement of the nozzle ring and impeller for such a radial turbine.

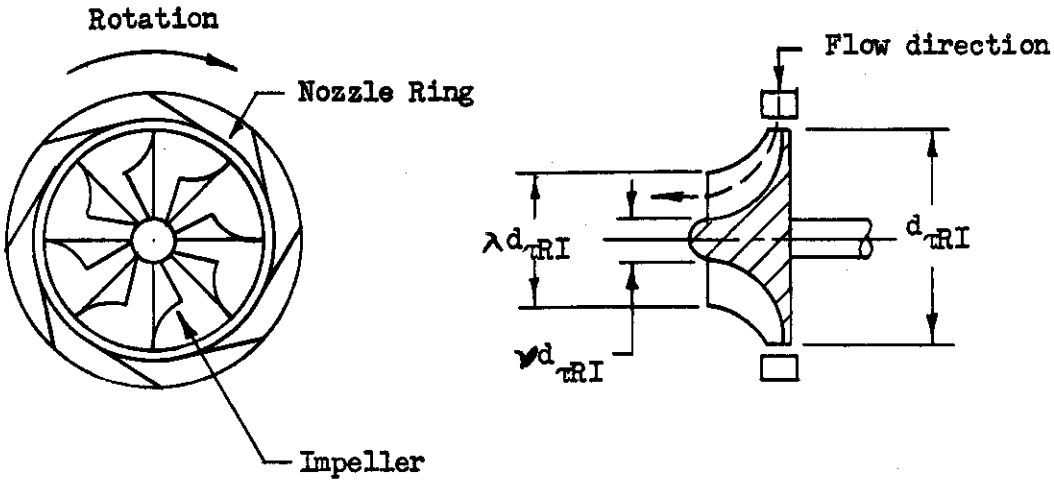

Figure VII-21. Schematic of typical radial turbine having radial blades.

The velocity diagrams at inlet and exit of a radial-vaned impeller are illustrated in Figure VII-22. The exit design is based on the condition of pure axial discharge.

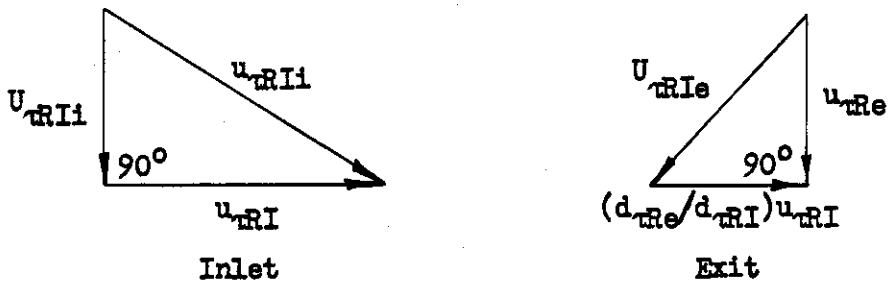

Figure VII-22. Velocity diagrams at inlet and exit of radial-vaned impeller having axial discharge.

Energy conversion within the turbine occurs in the stationary nozzles and in the rotating impeller. Thermal energy is converted into directed kinetic energy within the nozzle and is defined by

$$T^{o}_{\tau Ri} - T_{\tau RIi} = u^{2}_{\tau RIi}/2gJc_{p} \qquad \text{(VII-139)}$$

The energy conversion within the impeller passages is defined by

$$T_{\tau RIi} - T_{\tau Re} = \left[u^{2}_{\tau RI} - u^{2}_{\tau RI}(d_{\tau Re}/d_{\tau RI})^{2} + U^{2}_{\tau RIe} - U^{2}_{\tau RIi}\right]/2gJc_{p} \qquad \text{(VII-140)}$$

Since, however, with reference to Figure VII-22,

$$U^{2}_{\tau RIe} = u^{2}_{\tau Re} + u^{2}_{\tau RI}(d_{\tau Re}/d_{\tau RI})^{2} \qquad \text{(VII-141)}$$

and

$$U^{2}_{\tau RIi} = u^{2}_{\tau RIi} - u^{2}_{\tau RI} \qquad \text{(VII-142)}$$

the energy change across the turbine can be expressed by combining equations (VII-139), (VII-140), (VII-141) and (VII-142) to yield

$$T^{o}_{\tau Ri} - T_{\tau Re} = (2u^{2}_{\tau RI} + u^{2}_{\tau Re})/2gJc_{p} \qquad \text{(VII-143)}$$

The total temperature at exit of the turbine is related to the actual exit temperature and flow velocity by

$$T^{o}_{\tau Re} = T_{\tau Re} + u^{2}_{\tau Re}/2gJc_{p} \qquad \text{(VII-144)}$$

so that in combination with equation (VII-143), the total temperature change of the gas from inlet to exit of the turbine is expressed by

$$T^{o}_{\tau Ri} - T^{o}_{\tau Re} = u^{2}_{\tau RI}/gJc_{p} \qquad \text{(VII-145)}$$

By definition of turbine efficiency, the relation between total temperature ratio and total pressure ratio across the turbine may be shown to be

$$T^{o}_{\tau Re}/T^{o}_{\tau Ri} = 1 - \eta_{\tau R}\left[1 - (p^{o}_{\tau Re}/p^{o}_{\tau Ri})^{(k-1)/k}\right] \qquad \text{(VII-146)}$$

Hence, combination of equations (VII-145) and (VII-146) yields a definition of the required tip speed of the impeller as a function of the inlet temperature and pressure, exit pressure and turbine efficiency.

$$u^{2}_{\tau RI} = gJc_{p}\,\eta_{\tau R}T^{o}_{\tau Ri}\left[1 - (p^{o}_{\tau Re}/p^{o}_{\tau Ri})^{(k-1)/k}\right] \qquad \text{(VII-147)}$$

The ratio of impeller tip speed to the turbine's theoretical spouting velocity $\phi_{\tau R}$ is a parameter conventionally employed to define the range of maximum turbine efficiency. The theoretical spouting velocity is a measure of the total energy released within the turbine and is defined by

$$\text{theo. velocity} = \sqrt{2gJc_{p}T^{o}_{\tau Ri}\left[1 - (p^{o}_{\tau Re}/p^{o}_{\tau Ri})^{(k-1)/k}\right]} \qquad \text{(VII-148)}$$

Thus, by equations (VII-147) and (VII-148)

$$\phi_{tR} = \sqrt{\eta_{tR}/2} \qquad \text{(VII-149)}$$

Test results of various radial turbines indicate that the value of the parameter ϕ_{tR} corresponding to maximum efficiency is in the range from 0.6 to 0.7, with the value of 0.7 corresponding to higher machine efficiencies.

The flow coefficient of a radial turbine is defined as the ratio of the axial component of the exit velocity to the impeller tip speed, i.e.,

$$\varphi_{tR} = u_{tRe}/u_{tRI} \qquad \text{(VII-150)}$$

This parameter is useful for evaluating the air capacity of the turbine. Studies of the effects of the flow coefficient on turbine performance, References VII-11 and VII-12, indicate that maximum efficiency occurs when the flow coefficient is within the range of 0.3 to 0.5. In the present study the value of the flow coefficient is assumed to have no effect on the turbine efficiency since, in general, it is possible to design the turbine to operate within the mentioned range. The rotational speed required of the turbine varies directly as the square root of the flow coefficient for any specified flow rate, expansion pressure ratio, and fixed geometry of the impeller.

The impeller's diametrical proportions may be defined in terms of the impeller tip diameter. The hub diameter is assumed equal to 20% of the tip diameter. Thus,

$$\nu_{tR} = 0.20 \qquad \text{(VII-151)}$$

Examination of existing impeller designs indicates the ratio of 0.20 to be representative. The outer diameter at the turbine exit plane is defined by

$$\lambda_{tR} = d_{tRe}/d_{tRI} \qquad \text{(VII-152)}$$

Present design practice indicates that values of this diameter ratio should be within the range of 0.5 to 0.7. Variation in design from the average of this range would be governed by matching the turbine performance to that required of the component operating as the load for the turbine. A study indicates that variation of the diameter ratio λ_{tR} within the range 0.5 to 0.7 has little or no effect on the turbine efficiency.

The flow capacity of a radial turbine is limited by the impeller dimensions and the permissible velocity at the turbine exit. The exit velocity is assumed to be axial and uniform throughout the exit

flow area. The exit flow area is defined by

$$A_{tRe} = (\pi/4)(d_{tRI})^2(\lambda_{tR}^2 - 0.2^2) \qquad \text{(VII-153)}$$

The specific weight of the air at the exit of the turbine is defined by

$$\gamma_{tRe} = (p/RT)_{tRe} \qquad \text{(VII-154)}$$

For convenience of analysis and evaluation, the exit temperature and pressure are expressed in terms of the turbine inlet total temperature and pressure. The ratio of total to static temperature at exit of the turbine is

$$T^o_{tRe}/T_{tRe} = \beta_{tRe} = 1 + 0.2\, M^2_{tRe} \qquad \text{(VII-155)}$$

which, when combined with equation (VII-146), yields

$$T_{tRe} = T^o_{tRi}\left\{1 - \eta_{tR}\left[1 - (p^o_{tRe}/p^o_{tRi})^{1/3.5}\right]\right\}/\beta_{tRe} \qquad \text{(VII-156)}$$

Also,

$$p_{tRe} = (p^o_{tRi})(p^o_{tRe}/p^o_{tRi})/(\beta_{tRe})^{3.5} \qquad \text{(VII-157)}$$

Combining equations (VII-150), (VII-155) and (VII-156) yields

$$1/\beta_{tRe} = 1 - \frac{\varphi^2_{tR}\,\eta_{tR}\left[1-(p^o_{tRe}/p^o_{tRi})^{1/3.5}\right]}{2\left\{1-\eta_{tR}\left[1-(p^o_{tRe}/p^o_{tRi})^{1/3.5}\right]\right\}} \qquad \text{(VII-158)}$$

The specific weight may then be expressed as a function of the inlet conditions by combining equations (VII-154), (VII-156) and (VII-157). Thus,

$$\gamma_{tRe} = \frac{p^o_{tRi}(p^o_{tRe}/p^o_{tRi})}{RT^o_{tRi}\left\{1-\eta_{tR}\left[1-(p^o_{tRe}/p^o_{tRi})^{1/3.5}\right]\right\}} \times \left[1 - \frac{\varphi^2_{tR}\,\eta_{tR}\left[1-(p^o_{tRe}/p^o_{tRi})^{1/3.5}\right]}{2\left\{1-\eta_{tR}\left[1-(p^o_{tRe}/p^o_{tRi})^{1/3.5}\right]\right\}}\right]^{2.5} \qquad \text{(VII-159)}$$

The flow rate in pounds per hour is expressed by the steady-state equation of continuity,

$$w_{tR} = 3600\,(\gamma A u)_{tRe} \qquad \text{(VII-160)}$$

which with equations (VII-150), (VII-153) and (VII-159) reduces to

$$\frac{w_{\tau R}\sqrt{\theta^{o}_{\tau Ri}}}{\delta^{o}_{\tau Ri}\, d^{*2}_{\tau Ri}} = 2650\,\varphi_{\tau R}(p^{o}_{\tau Re}/p^{o}_{\tau Ri})(\lambda^{2}_{\tau R} - 0.04)\ x$$

$$\frac{\sqrt{\eta_{\tau R}\left[1-(p^{o}_{\tau Re}/p^{o}_{\tau Ri})^{1/3.5}\right]}}{1-\eta_{\tau R}\left[1-(p^{o}_{\tau Re}/p^{o}_{\tau Ri})^{1/3.5}\right]}\ x$$

$$\left[1-\frac{\varphi^{2}_{\tau R}\,\eta_{\tau R}\left[1-(p^{o}_{\tau Re}/p^{o}_{\tau Ri})^{1/3.5}\right]}{2\left\{1-\eta_{\tau R}\left[1-(p^{o}_{\tau Re}/p^{o}_{\tau Ri})^{1/3.5}\right]\right\}}\right]^{2.5} \qquad \text{(VII-161)}$$

The variation in corrected air flow capacity per square inch of impeller frontal area is presented in Figure VII-23 as a function of the total pressure ratio and the flow coefficient $\varphi_{\tau R}$, assuming the turbine effi-

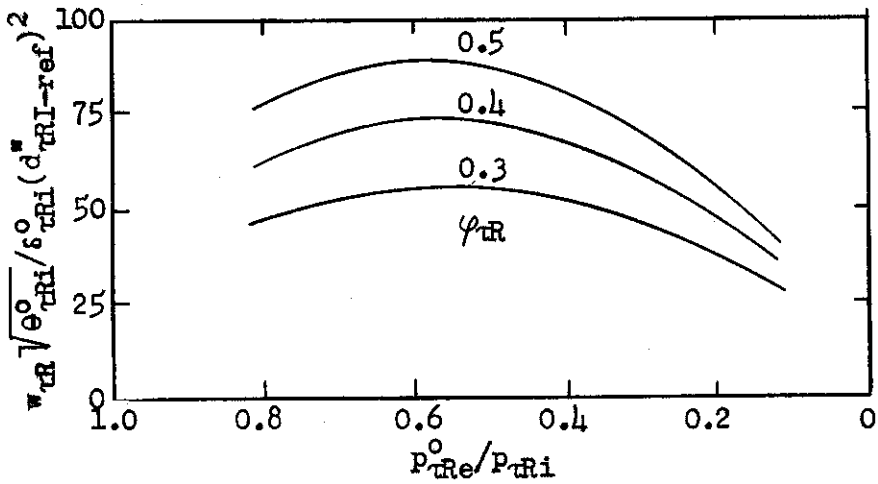

Figure VII-23. Chart for evaluation of flow capacity or impeller diameter of radial turbines.

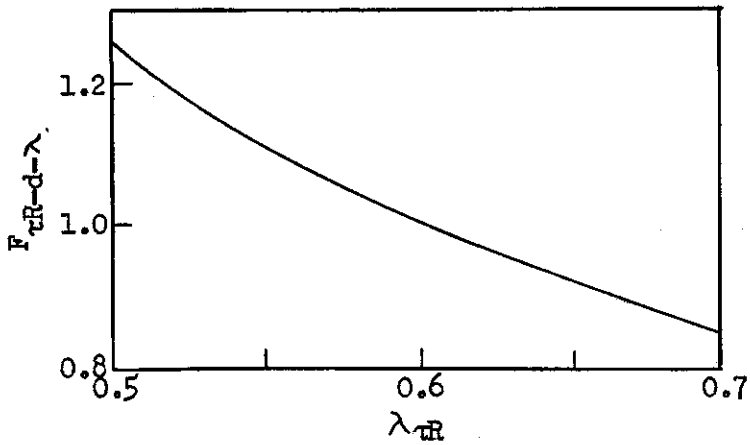

Figure VII-24. Correction factor for evaluation of the effect of the impeller diameter ratio on the required impeller diameter of radial turbines.

ciency to be 80% and $\lambda_{\tau R}$ as 0.6. For values of $\lambda_{\tau R}$ different than 0.6, the value of the ordinate read from Figure VII-23 must be multiplied by $(\lambda^2_{\tau R} - 0.04)/0.32$. Numerical values of this diameter correction factor $F_{\tau R-d-\lambda}$ are presented in Figure VII-24. Similarly, for turbine efficiencies different than 80% the correction factor $F_{\tau R-d-\eta}$ to be applied to the impeller diameter is presented in Figure VII-25 as function of the total pressure ratio. Since the diameter ratio and the efficiency correction factors are independent of each other, the impeller diameter may be evaluated as the product of the reference diameter, the diameter ratio correction factor, and the efficiency correction factor, i.e.,

$$d_{\tau RI} = (d_{\tau RI-ref})(F_{\tau R-d-\lambda})(F_{\tau R-d-\eta}) \qquad \text{(VII-162)}$$

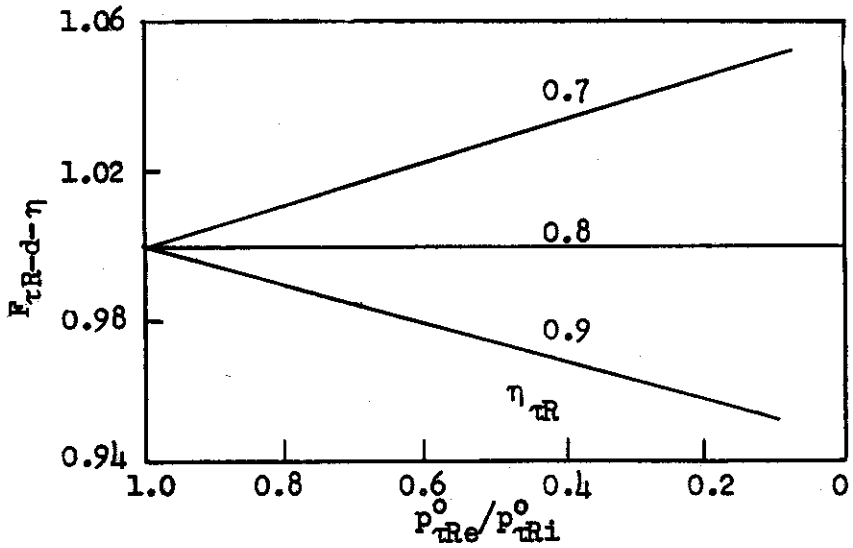

Figure VII-25. Correction factor for evaluation of the effect of efficiency on the impeller diameter of radial turbines.

The flow capacity with the nozzles operating under "choked flow" must be evaluated to determine its effect on the design procedure. Choking occurs when the throat velocity of the nozzles becomes nearly sonic. This condition is expressed approximately by

$$u_{\tau RIi} = \sqrt{kgRT^o_{\tau Ri}/1.2} = u_{\tau RI}(u_{\tau RIi}/u_{\tau RI}) \qquad \text{(VII-163)}$$

where the ratio $u_{\tau RI}/u_{\tau RIi}$ is the cosine of the nozzle angle. If the impeller tip speed defined by this equation is substituted into equation (VII-147), the overall turbine pressure ratio for sonic nozzle velocity is

$$p^o_{\tau Re}/p^o_{\tau Ri} = \left\{1 - \left[(u_{\tau RI}/u_{\tau RIi})^2/3\,\eta_{\tau R}\right]\right\}^{3.5} \qquad \text{(VII-164)}$$

For nozzle angles of zero and 30° the required turbine pressure ratios

are 0.151 and 0.269, respectively. Inspection of Figure VII-23 reveals that these values are in the range of decreasing flow capacity; hence, once sonic nozzle velocity is reached, the nozzle width or the nozzle angle may be decreased as the pressure ratio is increased. Thus, choking of the nozzles is not a determining factor for the turbine flow capacity.

An expression for the nozzle width may be derived by equating the flow through the nozzle to the flow through the exit. Since the inner diameter of the nozzle ring is nearly equal to the impeller diameter, the flow equation may be expressed by

$$\gamma_{Ii}\, U_{Ii}\, \pi\, d_{tRI}\, L_{tRn} = \gamma_{tRe}\, u_{tRe}\, \pi\, d_{tRI}^2 \left[\lambda_{tR}^2 - 0.04\right] / 4$$

Or, the ratio of the nozzle width to the impeller diameter is

$$b_{tRn} = L_{tRn}/d_{tRI} = \gamma_{tRe}\, u_{tRe} \left[\lambda^2 - 0.04\right] / (4\, \gamma_{tRIi}\, U_{tRIi}) \quad \text{(VII-165)}$$

For very small pressure ratios the specific weight of the air at the inlet would be nearly equal to the specific weight at the exit. At this condition, the nozzle width would be a maximum for any ratio of the exit velocity to the impeller inlet velocity since the exit flow area and impeller diameter would be small. For equal velocities at inlet and exit of the impeller, an exit diameter ratio of 0.6 and a hub diameter ratio of 0.2, the ratio of nozzle width to impeller diameter is 0.08 for pressure ratios near unity and decreases to about 0.035 for a pressure ratio of 0.2.

The efficiency of the radial turbine is primarily a function of the machine Reynolds number and pressure ratio, and is secondarily a function of the flow coefficient, the exit diameter ratio, and the gen-

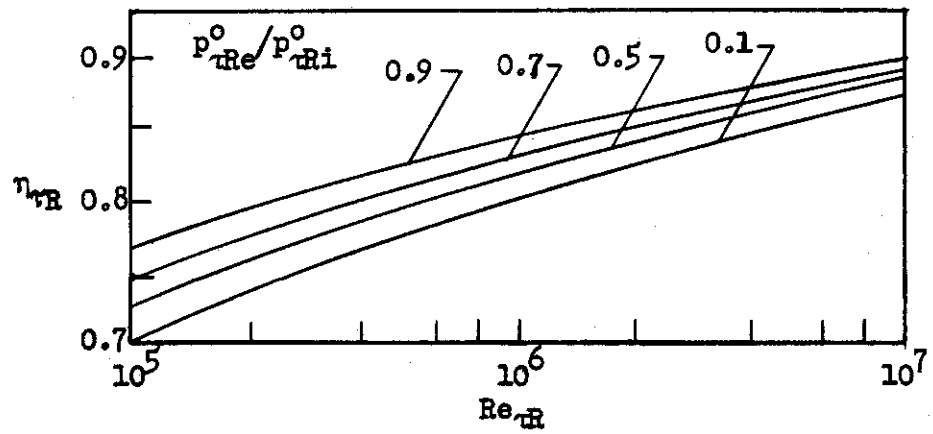

Figure VII-26. Efficiency of radial turbines as function of the machine Reynolds number and the pressure ratio.

eral design features of the turbine. A study of the efficiency characteristics of radial turbines indicates that for flow coefficients in the range 0.3 to 0.6 and exit diameter ratios from 0.5 to 0.7, the effects of the flow coefficient and the diameter ratio on the efficiency may be neglected. It is assumed that the general design features of all turbines are such as to yield optimum efficiency. Hence, the efficiency may be presented as a function of the pressure ratio and the machine Reynolds number only. Typical efficiency variations are presented in Figure VII-26.

The machine Reynolds number is defined by

$$Re_{\tau R} = \gamma_{\tau Ri}\, u_{\tau RI}\, d_{\tau RI}/g\, \mu_{\tau Ri} \qquad \text{(VII-166)}$$

The specific weight of the air at turbine inlet is

$$\gamma_{\tau Ri} = p_{\tau Ri}/RT_{\tau Ri} = p^{o}_{\tau Ri}\Big/\left[RT^{o}_{\tau Ri}(\beta_{\tau Ri})^{2.5}\right] \qquad \text{(VII-167)}$$

The inlet Mach number of the turbine has only a minor effect on the Reynolds number. Hence, the term $\beta_{\tau Ri}$ will be considered constant and equal to 1.025, corresponding to an inlet Mach number of 0.35. For the probable operating temperature range of the turbine, i.e., 0° to 600°F, the absolute viscosity of air may be expressed quite accurately by the empirical equation

$$\mu = 4.16 \times 10^{-9}\, T^{0.72} \qquad \text{(VII-168)}$$

Combining equations (VII-147), (VII-166), (VII-167) and (VII-168), and introducing the definitions of corrected pressure δ and corrected temperature Θ, a generalized expression for the machine Reynolds number is obtained. It is

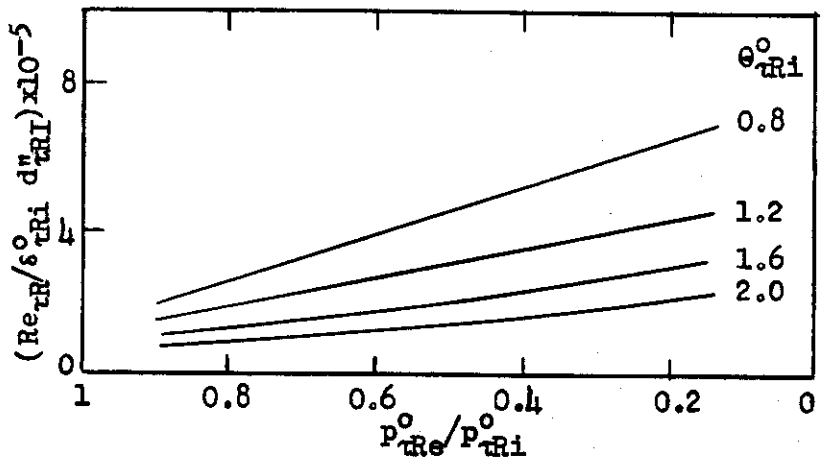

Figure VII-27. Machine Reynolds number of radial turbines as function of inlet temperature and pressure ratio.

$$Re_{\tau R}/(\delta^{o}_{\tau Ri} d^{*}_{\tau RI}) = 8.75 \times 10^{5} \sqrt{\eta_{\tau R}\left[1 - \left(\frac{p^{o}_{\tau Re}}{p^{o}_{\tau Ri}}\right)^{1/3.5}\right]} \Big/ (\theta^{o}_{\tau Ri})^{1.22} \qquad \text{(VII-169)}$$

The corrected Reynolds number per inch of impeller diameter is presented as a function of the pressure ratio and the corrected inlet temperature $\theta^{o}_{\tau Ri}$ in Figure VII-27. A turbine efficiency of 80% is used to define the Reynolds number. If the turbine efficiency is 70%, the Reynolds number would be 94% of the value indicated in Figure VII-27. This variation in Reynolds number would produce a negligible change in the turbine efficiency.

The total temperature and pressure ratios across the turbine are related as indicated by equation (VII-146). Once the efficiency has been determined and either the temperature or the pressure ratio of the turbine is known, the other may be evaluated directly.

The power delivered by the turbine shaft is equal to the energy removed from the air less the energy required to overcome mechanical losses. It is assumed that energy lost because of mechanical losses is transferred to a thermal sink other than the air passing through the turbine, and that this loss may be expressed as a fraction of the theoretical power output of the turbine. The power removed from the air is

$$P_{\tau R\text{-air}} = w_{\tau R}\, c_p (T^{o}_{\tau Ri} - T^{o}_{\tau Re}) \qquad \text{(VII-170)}$$

or,

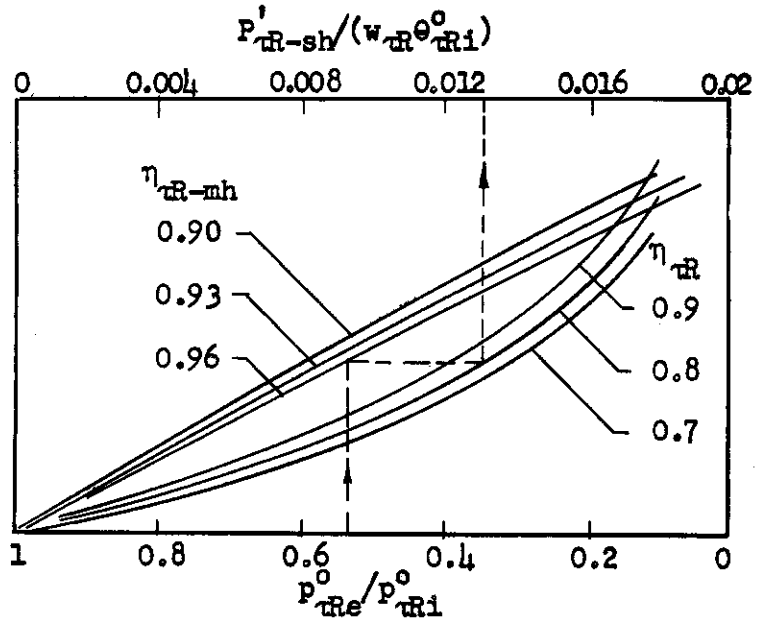

Figure VII-28. Chart for evaluation of shaft power delivered by radial turbines.

$$P_{\tau R\text{-air}} = \eta_{\tau R}\, w_{\tau R}\, c_p\, T^{\circ}_{\tau Ri}\left[1 - (p^{\circ}_{\tau Re}/p^{\circ}_{\tau Ri})^{(k-1)/k}\right] \qquad \text{(VII-171)}$$

The shaft horsepower expressed on a corrected basis is

$$P'_{\tau R\text{-sh}}/(w_{\tau R}\theta^{\circ}_{\tau Ri}) = 0.049\, \eta_{\tau R}\, \eta_{\tau R\text{-mh}}\left[1 - (p^{\circ}_{\tau Re}/p^{\circ}_{\tau Ri})^{1/3.5}\right] \qquad \text{(VII-172)}$$

In Figure VII-28 the schematic of a working chart for evaluation of the corrected horsepower is presented as a function of the turbine pressure ratio, turbine efficiency, and mechanical efficiency.

The rotational speed of the turbine is related to the peripheral speed and diameter of the impeller by the expression

$$n_{\tau R} = 720\, u_{\tau RI}/(\pi\, d^{w}_{\tau RI}) \qquad \text{(VII-173)}$$

Combining this equation with (VII-147), and using the definition of corrected temperature, yields

$$n_{\tau R}/1000 = 406\sqrt{\eta_{\tau R}\,\theta^{\circ}_{\tau Ri}\left[1 - (p^{\circ}_{\tau Re}/p^{\circ}_{\tau Ri})^{1/3.5}\right]}\Big/ d^{w}_{\tau RI} \qquad \text{(VII-174)}$$

A schematic of a working chart for evaluation of the rotational speed of a radial turbine is presented in Figure VII-29.

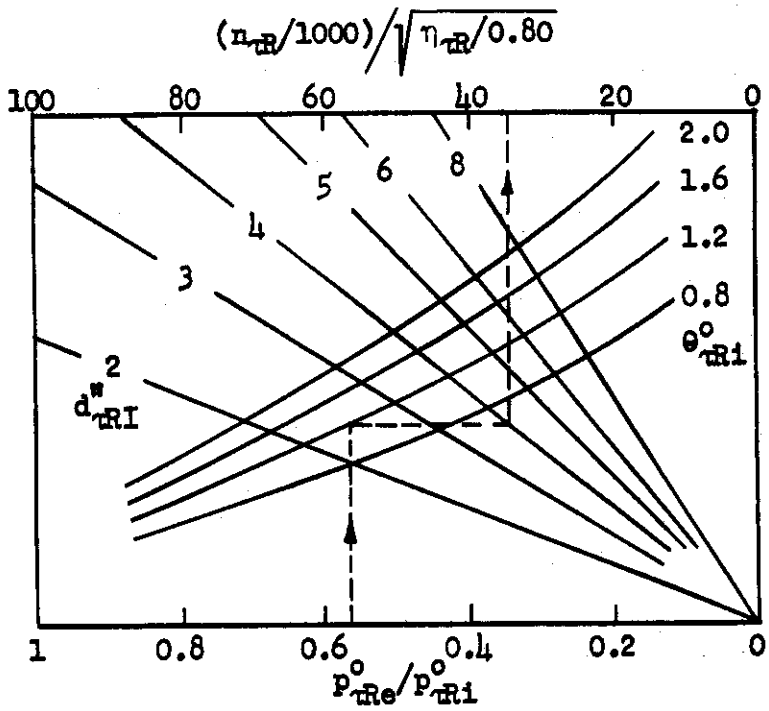

Figure VII-29. Chart for evaluation of rotational speed of radial turbines.

Evaluation of radial turbines for application in aircraft cooling systems requires also knowledge of their size and weight. A study of existing design practice indicates that approximate relationships may be established to define these characteristics. An average value of the maximum external diameter would be equal to twice the impeller diameter, and the axial length, including the housing, would be approximately 30% of the impeller diameter, i.e.,

$$b_{\tau R} = 0.3 \tag{VII-175}$$

Based on the dimensions of existing units, it appears that spatial requirements of radial turbines may be represented approximately by the expression

$$V''_{\tau R} = (d''_{\tau RI})^3 \tag{VII-176}$$

Similarly, the weight may be defined approximately by

$$W_{\tau R} = C_{\tau R}(d''_{\tau RI})^3 \tag{VII-177}$$

where the constant $C_{\tau R}$ varies in the range of 0.02 to 0.06, depending upon the size and general design of the turbine.

2. Axial Turbines

The axial turbine is a turbomachine in which the effective gas flow is parallel to the axis of rotation. This type of turbine might be used in aircraft cooling systems as an expansion device for the production of power or a cooling effect.

Performance and physical characteristics of axial turbines are evaluated for units designed on the basis of constant angular momentum theory. Turbines designed on this basis yield fairly high operating efficiencies. The condition of design for constant angular momentum is based on the radial variation of the gas velocity in the clearance space between the nozzle ring and the impeller buckets. Within this clearance space, the product of the whirl component of the absolute velocity and the radial distance from the axis of rotation is constant for all radii from the root section to the tip section of the turbine stage. In equation form, this condition of design is defined by

$$(u_{\tau AIi-wh})(d_{\tau AI}) = \text{constant} \tag{VII-178}$$

If in addition to the condition of constant angular momentum, the axial component of the velocity in this space is constant over the flow annulus, i.e.,

$$u_{\tau AIi-a} = \text{constant}, \tag{VII-179}$$

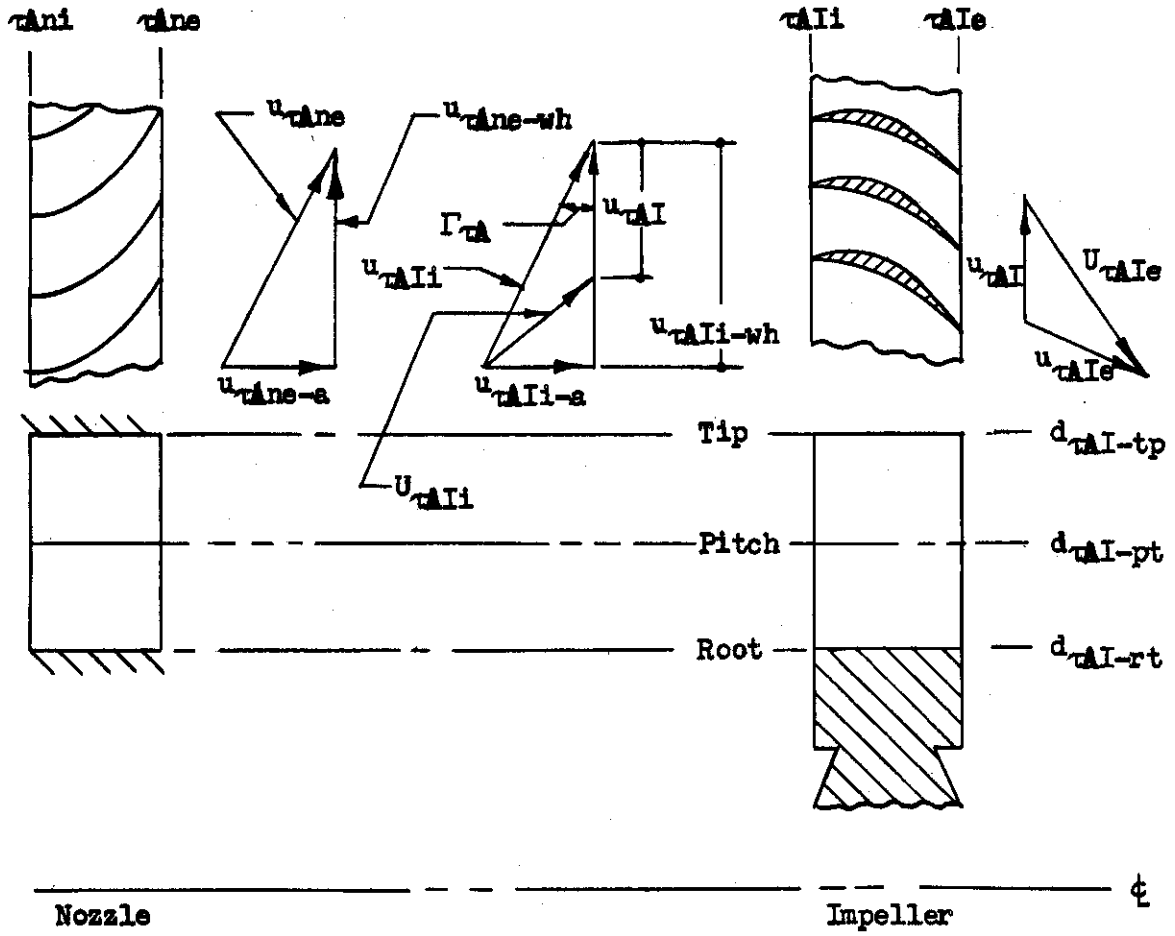

Figure VII-30. Velocity diagrams for nozzle and impeller of axial turbine stage.

a condition of radial equilibrium is established such that the resulting radial pressure gradient exactly counteracts the effect of centrifugal force of the fluid particles created by their whirl components of velocity, and the flow proceeds uniformly through the turbine stage rather than crowding to the tip section of the buckets. Results of actual measurements of gas velocities in a turbine stage designed on this basis are presented in Reference VII-16 and show good agreement with the design or theoretical values, except in the regions of boundary layer flow. Figure VII-30 illustrates the arrangement of the nozzle ring and impeller of a turbine stage, the velocity diagrams and nomenclature employed in this study.

Since, in general, the absolute velocity of the gas issuing from the impeller varies to some extent both in magnitude and direction with respect to the diameter, the analysis is conducted on the basis of the flow conditions at the pitch diameter of the impeller. At this diameter the exit velocity is assumed to be directed axially and to repre-

sent the mean value of all exit absolute velocities. Generalized equations presented in the following sub-sections are derived on the basis of conventional thermodynamic and fluid dynamic principles combined with typical generalized performance characteristics of axial turbines. Schematic diagrams representing graphical solutions and working charts for evaluation of turbine performance and physical characteristics are presented.

The required impeller speed of a turbine designed for pure impulse at the root section is a function of turbine efficiency, pressure ratio, angle of the absolute velocity at entrance to the impeller and total inlet temperature.

Since the losses of the turbine are equal to $(1-\eta_{\tau A})$ times total-to-total isentropic energy release, the energy available for conversion to velocity at the root section, without diffusion in the impeller passages, equals the output work of the impeller plus the axial exit kinetic energy. Hence, in equation form,

$$u^2_{\tau AIi-rt}/(2gJ) = c_p \eta_{\tau A} T^o_{\tau Ai} \left[1-(p^o_{\tau Ae}/p^o_{\tau Ai})^{1/3.5}\right] + u^2_{\tau AIe}/(2gJ) \quad \text{(VII-180)}$$

For turbines designed on the basis of pure impulse at the root section, the axial component of velocity at the root section of the impeller exit may be considered approximately equal to the axial velocity at the impeller inlet. Thus,

$$u_{\tau AIe} = u_{\tau AIe-a} = u_{\tau AIi-rt} \sin \Gamma_{\tau A-rt} \quad \text{(VII-181)}$$

Combining equations (VII-180) and (VII-181) yields

$$u_{\tau AIi-rt} = \sqrt{2gJ \eta_{\tau A} c_p T^o_{\tau Ai} \left[1-(p^o_{\tau Ae}/p^o_{\tau Ai})^{1/3.5}\right]} \Big/ \cos \Gamma_{\tau A-rt} \quad \text{(VII-182)}$$

The unit output of the turbine with axial exit velocity may be expressed by

$$u_{\tau AI-tp}\, u_{\tau AIi-wh-tp}/g = \eta_{\tau A} J c_p T^o_{\tau Ai} \left[1-(p^o_{\tau Ae}/p^o_{\tau Ai})^{1/3.5}\right] \quad \text{(VII-183)}$$

The whirl component of velocity at the tip section is equal to the root-to-tip diameter ratio multiplied by the whirl component of velocity at the root section. Hence, the impeller tip speed may be determined by combining equations (VII-182) and (VII-183) to yield

$$u_{\tau AI-tp} = \sqrt{2gJ \eta_{\tau A} c_p T^o_{\tau Ai} \left[1-(p^o_{\tau Ae}/p^o_{\tau Ai})^{1/3.5}\right]} \Big/ 2\upsilon_{\tau A} \quad \text{(VII-184)}$$

The flow velocity at the pitch section is used to define the flow capacity of the turbine. The axial velocity is assumed constant over the flow annulus. With reference to Figure VII-30 and equation (VII-182), the axial velocity may be expressed by the relationship

$$u_{\tau A1i\text{-}a} = \sqrt{2gJ\eta_{\tau A}c_pT^o_{\tau Ai}\left[1-(p^o_{\tau Ae}/p^o_{\tau Ai})^{1/3.5}\right]}(\tan\Gamma_{\tau A\text{-}rt}) \qquad \text{(VII-185)}$$

Since the whirl velocity varies inversely with the diameter, the whirl velocity at the pitch section is expressed by

$$u_{\tau A1i\text{-}wh\text{-}pt} = \left[2\nu_{\tau A}/(1+\nu_{\tau A})\right]\sqrt{2gJ\eta_{\tau A}c_pT^o_{\tau Ai}\left[1-(p^o_{\tau Ae}/p^o_{\tau Ai})^{1/3.5}\right]} \qquad \text{(VII-186)}$$

With reference to Figure VII-30, equations (VII-185) and (VII-186) may be combined to define the pitch-line spouting velocity of the nozzles.

$$u_{\tau A1i\text{-}pt} = \sqrt{2gJ\eta_{\tau A}c_pT^o_{\tau Ai}\left[1-\left(\frac{p^o_{\tau Ae}}{p^o_{\tau Ai}}\right)^{1/3.5}\right]\left[\tan^2\Gamma_{\tau A\text{-}rt}+\left(\frac{2\nu_{\tau A}}{1+\nu_{\tau A}}\right)^2\right]} \qquad \text{(VII-187)}$$

Since the turbine stage design has been defined on the basis of the velocity relationship in the clearance space between the nozzles and the buckets, the flow capacity of the turbine is most conveniently described by the state of the air in this space. The axial flow area is

$$A_{\tau A1i} = (\pi/4)(1-\nu^2_{\tau A})(d^2_{\tau A1\text{-}tp}) \qquad \text{(VII-188)}$$

The velocity component defining the flow through this area is the axial component of the nozzle velocity, as defined by equation (VII-185). By conservation of energy,

$$T_{\tau A1i\text{-}pt} = T^o_{\tau Ai}\left[1-u^2_{\tau A1i\text{-}pt}/(2gJc_pT^o_{\tau Ai})\right] \qquad \text{(VII-189)}$$

Combining equations (VII-187) and (VII-189) yields

$$T_{\tau A1i\text{-}pt} = T^o_{\tau Ai}\left\{1-\eta_{\tau A}\left[1-\left(\frac{p^o_{\tau Ae}}{p^o_{\tau Ai}}\right)^{1/3.5}\right]\left[\tan^2\Gamma_{\tau A\text{-}rt}+\left(\frac{2\nu_{\tau A}}{1+\nu_{\tau A}}\right)^2\right]\right\} \qquad \text{(VII-190)}$$

and, by introducing the nozzle efficiency

$$\frac{p_{\tau A1i\text{-}pt}}{p^o_{\tau Ai}} = \left\{1-\left(\frac{\eta_{\tau A}}{\eta_{\tau An}}\right)\left[1-\left(\frac{p^o_{\tau Ae}}{p^o_{\tau Ai}}\right)^{1/3.5}\right]\left[\tan^2\Gamma_{\tau A\text{-}rt}+\left(\frac{2\nu_{\tau A}}{1+\nu_{\tau A}}\right)^2\right]\right\}^{3.5} \qquad \text{(VII-191)}$$

A study of losses in axial turbines indicates that at design operational conditions nozzle losses represent about 40% of the turbine losses. Hence, the nozzle efficiency may be defined approximately by

$$\eta_{\tau An} = 0.6 + 0.4\eta_{\tau A} \qquad \text{(VII-192)}$$

The specific weight of the gas at the pitch section is defined by combining equations (VII-190) and (VII-191) with the perfect gas law. Combining this relationship for the specific weight with equations

(VII-185), (VII-188), (VII-192) and the equation of continuity yields

$$\frac{w_{\tau A}\sqrt{\theta^{o}_{\tau Ai}}}{\delta^{o}_{\tau Ai} d^{*2}_{\tau AI-tp}} = 3740(1-\nu^{2}_{\tau A})(\tan\Gamma_{\tau A-rt}) \times (0.6+0.4\eta_{\tau A})^{-3.5}\sqrt{\eta_{\tau A}\left[1-(p^{o}_{\tau Ae}/p^{o}_{\tau Ai})^{1/3.5}\right]} \times\left\{1-\eta_{\tau A}\left[1-\left(\frac{p^{o}_{\tau Ae}}{p^{o}_{\tau Ai}}\right)^{1/3.5}\right]\left[\tan^{2}\Gamma_{\tau A-rt}+\left(\frac{2\nu_{\tau A}}{1+\nu_{\tau A}}\right)^{2}\right]\right\}^{2.5} \quad \text{(VII-193)}$$

The maximum obtainable efficiency of an axial turbine is primarily a function of turbine pressure ratio and machine Reynolds number, and secondarily of leakage, windage, heat losses and flow angles. The secondary factors are assumed to have a consistent effect on the efficiency level of the turbine, so that turbine efficiency may be defined as a function of pressure ratio and Reynolds number only. Figure VII-31 presents a chart for the evaluation of the efficiency. The efficiency is defined on the basis of total pressures at inlet and exit of the turbine. The effect of machine Reynolds number $Re_{\tau A}$ on turbine efficiency is defined on the basis of data presented in References VII-18 and VII-17.

The machine Reynolds number is defined by

$$Re_{\tau A} = \gamma_{\tau Ai}\, d_{\tau AI-tp}\, u_{\tau AI-tp}/g\mu_{\tau Ai} \quad \text{(VII-194)}$$

For the normal range of air velocity at entrance to the turbine nozzles and the viscosity of air expressed by the relationship

$$\mu = 4.16 \times 10^{-9}\, T^{0.72} \quad \text{(VII-195)}$$

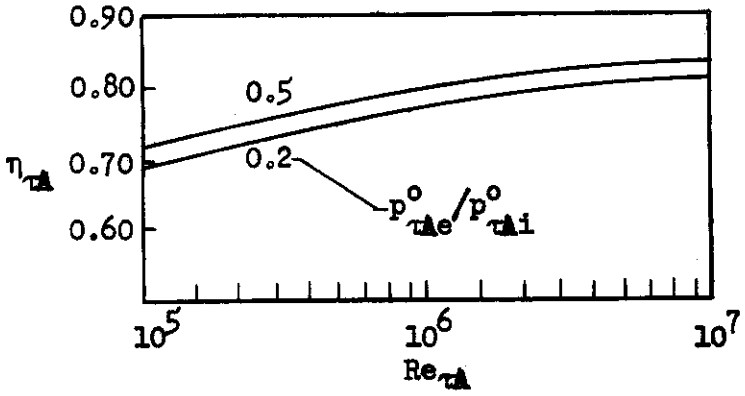

Figure VII-31. Efficiency of axial turbines.

the Reynolds number equation may be generalized as

$$Re_{tA}/(\delta^{o}_{tAi} d''_{tAI-tp}) = 500\, u_{tAI-tp}/(\theta^{o}_{tAi})^{1.72} \qquad \text{(VII-196)}$$

The required rotational speed of an axial flow turbine is related to the impeller tip speed and diameter by the equation

$$n_{tA} = 229\, u_{tAI-tp}/d''_{tAI-tp} \qquad \text{(VII-197)}$$

The shaft power delivered by an axial flow turbine equals the power developed by the impeller less the power required to overcome mechanical losses. Mechanical losses, which include bearing friction, windage, etc., cannot be evaluated accurately for variable operational conditions of the turbine, but their effect on turbine power output may be approximately defined by use of a mechanical efficiency. Thus, the corrected shaft power per pound of air is defined by

$$P'_{tA-sh}/(\theta^{o}_{tAi} W_{tA}) = 0.049\, \eta_{tA}\, \eta_{tA-mh}\left[1-(p^{o}_{tAe}/p^{o}_{tAi})^{\frac{1}{3.5}}\right] \qquad \text{(VII-198)}$$

In many designs, the permissible blade stress level may be a primary factor in establishing the required operating speed and/or size of an axial turbine. It is conventional practice in the design of turbines to define the maximum permissible stress level on the basis of the stress induced in the root section of the rotating blades by action of the centrifugal load of the blades. This obviates the consideration of vibratory, gas bending and secondary loads on the blades and discs.

Assuming the cross-sectional area of the blades to decrease linearly from the root to the tip section, the stress level at the blade root section due to centrifugal force is defined by

$$\text{Stress}_{rt} = \frac{(\gamma_{blade} u^{2}_{tAI-tp})(1-\nu^{2}_{tA})}{288\, g}\left[1-\frac{(1-\alpha_{blade})(2+\nu_{tA})}{3(1+\nu_{tA})}\right] \qquad \text{(VII-199)}$$

where the parameter α_{blade} represents the ratio of the blade tip area to the blade root area. Since the impeller blades of axial turbines employed in cooling systems would normally be subjected to relatively low temperatures, the allowable stress level may be considered greater than commonly employed in gas turbine design practice. The maximum permissible stress is set at 35,000 pounds per square inch for steel blades and at 12,000 pounds per square inch for aluminum blades. The parameter α_{blade} should be as low as is practical from the standpoint of manufacture and fatigue. A typical value of α_{blade} equal to 1/3 will be used. For these conditions, equation (VII-199) may be reduced to the form

$$(u^{2}_{tAI-tp})(1-\nu^{2}_{tA})\left[1-0.222(2+\nu_{tA})/(1+\nu_{tA})\right] = 6.68 \times 10^{5} \qquad \text{(VII-200)}$$

or

$$(u^2_{\tau AI\text{-}tp}/1000)^2(1-\nu_{\tau A})(5+7\nu_{\tau A}) = 6.0 \qquad \text{(VII-201)}$$

and is applicable either for steel or aluminum blades.

Very little design information dealing with size and weight of small axial turbines is available. The physical characteristics of an axial turbine may be determined with fairly good accuracy by similarity considerations of larger turbines. For comparative purposes, the maximum external dimension parallel to the plane of rotation can be expressed by an external diameter defined as

$$d''_{\tau Ae} = 1.25\, d''_{\tau AI\text{-}tp} \qquad \text{(VII-202)}$$

The nozzle ring and impeller blades forming one stage would have an axial length of approximately $0.2\, d''_{\tau AI\text{-}tp}$. At both the inlet and exit of the axial turbine an air collector ring would be necessary. The air velocity in the collector ring at inlet would be approximately equal to the axial air velocity through the turbine. Consequently, the collector at inlet would have approximately the same flow area as the annulus. If the inlet collector is assumed circular in cross section and the outlet collector is assumed cylindrical with the outlet centered about the axis of rotation, the turbine axial length can be represented approximately by

$$L''_{\tau A} = 1.15\, d''_{\tau AI\text{-}tp} \qquad \text{(VII-203)}$$

The spatial requirements may be determined by calculating the volume of the turbine with the dimensions given by equations (VII-202) and (VII-203). Thus,

$$V''_{\tau A} = 1.4\, d''^2_{\tau AI\text{-}tp} \qquad \text{(VII-204)}$$

The weight of an axial turbine may only be roughly established. Due to the greater amount of duct work required for flow passages in the axial turbine unit in comparison with the radial turbine, the bulk density would be less. On the basis of this assumption, the axial turbine weight can be expressed approximately by

$$W_{\tau A} = 0.03\, d''^3_{\tau AI\text{-}tp} \qquad \text{(VII-205)}$$

REFERENCES

VII-1 Patterson, G. N., Modern Diffuser Design, Aircraft Engineering, London, England, Sept. 1938.

VII-2 Rogallo, F. M., Internal-Flow Systems for Aircraft, Report No. 713, National Advisory Committee for Aeronautics, Washington, D.C., 1941.

VII-3 Roberts, H. E. and Langtry, B. D., The Influence of Design Parameters on the Performance of Subsonic Air Inlets, Journal of the Institute of Aeronautical Sciences, New York, N.Y., July 1950.

VII-4 Hoerner, S. F., Aerodynamic Drag, The Otterbein Press, Dayton, Ohio, 1951.

VII-5 Balje, O. E., A Contribution to the Precalculation of Radial Compressors, U.S. Air Force Tech. Report No. F-TR-2211-ND, Air Materiel Command, Wright Field, Ohio.

VII-6 Wosika, L. R., Radial Flow Compressors and Turbines for the Simple Gas Turbine, Paper No. 52-S-13, American Society of Mechanical Engineers, New York, 1952.

VII-7 The 1943 Supercharger Compressor Symposium Lecture Book, The General Electric Company, 1943.

VII-8 Hudelson, G. D., An Analytical Study to Determine the Optimum Inlet Diameter and Maximum Air Capacity of Centrifugal Compressors, Thesis, The Ohio State University, Columbus, Ohio, 1951.

VII-9 Vincent, E. T., The Theory and Design of Gas Turbines and Jet Engines, McGraw-Hill Book Co., Inc., New York, 1950.

VII-10 Howell, A. R., Fluid Dynamics of Axial Compressors, Development of the British Gas Turbine Jet Unit, The Institution of Mechanical Engineers, London, Reprinted by the American Society of Mechanical Engineers, New York, 1947.

VII-11 Knörnschild, E., The Radial-Flow Turbine in Comparison with the Axial Turbine, USAF Tech. Report No. F-TR-1198-IA, Air Materiel Command, Wright-Patterson Air Force Base, Ohio.

VII-12 von der Nuell, W. T., The Radial Turbine, USAF Tech. Report No. F-TR-2149-ND, Air Materiel Command, Wright-Patterson Air Force Base, Ohio.

VII-13 Coulter, E. E., Larkin, R. G., and Gabriel, D. S., Efficiency of a Radial-Flow Exhaust-Gas Turbosupercharger Turbine with a 12.75-Inch Tip Diameter, National Advisory Committee for Aeronautics, Report No. E6F03, Lewis Memorial Laboratory, Cleveland, Ohio, July 1946.

VII-14 Rebeske, J. J., Jr., Parisen, R. B., and Schum, H. J., Investigation of a Centrifugal Compressor Operated as a Centripetal Refrigeration Turbine, National Advisory Committee for Aeronautics, Report No. RM-E50120, Lewis Memorial Laboratory, Cleveland, Ohio, December 1950.

VII-15 Balje, O. E., A Contribution to the Problem of Designing Radial Turbomachines, Paper No. 51-F-12, American Society of Mechanical Engineers, New York, 1951.

VII-16 Goldstein, A. W., Analysis of the Performance of a Jet Engine from Characteristics of the Components. I - Aerodynamic and Matching Characteristics of the Turbine Component Determined with Cold Air, Flight Propulsion Research Laboratory, National Advisory Committee for Aeronautics, Cleveland, Ohio, Report No. 1459, October 1947.

VII-17 Channes, E. R. and Carman, R., The Effect of Inlet Temperature and Pressure on the Efficiency of a Single-Stage Impulse Turbine Having a 13.2 Inch Pitch-Line Diameter Wheel, Report No. E5H10, Aircraft Engine Research Laboratory, National Advisory Committee for Aeronautics, Cleveland, Ohio, September 1945.

VII-18 Davis, H., Kottas, H., and Moody, A. M. G., The Influence of Reynolds Number on the Performance of Turbomachinery, Paper No. 50-A-99, The American Society of Mechanical Engineers, New York, 1950.